Duplicated *SEPALLATA* transcription factors govern the robustness of flower development in *Arabidopsis thaliana*

Richa Kishor Yeshvekar

Submitted in accordance with the requirements for

the degree of

Doctor of Philosophy

The University of Leeds

School of Biology

September 2021

The candidate confirms that the work submitted is his/her own and that appropriate credit has been given where reference has been made to the work of others.

.

Acknowledgements

Thanks first and foremost to my supervisor Professor Brendan Davies for giving me the opportunity to work on this project. I am grateful to him for his guidance, excellent supervision, and support throughout my time in the lab. I am also thankful to him for his help in navigating my PhD through the COVID-19 pandemic and lockdowns, and for successfully trying to get me additional funding during the COVID-19 associated extension. I also thank Dr Antoine Larrieu for the insightful discussions and all the help he has given me. This thesis would have been incomplete without Antoine's support. I appreciate the valuable suggestions and feedback from my co-supervisors and assessors, Prof. Peter Meyer, Dr Laura Dixon, and Dr Tom Bennet. Thanks to Dr Martin Fuller, Dr Alex Kulak, and Dr Stuart Micklethwaite for their technical support with sample preparation and SEM imaging of the floral meristems. Special gratitude to Dr Ruth Hughes and Dr Sally Boxall for training to use the confocal microscope and being around (sometimes after hours) to ensure that I obtained good quality images. Thanks to Dr Chris West and Dr Alastair Plant for sharing the material and the unpublished know-how from their lab to generate the CRISPR/Cas9 KOs essential for this project.

I thank the Indian Council for Agricultural Research for funding me through the Netaji Subhas International PhD Scholarship during the first three years of my PhD. I am extremely thankful to the FBS graduate school for providing six months' funding through the COVID-19 hardship fund. These funds enabled me to finish the experiments necessary for completing this thesis.

Additionally, I thank the Davies lab members for their untiring support (Antoine, Barry, Jelena, Tayah, Mary, Zach, Beth, Lin, Esther, and Tas). They were a pleasure to work with. It would have been impossible to go through these four years without the administrative help from Lucy Parker and Caroline Murphy, the members of the FBS graduate school. Thanks to the members of CPS for good times at lunch and the pub (Katie, Grace, Liam, Martina, Phil, Sam, Mike, Kate, Pablo, Khushboo, and Roz). Special thanks go to my lovely friend Rachel, whom I could call on at any time of the day.

Although I was away from home, my friends in Leeds made sure that I was never indeed left alone. The small Indian community in FBS and UoL (Tarun, Badri, Mrunal, Payal,

and Susmita) were always around to offer a cup of chai with a healthy dose of advice. I am also thankful to my housemates turned friends (Rosa, Becca, Craig, and Sam) for keeping me sane during the COVID-19 lockdown. Friendships are easier to keep when you can see your friends regularly in person. I am grateful to Soham, Kaivalya, Arunima, Samia, and Tejal for their constant encouragement from different continents. Noopur and Ashwini went above and beyond in their friendship with me, managing to be my strongest support system while being in different corners of the world. I also thank my uncle Swapnil for helping make the figures in the thesis more artistic.

I am immensely grateful to Jonathan for his unwavering encouragement, infectious optimism, and curiosity in my work. I also thank his parents for being my family away from home. Finally, and most importantly, I thank my parents for always being encouraging and supportive at every step of my career, long before I even dreamt of doing a PhD. This would not have been possible without their blessings and safety net.

Abstract

Plants require a delicate balance between phenotypic plasticity and robustness in order make their lifecycle most efficient. Most phenotypes such as vegetative growth, defence response, and initiation of flowering are highly plastic, changing in response to external stochastic variations. In contrast, flower development is highly robust even under continuously changing environmental conditions. Most angiosperm flowers have an invariant floral structure and a uniform floral plan that is not affected by changes in external conditions. Genetic network architecture confers robustness upon a biological system with the help of multiple regulatory pathways, network hubs, and redundant genes. Genetically redundant *SEPALLATA* (*SEP*) transcription factors play a significant role in flower development in the model plant *Arabidopsis thaliana*. *SEP*s are present in multiple copies across flowering plants and have evolved through whole-genome duplication (WGD) events. There are four copies of *SEP*s in Arabidopsis that, in combination, are essential for flower development. Previous reports indicate that Arabidopsis *SEP1-4* are duplicate copies of each other such that single *sep* mutants lack a significant phenotype. The present study shows that *SEP1/2/4* and *SEP3* sub-clades diversified before the evolution of the most basal extant angiosperm *Amborella* and evolved independently throughout angiosperms. We describe novel and distinct phenotypes of *sep* mutants and, thereby, non-redundant functions of individual *SEP* genes. *SEP1* and *SEP2* play a redundant role in specifying decussate petal symmetry, even under variable temperature conditions, thereby ensuring the robust development of a typical crucifer flower. *SEP1* and *SEP2* also play a significant role in the development of lateral *sep*als. *SEP3* did not show any distinct functions, while *SEP4* showed environment-independent regulation of the number of floral organs. Identification of targets of *SEP1* and *SEP2* led to increased understanding of the molecular mechanisms involved in the robust formation of a decussate flower and expansion of lateral *sep*als. *SEP1* and *SEP2* regulate collective as well as *sep*arate sets of genes associated with biological robustness. Together, *SEP1* and *SEP2* suppress genes such as *NUBBIN, FBRNI,* and *PRP2*, contributing to lateral *sep*al expansion. This suggests that duplicate *SEPs* have diversified to retain partially redundant functions and acquire non-redundant functions, through which they confer robustness upon flower development in changing environmental conditions.

Table of Contents

List of Tables

List of Figures

List of Abbreviations

A. thaliana/Arabidopsis/At	*Arabidopsis thaliana*
ABAP	Angle between adjacent petals
Agrobacterium	*Agrobacterium tumefaciens*
bp	Base pairs
cDNA	Complementary DNA
ChIP	Chromatin Immuno Precipitation
Col-0	Columbia ecotype 0
CRISPR	Clustered Regularly Interspaced Short Palindromic Repeats
Cas9	CRISPR-associated protein 9
DNA	Deoxyribonucleic acid
dNTPs	Deoxyribonucleic acid mix of A, T, G, C
E. coli	*Escherichia coli*
e-value	Expectancy value
et al.	et alia (and others)
Fig.	Figure
FDR	False discovery rate
GC	Guanine cytosine
GFP	Green fluorescent protein
GRN	Gene regulatory network
GO	Gene ontology
HRM	High Resolution Melting-curve analysis
HSP	Heat shock protein
ID	Identifier
Kb	Kilo base (pair)
KDa	Kilo Dalton
LB	Luria Bertani medium
M	Molar
mRNA	Messenger RNA
MS	Murashigae Skoog medium
MYA	Million years ago
N	Random nucelotide

Nt	nucleotide
P	(prefix) plasmid
PAM	Protospacer adjacent motif
PCR	Polymerase chain reaction
qPCR	Quantitative polymerase chain reaction
RNA	Ribonucleic acid
rpm	Revolutions per minute
ST	Stable temperature
TE	Tris-HCl Ethylenediaminetetraacetic acid
TF	Transcription factor
SAM	Shoot apical meristem
SEP1-4	SEPALLATA 1-4
UTR	Untranslated region
VT	Variable temperature
v/v	Volume by volume
w/v	Weight by volume
WGD	Whole-genome duplication
WT	Wild type

1 Chapter 1: Introduction

1.1 Robustness in biological systems

Plants are sessile organisms that have evolved over millions of years to thrive in changing climatic conditions. This fact is indicative of their ability to adapt to varying conditions and reproduce generation after generation, while encountering constantly changing environments. In order accomplish this, a balance between plasticity and robustness is essential (Lenski et al., 2006). Phenotypic plasticity is an organism's ability to consistently change phenotype in order to survive when exposed to varying environmental conditions (Pigliucci et al., 2006). For example, the switch from vegetative to reproductive state, marked by initiation of flowering, is subject to seasonal cues such as temperature and photoperiod (Taylor et al., 2019). This phenotypic plasticity helps maximise the reproductive outcome for the plant, thereby contributing to overall reproductive fitness and survival. Robustness, also described as canalization, is a property of biological systems that describes an organism's ability to produce an invariable response to stochastic perturbations, resulting in a predetermined phenotype (Whitacre & Bender, 2010). Once flowering plants enter the reproductive phase, they commit to the development of very robust and uniform floral structures with a conserved floral plan, regardless of stochastic variations in the environment. Robustness, however, is not the literal opposite of plasticity. While plasticity is a phenotypic response to environmental perturbations, robustness can be generalized as producing a uniform output, regardless of intrinsic and extrinsic noise. The opposite of robustness is rather 'sensitivity', which would mean huge phenotypic variation in response to the smallest perturbation (Félix and Barkoulas, 2015b). Plasticity and robustness are generally interdependent, and their integration contributes to development and adaptation in systems (Bateson and Gluckman, 2012).

In a system, the robustness of a measured phenotype/trait depends on a definite set of perturbations and the genetic background (Whitacre, 2012). Importantly, robustness associated with a particular phenotype or trait may not be applicable to other phenotypes in the same population. For example, the robust spatial distribution and positioning of new organs at the Arabidopsis SAM is regulated by auxin-driven inhibitory fields (Vernoux et al., 2011). However, this auxin regulated robustness is not extended to the plastochron in the same population (Besnard et al., 2013). Instead, plastochron

robustness is governed by cytokinin signalling and AHP6 movement (Besnard et al., 2013; Mirabet et al., 2012). Similarly, the invariable response is conditional to specific set of perturbations. For instance, in Arabidopsis, the *BEH4* gene maintains robustness of hypocotyl elongation in the dark (Lachowiec et al., 2018). However, *beh4* plants grown in light do not show a significant difference in robustness of hypocotyl length, showing that the robustness is specifically associated with dark growth conditions. Similarly, robustness in response to environmental perturbations is not comparable with robustness associated with noise in gene expression. Overall, robustness can be measured as the degree of accuracy or symmetry with which a phenotype is produced in a population of similar genetic background (Clarke, 1998).

Various studies have attempted to uncover the how biological systems buffer stochastic perturbations resulting in an invariable output; however, their full understanding remains elusive. There is a network of multiple system principles that collectively contribute to robustness. For instance, 'master regulators' of gene networks, regulation of gene expression, and genetic and local functional redundancy are thought to confer robustness (Whitacre, 2012). The way these multiple mechanisms regulate the buffering of incoming perturbations has been studied in various systems, indicating that they share some similarities.

1.1.1 **Master regulators in genetic networks**

Genetic networks governing multiple functions and complex traits often have a 'master regulator' that buffers noise to avoid perturbations in key developmental processes. Such master regulators denote network hubs or fragile nodes in gene regulatory networks, which are involved in multiple pathways and buffer any genetic variation in their associated network to minimize phenotypic variation (Queitsch et al., 2002). Over 300 'master regulators of robustness' have been identified in the yeast *Saccharomyces cerevisiae* (Levy and Siegal, 2008). Most of these regulators include genes involved in chromosome organization, transcription, protein modification, and stress response. Perturbation of any one of these genes resulted in morphological variation. The best example of a master regulator is the heat shock protein 90 (HSP90) across various species. HSPs are molecular chaperones, responsible for folding and localization of proteins as well as for regulation of protein accumulation and denaturation. The HSP family contributes to various functions such as abiotic stress tolerance, in particular heat

stress and various developmental stages (Queitsch et al., 2000). HSP90 functions as a network hub in gene regulatory networks and has the capacity to buffer many developmental phenotypes (Sangster and Queitsch, 2005). In Arabidopsis, perturbing HSP90 resulted in phenotypic variation with respect to multiple traits such as root elongation, defence and response to stress (Sangster et al., 2008). Additionally, it is also speculated that when regulators are connected to multiple genetic networks, their contribution to each network is balanced. If this balance is disrupted, phenotypic variance is seen. For example, HSP90's capacity to buffer genetic polymorphisms diminishes during heat stress, resulting in expression of polymorphism related phenotypes (Sangster et al., 2007).

1.1.2 Regulation of gene expression

Noise in gene expression is known to affect development and transitions in developmental phases (Forde, 2009). Stochastic expression fluctuations are often regulated by microRNAs and small RNAs in plants (Hornstein and Shomron, 2006). microRNAs act in two different ways to buffer noise in gene expression: (1) miRNA mediated repression of 'leaky' target mRNAs in tissues where they would cause undesirable phenotypes. In developmental processes such as cell differentiation, certain genes are required to express only in a particular tissue. In such conditions, microRNA and their targets are expressed in mutually exclusive cells, restricting target expression in cells where microRNAs are produced. For instance, in both Arabidopsis and maize, miR166 plays a role in determining leaf polarity by restricting accumulation of *HD-ZIPIII* mRNA, which is required for adaxial cell fate specification; thus, cells lacking HD-ZIPIII form the abaxial side (Juarez et al., 2004; Kidner & Martienssen, 2004) (2) Co-expression of miRNAs with their targets to achieve posttranscriptional control of genetic noise. Gene expression requires activation of promoters, which results in random fluctuations of transcript number. This genetic 'noise' may perturb the nominal function of the genetic program and thus be detrimental to phenotype. Co-expression of miRNAs regulates the transcript number, creating a limiting step for protein production and reducing noise. For example, PHO2 shows high expression levels in Arabidopsis leaves under low phosphate conditions during senescence, which is contradictory to its function of repressing phosphate transport. However, miR399 that is co-expressed with PHO2 plays a regulatory role, leading to leaf senescence (Thatcher

et al., 2015). In plants, other classes of small RNAs such as siRNAs, tasiRNAs and ncRNAs have also been shown to play similar roles (Plavskin et al., 2016).

1.1.3 Genetic and functional redundancy

Duplicate genes or paralogs are common in plant genomes as a result of whole genome duplication events (Sémon and Wolfe, 2007). Several mechanisms have been proposed to explain paralog retention. For example, various functions of the ancestral gene may be divided between the paralogs, resulting in sub-functionalization (Lynch and Force, 2000). Another way of retaining a paralog is neofunctionalization, wherein one of the paralogs acquires a novel function (Assis and Bachtrog, 2013). Furthermore, selection for absolute gene dosage can also explain paralog retention (Kuzmin et al., 2020). Stoichiometric constraints in macromolecular complexes or pathways are also alternative explanations (Qian et al., 2010). However, duplicate genes with the same function exist in the genome and are termed 'genetically redundant'. It might be possible that duplicated genes bestow robustness to noisy biological systems, resulting in production of invariant outputs despite perturbed inputs. This can be achieved in two ways: (1) Compensation, wherein, duplicated genes show considerable divergence in expression from their paralogs. Thus, when the expression of one paralog decreases, and that of the other increases, their average gene expression is sufficient to produce the subsequent protein, associated with the trait (Levy and Siegal, 2008; Hanada et al., 2009). (2) Combinatorial gene interaction, in which each paralog contributes toward achieving the ultimate phenotype, maintaining an invariable output to counter noise. Duplicate genes often act as 'master regulators' of genetic networks, offering a two-fold layer of robustness (Levy and Siegal, 2008). It is important to note that duplicate genes are often partially redundant, implying that they have some unique functions in addition to their overlapping functions. Such genes show cryptic genetic variation that is phenotypically silent until revealed by exposure to environmental or genetic perturbations (Paaby and Rockman, 2014).

1.2 Robustness in flower development

Plant growth requires a balance between plastic and robust traits in order to maximise the efficiency of the plant life cycle. Flower development, being a crucial aspect of reproduction, is highly robust. Most higher angiosperms have a conserved floral scheme in terms of organ type, composition, and arrangement, that does not vary with stochastic

noise associated with external conditions (Espinosa-Soto et al., 2004; Rudall & Bateman, 2003). For example, plants from the Brassicaceae family produce uniform flowers with the same number of organs and cruciferous floral architecture, irrespective of constantly changing environmental conditions.

A typical angiosperm flower is comprised of four whorls – the first and outermost whorl is made up of *sep*als and the second whorl of petals, while the third and fourth whorls constitute the male and female reproductive organs, the stamens, and carpels. *Arabidopsis thaliana* is a crucifer that produces flowers with four *sep*als, four petals, six stamens and two fused carpels. The *sep*als and petals are arranged in a cross-like structure which is characteristic of cruciferous flowers. With this context, it would be interesting to discover the underlying mechanisms that promote robustness of flower development in Arabidopsis.

1.3 Mechanisms underlying flower development

1.3.1 Flower development in *Arabidopsis thaliana*

Flowers play an important role in seed plants as they produce the gametophytes that are essential for pollination, fertilisation, and seed production for propagation (Kaufmann et al., 2005b). For most plants, it is fundamental to match the timing of reproduction with the local growing season. Thus, the transition from vegetative to reproductive stage depends on the developmental stage as well as seasonally changing environments (Blackman, 2017). The synchronisation of developmental stages with environmental cues in order to achieve reproductive fitness is accomplished through developmental plasticity (Blackman, 2017). Flower development can be roughly divided in four stages. At the first stage, environmental cues such as light, temperature, vernalization, and photoperiod influence the expression of flowering time genes (Blázquez et al., 2003; Lee et al., 2007; Mockler et al., 2003) alongside endogenous phytohormone signals (Bao et al., 2020; Domagalska et al., 2010). For example, flowering during long-days is initiated by the coincident expression of *CONSTANS (CO)* in the light phase (Putterill et al., 1995). *CO* is regulated by *GIGANTEA (GI)*, a gene that regulates time measurement in the circadian clock (Sawa and Kay, 2011). *CO* and *GI* activate *FLOWERING LOCUS T (FT),* the first flowering time gene to be identified from Arabidopsis that is essential for initiation of flowering (Corbesier et al., 2007). Another factor that influences flowering time is vernalization, that is, prolonged exposure to cold

that induces the onset of flower development. Vernalization promotes flowering by supressing *FLOWERING LOCUS C (FLC),* an inhibitor of flowering (Michaels and Amasino, 1999). Similarly, during ambient temperature flowering, expression of genes such as *SHORT VEGETATIVE PHASE (SVP)*, and miR172 is induced (Lee et al., 2007; Zhu and Helliwell, 2011).

In the second step, these genes regulate the activity of floral integrators such as *SUPPRESSOR OF CONSTANS (SOC), LEAFY (LFY)*, and *FT* that are responsible for supressing the genes responsible for maintaining the vegetative stage while activating genes important for the specification of inflorescence and floral meristem identity (Nilsson et al., 1998; Yoo et al., 2005). In the third step, *LFY* regulates the activity of genes such as *AP1* and *CAULIFLOWER (CAL)*, that promote inflorescence meristem identity (Goslin et al., 2017). Once the inflorescence meristem identity is established, in step four, floral organ identity genes are activated. The floral organ identity genes regulate specification of different cell types and their development into different organs by regulating downstream genes (Jack, 2001; Krizek and Fletcher, 2005).

1.3.2 **Discovery of floral homeotic genes**

The discovery of floral homeotic mutants was pioneering for research on flower development. The 'double flower' phenotype that shows multiple whorls of *sep*als and petals, but lacks stamens and carpels, was reported in Matthiola over more than 400 years ago (Saunders, 1921). Double flowers from other species such as Cherianthus (Masters, 1869), Arabis (Bateson, 1913), and Petunia (Sink, 1973) also showed homologous phenotypes (Reynolds and Tampion, 1983). The Arabidopsis double flower mutant termed '*agamous*' was described in detail along with other mutants such as *apetala2-1* (leaflike *sep*als), *apetala2-2* (carpelloid *sep*als, absence of petals and stamens) , *apetala3-1* (*sep*aloid petals and carpelloid stamens), and *pistillata* (*sep*aloid petals, no stamens) (J. Bowman et al., 1989; Hill & Lord, 1989; Komaki et al., 1988; Meyerowitz et al., 1989). Later these phenotypes were linked to the mutations in the genes *AGAMOUS (AG), APETALA2 (AP2), APETALA3 (AP3),* and *PISTILLATA (PI),* respectively (Kunst et al., 1989; Yanofsky et al., 1990). Similarly, various homeotic mutants that showed defective or absent floral organs were identified for Antirrhinum (Carpenter and Coen, 1990). By the early 1990s, phenotypes of homeotic mutants were linked to different organ identity genes. *AGAMOUS* from Arabidopsis and *PLENA* from Antirrhinum were linked to formation of stamens and carpels (Yanofsky et al, 1990).

AP3, PI from Arabidopsis and *DEF*, *GLO* from Antirrhinum were found to be responsible for petal and stamen formation (Jack et al., 1992; Schwarz-Sommer et al., 1992). Whereas Arabidopsis *AP1, AP2* and Antirrhinum *SQUA* were confirmed to be responsible for *sep*al and petal identity (Kunst et al., 1989; Irish and Sussex, 1990). In two remarkable studies that describe the permutations and combinations of these homeotic mutants, the ABC model of flower development was proposed (Bowman et al., 1991; Coen & Meyerowitz, 1991). The ABC model of floral organ identity postulates the existence of three gene activities, A, B and C, which act in combination to specify the development of these four whorls (Bowman et al, 1991; Coen and Meyerowitz, 1991). The A-activity specifies organ identity in *sep*als, a combination of A and B activities is required for petal development; B and C-activity genes function together to form stamens, while C-activity specifies carpel formation. (Figure 1-1). Thus, in Arabidopsis, *AP1* and *AP2* are A-activity genes, *AP3* and *PI* specify B-activity, and *AG* specifies C-activity.

1.3.3 **ABCE model of flower development**

Although the A, B and C-activity genes were found to be essential for the specification of floral organ identity, ectopic expression of these genes in Arabidopsis leaves did not lead to formation of flowers (Honma & Goto, 2001; Pelaz et al., 2000a). Thus, it was established that these genes were not sufficient for flower development. The discovery of genetically redundant *SEPALLATA* transcription factors led to modification of the ABC model. The *sep1 sep2sep3* mutant produced indeterminate flowers composed of multiple whorls of *sep*als, indicating that *SEP*s are required for development of petals, stamens, and carpels. The *sep1 sep2sep3sep4* quadruple mutant made only whorls of leaf-like structures instead of flowers (Ditta et al., 2004; Pelaz et al., 2000c). Ectopic expression of *SEP3* with *AP1, AP3*, and *PI* converted rosette leaves to petaloid organs. Overexpression of *SEP2* and *SEP3* in plants constitutively expressing A and B activity genes resulted in a more complete transformation of leaves to petals (Pelaz, Tapia-López, et al., 2001). Ectopic expression of *PI, AP3, AG* and *SEP3* led to conversion of leaves to stamenoid organs (Honma and Goto, 2001). Thus, it was established that specification of floral organ identity requires another set of MADS-box genes, *SEPALLATA (SEP1/2/3/4),* that constitute the E-activity. The modified 'ABCE model' postulates that A+E activity is needed for development of *sep*als, A+B+E activity for petals, B+C+E activity for stamens, and C+E activity for carpels (Honma and Goto, 2001).

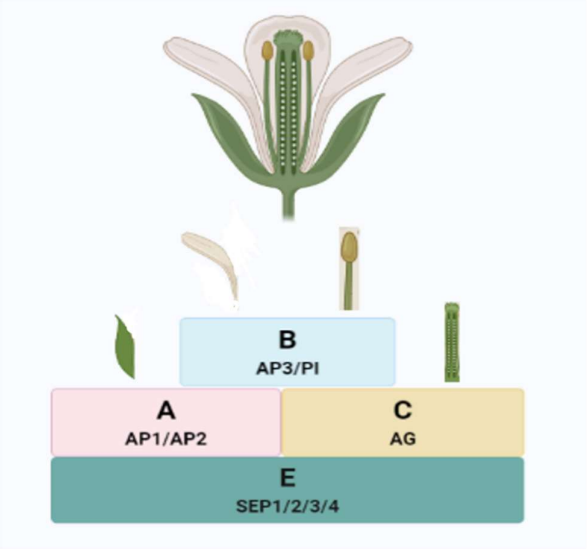

Figure 1-1: ABCE model of flower development: A+E function genes specify *sep*al formation, A+B+E function genes specify petal formation, B+C+E function genes specify stamen formation and C+E function genes specify carpel formation

1.3.4 **The (A)BC model of flower development**

The ABC model of flower development was proposed based on the activity of homeotic genes from Arabidopsis and Antirrhinum. However, a true recessive mutant for A-function has not been identified from any other species except for Arabidopsis (Heijmans et al., 2012). In Antirrhinum, a mutant that exhibited a typical loss of A-function phenotype, that is, conversion of *sep*als and petals to carpels and stamens, was found to be an ectopic expression of *PLE*, a C-function gene (Bradley et al., 1993). In Arabidopsis, loss of AP1 or AP2 not only shows the predicted carpel, stamen, stamen, carpel arrangement of whorls with affected perianth organ identity, but also shows additional phenotypes, such as leaf or bract-like structures in whorl 1 and secondary flowers in whorl 2 (Litt, 2015). These phenotypes cannot be explained by the classical ABC model of flower development. Additionally, AP1/AP2 are not essential for petal identity as seen from the development of *sep*als and petals in *ap1* mutant plants with constitutive SEP3 expression (*ap1 35S:SEP3)*(Castillejo et al., 2005). Moreover, the expression pattern of the Arabidopsis A-function genes, AP1 and AP2 does not fit within the classical ABC model. According to that model, genes belonging to each function should be expressed in two adjacent whorls; for example, expression of AP3 and PI is predominantly found in whorls 2 and 3 (Weigel and Meyerowitz, 1994). However, AP1 is expressed in the inflorescence and floral meristems to specify the meristem identity. After this stage, AP1 expression is restricted to whorls 1 and 2 in order to specify perianth organ identity (Alejandra Mandel et al., 1992; Gustafson-Brown et al., 1994). Unlike *AP1, AP2* is found to be expressed in all four floral whorls as well as in vegetative organs (Jofuku et al., 1994; Würschum et al., 2006). Other than specifying perianth organ identity, AP2 plays two important roles, that are, to restrict the expression of AG to whorls 3 and 4, and a role in ovule and seed coat development (Bowman et al., 1989; Jofuku et al., 1994; Smyth et al., 1990). Overall, there is little evidence for the A-function to be essential for *sep*al and petal identity in plants other than Arabidopsis. Hence, the new (A)BC model was proposed to include representation of other species (Causier et al., 2010). The (A)-function play a role in specifying floral meristem identity, restricts the expression of B- and C-functions genes, and supports their role of specifying floral organ identity (Figure 1-2). The new (A)-function also includes the E-function *SEP* genes that contribute to both B- and C-functions as well as specification of floral meristem identity (Ditta et al., 2004).

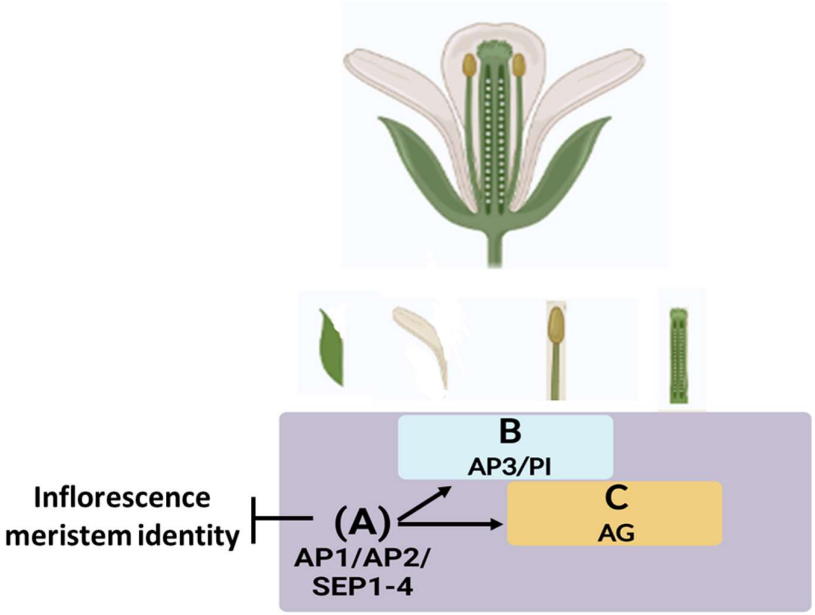

Figure 1-2: Schematic representation of the (A)BC model of flower development. The (A)-function (shown by a purple rectangle) represses the inflorescence meristem (shown by a flat-capped arrow). It regulates B- and C-function genes (shown by pointed arrows towards blue and yellow rectangles), *AP3, PI*, and *AG*, and establishes boundaries to restrict their expression to specific domains. The (A)-function comprises of *AP1*, *AP2*, and the E-function *SEP1-4* genes. Thus, *sep*al identity is specified by (A)-function proteins, petal identity is specified by (A)- and B-function proteins, stamens are specified by (A)-, B- and C-function proteins, and the carpel is made by (A)- and C-function proteins.

1.3.5 **Floral quartet model**

Although the ABC and further improved ABCE model explains the necessity of different gene functions to specify identity of different floral organs, it did not provide a molecular mechanism through which the floral homeotic genes interacted. In 1996, Davies *et al.* used yeast two hybrid (Y2H) studies to determine that B-function DEF and GLO proteins from *A. majus* form specific heterodimers with each other, but not with the C-function protein PLENA (Davies et al., 1996). Similarly, Reichmann et al (1996) reported that the Arabidopsis homeotic proteins AP1, AP3, PI, and AG could form specific dimers, wherein B-function proteins AP3 and PI formed a dimer with each other, but not with a C-function protein such as AG (Reichmann et al, 1996). Moreover, C-function proteins AG and PLENA form dimeric complexes with all AGL2-like (SEP1-like) proteins (Theißen, 2001). The specificity of dimer formation rendered the possibility of interaction between A, B and C-function proteins unlikely. However, the formation of larger multimeric complexes by SQUA, DEF and GLO proteins were shown by EMSA and Y2H assays (Egea-Cortines et al., 1999). The multimeric complexes were tetramers consisting of a SQUA-SQUA homodimer and a DEF + GLO heterodimer. In Arabidopsis, each of the A, B, and C-function proteins were shown to interact with the E-function SEP proteins (Pelaz et al., 2000a). Thus, the floral quartet model can be used to describe the role of MADS box transcription factors in floral organ development. Two homeotic proteins form a homo/hetero dimer (i) within the same function or (i) with an E-function protein. Two such dimers form a larger tetramer that binds to two CArG boxes in the promoter region of a target gene required to specify floral organ identity. This subsequently generates a DNA loop between the two binding sites (Smaczniak *et al*., 2012[a]). The SEP transcription factors play an essential role in formation of these tetramers, as mediators of higher order complex formation (Immink *et al*., 2009; Smaczniak *et al*., 2012). SEPs, especially SEP3 acts as a 'glue' during the formation of these tetramers, wherein the subdomain, K3 plays essential role (Immink *et al*., 2009; Melzer and Theissen, 2009). Thus, according to the floral quartet model, AP1+AP1+SEP+SEP forms *sep*als, AP1+AP3+PI+SEP forms petals, AP3+PI+AG+SEP forms stamens and AG+AG+SEP+SEP forms carpels in Arabidopsis Figure 1-3. Additionally, other proteins such as nucleosome remodelling factors and homeobox transcription factors were found to make larger complexes with these tetramers (Smaczniak et al., 2012). Thus, the core ABCE complexes found in the original floral quartet model are a part of

larger complexes with other non-MADS-Box proteins to specify floral organ identity. Moreover, the floral quartet model is based on the role of the A-function from the original ABC model. However, according to the (A)BC model, it has been shown that constitutive expression of SEP3 (35S:SEP3) in *ap1, ap1 ag,* or *ap1 agl24* mutants is sufficient for petal development, making AP1 nonessential for specifying A-function. Therefore, corresponding changes in the floral quartet model would mean that the (A)-function proteins include the former A- and E-function proteins.

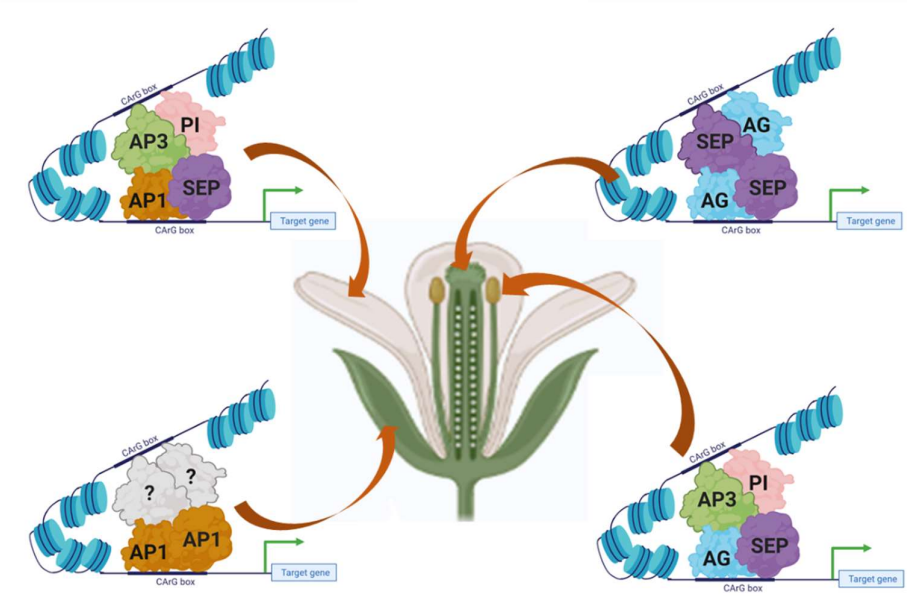

Figure 1-3: Floral quartet model. The MADS-box proteins AP1, AP3, PI, AG, and SEPs act in combination to specify identity of each floral organ. Combination of A and E-functions (AP1, SEPs, other unknown proteins) is required to specify *sep*al identity, AP1-AP3-PI-SEP specifies petal identity, AP3-PI-AG-SEP specifies stamen identity, and AG-AG-SEP-SEP specifies carpel identity. The tetramer complex formed by the homeotic proteins co-operatively binds two CArG boxes in the promoter region to regulate transcription of downstream genes.

1.3.6 **MADS box genes**

All the genes involved in floral organ specification, that is, the A, B, C and E function genes (*AP1, AP2, AP3, PI, AG, SEP1, SEP2, SEP3,* and *SEP4,*) belong to the MADS box family (Kaufmann et al., 2005; Weigel & Meyerowitz, 1994), with the exception of *AP2* (Kunst et al., 1989). MADS box genes encode transcription factors (Gramzow et al., 2010). The name MADS is an acronym from four representative proteins belonging to a diverse class of organisms, MCM from *Saccharaomyces cerevisiae*, AGAMOUS from *A. thaliana*, DEFICIENS from *Antirrhinum majus*, and SRF from humans (Theissen, Becker, Rosa, et al., 2000). It is evident that these genes are involved in regulation of fundamental, complex, and diverse biological functions over a wide range of organisms. In yeast, they are responsible for pheromone response during mating (Mead et al., 2002), while in animals the SRF genes regulate a variety of processes such as cardiac muscle development (Nelson et al., 2005). In plants, MADS box genes are responsible for regulation of flower initiation and development, as well as leaf, root, and fruit development (Reichmann and Meyerowitz, 1997; Liljegren et al, 1998; Kauffman et al, 2005).

1.3.7 **Evolution of MIKC genes**

The MADS box family is present in most eukaryotes (Gramzow et al., 2010; Theissen, Becker, di Rosa, et al., 2000). Fungi, animals, and protists have been reported to contain a small number of MADS box genes (Gramzow and Theissen, 2010). However, these genes are present in abundant numbers in plants (Becker et al., 2000; Theissen, Becker, Rosa, et al., 2000). The most recent ancestor of MADS box genes in prokaryotes can be traced back to subunit A of Topoisomerase-II A in prokaryotes (Gramzow et al., 2010). TOPOIIA-A has the ability to bind to DNA that enables its various functions related to managing the untangling of DNA strands during replication, transcription, recombination, and chromosome segregation. Thus, it is not surprising that the MADS box evolved to have a more specific mechanism of DNA interaction through the CArG boxes. Eukaryotic MADS box genes can be classified into Type I (SRF-like) and Type II (MEF2-like) lineages. These two types are estimated to be generated by a gene duplication event preceding the divergence of plants and animals more than a billion years ago (Alvarez-Buylla et al., 2000).

Type I genes share high similarity with the MADS domain of SRF and contribute to functions such as regulation of growth factors in animals (Wang et al., 2002). In plants,

type I genes form three sub-families, Mα, Mβ, and Mγ. These genes are mostly encoded by a single exon and are distributed over chromosomes 1 and 5 in Arabidopsis. The lack of type I MADS genes on other Arabidopsis chromosomes indicates that the multiple copies most likely arose from intrachromosomal duplications (Alvarez-Buylla et al., 2000). These genes are predominantly expressed in male and female gametophytes, embryo and endosperm (Tiwari et al., 2010). The first type I MADS gene to be studied from Arabidopsis is the *AGL80/FEM11* gene belonging to the Mγ subfamily, which functions in initiation of endosperm development (Portereiko et al., 2006). AGL80 is known to interact with an Mα protein AGL61/DIANA to specify central cell fate during reproduction. Type I proteins from one sub-family are shown to preferably interact with proteins from another sub-family (de Folter et al., 2005a). Although there are exceptions there are no significant reports on type I and II proteins interacting with each other (de Folter et al., 2005a).

The MADS domain of type II genes is highly similar to the MEF2 MADS domain. These genes are extensively found in animal, fungi, and plants; however, they have been studied in more detail in plants. The highly conserved type II MADS domain has functions pertaining to DNA-binding and dimerization. The type II genes recruited an intervening (I) domain and a keratin-like (K) domain before Streptophytes diverged (Figure 1-4). The K-box constitutes conserved repeats of hydrophobic residues that form amphipathic α-helices that function in protein dimerization and tetramerization (Kaufmann et al., 2005; Theißen & Gramzow, 2016). The MIKC genes can be classified into MIKC* and MIKC^c (c stands for classic). MIKC* genes have more variable and longer I and K domains.

1.4 MIKC^c genes have multiple copies

MIKC^c genes are highly conserved and have multiple copies in both gymnosperms and angiosperms. Most recent reports, based on whole genome sequences and large-scale transcriptomes of representative gymnosperms and angiosperms, classify the MIKC^c genes into 14 sub-clades, namely *SVP, MADS32, AGL32, AGL15, AG, ANR1, AG12, SOC1, GMADS, FLC, AGL6, AP3/PI, AP1*, and *SEP* (F. Chen et al., 2017). Amongst these, floral organ identity genes belonging to A, B, and E-function, i.e., *AP1, AP3/PI*, and *SEP* sub-clades are found only in angiosperms Figure 1-5. C-function genes, i.e., *AG* was found in both gymnosperms and angiosperms indicating that the most recent

ancestor of seed plants possessed this gene. Additionally, genes specifying A-, B-, and C-functions have only single copies, especially in Arabidopsis. For example, the *AP1* sub-clade is comprised of *AP1*, *CAL*, and *FRUITFUL (FUL)* in Arabidopsis, only *AP1* specifies A-activity, whereas *AP1, CAL* and *FUL* redundantly regulate floral meristem identity (Ferrandiz et al., 2000; Irish & Sussex, 1990).

Similarly, the Arabidopsis *AP3/PI* sub-clade constitutes of only two genes, *AP3* and *PI*, which specify B-function (Wuest et al., 2012). Although the *AG* sub-clade is comprised of *AG* and *AGAMOUS-LIKE (AGL)* genes, the members of the sub-clade show sub- and neo-functionalisation (Ó'Maoiléidigh et al., 2013; Zahn et al., 2006). An exception to this is the Arabidopsis *SEP* sub-clade, that constitutes of four genes, *SEP1-4*, which redundantly specify E-function (Pelaz et al., 2000a).

Evolution of MIKC genes. The plant type-I MADS-box genes contain a conserved DNA-binding MADS-domain and were present in early Chlorophytes. The plant type-II MADS-box genes were formed by recruiting the I, K-box (keratin-like domain), and C domains > 1 BYA, before the evolution of Charophytes. The K-box then diverged to form MIKC* and MIKCc genes in Bryophytes. The MIKC* proteins are longer than MIKCc proteins due to their longer K-box. In Angiosperms, the K-box consititutes of three conserved regions – K1, K2, and K3, that are essential for protein-protein interaction.

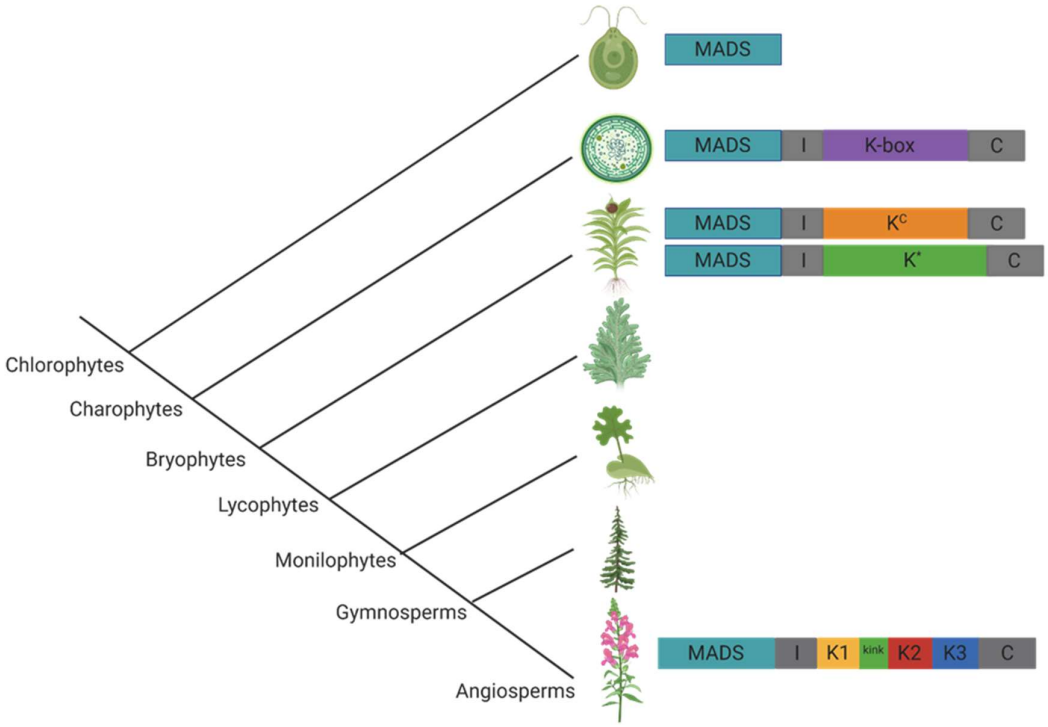

Figure 1-4: Evolution of MIKC genes. The plant type-I MADS-box genes contain a conserved DNA-binding MADS-domain and were present in early Chlorophytes. The plant type-II MADS-box genes were formed by recruiting the I, K-box (keratin-like domain), and C domains

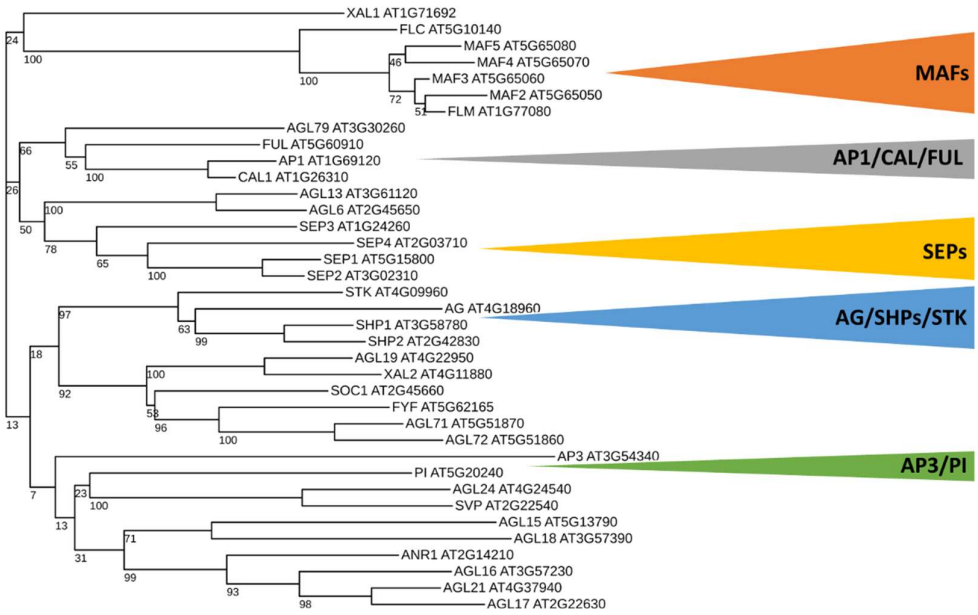

Figure 1-5: Representative phylogeny of MADS-box genes in Arabidopsis. The homeotic genes in Arabidopsis form *sep*arate sub-clades. The *SEP* subclade constitutes of the four *SEP* genes (*SEP1-4*, shown by a yellow triangle). *AP1* is part of the *AP1/CAL/FUL* sub-clade that functions non-redundantly in specifying floral meristem identity. The B-function genes *AP3* and *PI* form a *sep*arate sub-clade with *SVP* and *AGL24*. The C-function *AG* forms a sub-clade with *SHP1/SHP2/STK* genes.

1.5 Structure and function of *SEPALLATA* transcription factors

The *SEP* subfamily in *A. thaliana* is comprised of four MIKC^c type MADS-box genes, *SEP1-4*. The 4 genes are located on different chromosomes (Figure 1-6 A). The genes are 2.5 – 3 kb in size and encode ~ 250 aa proteins (Table 1-1). Like most MADS-box genes, *SEP*s are comprised of 7-8 exons; *SEP1* and *SEP2* have 7 exons each, while *SEP3* and *SEP4* have 8 exons each (Figure 1-6 B). *SEP* genes identified and characterised from different species have been reported to have 8 exons, except for *SEP1* and *SEP2* from *Brassicaceae* and *AGL2.5* from *Elaeis guineensis*. In Brassicaceae *SEP1* and *SEP2* genes, the possible loss of intron 5 led to fusion of exon 5 (42 bp) and exon 6 (42 bp) to form a longer exon (84 bp), thereby resulting in 7 exons. Although the *SEP1* and *SEP3* clades have undergone few structural changes during the course of evolution, there has been no major disruption to the intron-exon structure. It can be safely concluded that *SEP1*-like gene in the MRCA of extant angiosperms contained eight exons, with the lengths of 185, 79, 62, 100, 42, 42, 137, and 85 bp, respectively (Yu et al, 2016)

Table 1-1: Features of Arabidopsis SEP genes

Gene	ID	Chromosome no.	Chromosomal location	Gene size (bp)	Exons	Protein length (aa)
SEP1	AT5G15800	5	5151334..5154253	2920	7	251
SEP2	AT3G02310	4	559830..562664	2835	7	250
SEP3	AT1G24260	1	8593536..8596123	2588	8	251
SEP4	AT2G03710	2	1129229..1131838	2610	8	258

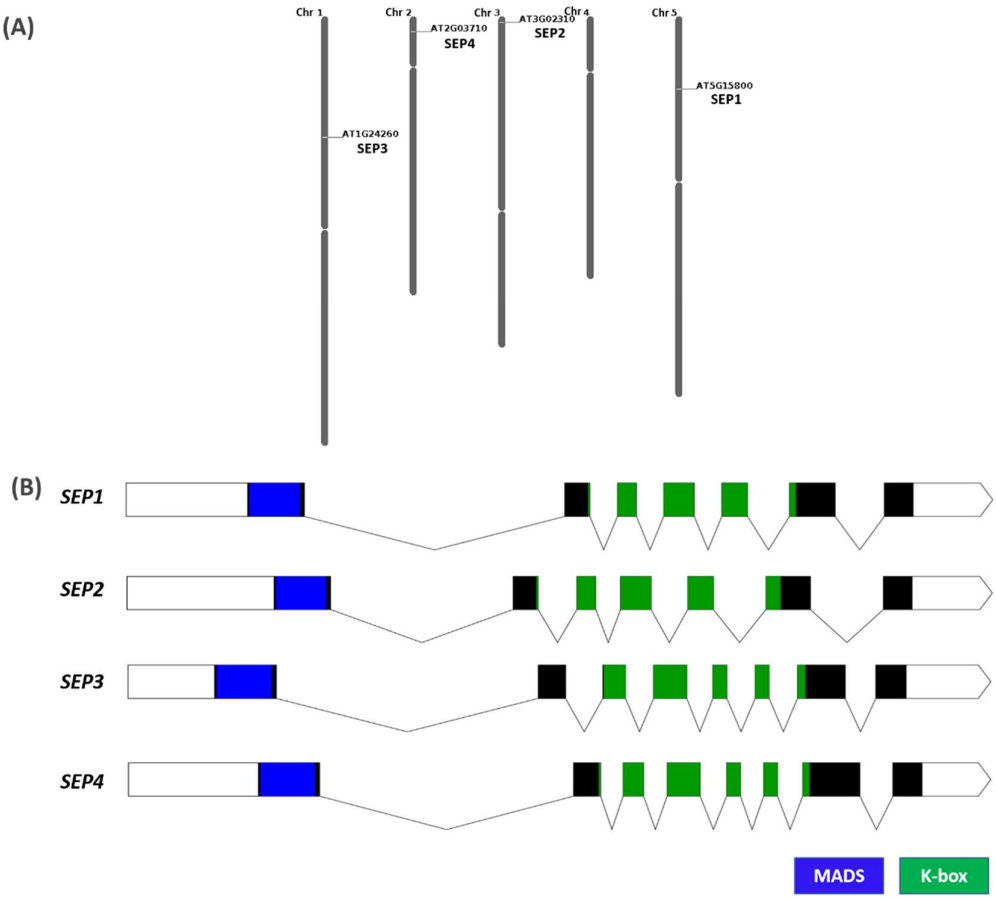

Figure 1-6: Structure and distribution of Arabidopsis SEP genes. (A) Chromosomal location of Arabidopsis *SEP* genes. *SEP1* is located on Chromosome 5, *SEP2* is located on Chromosome 3, *SEP3* is located on Chromosome 1, *SEP4* is located on Chromosome 2 (B) Intron-exon structure of *SEP* genes shows that *SEP1* and *SEP2* have 7 exons each (shown by boxes) with 6 introns (shown by zig-zag lines), whereas *SEP3* and *SEP4* have 8 exons each with 7 introns. The blue boxes show exons encoding the MADS domain, followed by a black box denoting exon encoding the I-domain. The green boxes show exons encoding the K-domain, and the following black boxes show exons encoding the C-domain.

SEP exon one contains the ~180 bp long DNA-binding MADS domain. The 58 aa MADS domain forms a 14 aa long N-terminal, followed by an amphipathic α-helix and two β-sheets (Santelli and Richmond, 2000). The motif KR[K/R]X4KK found between 22-30 nt constitutes a nuclear localization signal that transports the translated protein to the nucleus (Gramzow and Theißen, 2010). The MADS domain facilitates co-operative binding to CArG boxes [5'-CC(A/T)$_6$GG-3']. A MIKC heterotetramer binds to two different CArG boxes in promoter regions to regulate transcription of downstream genes (Melzer et al., 2009) (Figure 1-7 A). Different SEPs show differential binding co-operativity depending upon the distance between and orientation of two CArG boxes. For example, SEP1 and SEP3 containing heterotetramer complexes can bind to CArG boxes *sep*arated over 2 to 9 helical turns. SEP2 binds only to CArG boxes *sep*arated by more than 4 helical turns while SEP4 binds only to CArG boxes *sep*arated by less than 6 helical turns (Jetha et al., 2014). Overall SEP1, SEP2 and SEP3 show maximum binding preference towards CArG boxes *sep*arated by 6 helical turns, whereas SEP4 preferentially binds CArG boxes *sep*arated by 4 helical turns (Jetha et al., 2014). The binding affinity also changes depending on the number and position of A and T nucleotides, and the conformation of the DNA. SEP3 employs a shape readout mechanism based on presence of A tracts in the CArG boxes. A conserved arginine residue at the 3rd position in the MADS domain (R3) shows high DNA binding affinity with CArG boxes in the minor groove (Kappel et al, 2018) (Figure 1-7 B). As this arginine residue is conserved throughout the MIKC genes, it is quite possible that most MIKC TFs employ this mechanism to bind to target DNA.

Exon two encodes the intervening (I) domain that is involved in determining the specificity of protein-protein interactions (Kaufmann et al., 2005). Exons 3 to 6 (in *SEP1/2*) or 7 in (*SEP3/4*) encode the keratin-like domain, K-box. The K-box is comprised of three K1, K2 and K3 sub-domains (Figure 1-8 A). Each subdomain is a heptad repeat, in the form of [abcdefg]$_n$, with highly hydrophobic amino acids occupying 'a' and 'd' positions (Yang et al, 2003; Yang and Jack, 2004). This aids in formation of a coiled-coil structure bearing an α-helix (Figure 1-8 B). The hydrophobic heptad residues present at the surface of the coiled-coil facilitate protein-protein interactions with another coiled-coil (Mason et al, 2009). According to the crystal structure of the SEP3 K-domain reported by Puranik et al (2014), K1 and K2 sub-domains form two amphipathic α-helices each, that are involved in dimerization of two

SEP3 monomers. These are *sep*arated by a rigid kink region that prevents intramolecular interaction between these sub-domains. The K3 sub-domain facilitates interaction of two SEP3 dimers, resulting in formation of a tetramer. Twelve highly conserved leucine residues play an important role in intra- and intermolecular interactions leading to oligomerisation, allowing homotetramer and heterotetramer formation (Rumpler et al, 2019). Thus, SEP3, and other SEPs, have the ability to form tetramers with other MIKC type proteins, thereby acting as a glue that holds together interactions with other MIKC type proteins. Interestingly, within the ABCE model, SEP3 is known to interact with PI and AP3. SEP3 also interacts independently with AG. However, the B-function proteins AP3 and PI interact with the C-function AG only in the presence of SEP3 (Honma and Goto, 2001). This suggests that the SEP sub-family forms a network hub that regulates gene expression pertinent to flower development (Figure 1-8 C).

Exons 7/8 encode the C-terminal domain which is the least conserved. However, with the SEP subfamily, two slightly conserved motifs, SEP-I and SEP-II, have been reported (Zahn et al, 2004). Some monocot SEPs lack the SEP-II motif owing to a frameshift mutation in the LHS clade prior to duplication (Vandenbussche et al, 2003a). The motifs are comprised of hydrophobic and polar amino acids, with no reported functions in *SEP* genes so far. In AP3 and PI, the C-terminal motif was found to be dispensable in specifying floral organ identity; however, in AP3, the protein expression levels were affected in lines with truncated C-terminal (Piwarzyk et al., 2007). This suggests that the specificity of floral organ identity determination lies in the MIK domains, and not in the C-domain (Su et al., 2008). Although the exact function C-terminal motifs could possibly contribute to activation or repression of MIKC proteins.

Figure 1-7: MADS domain (A) Interaction of the MADS domain with DNA, (B) consensus sequence of the MADS domain with arrow pointing to the R3 residue essential for binding CArG boxes in minor groove (Käppel et al., 2018)

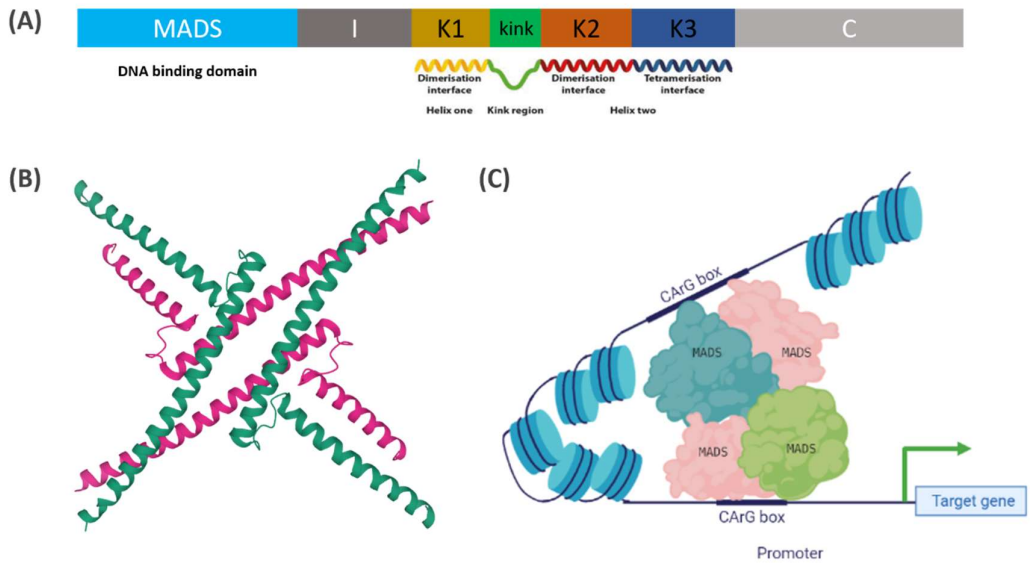

Figure 1-8: Protein-protein interactions of MIKC genes (A) Structure of MIKC gene (B) 3D structure of SEP3 keratin-like domain showing tetramer formation (C) Schematic of a MADS tetramer binding to two CArG boxes in the promoter region to regulate transcription of downstream gene

1.6 Hypothesis and scope of the thesis

The development of uniform flowers, despite highly variable environmental conditions, is an excellent example of robustness in biological systems. As a set of core, duplicated genes, models of the molecular mechanisms underlying robustness point towards the possible activity of *SEP*s in conferring robustness to flower development. It is hypothesized that retention of duplicated, redundant genes may enhance the robustness and evolvability of a complex system or essential process at multiple levels (Geuten et al., 2011). SEP transcription factors are present in multiple copies across angiosperms, with four copies in Arabidopsis (Malcomber and Kellogg, 2005). However, there is no mechanistic rationale behind retaining four copies of SEPs with redundant function. Duplicate genes suffer two possible fates – they either acquire deleterious mutations and become non-functional, or they acquire advantageous mutations and undergo sub-functionalisation and neo-functionalisation (Lynch and Conery, 2000; Hanada et al., 2009). However, loss of a single *SEP* has not been reported to have a striking effect on floral organ identity or architecture, suggesting that they are functionally redundant (Pelaz et al., 2000a). Additionally, the ability of SEPs to form tetramers with other MIKC proteins make them a 'network hub' (Rümpler et al., 2018). They act as a glue that holds together complexes of homeotic proteins and regulate transcription of genes essential for flower development. Thus, *SEP*s possess properties that theories of robustness suggest to be essential to buffer perturbations and provide a consistent output in the form of a uniform flower.

Although SEPs have been reported to be functionally redundant, the differential co-operative DNA-binding demonstrated by individual *SEPs* points towards *sep*arate functions of these genes (Jetha et al., 2014). Thus, it is hypothesized that *SEPs* show partial functional redundancy. The DNA-binding cooperativity of MADS-box genes also hampers the phenotypic characterisation of mutants belonging to this family, thereby making it difficult to assess true functional redundancy. Meticulous phenotypic analysis and quantification can expose subtle phenotypes that are generally overlooked (Kieffer et al., 2011). However, phenotypic analysis is carried out in standard, controlled growth conditions, which can mask robustness related phenotypes. Although limiting variation in the environment allows precise phenotypic measurements, it also constrains our understanding of subtle phenotypic changes that are influenced by the

variability in environment. Thus, it is important to carry out a meticulous phenotypic analysis of *sep* mutants in variable environmental conditions.

With this context, it would be interesting to evaluate the mechanisms employed in Arabidopsis to achieve the robustness of flower development. This was evaluated by using the following approach in this thesis:

i. A phylogenetic analysis of *SEP* genes was performed, based on sequences available from the new whole genome sequencing and transcriptome data for different plant species. Additionally, a synteny based approach was used to study the conservation and evolution of SEPs. The results from this study was used to understand how the gene family has diversified in Angiosperms.
ii. The redundancy of SEPs was assessed by closely analysing the phenotypes of individual *sep* mutants to identify any phenotypes unnoticed in previous reports. In order to study if and how SEPs contribute to developmental robustness, *sep* mutants was investigated for phenotypic variability under standard laboratory growth conditions and variable growth conditions. Additionally, the functional redundancy of SEPs was assessed by promoter-swap experiments to determine the specificity of each *SEP* gene in flower development.
iii. To understand the molecular mechanisms involved flower development, especially in association with the development of uniform flowers, RNAseq was used to identify putative targets of SEPs. A few candidate genes was selected and their role in flower development was experimentally validated.

2 Chapter 2: Materials and Methods

2.1 General materials

2.1.1 Chemicals, reagents and antibiotics

All chemicals, reagents and antibiotics of analytical quality were purchased through Science Warehouse from Sigma-Aldrich and Merck.

2.1.2 Enzymes and kits

Restriction enzymes were purchased from New England Biolabs. Molecular biology kits were purchased from Machery Nagel, Qiagen, Monarch, and Invitrogen. Primers and oligos were obtained from Integrated DNA Technologies.

2.1.3 Media

The following media were used in this study (Table 2-1). The media were prepared in aliquots of 400 mL in a 500 mL capacity Schott Duran bottle and sterilized by autoclaving at 120˚C, 15 PSI for 20 min.

Table 2-1: Composition of various media used in this study

Media	Component	Volume (g/L)
Luria Bertani (LB)	Tryptone	10
	Sodium Chloride	10
	Yeast Extract	5
	Agar (to be added for solid media)	15
	Distilled water	up to 1 L
YEB	Beef extract	5
	Yeast extract	1
	Peptone	5
	Sucrose	5
	MgCl2	0.5
	Agar (to be added for solid media)	15
	Distilled water	to 1 L
½ Murashigae Skoog (MS)	MS salts	2.16
	KOH	Adjust pH to 5.7
	Agar (to be added for solid media)	8
	Distilled water	to 1 L

2.1.4 Vectors

Following vectors were used in the present study as described in Table 2-2

Table 2-2: Details of vectors and constructs used for cloning

Purpose	Vector Name	Type	Resistance	AddGene catalogue no.	Function
GreenGate Cloning	pGGA004	35S	Ampicillin	48815	Plant promoters
	pGGA012	RPS5A	Ampicillin	48818	Plant promoters
	pGGB003	B-dummy	Ampicillin	48821	N-tags
	pGGD001	linker-GFP	Ampicillin	48833	C-tags
	pGGE001	RBCS	Ampicillin	48839	Terminators
	pGGF002	p35S:BastaR:t35S	Ampicillin	48843	Resistance
	pGGA000	promoter	Ampicillin	48856	Empty entry vectors (ccdB+)
	pGGB000	N-tag	Ampicillin	48857	Empty entry vectors (ccdB+)
	pGGC000	CDS	Ampicillin	48858	Empty entry vectors (ccdB+)
	pGGD000	C-tag	Ampicillin	48859	Empty entry vectors (ccdB+)
	pGGE000	terminator	Ampicillin	48860	Empty entry vectors (ccdB+)
	pGGZ003	Plant resistance at left border	Spectinomycin/Basta	48869	Empty destination vectors (ccdB+)
CRISPR cloning	pEn-Chimera		Ampicillin	61432	Entry vector for sgRNA
	pDeCas9		Spectinomycin/Basta	61433	Destination vector for sgRNA

2.1.5 Bacterial strains

Escherichia coli DH5α was used for standard bacterial cloning. *Agrobacterium tumefaciens* GV3101 was used for plant transformations. Both cultures were obtained from previous stocks in the lab.

2.2 Plant methods

2.2.1 Plant materials and genotypes

Arabidopsis thaliana plants belonging to the ecotype Columbia (Col-0) were used in the present study. *sep* mutant lines and wild-type control were obtained from previous stocks in the lab. Of these, *sep1-1, sep2-1, sep3-2* and *sep4-1* have been previously described (Pelaz et al, 2000; Ditta et al, 2004). *sep2-2* is a GABIKAT insertion line and *sep3Δ* was formed by a deletion in *sep3-2* due to excision of the En-1 transposon. New alleles *sep1-3, sep2-3*, *sep2-4, sep4-2* are SALK T-DNA insertion lines. These lines were obtained from the Nottingham Arabidopsis Stock Centre (NASC). The details of these lines are listed in Table 2-3 and belowTable 2-4. The genotypes of all lines were confirmed by PCR (see section 2.3.3)

Table 2-3: Details of *sep* single mutants used in the present study

Sr. No.	Allele	Type	Location	Co-ordinates	Insertion line ID	NASC ID
1	*sep1-1*	T-DNA, DuPont	Intron	1354		
2	*sep1-2*	T-DNA, SALK	Exon	W/5151673-5151791	SALK_011077	N654065
3	*sep1-3*	T-DNA, SALK	Exon	W/5153719-5154077	SALK_121233	N663849
4	*sep2-1*	En1 transposon	Intron	1889		
5	*sep2-2*	GABI-KAT	3'-UTR	C/464135-464383	246B03	N423535
6	*sep2-3*	T-DNA, SALK	Exon	C/465655-465655	SALK_099222	N599222
7	*sep2-4*	T-DNA, SALK	Intron	W/466145-466145	SALKseq_138299	N638299
8	*sep3-2*	En1 transposon	Exon	48		
9	*sep4-1*	T-DNA, Wisconsin	Intron	307		
10	*sep4-2*	T-DNA, SALK	Intron	319	SALK_006229	N506229

Table 2-4: Details of *sep* double mutants used in the present study

Sr. No.	Double mutant	Alleles	Zygosity
1	*sep1 sep2*$^{+/-}$	*sep1-1, sep2-1*	Homozygous for *sep1-1*, heterozygous for *sep2-1*
2	*sep1 sep2*	*sep1-1, sep2-1*	Homozygous
3	*sep1sep3*	*sep1-1, sep3-2*	Homozygous
4	*sep1sep4*	*sep1-1, sep4-2*	Homozygous
5	*sep2sep3*	*sep2-1, sep3-2*	Homozygous
6	*sep2sep4*	*sep2-1, sep4-2*	Homozygous
7	*sep3sep4*	*sep3-2, sep4-2*	Homozygous

2.2.2 Plant growth conditions

2.2.2.1 Growth chamber and glasshouse

A. thaliana seeds were sown in 5 X 4 X 5 cm seed tray inserts containing a compost mixture. The pots were incubated at 22°C under short day conditions (8h/16h light/dark), with 65% relative humidity. Seedlings were re-potted after germination such that each pot had one seedling. Plants were transferred to long day conditions (16h/8h light/dark) 7 days post germination (dpi), with either constant temperature (22°C) or temperature varying between 16 to 28°C. For varying temperature condition, the temperature gradually increased from 16°C at 9:00 hours to reach a maximum of 28°C at 15:00. The temperature gradually decreased again to 16°C by next morning 9:00 hours, to complete a cycle of 24 hours (Figure 2.1). This program was designed to mimic naturally occurring temperature changes throughout a day in summers. Similar potting and germination methods were used while growing plants in a glasshouse.

2.2.2.2 Surface sterilization and in vitro cultivation

A. thaliana seeds were surface sterilized by incubating in a 30% sodium hypochlorite solution for 10 minutes. After removing the bleach, seeds were incubated in 70% ethanol for 30 seconds and then washed three times with sterile distilled water. Alternatively, a vapour-phase sterilization method was used. Less than ~100 seeds were placed in sterile tubes on a rack. The rack was then placed in a desiccator jar in a fume hood, with a 250 mL beaker containing 100 mL of 30 % (v/v) sodium hypochlorite. 3 mL of concentrated HCl was added to the beaker and the desiccator jar was sealed immediately. Sterilization by chlorine fumes was allowed to proceed for 3 to 4 hours.

The seeds were then suspended in top agar (0.1 % agar) and were plated on 1/2 MS Agar plates (1.1 g/l MS, 0.8 % Agar, pH 5.8) using a micropipette. The plates were sealed with micropore tape and incubated for 7-14 days at 20°C and 16/8 hours day /night.

2.2.3 Crossing

All siliques and mature flowers from a branch of the acceptor plant were removed, along with very young buds. Closed flowers with non-dehisced pollen were selected for emasculation. All petals and anthers on the acceptor flower were removed using a pair of fine forceps. The stigma of the carpels was pollinated with pollen from the donor

plant. The crossed flower was marked, and the plants were allowed to grow until the siliques matured. Seeds from these crosses were sown to obtain F1 plants.

2.2.4 Phenotyping

The plants were observed for their growth rate and flowering time according to the Biologische Bundesanstalt, Bundessortenamt und Chemische Industrie (BBCH) scale (Meier et al, 2001). Growth rate was measured by counting the number of rosette leaves after every two days. Flowering time was recorded as days to bolting.

2.2.4.1 Flower phenotype

Open flowers on the main stem of *sep* mutant and control plants were chosen for phenotypic studies. The first four flowers on the main stem were excluded from the analysis. The flowers were characterized with respect to (i) number of floral organs in each whorl, and (ii) arrangement of *sep*als. Arabidopsis Col-0 produces two to three open flowers over a period of one day. Six open flowers each were harvested from four biological replicates and were preserved in 70% ethanol. The flowers were dissected using a fine pair of forceps and scalpel under a dissecting microscope. The number of *sep*als, petals, stamens and carpel was manually counted and recorded. In order to study the arrangement of floral organs in *sep* mutants, open flowers were harvested and mounted on a petri dish containing agar. A pinch of bromophenol blue was added to the agar to improve contrast for imaging. Keyence microscope (VHX-7000) was used to observe the flowers at 50X magnification. The 'Depth composition and 3D' setting was used to obtain Z-stacks that produced a high-resolution image wherein all parts of the flower were in focus. The resulting images were used to measure the angle between adjacent petals in ImageJ (v1.52a). The carpel was denoted as the centre of a circle. The centre and the farthest point on the petal were joined to form the median of the petal. Angle between adjacent petals was recorded using the built-in measure function. Four angles were per flower were measured and the quality of measurement was checked to make sure that the sum total of all four angles equalled 360º.

2.2.4.2 Characterization of siliques and seeds

Similar to flower production, Arabidopsis main stem produces two to three mature siliques over a period of 24 hours. Six fully elongated, mature siliques (greenish brown in colour) were collected from the main stem of four biological replicates (n=24). Individual siliques were places in 1.5 mL microfuge tubes and dried at 60°C for 48

hours. When the siliques were completely dry, a pair of forceps was used to gently open the silique. The outer shell was placed on a glass slide with double-sided tape. Silique length was determined by imaging these siliques by using the Keyence microscope and using ImageJ to measure the length. The seeds from the microfuge tube were tapped on a clear white paper and the number of seeds was counted. This data was used to calculate the number of seeds/silique.

2.2.5 Plant Transformation

2.2.5.1 Floral dipping

Plants were transformed by using the "floral dip" method (Clough and Bent, 1998). Approximately 8 plants of each genotype were grown in pots. The main stems were cut 10 days prior to transformation to increase the number of side shoots. Two days prior transformation, positive Agrobacterium colonies (see section 2.3.6) were spread on YEB plates with appropriate antibiotics and incubated at 28°C for 48 hours, to obtain a lawn growth. The bacterial lawn was scraped off the plate and suspended in 20 mL of YEB broth. This suspension was added to 130 mL of sucrose solution (5%) with Silwet L-77 (0.05 %) before dipping the plants. Plants were dipped in this solution for about 30 seconds, such that all the young buds were coated with the solution. The pots were sealed with plastic sleeves to maintain humidity, placed horizontally in a tray, and kept in dark for 24 hours. Next day, the plastic sleeves were opened and the plants were allowed to grow under glasshouse conditions.

2.2.5.2 Transformant selection

T0 seeds were sown in compost on a 30 x 22 cm tray and grown at 22°C, 16 hour light photoperiod. 4 days post germination, the seedlings were sprayed with a solution of 120 mg Basta (glufosinate ammonium) in 1 Litre water, with 500 µL Silwet L-77. Basta treatment was repeated every 3 days until non-transformed plants showed yellowing of cotyledons. Maximum three treatments were performed. The surviving seedlings were transferred to new pots. These T1 plants were genotyped to confirm their background, the presence of transgene (see section 2.3.3) and were observed under confocal microscopy to confirm the expression of GFP (see section 2.4.2).

2.3 Molecular methods

2.3.1 DNA extraction

A small amount of plant tissue was put in a 1.5 mL microfuge tube and ground to fine powder using liquid nitrogen and microfuge pestle. 300 µL extraction buffer (200 mM Tris-HCl, 250 mM NaCl, 25 mM EDTA and 0.5 % SDS, pH 7.5) was added and centrifuged at 14000 rpm for 2 minutes. 250 µL supernatant was transferred to a new microfuge tube containing equal volumes of isopropanol, inverted 5 times and centrifuged for 5 minutes at 14000 rpm. The supernatant was removed and the pellet washed in 1 mL 70 % ethanol. The pellet was air-dried and suspended in 400 µL of TE buffer (10 mM TRIS-HCL, pH 7.6, 1 mM EDTA, pH 8). The prepared genomic DNA was stored at – 20° C and used for PCR based genotyping.

2.3.2 Plasmid DNA extraction

Bacterial culture was inoculated in 5 mL of Luria Bertani broth and was grown overnight at 37° C. 3 mL of the culture was centrifuged at 10,000 x g for 1 min and the supernatant was discarded. Plasmid DNA was isolated by using the QIAprep Miniprep Kit (Qiagen) according to the manufacturer's protocol. The obtained plasmid DNA was suspended in ~45 µL of elution buffer.

2.3.3 Genotyping

The genotype of the mutants was confirmed by performing PCR to amplify the insertion. PCR for the wild type allele was performed to determine whether the mutant was homozygous or heterozygous.

2.3.3.1 Primer design

Genotyping primers for SALK insertion lines were designed by using the T-DNA primer Design tool [http://signal.salk.edu/tdnaprimers.2.html]. Border primers were selected as specified on the T-DNA Express website. Other primers were designed by using Primer3Plus [https://www.bioinformatics.nl/cgi-bin/primer3plus/primer3plus.cgi/] (Untergasser et al, 2007).

2.3.3.2 Polymerase chain reaction (PCR)

In order to genotype mutants, two PCR reactions were set up (i) to confirm the presence of insertion (gene specific forward/reverse primer + border primer) and (ii) to determine zygosity of the mutant (gene specific forward primer + reverse primer). The reaction

components are shown in Table 2-5. The cycling conditions were run as per recommended by GoTaq® Green MasterMix (Promega) manufacturers (Table 2-6).

Table 2-5: Components of a PCR reaction set up using GoTaq® Green MasterMix

Component	Volume
GoTaq (2X)	10 µL
Forward primer	1 µL
Reverse primer	1 µL
Genomic DNA	1 µL
Nuclease free water	7 µL

Table 2-6: PCR thermal cycling conditions for genotyping *sep* mutants

Step	Temperature	Time	No. of Cycles
Initial denaturation	95°C	30 sec	
Denaturation	95°C	30 sec	35X
Annealing	55°C	30 sec	
Extension	72°C	1 min	
Final extension	72°C	5 min	
Hold	4°C	∞	

2.3.3.3 Agarose gel electrophoresis

Gels were made containing either 1 % (w/v) or 2 % (w/v) agarose and 0.05 µL/mL SYBR green in 1X TAE buffer. Electrophoresis was performed in 1X TAE buffer at 100 V until the reference dye reached the bottom of the gel. Separated DNA bands were visualised using Syngene gel documentation system

2.3.4 GreenGate Cloning

2.3.4.1 Primer design

Forward and reverse primers were designed such that they spanned 12-15 nt sequence specific to *SEP1-4* promoters, genes and terminators. The nucleotides 5'-AACA-GGTCTC-A-NNNN (nn)-3' were added to the forward primer in front of the gene specific sequence and to the reverse primer followed by the reverse complement of the specific sequence. GGTCTC represents the *Bsa*I recognition site, AACA was added because the enzyme does not cut if the restriction site is at the extreme ends of PCR products. NNNN represents overhang specific to the entry vectors. 2 additional

nucleotides (nn) were added in case of the coding sequence to bring the modules into frame (NNN represents an in-frame coding triplet in the overhangs). The primer sequences are enlisted in Table S1

2.3.4.2 PCR

The promoter region, gene and terminator of *SEP1* and *SEP2* were amplified by using Phusion® High-Fidelity DNA Polymerase (NEB). 50 ng of Col-0 DNA was mixed on ice with 10 µL of 5X Phusion buffer (containing $MgCl_2$), along with dNTPs to a final concentration of 0.2 mM. Primers were added to the final concentration of 0.5 µM and 1 unit of Phusion polymerase was added. The total volume was made up to 50 µL with sterile water. Samples were initially denatured for 2 min by incubating at 98˚C followed by 30 cycles of denaturation (30 sec at 98˚C), annealing (30 sec at 55-60˚C) and extension (2.5 min at 72˚C). A final 10 min extension step was performed at 72˚C.

2.3.4.3 Cloning

After amplification, the PCR reactions were run on 1% agarose gels, and the appropriate band was excised and purified by using the QIAquick Gel Extraction Kit (Qiagen). The purified PCR product and the respective empty entry modules (~100 ng) were mixed and digested with BsaI (37°C, 1 h). The restriction enzyme was inactivated by incubating at 65°C for 5 minutes. The digested products were ligated with T4 DNA ligase at room temperature, 5 minutes (Quick Ligation kit, NEB) and the ligase was heat-inactivated (65°C, 5 min). 5 µL of the ligated product was mixed with 25 µL of competent ccdB sensitive *E.coli* DH5α cells and were kept on ice for 20 minutes. The cells were heat shocked at (42°C, 90 seconds). 1 mL of LB broth was added, and the cells were recovered at 37°C for 1 h. Cells were then plated on LB agar containing appropriate antibiotic (100 µg/mL ampicillin) and incubated at 37˚C overnight to allow bacterial colonies to grow.

2.3.4.4 Colony PCR

Colony PCR was performed to screen for positive transformants. A colony was picked from the plate, suspended in 20 µL of sterile water and denatured at 95°C for 10 minutes. The lysed colony was used as a template along with M13_F and SP6 primers in a GoTaq master mix. PCR cycling conditions were similar to those mentioned earlier. The PCR products were checked by agarose gel electrophoresis. Positive colonies were

inoculated in LB broth and were incubated overnight at 37. Plasmid DNA was extracted from these overnight grown cultures as mentioned in section 2.3.2.

2.3.4.5 Glycerol stock preparation

For cultures that were tested positive in colony PCR, 1 mL of overnight grown culture was added to a sterile 2 mL microcentrifuge tube. Sterile 80 % glycerol was added to this and the tube was gently inverted 4-6 times, flash frozen in liquid nitrogen and was stored at -80° C until further use.

2.3.4.6 GreenGate assembly

The GreenGate reaction was performed by mixing 1.5 µL plasmid of each of the six modules were mixed with 1 µL of the destination vector (pGGZ001), 1.5 µL T4 DNA ligase buffer, 1 µL T4 DNA ligase (30 µg/mL) and 1 µL FastDigest Eco31I in a total volume of 15 µL. 30 cycles of 37°C for 2 minutes and 16°C for 2 minutes each, followed by 50°C for 5 minutes and 80°C for 5 minutes. 6 µL of the reaction were used for heat-shock transformation of *E. coli* DH5α cells. $1/10^{th}$ dilutions were plated on LB Agar with spectinomycin (50 µg/mL) for selection. Positive colonies were screened by colony PCR by using multiple primers spanning the whole construct.

2.3.5 Cloning and genotyping of CRISPR-Cas9 constructs

CRISPR-Cas9 mediated gene knock-down was used to validate the function of downregulated targets of SEP1 and SEP2. pEnChimera and pDeCas9 vectors were provided by Dr. Chris West along with technical knowhow about the cloning strategy.

2.3.5.1 sgRNA design

A single guide RNA (sgRNA) was designed for each target gene by using the CCTop tool [https://crispr.cos.uni-heidelberg.de/] (Stemmer et al, 2015). The sgRNA protospacer was 20 nt long with an NGG protospacer adjacent motif (PAM) at the 3' end. The total GC content of the sgRNA was between 45-60%. The core region spanned 12 nt, with the maximum number of total mismatches limited to <4. It was confirmed that the sgRNA did not have any off-targets in Arabidopsis by using the CCTop off-target prediction tool (Labuhn et al, 2017) as well as by running BLAST search on the TDNA Express website. A 5'ATTG overhang was added to the protospacer, while a 5'AAAC overhang was added to the protospacer reverse complement, and there were ordered as oligos from Integrated DNA Technologies.

2.3.5.2 Cloning in pEnChimera

In order to anneal the protospacer oligonucleotide to its reverse complement oligonucleotide, 2 µL of each 100 µM oligo was added to 46 µL of water and incubated at 95°C for 5 min. The reaction was cooled at room temperature for 20 min. pEn-Chimera was restrict digested using BbsI, by incubating the reaction components shown in Table 2-7 at 37°C for 1 hour. The digested product was run on 0.8% gel at 70 V such that the digested and undigested plasmid bands were *sep*arated. The band corresponding to the digested plasmid was gel extracted and purified using Qiagen Gel Extraction kit.

2 µL of digested pEn-Chimera, 3 µL of annealed oligos, 1 µL of T4 ligase and 5 µL of Quick Ligase buffer were gently mixed together and incubated at RT for 5 min, in order to ligate the annealed oligos within the pEn-Chimera vector. 5 µL of the ligation mixture was used to transform *E. coli* DH5α cells with a selection of Ampicillin (100 µg/mL). A colony PCR using ChiSeq_F primer with the reverse protospacer oligo (annealing temperature 56°C, elongation 30 sec, 30 cycles) was performed to identify positive colonies. The expected band size was 370 bp. A positive colony was inoculated in 5 mL LB broth and grown overnight at 37°C, 200 rpm. The culture was used to miniprep the pEnChimera-sgRNA plasmid. The plasmid was sequenced using ChiSeq_F primer to confirm that the sgRNA had integrated at the correct site.

Table 2-7: Composition of reaction for restriction digestion of pEn-Chimera

Component	Volume
pEn-Chimera	10 µL
10X NEB Buffer	2 µL
BbsI	1 µL
Nuclease free water	7 µL

2.3.5.3 Gateway cloning in pDeCas9

A Gateway LR reaction was set up as described in Table 2-8 to integrate the sgRNA in pDeCas9. The microfuge tube was vortexed to mix all components, briefly centrifuged and incubated at room temperature for 2 hours. 1 µL of Proteinase-K was added to the reaction and it was incubated at 37 for 10 min. 10 µL of this reaction was used to transform *E. coli* DH5α cells as described previously, with a selection of Spectinomycin (50 µg/mL). The transformation efficiency should be 100% at this step; however, a colony PCR was performed with primers SS42 and protospacer forward oligo

(annealing temperature 60°C, elongation 1 min, 35 cycles), with an expected band size of 1070 bp. A positive colony was inoculated in 5 mL LB broth and grown overnight at 37°C, 200 rpm. The culture was used to miniprep the pDeCas9-sgRNA plasmid. The plasmid was sequenced using SS42 primer to confirm the presence of sgRNA and Cas9. This vector was used to transform Agrobacterium.

Table 2-8: Composition of Gateway reaction to clone sgRNA in pDeCas9

Component	Volume
pEn-Chimera-sgRNA	2 µL
pDeCas9	3 µL
TE Buffer (pH 8)	4 µL
LR Clonase II	1 µL

2.3.5.4 Genotyping of transformants by high-resolution melt curve analysis

Genomic DNA from T1 plants was extracted as described previously. Primers flanking the edited size were designed to produce an amplicon size of 80-120 bp, Tm at 58 ± 2ºC and GC% not exceeding 65 % (Laurie and George, 2009). For HRM analysis, the PCR mix was prepared as shown in Table 2-9. The cycling conditions were as shown in Table 2-10. The melt curve was obtained on BioRad qPCR machine and was analysed using the LightScanner software.

Table 2-9: PCR components for high-resolution melt cure analysis

Component	Volume
Precision Melt Supermix, BioRad (2X)	5 µL
Forward primer	0.5 µL
Reverse primer	0.5 µL
Genomic DNA	4 µL
Total Volume	10 µL

Table 2-10: PCR cycling conditions for high-resolution melt curve analysis

Step	Temperature	Time	No. of Cycles
Initial denaturation	95°C	5 sec	
Denaturation	95°C	5 sec	40X
Annealing	55°C	5 sec	
Extension	72°C	30 sec	
Melt curve start	94°C	30 sec	
Melt cure end	25°C	30 sec	
Hold	4°C	∞	

2.3.6 Agrobacterium transformation

To transform the plasmid containing the assembled vector in Agrobacterium, 1 µL of plasmid was mixed with 50 µL of *Agrobacterium tumefaciens* GV3101 competent cells and incubated on ice for 20 minutes. The mixture was transferred to pre-chilled electroporation cuvettes such that it was in contact with both the electrodes. The cells were electroporated by applying a pulse of 18 kV/cm. Immediately, 1 mL of LB broth was added to the cells and they were recovered for 3 hours at 28°C. The cells were plated on YEB agar containing rifampicin (10 µg/mL), gentamycin (30 µg/mL) and spectinomycin (50 µg/mL). The plates were incubated at 28°C for 48 h. Colony PCR was performed as mentioned earlier to identify positive clones.

2.3.7 RNA extraction

Fresh floral meristem and buds were harvested from plants right after bolting. Open flowers were removed by using a pair of fine forceps. The tissue was frozen in liquid nitrogen and stored at -80° C until further use. Total RNA was extracted by using NucleoSpin RNA extraction kit (Macherey-Nagel) according to manufacturer's protocol. The RNA was quantified using NanoDrop and the quality of RNA was checked by performing agarose gel electrophoresis. Extracted RNA was stored at -80°C.

2.3.8 cDNA synthesis and qPCR

cDNA was synthesized by using the FirstStrand cDNA synthesis kit (Thermo Fischer scientific). A mixture1 was prepared as mentioned in Table 2-11 and the volume was made up to 12 µL with nuclease free water. Mixture 1 was incubated at 65°C for 5

minutes. Mixture 2 containing the reverse transcriptase was added, mixed well and incubated at 42°C for 50 minutes, followed by 70°C for 15 minutes to inactivate the enzyme. The synthesized cDNA was diluted 5000 times using nuclease free water and used as a template for qPCR. Quantitative Real-time PCR (qPCR) was performed on an Opticon continuous fluorescence detection system (C1000 Thermal Cycler, Biorad) using the IQ SYBR Green Supermix (Biorad). Reactions were performed in a total volume of 50 µL as shown in Table 2-12 and the cycling programme was used according to the manufacturer's instructions (Table 2-13). Gene expression was calculated relative to TIP1.4 reference gene using the standard curve method.

Table 2-11: Composition of reaction used for cDNA synthesis

Mixture 1	
Oligo(dT)	1 µL
Random primers	1 µL
RNA (500 ng)	
dNTP	1 µL
Total volume	12 µL
Mixture 2	
First strand buffer	4 µL
0.1 mM DTT	2 µL
SSII	1 µL
Total volume	7 µL

Table 2-12: Components of a qPCR reaction

PreMix	**5 µL**
Forward primer	0.01 µL
Reverse primer	0.01 µL
cDNA	45 µL (1:5000 dilution)

Table 2-13: Thermal cycling conditions for qPCR and melt curve analysis

Polymerase activation and DNA denaturation at	**95°C**	**3 min**	
Denaturation	95°C	10 sec	40 cycles
Annealing	60°C	30 sec	
Melt Curve Analysis	55°C – 95°C, 0.5°C increment 2-5 sec. / step		

2.4 Microscopy

2.4.1 Light microscopy

Keyence microscope (specifications) was used to record all images. The images were modified or analysed by using ImageJ (v1.52a).

2.4.2 Confocal microscopy

Confocal microscopy was used to study the floral meristem architecture and the expression of GFP, as described by Prunet (2017). Meristems from freshly bolted plants were harvested and mounted on 2% agarose in a 50mm X 15mm petri dish. All open flowers and big buds were removed using forceps. The buds were removed until a bright green meristem was spotted under the dissecting microscope. The samples were stained with 20 µL of 1 mg/mL propidium iodide (PI) solution for 2 min. The samples were rinsed twice with sterile deionized water. A Zeiss LSM880 with Airyscan Inverted Microscope with a 40X water immersion lens (specifications) was used to image the meristem and buds. The imaging dish was placed upside down on the microscope stage. A drop of sterile deionized water was placed on the lens, and the stage was lowered until the sample touched the water drop on the lens to form a water coloumn. Fixed imaging parameters were adjusted according to different samples. However, the pinhole was always set to 1 airy unit and the XY resolution was 512 X 512. The Z resolution was altered according to the size if the sample. The excitation wavelength for PI was 488nm and detected in the range 566 to 630 nm. The images were saved in CZI format and were edited and analysed using FIJI-ImageJ(v1.52i). The final images were exported in TIFF and JPEG format.

2.4.3 Scanning electron microscopy

Scanning electron microscopy (SEM) was used to obtain detailed images of floral buds and meristems. Samples were fixed in paraformaldehyde according to Franks (1963) and critical point dried with help from Mr. Martin Fuller, Astbury Biostructure Laboratory. Fixed meristems were imaged on a FEI Nova NanoSEM450 with help from Dr Stuart Micklethwaite at Leeds Electron Microscopy And Spectroscopy Centre (LEMAS), University of Leeds.

2.5 Bioinformatics methods

2.5.1 RNAseq sample preparation and sequence analysis

Global RNA expression levels in three biological replicates of *sep1-1 and sep2-1* mutants, grown under stable temperature and screenhouse conditions, were measured via high-throughput next generation Illumina sequencing. Three dissected meristems were pooled for one biological replicate. Three biological replicates each of Col-0 grown under stable and natural environmental conditions were used as control. Library preparation and sequencing services were provided by the Next Generation Sequencing Facility, University of Leeds. FastQ files obtained from sequencing the libraries were run through the FastQC software to ensure good read quality (Andrews, 2010). Adapter sequence at the end of the reads was trimmed by using TrimGalore. The reads were aligned to the indexed Arabidopsis genome (v. TAIR 10) by using STAR aligner (Dobin et al, 2013). The Cufflinks and Cuffdiff packages were used to determine the number of reads mapped to each transcript and for differential expression analysis, where the expression of each gene from the *sep* mutant samples was normalized with respect to its expression in Col-0 (Trapnell et al, 2010). The data was visualized using CummeRbund(v3.8) package from R(v3.5.2) (Goff et al, 2019). The analysis was run on the High-Performance Computing (HPC) Facility at the University of Leeds to reduce processing time. Final output files comprising of Gene ID, number of reads, $\log_2$(fold change), P-value, and P_{adj}-value was generated for each biological replicate.

2.5.2 Other bioinformatics techniques

The following online databases were used to obtain information in this study (Table 2-14)

Table 2-14: Details of online databases and resources

Resource	Website	Reference
T-DNA express	http://signal-genet.salk.edu/Source/AtTOME_Data_Source.html	Alonso et al, 2003
Araport	https://bar.utoronto.ca/thalemine/begin.do	Krishnakumar et al, 2014
TAIR	https://www.arabidopsis.org/	Tanya et al, 2015
Gene Ontology	http://geneontology.org/	Mi et al, 2019
Clustal Omega	https://www.ebi.ac.uk/Tools/msa/clustalo/	Madeira et al, 2019
PlantPAN 3.0	http://plantpan.itps.ncku.edu.tw/	Chow et al, 2019
Arabidopsis EFP Browser	http://bar.utoronto.ca/efp2/Arabidopsis/Arabidopsis_eFPBrowser2.html	Winter et al, 2007
MEME Suite	https://meme-suite.org/meme/tools/meme	Bailey et al, 2009

3 Chapter 3: Evolution and Synteny of Arabidopsis *SEP* genes

3.1 Introduction

MADS-box genes play a central role in flower development. The origin of the MADS-box gene family is uncertain. However, the MADS-box genes can be found in extant fungi, animals, and plants, thus indicating that the last common ancestor of the eukaryotic taxa had at least one gene with a MADS-box more than 1 billion years ago (Theißen et al., 1996). The MADS-box gene family has since then grown through a series of gene duplications followed by functional diversification of the duplicated copies (Airoldi and Davies, 2012). In addition to the MADS-box, Type II genes constitute of Intervening, K-box, and C-terminal domains, forming the MIKC genes (Becker and Theissen, 2003). MIKC genes diverged into two subclasses, MIKC^c and MIKC*, in the ancestor of all land plants (Gramazow and Theissen, 2010). The MIKC^c genes can be further classified into 14 clades (*StMADS11, AGL17, AGL12, TM3, FLC, AGL6, AGL2/SEP, SQUA, AG, TM8, OsMADS32, DEF/GLO, GGM13, AGL15*), based on recent phylogenomic studies based on transcriptomic data from gymnosperms, basal and higher angiosperms (Chen et al, 2017). The AGL2/*SEP* clade constitutes E-activity specifying *SEPALLATA* genes that regulate flower development (Zhang et al, 2004; Chen et al, 2014; Gramzow and Theissen, 2010). *SEP* genes are essential for regulating flower development and specifying identity of floral organs. Therefore, the study of evolution and diversification of *SEPs* is expected to point towards important clues for understanding the morphological evolution of flowers.

SEP genes are angiosperm specific. The most basal angiosperms, Amborella, Magnolia, and Eschscholzia contain two *SEP* genes each. This indicates that the *SEP* family originated and underwent duplication before the diversification of extant angiosperms (Zahn et al., 2005). Unlike other several other homeotic genes, multiple copies of *SEPs* have been reported from plants belonging to other classes such as monocots, eudicots, rosids, and asterids (Christensen and Malcomber, 2012; Causier and Davies, 2014; Zhang et al., 2016). *SEPs* have four duplicate copies in the model plant *A. thaliana.* Although these copies have been reported to be functionally redundant (Pelaz et al., 2000a; Ditta et al., 2004), they have not been converted into pseudogenes or deleted

from the genome. It is difficult to explain the existence of four duplicated copies that show no functional divergence.

Arabidopsis thaliana has four duplicate *SEPs*, *SEP1-4*, that specify the E-function in flower development (Table 3-1) (Pelaz et al., 2000a; Malcomber and Kellogg, 2005). Amongst the four *SEPs* in *A. thaliana, SEP1 and SEP2* seem to be the product of a recent duplication (Ermolaeva et al., 2003). However, their relationship with *SEP3* and *SEP4* has been difficult to study. Early studies suggested that *SEP1* and *SEP2* have a closer association with *SEP3* as compared to that with *SEP4* (Yu and Goh, 2000; Ermolaeva et al., 2003). Other studies maintain that *SEP1*/2/4 form a Separate sub-clade from *SEP3* (Zahn et al, 2004). Additional sub-clades such as *LOFSEP* and FBP9/23 have been reported from monocots and rosids, respectively (Malcomber and Kellogg, 2005).

The most recent study on evolution and diversification of *SEP* genes was published ~ 15 years ago, making a newer look essential. The advent of Next Generation Sequenceing technology has made high quality whole genome sequence and transcriptome data available from several plants. Moreover, although the conservation of some MADS-box genes has been studied by synteny (Zhao et al., 2017), an approach specific to *SEP* genes is lacking. This chapter aims to identify *SEPALLATA* genes from plants belonging to all clades and conduct a phylogenetic analysis to understand their evolution and diversification.

Aims of studying the evolution and diversification of *SEP*ALLATA transcription factors:

1. To determine the sequence and structural features that distinguish *SEPs* from other MADS-box TFs
2. To study the phylogenetic relationship between At*SEPs* and their orthologs
3. To determine the conservation of *SEPs* throughout Angiosperms based on synteny analysis

3.2 Characteristics of *A. thaliana SEP*ALLATA genes

Arabidopsis thaliana has four duplicate *SEPALLATA* genes. These genes are located on different chromosomes (Table 3-1) and are possibly a product of a *sep*arate gene duplication events. The genes were classified and initially named as *AGAMOUS-LIKE (AGL)* based on sequence similarity to the homeotic gene *AGAMOUS* (*AG*). However, they were later named *SEPALLATA* due to the *sep*alloid flower phenotype of the *sep1 sep2sep3* mutant (Pelaz et al, 2001). *SEP1-4* proteins are approximately 250 to 258 amino acids (aa) long, with the MADS domain spanning from 3-57 aa and the K-box spanning from 88-178 aa (with the exception of *SEP3*, where the K-box is comprised of 91-191 aa) (UniProt). The MADS box and K-box predominantly form α-helical secondary structures with interspersed random coils and coiled-coils (Puranik et al., 2014). The K-box α-helices interact with each other to form homodimers and heteromeric complexes with other proteins (Yang, 2004).

Table 3-1:Details of chromosomal location, gene and protein length and domain structure of Arabidopsis *SEP* genes

Gene	Aliases	ID	Chromosomal location	Gene Length (bp)	Protein length (aa)	MADS (aa)	K-box (aa)
SEP1	*AGL2*	AT5G15800	Chr5: 5151334-5154253	2920	251	3-57	88-178
SEP2	*AGL4*	AT3G02310	Chr3: 464279-467151	2873	250	3-57	88-178
SEP3	*AGL9*	AT1G24260	Chr1: 8593536-8596123	2588	251	3-57	91-181
SEP4	*AGL3*	AT2G03710	Chr2: 1129229-1131838	2610	258	3-57	88-178

The Arabidopsis MADS-box is highly conserved (Figure 3-1 A). *SEP1* and *SEP3* MADS-boxes show 100 % identity while *SEP1* and *SEP2* show 96% identity with each other. Although the percent identity between *SEP2* and *SEP4* is the lowest, it still stands at 91 %. According to InterPro and ProSite, the secondary structure of the At*SEP* MADS-box constitutes of two α-helices, between residues 7 to 15 and 22 to 37, respectively. The At*SEP* K-box is less conserved as compared to the MADS box. *SEP1* and *SEP2* K-box sequences are 90 % identical, whereas the K-boxes from other At*SEPs* show 48 to 59% identity (Figure 3-1 B). The structure of the K-box is comprised of three amphipathic α-helices corresponding to K1, K2, and K3, that assemble into coiled coil structures (Yang, 2004). Helices α_1 and α_2 are joined by a coiled kink formed by

residues 112 to 120 LLGEDLGPL, conserved in *SEP1*, *SEP2* and *SEP3* (Figure 3-1 B). The kink region in *SEP4* varies, suggesting that the *SEP4* protein might adapt a different conformation. The C-terminal is the most variable region suggesting its role in functional divergence. This suggests that during the course of evolution each of these domains in *SEP* genes have acquired distinct functions. In order to understand how these domains have evolved through *SEP* genes in angiosperms, it was important to identify homologs from different species.

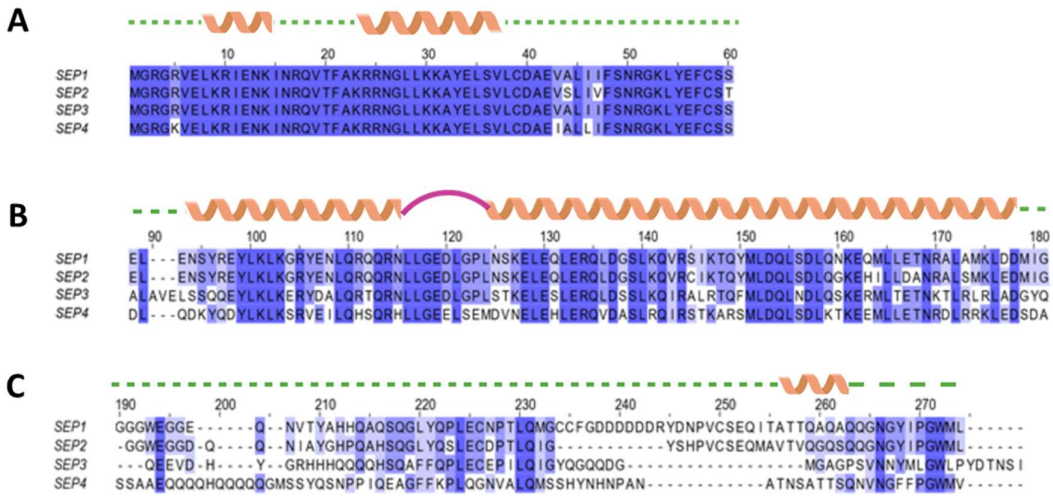

Figure 3-1: Alignment and secondary structure of Arabidopsis *SEPs*: CLUSTALx alignment of Arabidopsis *SEP1*, *SEP2*, *SEP3*, and *SEP4* amino acid sequences (A) Highly conserved MADS-box with two α-helical secondary structures (B) K-domain, showing two α-helices joined by a kink region (C) C-terminal with low sequence identity. The colour scheme corresponds to the standard CLUSTALx percentage identity scheme, with a threshold of 50 % identity, such that the darkest blue block denotes 100% identity while white block correspond to <50% identity. The protein secondary structure is shown by helices denoting α-helices and green dashed lines denoting random coils or β-sheets

3.2.1 **Distribution and Analysis of *SEP*ALLATA genes**

A comprehensive search for all *SEP* genes was performed against the Phytozome v13 database (Goodstein et al, 2012), such that a minimum of one plant species per family was included. BLASTP results were filtered to select sequences that showed a minimum of 200 similar nucleotides with the query sequences. A total of 145 protein sequences from 29 plant species belonging to basal angiosperms (1), Asterids (2), Rosid (2), Fabiaceae (3), Malphigiales (3), Malvales (2) Brassicaceae (6), other eudicot (1), and Monocots (8) were chosen. Analysis of the domain structure of these sequences by using Pfam and PROSITE (Bateman et al., 2004; Hulo et al., 2006) confirmed that the sequences contained SRF-like (MADS-box), K-box and two PROSITE domains MADS_box_1, MADS_box_2, corresponding to the MADS-box, thereby verifying that they belonged to MIKC^c class (Figure 3-2 A). The signature sequences of these motifs were scanned by using the MEME suite. Motif 1 corresponded to the MADS-box, while motifs 2, 3, and 4 corresponded to K1, K2 and K3 subdomains, respectively. (Figure 3-2 B). It was confirmed that the domains followed the order M, I, K, and C. Figure 3-2 C shows an example of motif distribution across the protein sequence. This step filtered out other MADS-box or MIKC* genes that could have been incorrectly picked up on the basis of high percentage identity. Six sequences were discarded as they showed erroneous order of motifs when analysed using MEME suite. Thus, a database of 139 protein sequences was used for further analysis.

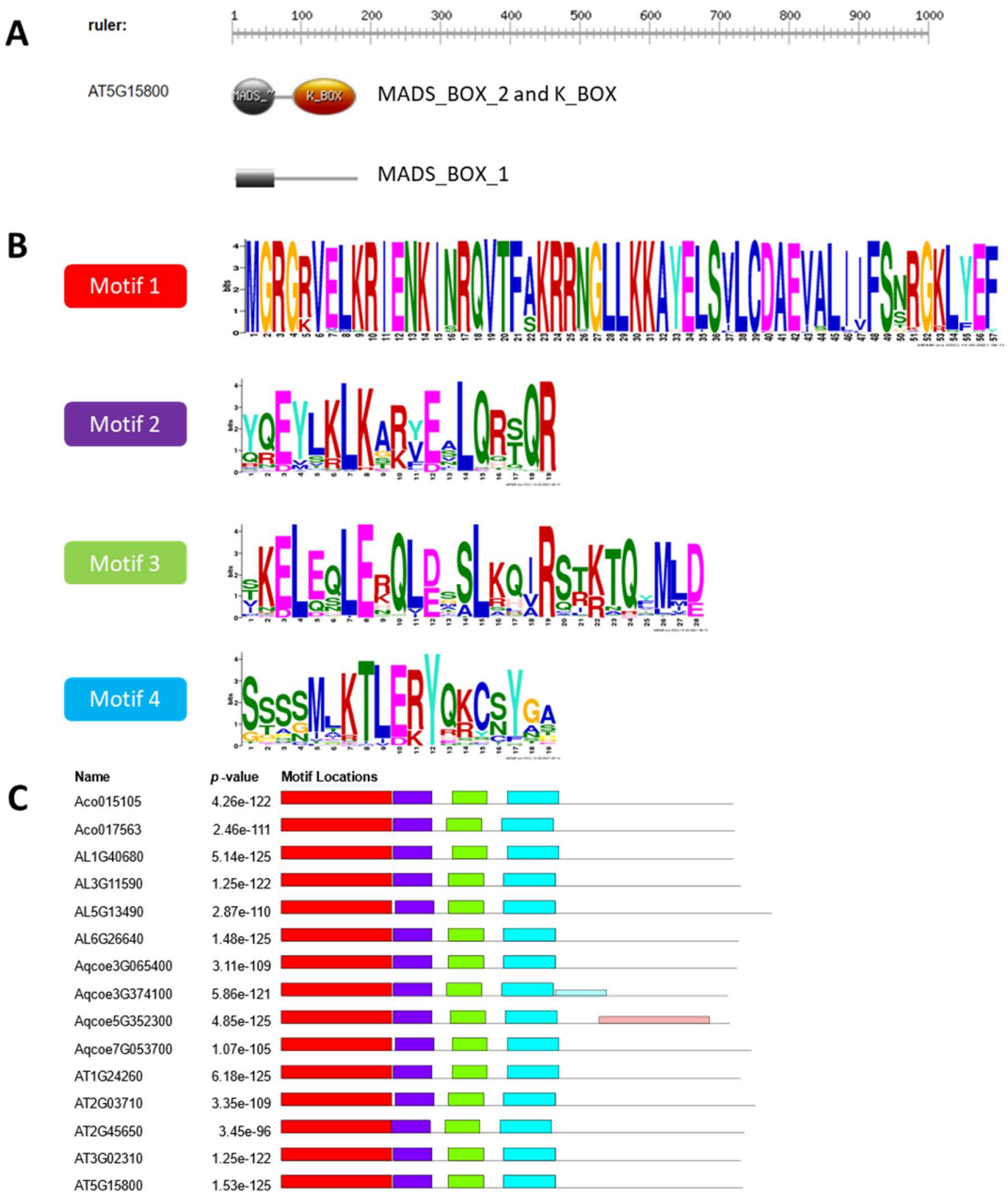

Figure 3-2: Conserved motifs in homologs of Arabidopsis *SEP* genes. (A) Identification of conserved motifs, MADS_box_1, MADS_box-2, and K-box in *SEP* homologs by using PROSITE. (B) Identification of ungapped motif patterns in *SEP* homologs by using MEME Suite (C) Distribution of motifs 1-4 along *SEP* homolog sequences, determined by using MEME suite. Accessions of homologues correspond to A. thaliana (AT), A. lyrate (AL), and Aquilegia coerulea (Aqcoe)

3.2.2 Alignment and Sequence Features of *SEP* homologs

3.3 Identification of conserved motifs from the K-domain

The developmental and functional versatility of *SEPs* might depend upon the specific features of their domains. A close look at the alignment of *SEP* genes across species might point to sequence features that either contribute to high conservation or functional diversity. The analysis of sequence features and alignment of *SEPs* genes in this section aims to identify conserved motifs signatures for each *SEP* subclade. CLUSTALX alignment of the selected 139 *SEP* sequences showed that the MADS domain was the most conserved across all species. The K domain was found to be the next highly conserved domain. The amino acid alignment of K-domain sequences showed that the sequence corresponding to helices α1 and α2 was highly conserved, along with LLGEDL residues that form the kink region that joins both the helices (Figure 3-3). The secondary structure comprises of three alpha-helices corresponding to the K1, K2 and K3 subdomains. Additionally, certain motifs were found to be specific to either SEP1/2 or SEP3. The At*SEP3* and other *SEP3* like proteins contain the RLMEG motif that was absent in other *SEPs* (shown in pink, Figure 3-3). Similarly, the motif KLDEMIGV was specific to *SEP1*/2 sequences from the Brassicaceae plants (shown in cyan, Figure 3-3). These signature motifs can aid in classification of newly identified *SEPs* from different species into SEP1/2 or SEP3 subclades. Additionally, these motifs can also be assessed in studies that aim to associate functions of different *SEPs* to their sequence. The heptad position 'g' was found to be occupied by lysine (K) and arginine (R) in these *SEP3* and *SEP1*/2 motifs respectively. This is concurrent with the report that positions 'e' and 'g' are generally occupied by polar or charged residues that are important for specificity of protein-protein interaction (Popatov et al, 2015).

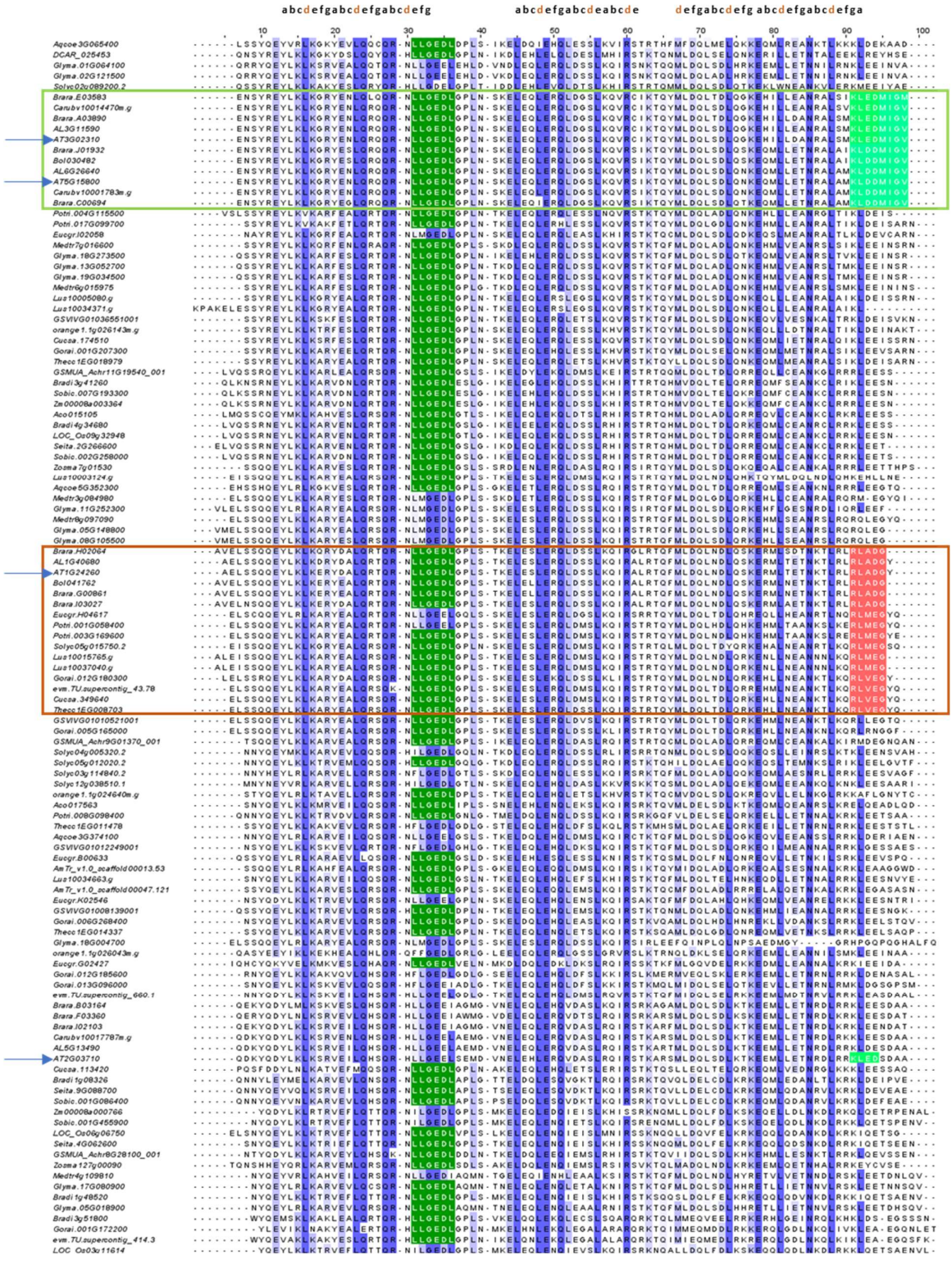

Figure 3-3: Multiple sequence alignment of K-domain from all identified *SEP* homologs. The sequence alignment was performed by using CLUSTALx algorithm and

viewed using JalView percentage identity colour scheme (threshold – 50 % identity). The conserved kink region LLGEDL is highlighted in green. The $[abcdefg]_n$ heptad repeat is denoted at the top of the alignment. The Arabidopsis *SEP* genes are indicated by a blue arrow on the left side of the panel. Coloured boxes show signature sequences for *SEP1*/2 sub-family in Brassicacea (cyan), and *SEP3* subfamily (pink).

3.4 Identification of conserved motifs from the C-domain

The C-domain has the most variable sequence in MIKC proteins. The alignment of *SEP* C-terminal regions showed very low overall identity; however, two relatively conserved *SEP* motifs, motif-I and motif-II were identified (Figure 3-4). These motifs are similar to the AG-I and AG-II motifs and the *SEP*-I and *SEP*-II motifs reported by Zahn et al (2004). However, these generic motifs account for smaller patterns that could be seen only in a few sequences. This warranted for a motif identification search by using the MEME Suite (Bailey et al., 2015), resulting in identification of five motifs (Figure 3-5). Motifs C1 (red) and C2 (green) were found to overlap with the *SEP*- motif I, while motif 4 (blue) corresponded to *SEP*-II described by (Zahn et al., 2005) (Figure 3-5). However, motifs 3 (purple) and 5 (yellow) were newly identified (Figure 3-5). In addition to these motifs, 4-5 signature amino acids, specific to a *SEP1/2*, *SEP3*, and *SEP4* sub-clades were found. The At*SEP3* subfamily showed a signature motif LNQL (highlighted in green, Figure 3-4) which was not found in other *SEPs*. The *SEP1*/2 subfamily exhibited residues R(S/H)HH (Figure 3-5) adjacent to motif 3. *SEP4* subfamily genes were specified by the characteristic Q stretches in the C-terminus (Figure 3-4).

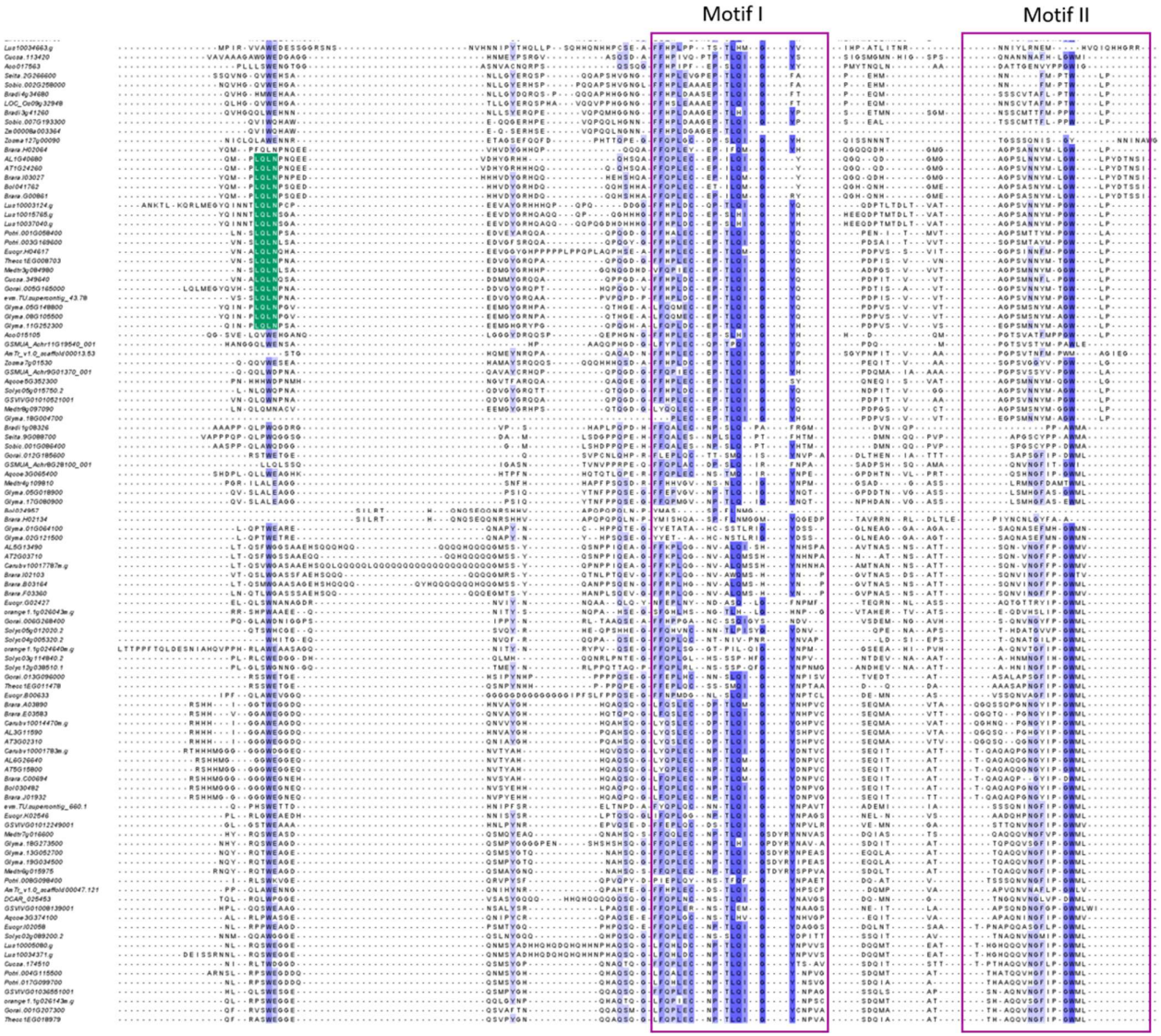
Motif I
Motif II

Figure 3-4: Multiple sequence alignment of the C-terminal region of *SEP* homologs. The C-domain is the least conserved among the M, I, K and C domains. The *SEP3* homologs have a conserved LQLN motif at the beginning of the C-terminus. The homologs show two conserved motifs, i.e., motif I and motif II shown within boxes. Evolution and Divergence of *SEP*ALLATA genes

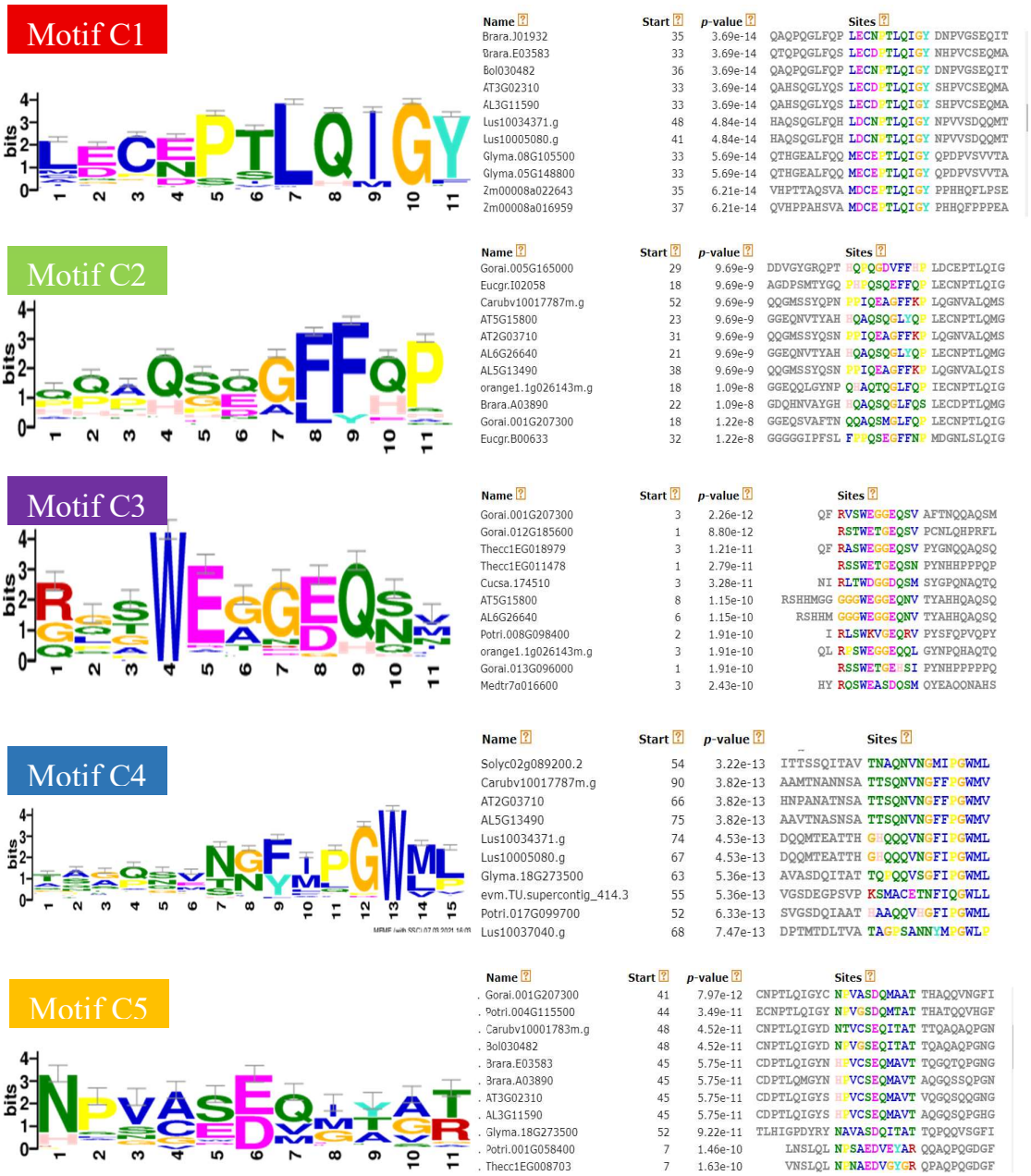

Figure 3-5: Motifs in the C-terminal identified by using MEME Suite. Each motif is represented by its consensus sequence logo and example of pattern identified in a few sequences. The colour of the label corresponds to the motif colour in figures 3.7 and 3.8

3.5 Phylogenetic analysis of *SEP* homologs

In order to determine the phylogenetic relationship and evolutionary origin of *SEPs*, the CLUSTALX alignment of the full amino acid sequence corresponding to the above 145 sequences was used to construct a phylogenetic tree. The *SEPs* formed clear clades, viz., *SEP3* (AGL9) and the *LOFSEP-SEP4-SEP1*/*SEP2* (*AGL2/3/4*) (Figure 3-6). *SEP* genes are angiosperm specific. The earliest extant angiosperm *Amborella trichopoda* contains two *SEPs*. This shows that *SEPs* originated and underwent duplication in the ancestor of extant angiosperms. One Amborella *SEP* coincides with the *SEP3* clade while the other branches at the base of *SEP1*/2/4 clades. This suggests that the two Amborella *SEPs* evolved *sep*arately to give rise to these clades.

Three *SEP* homologues were identified from *Aquilegia coerulea L.,* (Ranunculaceae), a lower eudicot that is sequenced, assembled, and well annotated. The gene Aqcoe5G352300 was found in the *SEP3* clade. The other two *SEP*s, Aqcoe3G065400 and Aqcoe3G374100 were in the *SEP4* clade. Thus, a duplication within the *SEP1/2/4* clade took place before the evolution of eudicots. *SEP* families from two lower Rosid species, *Eucalyptus grandis* and *Vitis vinifera* showed four *SEP* genes each which were distributed in *SEP3* (Eucgr.H04617, GSVIVG01010521001), *SEP4* (Eucgr.G02427, GSVIVG01012249001), and *SEP1/2* (Eucgr.K02546, Eucgr.B00633, GSVIVG01008139001, and GSVIVG01036551001) clades (Figure 3-6). This suggests that the diversification of *SEP1/2* and *SEP4* clades took place sometime after the diversification of eudicots but before the diversification of rosids.

Although *SEP* families from most higher eudicot species used in this analysis show multiple copies of *SEPs* in the *SEP1/2* sub-clade, they do not necessarily form fall within *sep*arate *SEP1* or *SEP2* sub-clades. Only genes from Brassicaceae showed clear distinction between *SEP1* and *SEP2* sub-clades (shown in orange, Figure 3-6). The *SEP1* sub-clade included genes Brara.J01932, Brara.C00694 (*B. rapa*), Carubv10001783 (*C. rubella*), and AL6G26640 (*A. lyrata*). Whereas the SEP2 sub-clade included Brara.A03890, Brara.E03583 (*B. rapa*), Carubv10014470 (*C. rubella*), and AL3G11590 (*A. lyrata*). This suggests that the duplication leading to the emergence of *SEP1* and *SEP2* was recent and restricted to the Brassicaceae.

SEP genes from the monocots are *sep*arated in *SEP3* and *SEP1/2/4* clades. The basal monocot *Acorus americanus* showed two *SEP* genes, Aco015105, in the SEP3 sub-

clade and Aco17563 that falls in the *SEP1/2/4* clade. Similarly, *Zostera marina* showed two genes, Zosma7g01530 in he SEP3 clade and Zosma127g00090 in the *SEP1/2/4* sub-clade. However, higher monocots such as *Zea mays, Brachypodium distachyon, Setaria italica, Sorghum bicolor,* and *Oryza sativa* showed multiple genes in both clades.

The *SEP* sister-family *AGL6*, which forms a *sep*arate clade, was used as an outgroup in this study. The *AGL6* family is present both in gymnosperms and angiosperms (Becker and Theissen, 2003; Nam et al, 2003). The high sequence similarity suggests that *AGL6* and *SEP* families evolved from a common MIKC gene present in the ancestor to extant gymnosperms and angiosperms, or that the *SEP* family evolved from *AGL6* in the ancestor of extant angiosperms. Alternatively, Zahn et al (2004) hypothesised that an ancestor of the *SEP* genes may have been lost in the ancestor of gymnosperms. In gymnosperms, the *AGL6* genes are expressed in the male and female cones, and therefore, have functions pertaining to sporophyte and gametophyte development (Dreni and Zhang, 2016). The *AGL6* sub-family has more than one copy in both angiosperms and gymnosperms. In petunia, the *PhAGL6* gene is considered to be functionally redundant with *FBP2* (*AGL2/SEP1*) (Rijpkema et al, 2009). It is possible that the *AtAGL6* acts redundantly with *AGL2* in specifying C and D function in the fourth whorl (Rijpkema et al, 2009).

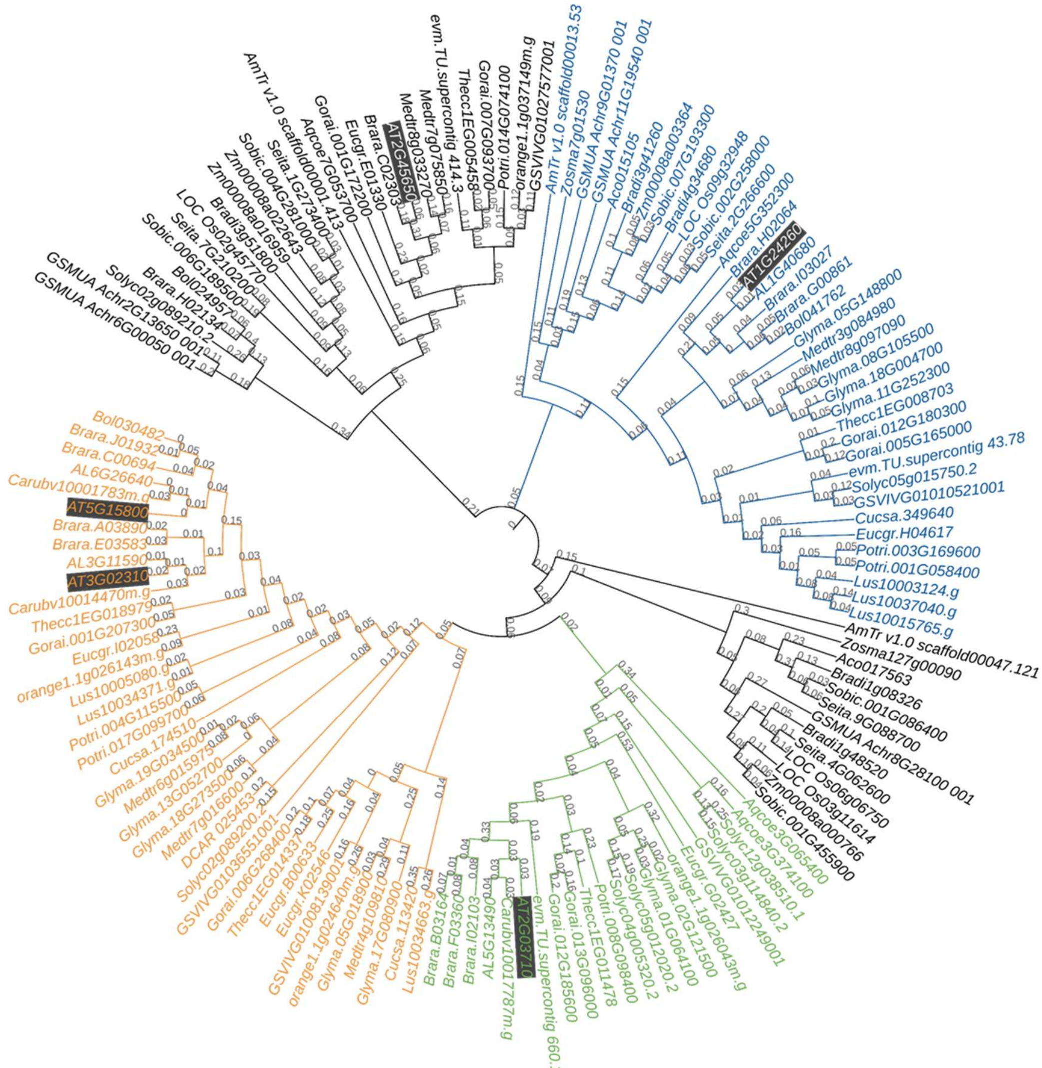

Figure 3-6: Phylogentic tree of At*SEPs* and their homologs. Maximum Likelihood tree was constructed using PhyML v3.0 (Guindon et al., 2010). The best model (JTT+G+I) was determined by using the Akaike Information Criterion (AIC) and the Bayesian Information Criterion (BIC) based on ProtTest 3 (Brewer et al., 2016; Darriba et al., 2011). The final tree was represented and edited using iTOL. *SEP* sub-clades are represented as *SEP3* (blue), LOF*SEP* (black), *SEP4* (green), and *SEP1*/*SEP2* (orange).

3.6 Synteny between *A. thaliana* SEP genes

The *SEP* genes are a product of multiple WGD events throughout evolution. To gain more insight about the evolution and diversification of Arabidopsis *SEP*s, synteny analysis was carried out by using the plant genome duplication database (PGDD). Chromosomal segments containing the *SEP1* and *SEP2* genes, that is, 5.05 – 5.25 Mb on Chromosome 5 and 0.36 – 0.56 Mb on Chromosome 3 showed high collinearity with each other, based on the large number of connectors (blue lines) between syntelogs seen in Figure 3-7 A. Thus, *SEP1* and *SEP2* have a common ancestor. Interestingly, both *SEP1* and *SEP2* showed synteny with *FUL* (Chromosome 5, 24.40 -24.60 Mb) (Figure 3-7 B, C); however, parts of chromosomal segments corresponding to only three genes showed collinearity.

SEP4 showed synteny with *AP1* and *CAL*. The *SEP4* containing chromosomal segment 1.03-1.23 Mb showed collinearity with Chromosome 1 segments 9.00 – 9.20 Mb (containing *FUL*) and 25.88 – 26.08 Mb (containing *AP1*). This shows that *SEP4*, *AP1* and *CAL* have a common ancestor. Although *SEP1, SEP2*, and *SEP4* fall in the same clade in the phylogenetic trees, PGDD did not yield results to show collinearity between *SEP1*, *SEP2* and *SEP4*. However, collinearity was found between *FUL, CAL*, and *AP1*, suggesting that they have a common ancestor. Thus, it can be hypothesised that the most recent common ancestor (MRCA) of *SEP1, SEP2, FUL* and MRCA of *AP1, CAL, SEP4* have a common ancestor (Figure 3-9). Interestingly, *SEP3* did not show collinearity or other tandem duplications in the Arabidopsis genome, showing that it diversified independently of the *SEP1/2/4* genes.

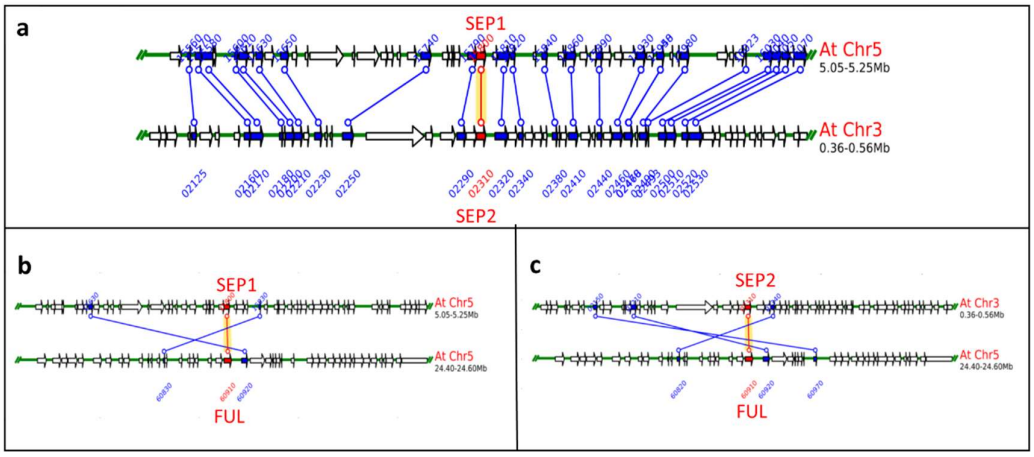

Figure 3-7: *SEP1* and *SEP2* share synteny. (A) *SEP1* and *SEP2* share a syntenic block of 0.2 Mb between chromosome 3 and chromosome 5 (B, C) *SEP1* and *SEP2* share synteny with *FUL*

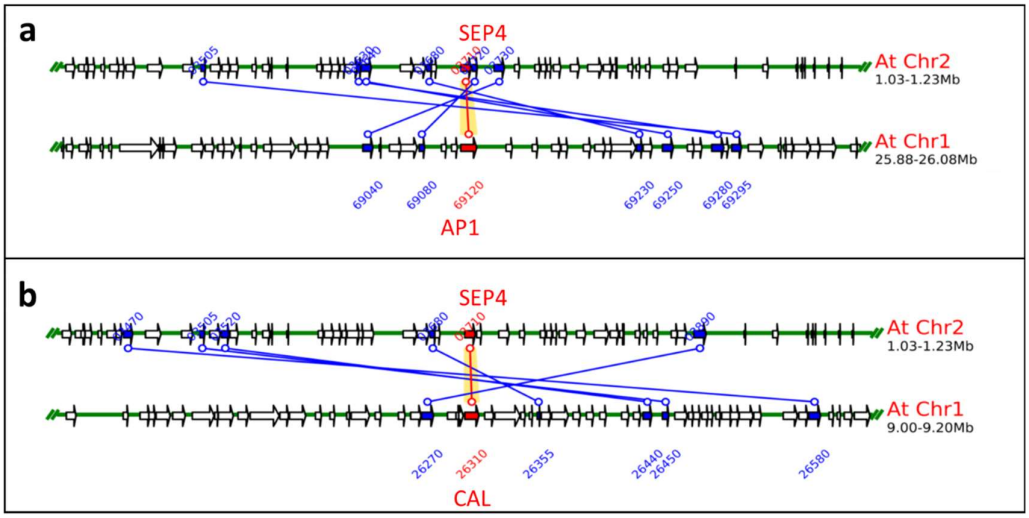

Figure 3-8: Syntenic partners of *SEP4*. Chromosome 2 co-ordinates 1.03 to 1.23 Mb containing the *SEP4* gene show synteny with (a) *AP1* gene block (25.88 to 26.08 Mb) on Chromosome 1 and (b) *CAL* gene block (9.0 to 9.2 Mb) on Chromosome 1

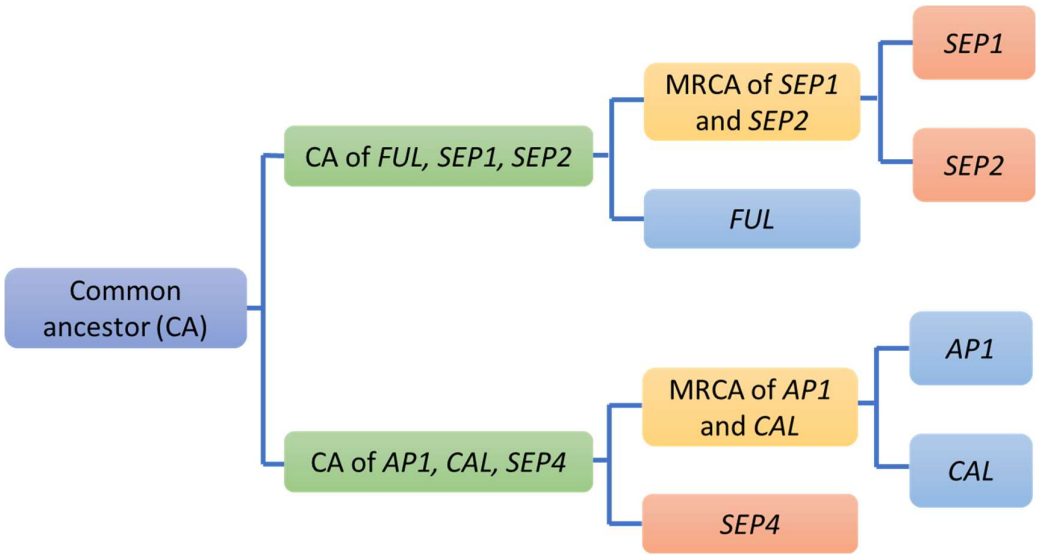

Figure 3-9: Schematic of duplication model deduced from synteny analysis of Arabidopsis SEPs demonstrating the relationship between *SEP1, SEP2*, and *SEP4*. The most recent common ancestor (MRCA) of *SEP1* and *SEP2,* and FUL have a common ancestor. Similarly, the MRCA of *AP1* and *CAL*, and *SEP4* have a common ancestor. These two common ancestors share an ancestor.

3.7 Discussion

3.7.1 Identification of sequence features is essential for functional characterisation of *SEPs*

Identification of conserved domains and motifs have improved our understanding of *SEP* structure and function. For example, the conserved MADS-box is known bind CArG motifs of DNA to regulate transcription of genes downstream (Jetha et al., 2014). The K-box, the second most conserved motif in MIKC proteins, determines protein-protein interactions. K1 and K2 subdomains are responsible for dimerization of the protein and K3 subdomain is essential for tetramerization (Yang et al., 2003; Yang, 2004; Acajjaoui et al., 2013). The most noticeable sequence feature of the K-domains is the frequent occurrence and high conservation of leucine residues (Figure 3-3). Leucine generally occupies position 'd' in the $[abcdefg]_n$ 7-residue repeat, that is characteristic of a leucine-zipper motif (Yang, 2004). These heptad repeats are present at the interaction interface for formation of homo- and hetero-tetrameric *SEP* complexes. Residues at heptad positions 'a' and 'd' form the hydrophobic core that is important for stability (Popatov et al, 2015). Leucine and other hydrophobic residues

form intra and intermolecular contact points. The K-domain forms coiled-coils that are involved in protein-protein interaction (Ma et al., 1991; Davies and Schwarz-Sommer, 1994; Riechmann and Meyerowitz, 1997; Puranik et al., 2014). These features may influence the ability of *SEP* proteins to form heterotetrameric complexes with a variety of other proteins and act as a 'glue' in the protein-protein interaction network that regulates flower development (Immink et al., 2009). Moreover, other MIKC proteins such as AP3 and PI have a lower number of conserved leucine residues at position 'd' or at the interaction interface (Rumpler et al, 2018b; Smaczniak et al., 2012; Zhao et al, 2017). This might limit their possibilities of forming heteromeric complexes, contributing to their very specific role in regulation of flower development. Leucine-zipper proteins show that the leucine residues occupying position 'd' have more favourable interactions with other amino acids as compared to another amino acid occupying the same position (Fong et al., 2004). This increases the possibility of *SEPs* interacting with other proteins, supporting their role as 'network hubs'. Along with heterotetramers, *SEPs* have the ability of forming homotetramers. *SEP3* homotetramers were shown to cooperatively bind two CArG boxes by DNA looping (Melzer et al, 2009). Such complexes have not been found to have a biological function *in planta*, mostly due to the lack of evidence about individual function of *SEPs* independent of other MIKC proteins. However, this cannot exclude the possibility of *SEP* homotetramers having functions relevant to formation of larger complexes by connecting other homeotic proteins. Identification of new conserved motifs from this study (Section 3.3) might provide sequence information for further structural and functional characterization of the K-domain

The function of the C-domain is poorly understood, but the fact that they have been preserved through evolution suggests that they play an important role. Although there is little evidence about C-domain function in *SEPs*, deletion of AG C-domain led to production of a dominant negative form of AG, implying that it is essential for full function of the protein (Mizukami et al, 1996). The non-conserved nature of C-terminal domains have contributed to the structural and functional divergence of MIKC proteins (Vandenbusche et al, 2003). This suggests that C-terminal may be responsible for a multitude of functional implications such as specification of protein-protein interaction or DNA-binding activity, forming higher order complexes necessary for transcription regulation or controlling the spatio-temporal expression of *SEPs* via post-translational

modifications. The small differences in MIK domain sequences are attributable to amino acid substitutions or small insertions and deletions. In contrast, diversification of the C-terminus is primarily attributable to frameshift mutations (Vandenbusche et al, 2003). Conserved motifs in C-terminus are usually flanked by long stretches of non-conserved residues. The evolution and diversification of the C-terminus has always remained ambiguous. The existence of multiple copies of transcriptionally active and functionally redundant *SEP* genes for hundreds of millions of years has always been a puzzle. The small variations in the C-terminus might allow duplicate *SEP* genes to develop new additional functions while fulfilling their primary functions of DNA-binding through the MADs-domain and protein-protein interaction through K-domian. The identification of newer C-terminal motifs in this study might aid in studies pertaining to determining the functional divergence of *SEPs* from different angiosperms.

3.7.2 **Arabidopsis SEPs form distinct clades**

The *SEP* genes belong to one of the most recently originated MADS-box subfamilies (Nam et al., 2003). The basal most exant angiosperm, Amborella and Eschscholzia were shown to contains two *SEP* genes in the present study, one belonging to the *SEP1/2/4* clade and the other belonging to the *SEP3* clade. This result, coupled with the report that *SEP* homologs have not been detected in gymnosperms suggests that the *SEP* family originated and underwent duplication in the ancestors of extant angiosperms (Zahn et al., 2005). However, it is also possible, that the multiple copies of *SEPs* resulted from multiple independent duplication events. The more likely possibility of an early duplication that occurred before the diversification of extant angiosperms resulted in two clades – the Arabidopsis *SEP1/2/4* clade and Arabidopsis *SEP3* clade. Both the *SEP1/2/4* and *SEP3* clades have representatives from other eudicots, monocots, and the basal-most angiosperms Amborella and Eschscholzia. The presence of *SEP* homologs in all major angiosperm lineages and their clear absence in the extant gymnosperms evidently points towards their critical role in the evolution of the flower and thereby, angiosperms (Irish, 2003).

The *AGL6* family that was used as an outgroup in the present study is considered to be a sister clade to the *SEP* family (Becker and Theissen, 2003). The *AGL6* family is present in both gymnosperms and angiosperms. The expression of *SEP* genes in the floral meristems of angiosperms and that of *AGL6* homologs in shoot meristems in

gymnosperms suggest an ancestral meristematic function for the common ancestor of the *SEP* and *AGL6* subfamilies (Zahn et al, 2005). The close association between these two clades imply that an ancestor of the *SEP* genes may have existed in the common ancestor of angiosperms and gymnosperms and was lost in the ancestor of the gymnosperms.

The phylogentic tree indicates that there is little reason to belive that the Arabidopsis *SEP*s are functionally redundant. The long-term coexistence of multiple duplicated copies that are functional, suggests that subfunctionalisation and/or neofunctionalisation may have occurred among paralogs in the *SEP* family. Although *SEPs* have been reported to be functionally redundant, the differential co-operative DNA-binding demonstrated by individual *SEPs* points towards *sep*arate functions of these genes (Jetha et al., 2014). Additionally, the *SEP1/2* genes are expressed in all four whorls, whereas *SEP3* is expressed in the inner three whorls but not in the outermost whorl and *SEP4* is expressed throughout the early floral meristem (Ditta et al., 2004). It is likely that the protein sequences coressponding to the genes do not differ adequately to cause changes functional diversification; however, the expression patterns, interaction partners, and downstream targets of these genes may change, thereby resulting in non-redundant functions.

3.7.3 **Synteny analysis shows that *SEP3* and *SEP1/2/4* clades have diversified *sep*arately**

Synteny aids in deduction of a common ancestor of two or more chromosomal segments, based on collinearity. More collinearity corresponds to recent duplication, whereas decrease in collinearity shows divergence due to chromosomal aberrations. The high number of connectors between chromosomal segments surrounding *SEP1* and *SEP2* support that reports that these two genes are a product of a recent duplication (Ermolaeva et al., 2003). They have not diverged significantly, supporting the hypothesis that they are genetically redundant. Conversely, the low number of syntelogs between *SEP1/2* and *FUL* show that although these genes have a common ancestor, they have diversified to gain *sep*arate functions (Rounsley et al., 1995; Ferrandiz et al., 2000; Pelaz et al., 2000a; Ditta et al., 2004).

SEP4, *CAL*, and *AP1* share synteny. *AP1* and *CAL* function redundantly in the regulation of meristem identity (Ferrandiz et al., 2000). *SEP4* has been reported to play

a role in meristem identity as well as floral organ identity specification (Ditta et al., 2004). The similar function of meristem identity specification shown by *SEP4*, *CAL*, and *AP1* would suggest that *SEP4* gained this function from their most recent common ancestor. It further sub-functionalised to play a role in floral organ identity specification. This is a clear example of duplication leading to diversification in the psatio-temporal gene expression, resulting in the creation of a novel function. Additionally, it is interesting that *SEP4* was not identified as a clear syntelog of *SEP1/2*. This could be due to the low sensitivity of PGDD resulting in missing out on highly dissimilar duplications. Alternatively, it can be hypothesised that the MRCA of *SEP1, SEP2, FUL* and MRCA of *AP1, CAL, SEP4* had a common ancestor. This could be further verified by running intergenomic microsynteny analysis on genomes of different species, including basal angiosperms and model gymnosperms. If *SEP1/2* have truly no direct collinearity with *SEP4*, it would suggest a possibilty of *SEP1/2* showing non-redundant functions with *SEP4*.

The synteny analysis also shows that *SEP3* showed no collinearity with other chromosomal segments in Arabidopsis. Thus, either the *SEP3* chromosomal segment never underwent duplication or duplicated pairs of *SEP3* have undergone deletion or non-functionalisation.

4 Chapter 4: SEP genes affect the robustness of flower development

Robustness is a property of biological systems that describes an organism's ability to produce an invariant phenotype in response to genetic or environmental perturbations, resulting in a predetermined phenotype (Whitacre & Bender, 2010). Flower development, being a crucial aspect of reproduction, is highly robust in angiosperms. Most plants produce flowers with uniform architecture, that is, consistent phyllotactic pattern, number of whorls, merism (number of floral organs per whorl), and symmetry, irrespective of changing environmental conditions (Abley et al., 2016a; Wils & Kaufmann, 2017). Floral architecture affects fruit development, maturation, seed set, and overall yield (Diggle, 1995; Dai et al., 2016). Variability in floral organ size may result in fruit abortion or negatively affect seed number or mass per fruit (Diggle, 1995). Thus, maintaining morphological uniformity in floral architecture is essential for reproductive success (Wyatt, 1982; Buide, 2004). Most angiosperm families have evolved to develop a very robust floral plan (Smyth, 2018). Especially plants belonging to Brassicaceae, one of the most prominent flowering plant families, show significant conservation of floral plan. Strong selection constraints on floral architecture through minimising structural variations from the floral ground plan in Brassica has evolved to ensure reproductive success (Endress, 1992). A model plant from the Brassicaceae, *A. thaliana,* produces flowers with *sep*als, petals, stamens, and carpels arranged in four *sep*arate whorls, in bilateral symmetrical arrangement (Nikolov, 2019). The first two whorls, consisting of *sep*als and petals, show a decussate symmetry, depicting a classic crucifer floral organ arrangement that remains invariable irrespective of changing environmental conditions.

Floral architecture is genetically controlled by different sets of genes responsible for establishing phyllotaxy within flowers, determining organ identity, and governing organ boundaries. Out of these, gene regulatory network determining floral organ identity has been the most thoroughly studied, leading to the postulation of the ABCE model of flower development. As described in chapter 1, combinations of A, B, and C-activity genes lead to the development of *sep*als, petals, stamens, and carpels (Bowman et al., 1991; Coen & Meyerowitz, 1991; Weigel & Meyerowitz, 1994). The homeotic genes dictate the identity, number, position, and pattern of floral organs (Bowman et

al., 1991). Although mutations in these homeotic genes lead to striking phenotypes showing the inability to develop a particular floral organ (e.g., *ap3* and *pi* flowers do not form petals and stamens), loss of these genes does not affect the floral ground plan (Smyth, 2018). Despite playing an important role in flower development, A, B and C-activity genes do not have multiple copies in Arabidopsis or across other angiosperms, suggesting that some other mechanism protects their function by buffering the stochasticity to guarantee unimpeded flower development. The activity of A, B, and C-activity genes is insufficient to specify organ identity and requires interaction with E-activity *SEP* genes to switch from a developmental ground state and establish a floral state (Pelaz et al., 2000b; Pelaz, Tapia-López, et al., 2001; Theißen & Saedler, 2001). This suggests a possibility of *SEP*s playing a role in the maintenance of that floral state.

The *SEP* family in *A. thaliana* comprises four closely related genes, which came about through duplications. Previous studies describe these genes as redundant (Ditta et al., 2004; Pelaz et al., 2000b). Single and double *sep* mutants have been largely overlooked or reported to show only subtle or insignificant phenotypes. Higher-order *sep* mutants exhibit striking phenotypes. The quadruple *sep1 sep2 sep3 sep4* mutant cannot form flowers and makes indeterminate whorls of leaf-like structures (Ditta et al., 2004). The triple *sep1 sep2 sep3* mutant generates flowers entirely composed of *sep*aloid whorls (Pelaz et al., 2000b). This indicates that the *SEP*s specify floral organ identity in a redundant manner where all four *SEP* genes contribute to flower development and can essentially substitute for each other (Jetha et al., 2014). However, there is no mechanistic rationale behind retaining duplicate copies of redundant *SEP* genes in *A. thaliana* or across other angiosperms. As seen in chapter 3, the earliest extant angiosperm, *Amborella trichopoda*, has two copies of *SEP*s, suggesting that the *SEP* family underwent duplications before the divergence of extant angiosperms. During the course of evolution, duplicate genes are generally lost by pseudogenisation, or they undergo functional divergence. In this case, the ancestral gene functions are divided between multiple copies through sub-functionalisation, or they acquire new functions through neo-functionalisation. With inadequate evidence of sub-functionalisation or neo-functionalisation within the *SEP* family, it is difficult to justify the evolutionary cost of maintaining four copies of redundant genes.

Plants have a higher retention rate of duplicate genes compared to animals. The mechanism and age of duplication and gene function influence the survival of duplicate

genes (Rody et al., 2017). According to the Gene Balance Hypothesis, multiple copies of genes encoding transcription factors and proteins that make multiple connections are retained to maintain optimal relative gene dosage (Rody et al., 2017). *SEP*s encode MADS-box transcription factors that form tetrameric complexes to bring together other MADS-box proteins to regulate flower development (Hugouvieux & Zubieta, 2018; Kaufmann et al., 2005; Rümpler et al., 2018). They also form multimeric, higher-order complexes with other MADS and non-MADS proteins to function in various developmental processes such as initiation of flowering, flower development and seed production (Kaufmann et al., 2005b). SEPs bind specifically to CArG boxes in promoter regions to modulate the expression of target genes and play a key role in regulating hormonal and developmental pathways (Kaufmann et al., 2009b; Lai et al., 2020). However, the ability to form multiple connections in massive networks (Immink et al., 2009) does not correlate with maintaining optimal gene dosage of *SEP*s. Single or double *sep* mutants do not exhibit significantly conspicuous phenotypes expected from disturbing such huge and crucial gene regulatory networks. Thus, based on studies so far, the advantage of having multiple copies of redundant *SEP* genes remains elusive. However, genetic redundancy and the ability to function as network hubs by forming multiple connections in gene regulatory networks are desirable characteristics for components that contribute to the robustness of a system (M. A. Félix & Barkoulas, 2015; Mestek Boukhibar & Barkoulas, 2016; Whitacre, 2012). Thus, it can be hypothesised that duplicate and genetically redundant SEP transcription factors have been retained as they govern the development of flowers with uniform morphologies irrespective of environmental conditions, thereby contributing to developmental robustness.

Much of our understanding of *sep* mutant phenotypes comes from plants grown under standard environmental conditions in controlled growth chambers. Limiting variation in the environment allows precise phenotypic measurements and reduces the number of variable factors to be considered that might affect the phenotype. However, it also constrains our understanding of more subtle phenotypic changes that are influenced by the variability of natural environments. Thus, in order to study developmental robustness, it is essential to use growth conditions that correspond to real-world, variable growth conditions. In this chapter, the hypothesis that SEPs govern the robustness of flower development was investigated by growing *sep* single and double

mutants in (i) ideal, stable temperature (ST) (22ºC) and (ii) variable temperature (VT) (16-28ºC). Single and double *sep* mutants was investigated to identify any phenotypes overlooked by previous studies. Further, phenotypic variability was assessed to determine whether the duplicated SEPs play any role in promoting the developmental robustness of the flower. If SEPs indeed act as a capacitor to produce uniform flowers, *sep* mutants should be expected to exhibit more variable phenotypes than wild type control plants. Moreover, the functional redundancy of SEPs was investigated by promoter-swap assays to determine whether different SEPs can substitute for each other. Overall, this chapter describes the analysis of *sep* single and double mutant phenotypes in ST and VT conditions.

Objectives

- To determine whether *sep* single and double mutant flowers show significant, undescribed phenotypes
- To assess the effect of a variable environment on *sep* phenotypes and determine their possible role in robustness
- To determine whether *SEP*s are functionally redundant

4.1 *sep* mutant alleles show subtle but distinct phenotypes

4.1.1 Characterisation of new *sep* mutant alleles

The activity of SEP genes has been described as redundant throughout the literature (Pelaz et al., 2001; Honma and Goto, 2001). Single or double *sep* mutants do not show a phenotype as striking as the higher-order *sep* mutants or other homeotic mutants. These studies were based on single alleles corresponding to each *SEP* gene, viz. *sep1-1, sep2-1, sep3-2,* and *sep4-1* (Pelaz et al., 2001; Ditta et al., 2004). Thus, it was important to identify new *sep* alleles and investigate their phenotypes. New alleles *sep1-2* (SALK_011077, insertion in exon 7), *sep2-3* (SALK_099222, insertion in exon 3), *sep2-4* (SALK_138299, insertion in intron 1) and *sep4-2* (SALK_006229, insertion in first intron) were obtained from NASC (Figure 4-1). All the alleles were genotyped to confirm homozygosity and used for further experiments.

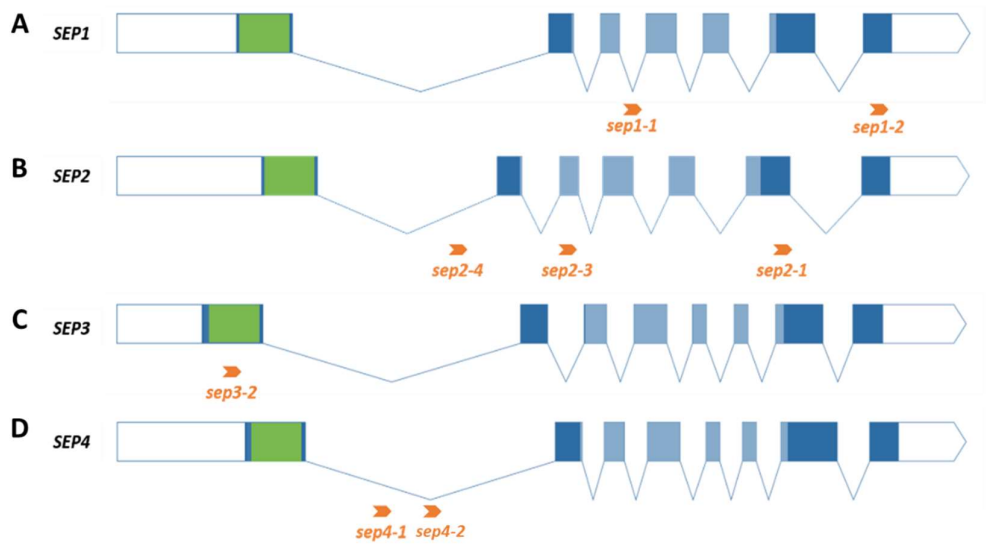

Figure 4-1: Location of insertion in *sep* mutant alleles used in this study (A) *sep1-1* has an insertion in intron 3, *sep1-2* insertion in exon 7 (B) *sep2-4* shows insertion in intron 1, *sep2-3* and *sep2-1* have insertions in exons 3 and 6 respectively (C) *sep3-2* insertion is present in exon 1 (D) *sep4-1* and *sep4-2* have insertions is in intron 1

4.1.2 *sep* mutant phenotypes under VT conditions

The behaviour of *sep* mutants grown under natural environmental conditions was previously studied by Davies, Kauffman, and Kohl labs. Single and double *sep* mutants were grown in a screenhouse by our collaborators, such that the plants experienced a naturally varying environment. This experiment was conducted in Summer, Spring and Winter 2017. Strikingly, in natural environmental conditions, individual *sep* mutants showed a variety of abnormalities affecting flower development. The distinct phenotypes showed that the *sep* mutant flowers were more variable across different seasons, concerning size and shape as compared to the wild-type (WT), suggesting that the phenotypes depended on genotype and environment both (Unpublished, Davies and Kauffman labs). The weather modelling data from the experiment indicated a range of environmental conditions, including minimum and maximum photo radiation, minimum and maximum temperatures, and varying daily temperature, that could most influence the *sep* phenotype. Out of these, we chose temperature ranging between extreme minimum and maximum during Spring, varying throughout the day, to investigate its effect on variability in flower morphology. To determine how changing temperature affected the *sep* phenotype, the plants were grown in VT in a controlled growth chamber at Leeds (16 to 28 ˚C, 16h/8h day/night, 60 % relative humidity (Figure 4-2). Appropriate controls were maintained at ST under identical growth chamber conditions but at constant temperature (22˚C, 16h/8h light/dark).

A typical Arabidopsis WT flower has four *sep*als, four petals, six stamens, and two fused carpels, with the *sep*als and petals showing crucifer symmetry. The flowers of wild type plants subjected to ST and VT conditions conformed to this pattern (Figure 4-2). Single and double *sep* mutants were observed to determine if they showed deviation from the standard WT flower regarding the number of floral organs, symmetry of floral organ arrangement or organ identity. In contrast to published reports (Ditta et al., 2004; Pelaz et al., 2000), flowers of *sep* mutants revealed distinct phenotypes upon close inspection. The phenotypes were either as (i) environment-dependent or (ii) environment independent. *sep1* and *sep2* showed environment-dependent phenotypes, with a skewed arrangement of petals (Figure 4-2), deviating from the characteristic crucifer arrangement seen in WT. Flowers from plants grown under both ST and VTs showed the skewed petal phenotype; however, the phenotype was exacerbated in *sep1* and *sep2* plants grown in VT (Figure 4-2). The loss of

symmetry was most obvious in *sep1 sep2* double mutant flowers, which show very significant deformation (Figure 4-2, Table 4-1). *sep1 sep2* flowers also showed an environment-independent decrease in the number of *sep*als (Table 4-1). These phenotypes was described in detail in the following sections.

Interestingly, *sep3-2* flowers did not show a significant phenotype. The plants produced a few early flowers (flower number one to four on the main stem) with *sep*aloid petals; however, this phenotype was rare (Figure 4-2). *sep4* mutant alleles showed an environment-independent increase in the number of *sep*als and petals (Figure 4-2). This was also evident in two *sep4* double mutants, i.e., all flowers from *sep1sep4* and *sep2sep4* showed an increase in the number of petals; however, *sep3sep4* flowers did not show this phenotype (Figure 4-2, Table 4-1).

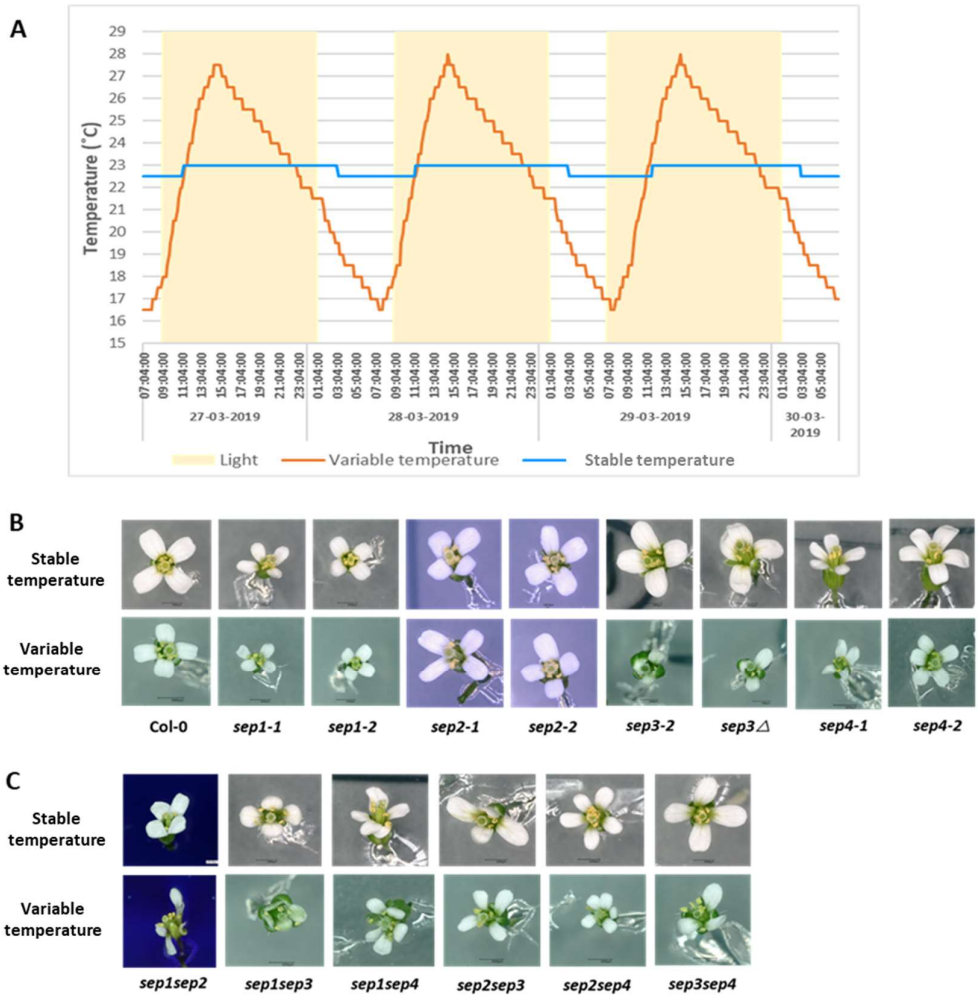

Figure 4-2: Effect of VT conditions on phenotypes of sep mutants (A) VT program showing a steady increase in temperature from 16 to 28 ˚C, from 7:00 am to 15:00, and decrease from 15:00 to 7:00. The control temperature used was 22 ˚C. The day/night conditions were 16/8h in both chambers. (B) Phenotypes of *sep* single mutants in constant temperature (ST) and variable temperature (VT) (C) Phenotypes of *sep* single mutants in ST and VT.

Table 4-1: Summary of floral organ phenotypes observed in *sep* single and double mutants. Arrows show increase (↑), decrease (↓), and variability (↕) in number (n=8)

Allele	Condition	Sepals	Petals	Stamen	Carpels
sep1-1	ST	-	Skewed	-	-
	VT	-	Skewed	-	-
sep1-2	ST	-	Skewed	-	-
	VT	-	Skewed	-	-
sep1-3	ST	-	Skewed	-	-
	VT	-	Skewed	-	-
sep2-1	ST	-	Skewed	-	-
	VT	-	Skewed	-	-
sep2-3	ST	-	Skewed	-	-
	VT	-	Skewed	-	-
sep2-4	ST	-	Skewed	-	-
	VT	-	Skewed	-	-
sep3-2	ST	-	Occasionally *sep*alloid	-	-
	VT	-	Occasionally *sep*alloid	-	-
sep4-1	ST	4↑	4↑	-	2↑
	VT	4↑	4↑	-	2↑
sep1-1sep2-1	ST	2↓	Skewed	-	2
	VT	2↓	Skewed	-	2
sep1-1sep3-2	ST	-	-	-	2
	VT	-	Occasionally *sep*alloid	-	2
sep1-1sep4-1	ST	4↑	4↑	-	2↑
	VT	4↑	4↑	-	2↑
sep2-1sep3-2	ST	-	-	-	2
	VT	-	-	-	2
sep2-1sep4-1	ST	4↑	4↑	-	2↑
	VT	4↑	4↑	-	2↑
sep3-2sep4-1	ST	-	-	-	2
	VT	-	-	-	2

4.2 Loss of *SEP1* and *SEP2* affects development of decussate flower, especially in VT

4.2.1 The skewed arrangement of petals in *sep1* and *sep2* is exacerbated in VT conditions

The standard cross-shaped symmetry in whorls 1 and 2 in a WT flower indicates that the ideal angle between adjacent petals (ABAP) is 90º, as well as the mean ABAP for a flower is 90º. (The mean of ABAP in a flower containing four petals will always theoretically be 90º. However, showing the mean is necessary to show the variance from the mean in this phenotype). A flower was considered to have skewed petals if the ABAP deviated from the standard 90º by ≥10%, that is, 90º >± 9º. In WT flowers grown under ST and VT conditions (Figure 4-3 A, B), the mean ABAP was 90º ± 6.90, and the variability of ABAP, shown by the size of box and outlier points, was very low (Table 4-2; Figure 4-4 A). The variability in ABAP around the mean was analysed by calculating the coefficient of variation (%CV) for the population (n=32). The %CV was 7% and 6% for ABAP in WT flowers grown under ST and VT conditions, respectively (Figure 4-4 C). Only 3 % of WT flowers showed skewed petals under ST, and 6 % under VT conditions (Figure 4-4 B). Overall, WT flowers showed little variation from the ideal ABAP.

In *sep1-1, sep1-2, sep1-3, sep2-1, sep2-3, and sep2-4* grown at ST, the arrangement of petals was skewed, compromising the characteristic cruciferous arrangement (Figure 4-3 C, E, G, I, K, M). Under VT conditions, the *sep1* and *sep2* flowers showed enhanced deviation from decussate symmetry (Figure 4-3 D, F, H, J, L, N). The dispersion of ABAP, evident from the size of boxes and outliers in the plot, was broader in *sep1* and *sep2* flowers than the WT (Figure 4-4 A). The % CV for ABAP in *sep1* and *sep2* flowers was significantly higher than that of WT (Figure 4-4 C), suggesting that loss of *SEP1* or *SEP2* affects the ability to form a decussate flower. This phenotype was enhanced in mutant flowers from plants grown under VT, indicating that exposure to VT further reduced the plants' ability to create a decussate flower. This analysis could not be carried out on the *sep1 sep2* double mutant because the angle between petals could not be measured due to extreme deformation in this mutant combination.

The phenotype had a higher penetrance under VT condition. 78 % of *sep1-1* flowers showed skewed petals under ST, which increased to 84 % when the plants were grown

in VT. Similarly, in *sep1-2* and *sep1-3*, 50 % and 40 % of the flowers showed skewed petals in ST, while 78 % and 81 % flowers showed skewed petals in VT conditions (Table 4-2, Figure 4-4-B). In *sep2* alleles, *sep2-1, sep2-3,* and *sep2-4* had 62 %, 46 %, and 46 % of flowers showing skewed petals under ST, respectively. This number increased to 68 %, 50 %, and 75 %, respectively, for plants grown in VT conditions (Table 4-2Figure 4-4-B).

Overall, this indicates that there is little deviation from the ideal 90º ABAP in the WT flowers. *sep1* and *sep2* flowers show significant variation from the perfect ABAP, suggesting that they are defective in defining decussate symmetry. Subjecting the plants to VT conditions enhances the number of flowers showing compromised decussate symmetry in WT and mutants; however, the increase in the number of flowers with skewed petals is significantly higher in the mutants than in WT. This suggests that when plants encounter varying conditions, the ABAP tends to deviate from the ideal. However, this deviation is buffered in the presence of *SEP1* and *SEP2*.

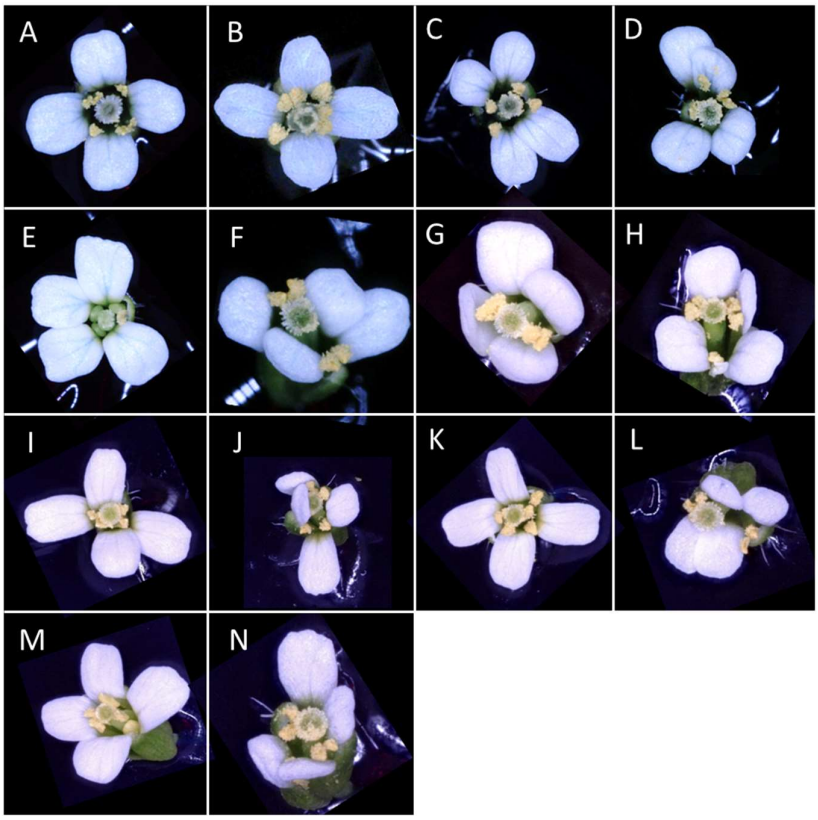

Figure 4-3: Loss of SEP1 or SEP2 affects decussate floral symmetry. The characteristic crucifer arrangement seen in WT Col-0 flowers remains undisturbed in (A) ST and(B) VT. Flowers from multiple *sep1* and *sep2* allele plants, that is, *sep1-1* (C, D), *sep1*-2 (E, F), *sep1*-3 (G, H), *sep2-1* (I, J), *sep2*-3 (K, L), and *sep2*-4 (M, N), grown in ST and VTs, respectively, show that the decussate arrangement of petals is affected.

Table 4-2: Analysis of *sep1* and *sep2* single mutants. Flowers were analysed at 22 ºC and VT regarding the angle between adjacent petals.

Genotype	% skewed flowers	Mean	Standard Deviation	Number of flowers analysed/number of plants
Col-0	3.12	90	6.90	32/4
Col-0 VT	6.25	90	5.58	32/4
sep1-1	78.12	90	23.75	32/4
sep1-1 VT	84.37	90	30.14	32/4
sep1-2	50.00	90	17.20	32/4
sep1-2 VT	78.12	90	31.34	32/4
sep1-3	40.62	90	14.07	32/4
sep1-3 VT	81.25	90	34.67	32/4
sep2-1	62.75	90	20.05	32/4
sep2-1 VT	68.50	90	23.32	32/4
sep2-3	46.87	90	14.31	32/4
sep2-3 VT	50.00	90	23.56	32/4
sep2-4	46.87	90	20.70	32/4
sep2-4 VT	75.00	90	24.72	32/4

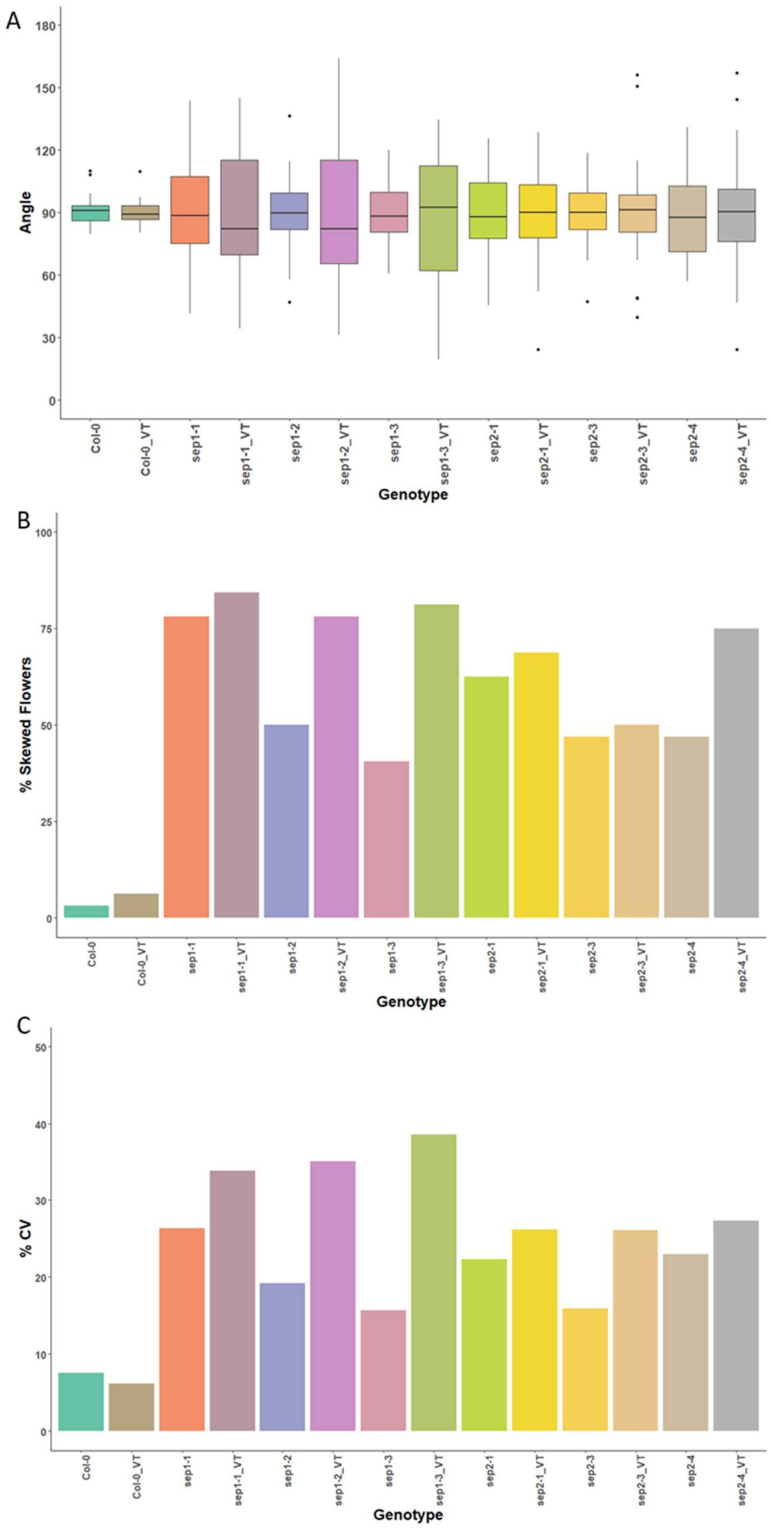

Figure 4-4: Assessment of skewed petal phenotype observed in *sep1* and *sep2* alleles. (A) Variability in angle between adjacent petals in WT, *sep1-1*, *sep1*-2, *sep1*-3, *sep2-1*, *sep2*-3, and *sep2*-4, grown in ST and VT (B) The percentage of flowers that showed

90º ± ≥10% deviation (C) Coefficient of variation in angle between adjacent petals for each genotype grown in ST and VT.

4.2.2 *SEP1-GFP* transgene complemented the skewed petal arrangement in *sep1-1*

To verify that the skewed petals observed in *sep1-1* were attributable to loss of *SEP1*, a C-terminal *SEP1:GFP* tagged construct under the control of its native promoter (2000 bp upstream of the start codon) was cloned and transformed into *sep1-1* (hereafter named *pSEP1:SEP1-GFP sep1-1*) and *sep1 sep2* mutants (hereafter called *pSEP1:SEP1-GFP sep1 sep2*). Multiple independent T1 lines were screened for both constructs. Out of these, lines that showed 3:1 segregation in the T2 were selected to ensure Mendelian segregation of a single transgene copy. Homozygous T3 plants were analysed for complementation. Ten independent T3 lines were analysed for expression of GFP by using confocal microscopy, from which four lines exhibited good expression of GFP and showed complementation. This confirms that the skewed petal phenotype is attributed to the loss of the *SEP1* gene. After identification of complementing lines, they were further assessed to determine the extent of complementation.

As described in the previous section, WT flowers have petals arranged in a decussate symmetry, such that the angle between adjacent petals approximates to 90º (Figure 4-5-A). The *sep1-1* mutant flowers, however, show a skewed arrangement of petals, such that the angles between adjacent petals vary (Figure 4-5-B). Flowers from two T3 lines with *pSEP1:SEP1-GFP sep1-1,* Lines 2, 4, 5, and 9 showed complementation by exhibiting a decussate symmetry (Figure 4-5-C, D). In plants subjected to VT conditions, the decussate arrangement of WT flowers was not affected, whereas the skewed angle phenotype in *sep1-1* flowers was exacerbated (Figure 4-5-E, F). Flowers from complemented Lines 2, 4, 5, and 9 reverted to decussate symmetry in VT as well, indicating complementation of *sep1-1* phenotype (Figure 4-5-G, H). Confocal microscopy of Line 2 plants grown in both ST and VT conditions showed GFP in the floral buds and meristems (Figure 4-5-I, J), confirming that the *SEP1-GFP* transgene was expressed. The GFP was prominently visible in young buds arising from the meristem, although not in the central meristem *per se*. SEM analysis of the *sep1-1* inflorescence meristem suggests that the initiation of *sep*al primordia is slightly askew (Figure 4-5-K); however, this could not be confirmed for the petal primordia. SEM of

Line 2 inflorescence meristem shows perfect decussate symmetry in the *sep*al primordia, indicative of complementation (Figure 4-5-L).

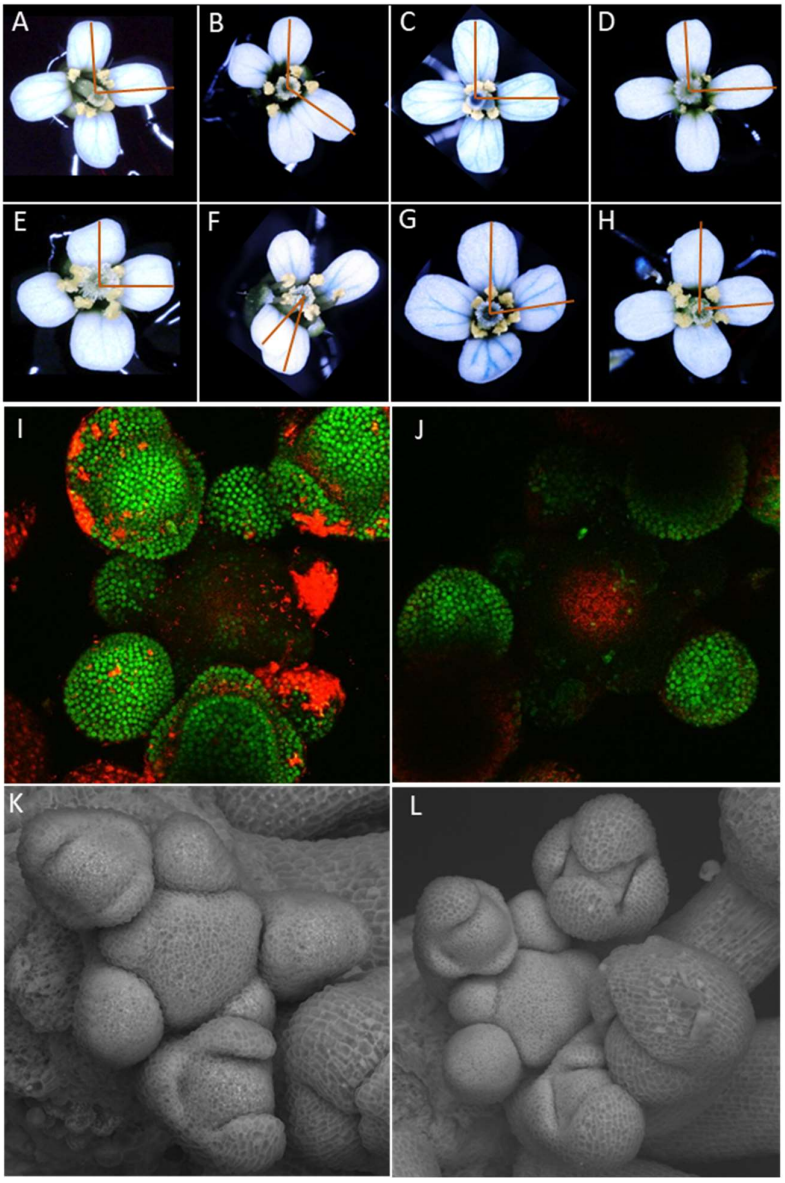

Figure 4-5: Complementation of skewed petal phenotype by *pSEP1:SEP1-GFP* transgene. The angle between adjacent petals, is shown using orange lines in A-H, for flowers from (A) WT (90^{oo} >± 9^{o}), (B) *sep1-1* (>90^{oo} >± 9^{o}), (C) *pSEP1:SEP1-GFP sep1-1* Line 2 (90^{oo} >± 9^{o}), (D) *pSEP1:SEP1-GFP sep1-1* Line 4 (90^{oo} >± 9^{o}), in ST, and (E) WT (90^{oo} >± 9^{o}), (F) *sep1-1* (<90^{oo} >± 9^{o}), (G) *pSEP1:SEP1-GFP sep1-1* Line 2 (90^{oo} >± 9^{o}), (H) *pSEP1:SEP1-GFP sep1-1* Line 4 (90^{oo} >± 9^{o}), in VT (90^{oo} >± 9^{o}), respectively. GFP was expressed (shown in green) in both (I) ST and(J) VT conditions.

The red zones indicate Chlorophyll B for reference. SEM analysis of (K) sep1-1 and (L) show that the pSEP1:SEP1-GFP sep1-1 Line 2 shows the initiation of sepal primordia.

The variability in angle between adjacent petals was assessed for WT, *sep1-1,* Line 2, Line 4, and Line 5 plants subjected to ST and VT (Figure 4-6). As expected, the WT flowers showed slight deviation from the characteristic 90º angle in either condition. The petal angles ranged between 87º (minimum value in the first quartile) and 93º (maximum value in the third quartile) for WT in ST and 87º and 92º for WT in VT. *sep1-1* flowers showed a significant increase in the distribution of petal angles ranging between 73º and 107º in ST. This was exacerbated in VT, such that the smallest angle measured 69º and the largest angle measured 114º, excluding the outliers. In the complemented lines, Line 2, Line 4, and Line 5, the petal angles ranged between 88º-93º, 88º-92º, and 88-93º in ST, 86º-92º, 87º-92º, and 86-92º in VT, respectively (Figure 4-6-A).

Along with decreased deviation in petal angle, the complemented lines showed a significant reduction in the percentage of flowers with skewed petals (Figure 4-6-B). Only 5% and 2% of flowers analysed from WT plants grown in ST and Vt conditions, respectively, showed skewed flowers. While 71% and 74% of the flowers analysed from *sep1-1* showed skewed petal arrangement, only 4% and 16% of Line 2 flowers in ST and VT, respectively. Similarly, 4% and 10% of Line 4 flowers and 6% and 12% of Line 5 flowers showed skewed petals in ST and VT, respectively.

The variability in petal angle was assessed by measuring %CV for each line. The CV for WT flowers from ST and VT did not differ significantly. However, the CV for *sep1-1* flowers was 3.8 times higher than WT in ST and 7.5 times higher than WT in VT. The variability of the complemented lines showed a significant difference from that of *sep1-1* ($p<0.05$). Overall, this shows that *pSEP1-SEP1-GFP* complemented the skewed petal phenotype in *sep1-1* through decreased variability in petal angle, as well as reduced number of flowers deviating from the ideal, decussate symmetry. This was observed in both ST and VT conditions, confirming that loss of SEP1 indeed affected the decussate arrangement of Arabidopsis flowers.

.

Table 4-3: Complementation of skewed petal phenotype by *pSEP1*:*SEP1-GFP* transgene. Flowers were analysed at ST and VT for the angle between adjacent petals

	Mean	**Standard deviation**	**% Skewed**	**Number of flowers/ number of plants**
Col-0	90	6.14	5.75	20/4
Col-0 VT	90	4.42	2.5	20/4
sep1-1	90	23.36	71.25	20/4
sep1-1 VT	90	33.40	73.75	20/4
Line 2	90	5.20	3.75	20/4
Line 2 VT	90	7.71	16.25	20/4
Line 4	90	4.99	3.75	20/4
Line 4 VT	90	6.15	10	20/4
Line 5	90	4.39	4	20/4
Line 5 VT	90	6.70	9.5	20/4

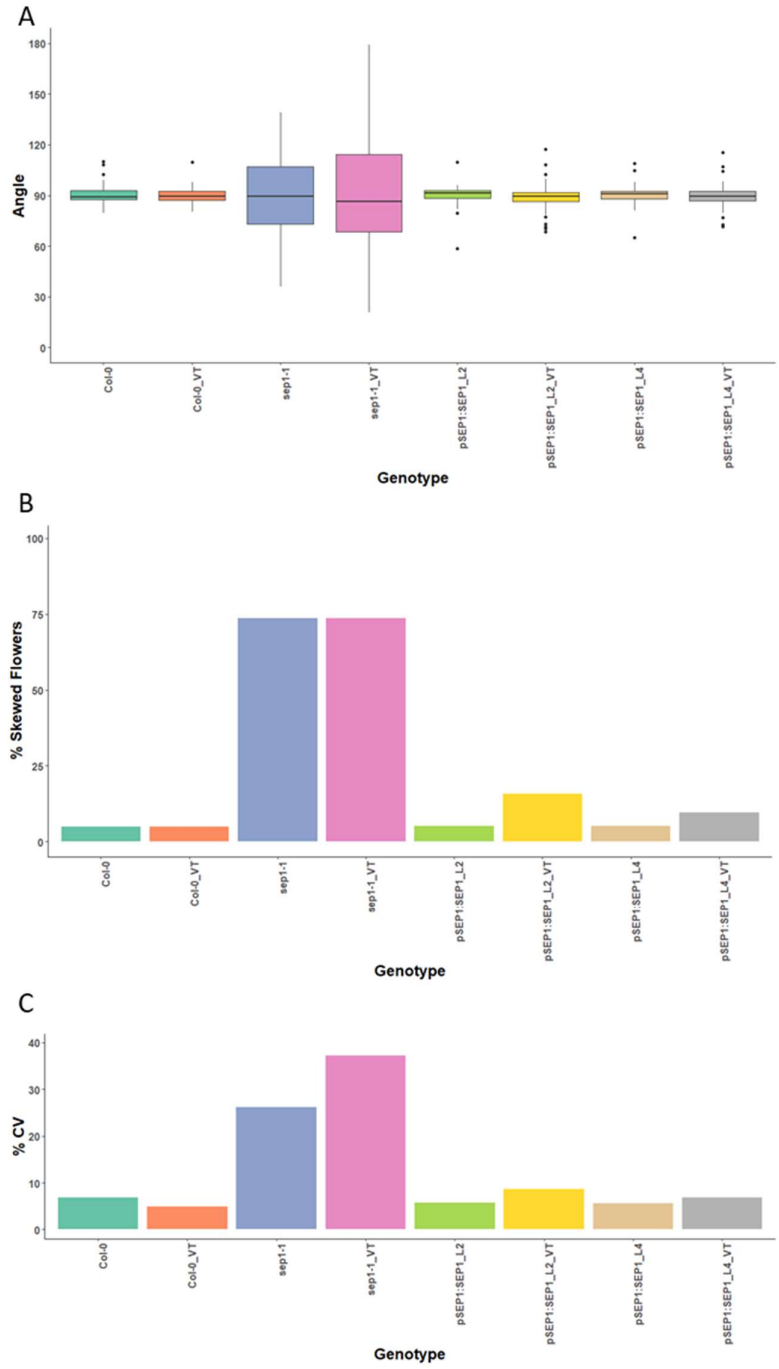

Figure 4-6: Complementation of skewed petal phenotype by *pSEP1*:*SEP1-GFP* transgene. (A) Variability in angle between adjacent petals in WT, *sep1-1*, *pSEP1*:*SEP1-GFP*_L2, and *pSEP1*:*SEP1-GFP*_L4 , grown in ST and VT (B) The percentage of flowers that showed 90º ± 10% deviation (C) Coefficient of variation in angle between adjacent petals for each genotype grown in ST and VT.

4.3 Loss of *SEP1* and *SEP2* suppressed growth of lateral *sep*als

4.3.1 Multiple *sep1 sep2* alleles develop fewer lateral *sep*als

The previous section elaborated on *sep1-1* and *sep2-1* mutant phenotype exhibiting a skewed petal arrangement in whorl 2. Interestingly, loss of both *SEP1* and *SEP2* are resulted in development of only two *sep*als (Figure 4-7-A). *sep1-1sep2-1* flowers showed an absence of lateral *sep*als, and occasional occurrence of *sep*aloid petals, shown by an arrow in Figure 4-7-B. Fully open flowers were found to possess only adaxial and abaxial *sep*als visible upon dissection (Figure 4-7-C, D). SEM analysis of *sep1-1 sep2-1* inflorescence meristem showed the presence of four or occasionally five *sep*al primordia (Figure 4-7-I). This implies that the lateral *sep*al primordia are initiated at the floral meristem, however, they remain rudimentary and do not expand further to form a fully grown *sep*al (Figure 4-7-J). To determine if this phenotype was observed in other *sep1 sep2* mutants, different *sep1* and *sep2* alleles were crossed. Flowers from heterozygous *sep1-2 sep2-3* and *sep1-2 sep2-4* plants showed the characteristic skewed floral organ arrangement found in *sep1-1 sep2-1* (Figure 4-7-E), along with reduced number of *sep*als. Figure 4-7-F shows *sep1-2*$^{-/-}$ *sep2-3*$^{+/-}$ flower with two fully formed and a third smaller *sep*al. Similarly, *sep1-2*$^{-/-}$ *sep2-4*$^{+/-}$ flowers showed a reduced number of *sep*als (Figure 4-7-G, H). However, homozygous *sep1-2 sep2-3* and *sep1-2 sep2-4* alleles could not be recovered to confirm this phenotype, suggesting that the homozygous seeds were unviable. This does not explain how *sep1-1 sep2-1* plants produce viable seeds. One possible reason could be the presence of T-DNA insertion is in Exon 7 in *sep2-1,* which might allow production of a partial protein. However, this claim needs to be clarified by further research.

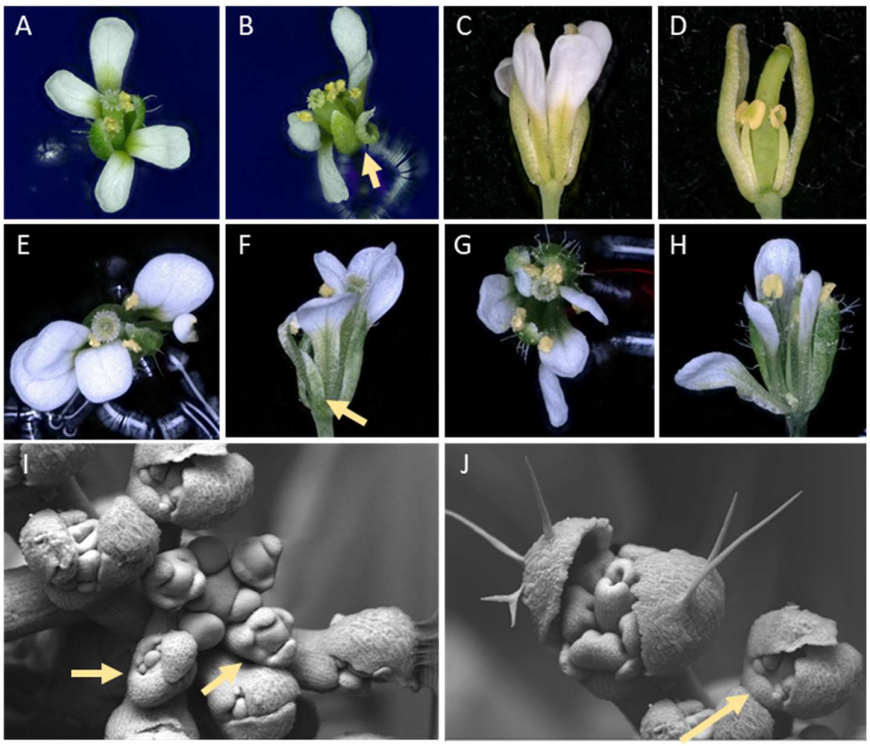

Figure 4-7: *sep1 sep2* alleles show supressed lateral *sep*als. (A) *sep1-1 sep2-1* flower only adaxial and abaxial *sep*als (B) *sep1-1 sep2-1* flower showing distorted arrangement of floral organs and a *sep*aloid petal highlighted by an arrow (C) Open flowers of *sep1-1 sep2-1* showing (lack of lateral *sep*als D) petals removed for clarity. (E) *sep1*-2 *sep2*-3 flower shows distorted arrangement of floral organs, and (F) a smaller third *sep*al, shown by an arrow (G) *sep1*-2 *sep2*-4 flower shows misshapen arrangement of floral organs, and variable number of petals and *sep*als. SEM analysis of *sep1-1 sep2-1* inflorescence meristems shows (I) four or five *sep*al primordia, and (J) rudimentary lateral *sep*al, shown by arrows.

4.3.2 *pSEP1:SEP1-GFP* and *pSEP2:SEP2-GFP* transgenes complement the *sep1 sep2* phenotype

In order to confirm that the suppression of lateral *sep*al development seen in *sep1 sep2* is attributable to loss of *SEP1* and *SEP2*, complementation studies were performed. As described previously, constructs with C-terminal GFP tagged *SEP1* and *SEP2* CDS under the control of their native promoters (2000 bp upstream of the start codon), and 3'-UTR were used to transform *sep1-1 sep2-1*$^{+/-}$ plants. Multiple T1 lines homozygous for the *sep1 sep2* mutations and the transgene were identified and are hereafter referred to as *SEP1-GFP sep1 sep2* and *SEP2-GFP sep1 sep2*. Out of these, lines that showed 3:1 segregation in T2 were selected to ensure Mendelian segregation of a single transgene copy. Homozygous T3 plants from *SEP1-GFP sep1 sep2* Line 22 and *SEP2-GFP sep1 sep2* Line 30 were analysed for complementation.

As described in the previous section, WT flowers have four *sep*als and four petals, arranged in a decussate symmetry (Figure 4-8-A). The *sep1 sep2* mutant flowers, however, showed only two *sep*als and a skewed arrangement of petals (Figure 4-8-B). Flowers from Line 22 and Line 30 were comprised of four *sep*als and exhibited decussate symmetry (Figure 4-8-C, D). Confocal microscopy of Line 22 and Line 30 inflorescences confirmed the expression of GFP in floral buds (Figure 4-8-E. F). As seen in Line 2, the GFP was prominently visible in buds surrounding the meristem but not in the central meristem. The transgene also showed significant expression in *sep*als. As seen in section 4.3.1, SEM analysis of the *sep1 sep2* inflorescence and developing flowers showed four *sep*al primordia, although the lateral *sep*al primordia did not expand to form full *sep*als (Figure 4-8-G). The complemented line Line 22 showed four *sep*al primordia that fully expanded to form a normal first whorl (Figure 4-8-H). Thus, the expression of either *pSEP1:SEP1-GFP* or *pSEP2:SEP2-GFP* transgenes in *sep1 sep2* restored growth and expansion of lateral *sep*als.

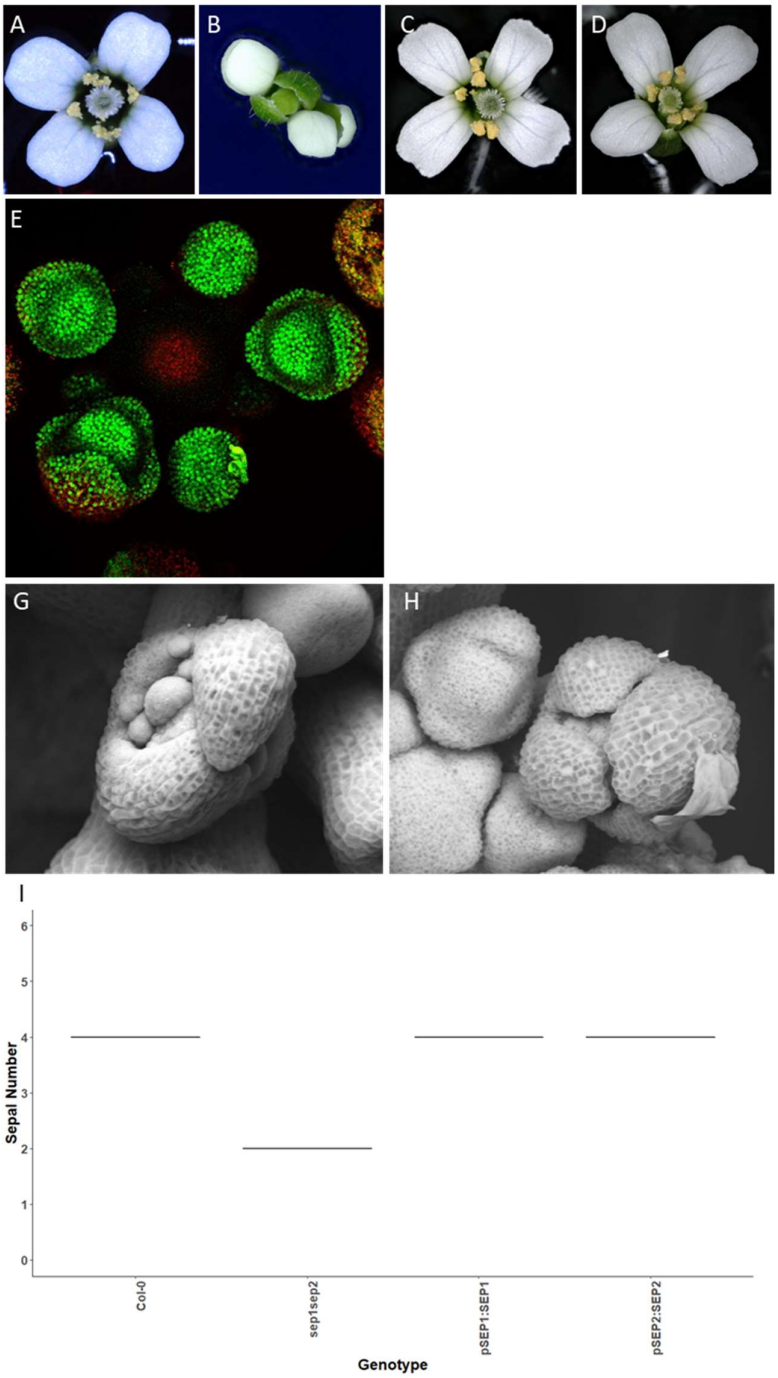

Figure 4-8: Complementation of *sep1-1sep2-1* phenotype by *pSEP1*:*SEP1-GFP* and *pSEP2*:*SEP2-GFP* transgenes. (A) WT flower showing uniform arrangement of floral organs (B) *sep1-1sep2-1* showing an aberrant arrangement of floral organs and two distinctive *sep*als. Flowers from (C) Line 22 and (D) Line 30 exhibit normal looking flowers, thereby complementing the *sep1 sep2* phenotype. Expression of the GFP transgene was confirmed by confocal microscopy of (E) Line 22 and (F) Line 30. SEM

images showed (G) two rudimentary (orange arrows) and two fully formed (green arrows) *sep*als in *sep1-1 sep2-1* (H) four fully formed *sep*als (green arrows) in Line 22. (I) The number of *sep*als in reverted to 4 in *pSEP1*:SEP1 and *pSEP2*:SEP2 lines.

4.4 *sep3* and *sep4* show phenotypes non-redundant with *sep1* and *sep2*

Although *sep1* and *sep2* mutants showed distinct phenotypes, the *sep3-2* mutant lacked any significant phenotype. Occasionally, *sep3-2* petals showed a subtle partial transformation to *sep*als. This was observed under both ST and VT conditions. However, this phenotype arose sporadically and was very rare. Thus, *sep3-2* was considered to be aphenotypic in this study. Interestingly, *sep4-1* and *sep4-2* showed an increase in floral organ number (Figure 4-9 A, B, C). Additionally, although *sep4* mutants showed extra organs, the number of organs was found to be variable. They showed 4-6 *sep*als, 4-7 petals, 5-7 stamens and sometimes 3 fused carpels (Figure 4-9 D, E, F, G) (n=8). The double mutants with *sep4,* that is, *sep1 sep4* and *sep2 sep4* also show an increase in organ number, except for the *sep3 sep4* double, which reverts to approximately 4 again (Figure 4-2 B). Also, that the increased organ number was independent of growth conditions.

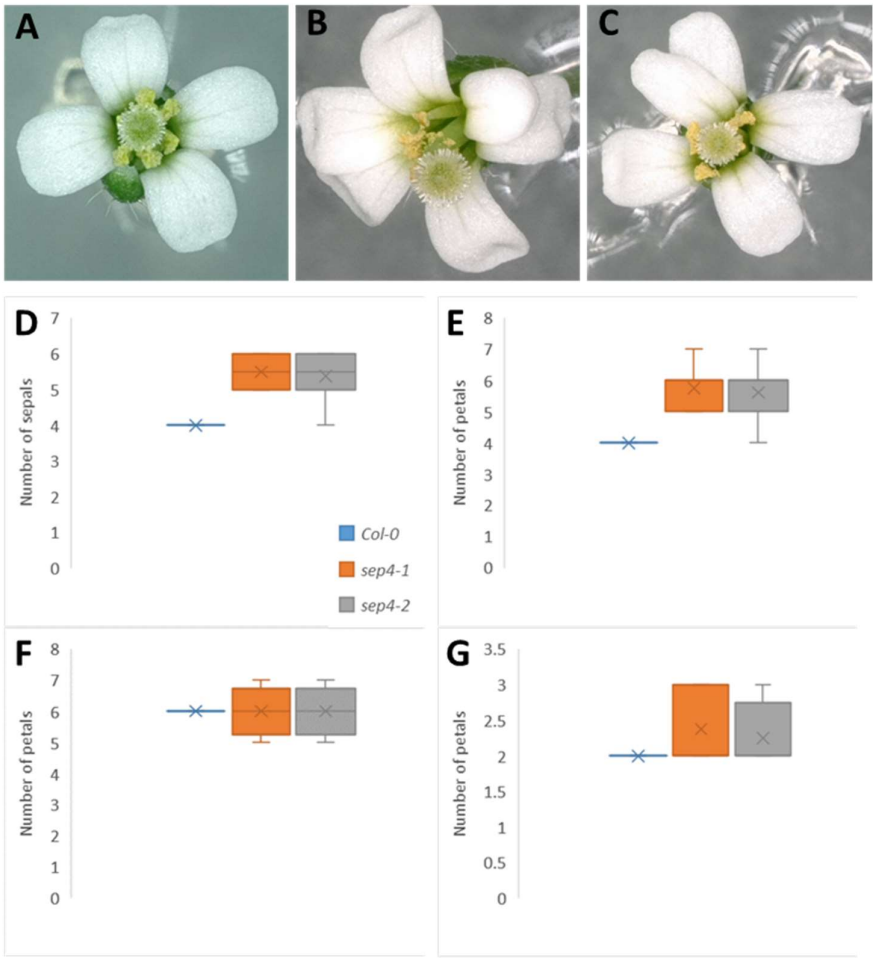

Figure 4-9: Phenotypic characterization of *sep4* mutants. (A)Wild type flower showing four petals, six stamens and two fused carpels (B) *sep4*-1 flower showing 6 petals (C) *sep4*-2 flowers showing 5 petals. The number of floral organs was increased and variable in *sep4*-1 and *sep4*-2 compared to the wild type (D) number of *sep*als (E) number of petals (F) number of stamens and (G) number of carpels.

4.5 SEP1 and SEP2 contribute to the robustness of decussate petal symmetry

4.5.1 *SEP1* and *SEP2* protein contributes to decussate symmetry

As seen in previous sections, SEP1 and SEP2 are both involved in setting petal angle and their expression makes the petal angle more robust towards fluctuations in temperature. The fact that SEP1 and SEP2 show common functions is underlined by the fact that the *sep1 sep2* double mutant shows a more severe phenotype of distorted petal angle symmetry. This phenotype is not observed in *sep3* and *sep4*. Moreover, the *sep1sep3* and *sep1sep4* doubles do not show a skewed petal phenotype as severe as *sep1 sep2.* This suggests that the phenotype could be a consequence of the SEP1 and SEP2 protein sequence. SEP1 and SEP2 are more closely related than SEP3 and SEP4 in terms of similarity in the protein sequence. Thus, the protein-protein interactions of SEP1 and SEP2 could differs from that of SEP3 or SEP4. Thus, the skewed petals phenotype could be caused by the SEP1/SEP2 protein sequences that cannot be caused by SEP3 or SEP4. It also could be a mixture of both expression and activity of the protein sequence.

To test whether the robustness of petal angle is driven by the expression of SEP1/SEP2 or by distinct properties of the SEP1 and SEP2 proteins, complementation assays were performed by using promoter swap constructs. Lines with *pSEP1:SEP1-GFP, pSEP1:SEP2-GFP, pSEP1:SEP3-GFP,* and *pSEP1:SEP4-GFP* transgenes were evaluated for their competence to restore robustness to decussate symmetry of the petal angle. The nomenclature of lines used is provided Table 4-4. The variability in angle between adjacent petals was assessed for *pSEP1:SEP1-GFP L2, pSEP1:SEP1-GFP L4, pSEP1:SEP2-GFP L13-5, pSEP1:SEP2-GFP L13-6, pSEP1:SEP3-GFP L14-6, pSEP1:SEP3-GFP L14-8, pSEP1:SEP4-GFP L15-7*, and *pSEP1:SEP4-GFP L15-8* plants subjected to ST and VT (Figure 4-10).

Table 4-4: Promoter swap lines generated for complementation analysis

Genotype/Line	Promoter	Gene	C-tag	Background	Phenotype Assessed
L-2	*pSEP1*	*SEP1*	*GFP*	*sep1-1*	Skewed petals
L-4		*SEP1*			
L-13-5		*SEP2*			
L-13-6		*SEP2*			
L-14-6		*SEP3*			
L-14-8		*SEP3*			
L-15-1		*SEP4*			
L-15-2		*SEP4*			
L-22		*SEP1*		*sep1 sep2*	Number of *sep*als
L-13-1		*SEP2*			
L-13-2		*SEP2*			
L-14-1		*SEP3*			
L-14-4		*SEP3*			
L-15-7		*SEP4*			
L-15-8		*SEP4*			
L16-2	*pSEP2*	*SEP1*			
L30-4		*SEP2*			
L-17-3		*SEP3*			
L-17-12		*SEP3*			
L-18-11		*SEP4*			
L-18-12		*SEP4*			

In the complemented lines *pSEP1:SEP1-GFP*_L2 and L4, the petal angles ranged between 88º-93º and 88º-92º in ST, 85º-92º and 88º-92º in VT, respectively (Figure 4-10-A). T3 lines with the *pSEP1:SEP2-GFP* transgene, L13-5 and L13-6, showed a slightly broader range of angles, ranging between 83º-94º and 86º-96º in ST, and 86º-94º and 83º-96º, in VT respectively. These petal angles showed less than 10% deviation from 90º, confirming that SEP1 and SEP2, driven by *pSEP1*, complemented the skewed arrangement of petals. The angles further deviated from 90º in *pSEP1:SEP3-GFP* lines, L14-5 and L14-6. The angle values ranged from 81º-99º, 73º-105º in ST and 72º-108º, 73º-107º in VT. Similarly, the petal angle values for *pSEP1:SEP4-GFP* lines, L15-1 and L15-2, ranged between 77º-105º and 74º-104º in ST, and 70º-108º and 77º-104º in VT, respectively. The distribution of angles in *pSEP1:SEP3-GFP and pSEP1:SEP4-GFP* lines was not significantly different from petal angles exhibited by *sep1-1* flowers in ST (75º-108º) and VT (71º-114º), indicating that SEP3 and SEP4 did not complement the skewed arrangement of petals, even under the control of *pSEP1* (Figure 4-10 A).

Along with decreased deviation in petal angle, the complemented lines showed a significant reduction in the percentage of flowers with skewed petals (Figure 4-10-B). While 71% and 74% of the flowers analysed from *sep1-1* showed skewed petal arrangement, only 4% and 16% of *pSEP1:SEP1_L2* flowers in ST and VT, respectively, showed this deviation. Similarly, 4% and 10% of *pSEP1:SEP1_L4* flowers showed skewed petals in ST and VT, respectively (Figure 4-10 B). Comparatively, a higher percentage of flowers showed skewed petals in *pSEP1:SEP2_L13-5* and *L13-6,* going up to 50% in L13-6 under VT conditions. In *pSEP1:SEP3* lines L14-5 and L14-6, as well as *pSEP1:SEP4* lines L15-1 and L15-2, more than 70% flowers showed skewed petals under both ST and VT (Figure 4-10 B), thus not complementing the skewed petal phenotype.

The variability in petal angle was assessed by measuring %CV for each line. The CV for WT flowers from ST and VT did not differ significantly. However, the CV for *sep1-1* flowers was 3.8 times higher than WT in ST and 7.5 times higher than WT in VT. The variability of the complemented lines showed a significant difference from that of *sep1-1* ($p<0.05$). The CV was reduced to less than 10% in *pSEP1:SEP1_L2* and *L4*. *pSEP1:SEP2_L13-5* and *L13-6* showed 10-30% CV. In contrast, *pSEP1:SEP3* lines L14-5 and L14-6, as well as *pSEP1:SEP4* lines L15-1 and L15-2 showed more than 30% CV (Figure 4-10 C). Overall, this shows that *pSEP1:SEP1-GFP* and *pSEP1:SEP2-*

GFP complemented the skewed petal phenotype in *sep1-1,* SEP3 and SEP4 could not substitute for SEP1/SEP2. This shows that the SEP1 and SEP2 proteins play a role in regulating the robustness of decussate petal angle.

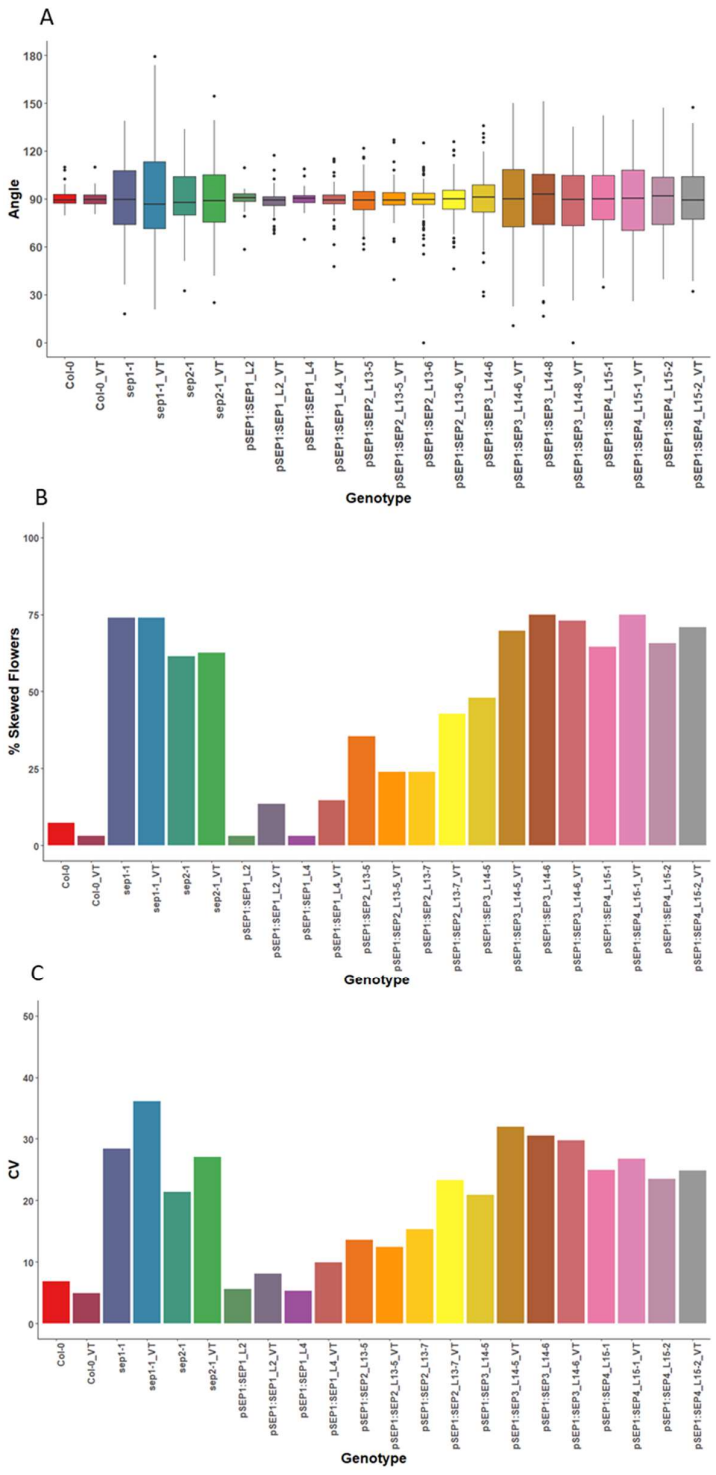

Figure 4-10: Complementation of skewed petal phenotype by *pSEP1:SEP1/2/3/4-GFP* transgenes. (A) Variability in angle between adjacent petals in WT, *sep1-1, pSEP1:SEP1-GFP*_L2, *pSEP1:SEP1-GFP*_L4, *pSEP1:SEP2-GFP*_L13-5,

*pSEP1:SEP2-GFP*_L13-7, *pSEP1:SEP3-GFP*_L14-5, *pSEP1:SEP3-GFP*_L14-6. *pSEP1:SEP4-GFP*_L15-1, *pSEP1:SEP4-GFP*_L15-2, grown in ST and VT (B) The percentage of flowers that showed 90º ± 10% deviation (C) Coefficient of variation in angle between adjacent petals for each genotype grown in ST and VT

4.5.2 SEP3 and SEP4 proteins can substitute SEP1 and SEP2 to regulate lateral *sep*al expansion

To test whether the lateral *sep*al expansion is driven by the expression pattern of SEP1/SEP2 or by their properties of their proteins, similar complementation assays were performed. Lines with *pSEP1:SEP1-GFP, pSEP1:SEP2-GFP, pSEP1:SEP3-GFP,* and *pSEP1:SEP4-GFP* transgenes were evaluated for rescuing the loss of lateral *sep*als in *sep1 sep2*. The *sep*al number was assessed for *pSEP1* driven lines *L22, L13-1, L13-2, L14-1, L14-4, L15-7*, and *L15-8* (Figure 4-11, Table 4-4). The wild type produces 4 *sep*als in Arabidopsis flowers whereas the *sep1 sep2* flowers produce only 2 *sep*als. All complemented lines showed 4 *sep*als (Figure 4-11 A). Thus, SEP3, and SEP4 proteins are capable of substituting for SEP1 and SEP2 to produce lateral *sep*als, when driven by the Sep1 promoter. Within the assessed flowers (n=24; 6 flowers per plant), 100% of flowers showed 4 *sep*als for all lines except *pSEP1:SEP4-GFP L15-8,* which contained 15% flowers with 2 *sep*als and 5% flowers with 3 *sep*als (Figure 4-11 A, C). The CV was zero in all lines except *pSEP1:SEP3-GFP* L14-1 and L14-4 with 10 and 13% CV, and *pSEP1:SEP4-GFP L15-8* with 30% CV. Lines *pSEP1:SEP3-GFP* L14-1 and L14-4 also showed a few flowers with 2, 3 and 4 *sep*als (Figure 4-11 B). However, the number of non-complemented flowers was negligible.

Similarly, the *sep*al number was assessed for *pSEP2* driven lines *L30, L16-2, L17-3, L17-12, L18-11,* and *L18-12* (Figure 4-12Figure 4-11, Table 4-4). All *pSEP2* driven lines, showed 4 *sep*als (Figure 4-12 A). Within the assessed flowers (n=24; 6 flowers per plant), 100% of flowers showed 4 *sep*als. The CV was zero in *pSEP2:SEP1-GFP L16-2* and *pSEP2:SEP2-GFP L30* lines. The CV was between 10-20% in *pSEP2:SEP3-GFP* L17-3 and L17-12, while the CV was less than 10% in *pSEP2:SEP4-GFP L18-11* and *L18-12* (Figure 4-12 B). Lines *pSEP2:SEP3-GFP* L14-1 and L14-4 also showed a few flowers with 2, 3 and 4 *sep*als (Figure 4-11 B). Lines *pSEP2:SEP4-GFP L18-11*, *L18-12, pSEP2:SEP3-GFP L14-1,* and *L14-4* showed less than 15% flowers with either 2, 3, or 5 *sep*als. Thus, the expansion of lateral *sep*als controlled by the SEP1/SEP2

proteins. The high similarity between SEP1-4 proteins allows SEP3 and SEP4 to substitute for SEP1 and SEP2 to redundantly regulate lateral *sep*al growth.

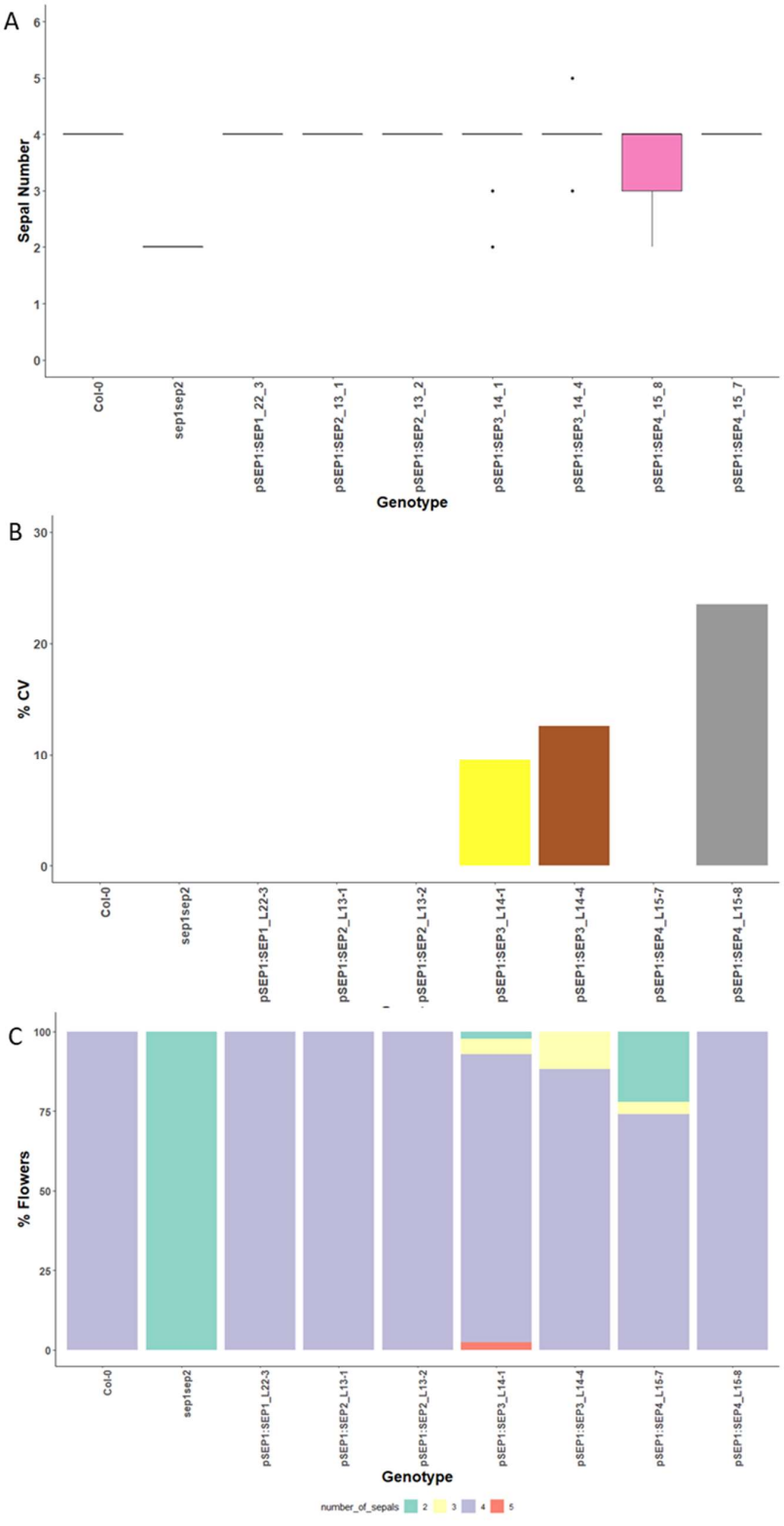

Figure 4-11: Complementation of supressed lateral *sep*al phenotype by *pSEP1*:*SEP1/2/3/4-GFP* transgenes. (A) Variability in angle between adjacent petals in

WT, *sep1-1*, *pSEP1*:*SEP1-GFP*_L22-3, *pSEP1*:*SEP2-GFP*_L13-1, *pSEP1*:*SEP2-GFP*_L13-2, *pSEP1*:*SEP3-GFP*_L14-1, *pSEP1*:*SEP3-GFP*_L14-4, *pSEP1*:*SEP4-GFP*_L15-7, *pSEP1*:*SEP4-GFP*_L15-8 (B) Coefficient of variation for number of *sep*als, for each genotype (C) Distribution of flowers with respect to number of *sep*als for each genotype.

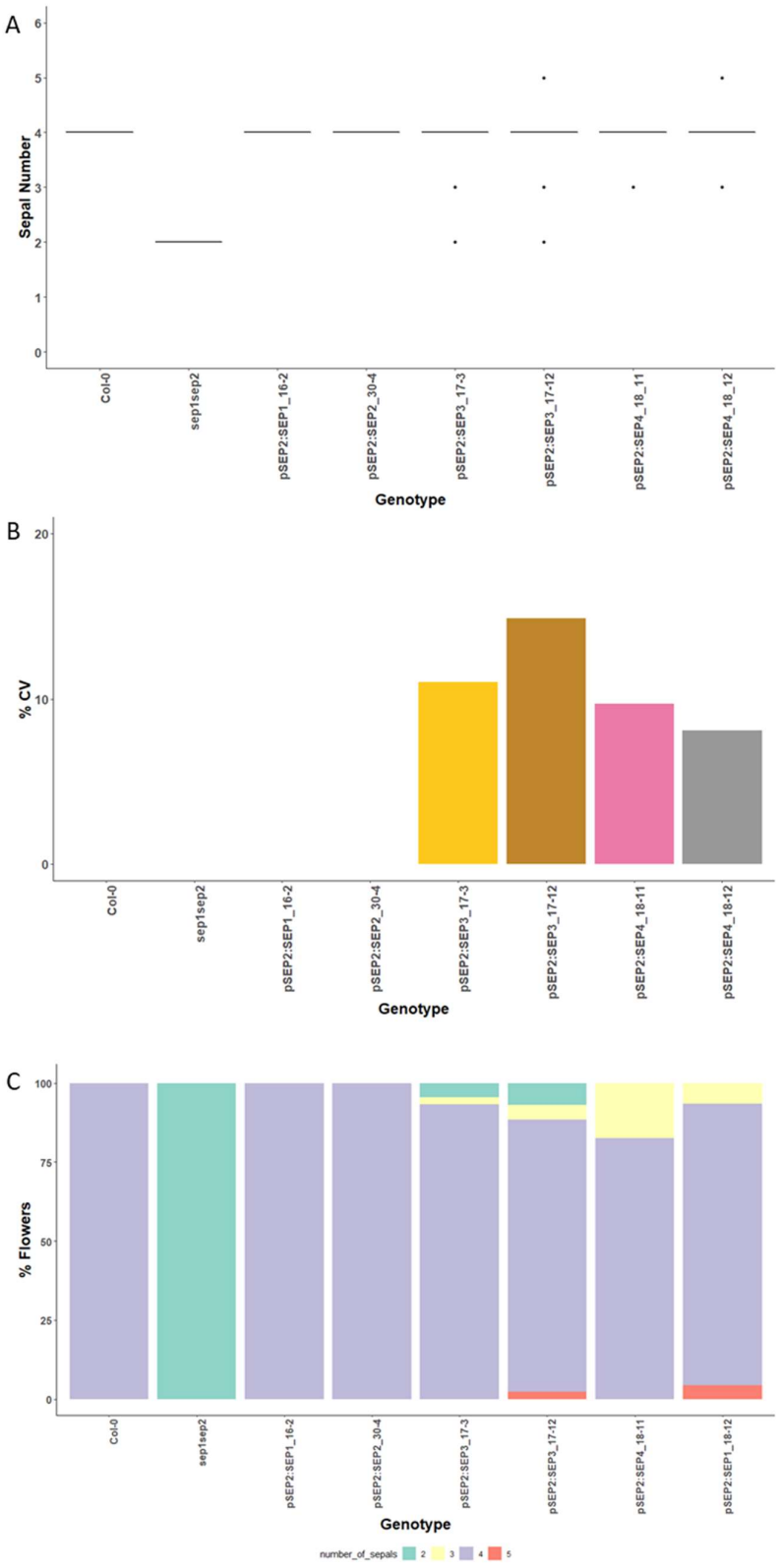

Figure 4-12: Complementation of supressed lateral *sep*al phenotype by *pSEP2*:*SEP1/2/3/4-GFP* transgenes. (A) Variability in angle between adjacent petals in

WT, *sep1-1*, *pSEP2*:*SEP1-GFP*_L16-2, *pSEP2*:*SEP2-GFP*_L30-4, *pSEP2*:*SEP3-GFP*_L17-3, *pSEP2*:*SEP3-GFP*_L17-12, *pSEP2*:*SEP4-GFP*_L18-11, *pSEP2*:*SEP4-GFP*_L18-12 (B) Coefficient of variation for number of *sep*als, for each genotype (C) Distribution of flowers with respect to number of *sep*als for each genotype.

4.7 Discussion

4.7.1 Growing plants in natural environments reveals hidden aspects of gene function

Plants grown in natural, real-world conditions experience incessantly changing environmental conditions. The environment varies not only due to the changing seasons but is also affected daily by multiple factors. Within a day, permutations and combinations of factors such as light intensity, spectrum of photosynthetic active light, UV-B, extreme temperatures, temperature variation, CO_2 levels, vapour pressure deficit, wind speed, and turbulence create a large variety in natural 'field' conditions. Exposure to such variable environmental conditions has the potential to strongly influence plant growth. Furthermore, as plants are sessile organisms, additional factors such as soil compaction, nutrient availability, and water supply contribute to random variability and stochasticity of growth conditions. Conducting experiments with too many random variables is difficult as the sheer number of treatments from combinations of different factors was challenging to design and execute. The complex nature of these experiments might impede data interpretation (Poorter et al., 2016). Although field experiments are routinely used for research in plant breeding and agronomy to great effect, they can limit molecular studies that require a more controlled approach. Although recent advances in crop modelling and high-throughput phenotyping offer promising methods to overcome these challenges, they are not feasible or available for all to use. Developmental research in plant sciences has been traditionally carried out by growing plants under controlled environmental conditions to overcome these problems. While studying developmental phenotype by performing expensive and time-consuming molecular and cellular analyses, it is essential to limit the number of factors to be considered that affect a particular phenotype. Growing plants in controlled environmental conditions limits the number of factors to be considered. It offers additional benefits by limiting variation and making the process of treatment and manipulation relatively easy. A large number of replicates can be evaluated by conducting experiments in controlled lab conditions to generate high-throughput and high-quality data.

Although such lab-based studies in controlled growth chambers offer benefits, it is not uncommon to find difficulties in extrapolating the results from these experiments to field conditions. Sometimes conditions used for a lab/glasshouse-based experiment are

scalable and correlate well with natural 'field' conditions; however, it is not rare to find no positive correlation between results of the same experiment carried out under lab, glasshouse, and field conditions (Bacilio et al., 2017). The use of controlled growth chambers to study development, physiology, and stress response offer valuable information. Nevertheless, it also constrains our understanding of how those plants grow and perform in real-world conditions. Large communities of plant scientists either work in the lab or the field depending on the traditional approach used to study the objectives of their interest. Each niche community has developed its concepts, protocols, and terminologies (Blum, 2014). However, the limited crosstalk between lab and field scientists might result in an undesirable cultural 'glass wall' (Kohler R.E., 2010), leading to oversight while designing experiments that might benefit from a different approach, mainly using natural growth conditions. Moreover, rules and regulations for studying mutants and transgenic plants sometimes make growing plants in natural environmental conditions difficult. Overall, these restrictions have impeded the number of studies that have evaluated the mutation-phenotype relationship in natural environments. Thus, mutations that exhibit a neutral or WT-like phenotype in a controlled environment but may show a different phenotype in response to environmental changes have remained largely unexamined.

Mainly while studying genes related to robustness, mutant phenotype may depend on specific environmental conditions and can be masked in controlled standard environments (Taylor et al., 2019). Robustness in biological systems is achieved through redundancy in duplicate genes or master regulators in the gene regulatory network (Bateson & Gluckman, 2012; Whitacre, 2012). Phenotypes associated with a mutation in a single gene belonging to a family of redundant genes are difficult to observe as the other genes compensate for gene disruption and buffer against any pernicious phenotype. Moreover, even if the single mutant shows a subtle phenotype, the probability of it being overlooked is very high as compared to the conspicuous phenotype exhibited by a double or higher-order mutant from the same gene family. Additionally, weak alleles produce residual protein that can mask phenotype, especially in ideal environmental conditions (Lloyd and Meinke, 2012). The mutation–phenotype relationship is further complicated by the complex relationships among genes that interact through multilevel networks to provide a robust output. Master regulators or network hubs that influence a large number of genes buffer against deleterious

phenotype. Environmental changes can affect this robustness such that mutations that are buffered in one state may be revealed when the state changes (Abley et al., 2016b; Masel & Siegal, 2009; Waddington, 1961).

So far, studies related to *sep* mutants from *A. thaliana* and other species were exclusively conducted in standard environmental conditions with the context of evaluating their role in flower development (Gao et al., 2010; Pelaz et al., 2000b; J. Zhang et al., 2018; Zhao et al., 2006). Moreover, *sep* mutant studies were restricted to controlled environment containment facilities due to the mutants being T-DNA insertion lines. In Arabidopsis, higher-order triple and quadruple *sep* mutants showed conspicuous phenotypes. In comparison, the single and double *sep* mutants appeared aphenotypic or showed subtle phenotype, suggesting that the duplicate *SEP* genes are functionally redundant (Jack, 2001). However, the interpretation that the *SEP* genes function completely redundantly is questionable for three reasons. Firstly, maintaining functional copies of four completely redundant *SEP* genes offers no selective advantage. Despite this, evolutionary analysis indicates that the *SEP* genes have been maintained in multiple copies in all extant angiosperms for millions of years. Secondly, the SEP genes have different expression patterns, that is, SEP1, SEP2, and SEP4 are expressed in all four floral whorls, while SEP3 is expressed only in whorls 1, 2, and 3 (Ditta et al., 2004; Flanagan & Ma, 1994; M. A. Mandel & Yanofsky, 1998; Savidge et al., 1995). Thirdly, *sep3-1* and *sep3-2* petals showed a subtle partial transformation to *sep*als, that was stronger in 35S::SEP3 antisense flowers, but was not observed in *sep1, sep2*, and *sep4* flowers (Pelaz, Gustafson-Brown, et al., 2001a). The difference in expression patterns and the independent phenotype reported for *sep3* suggest that these genes might have independent functions.

Previous studies from the Davies lab indicated that growing *sep* mutants under non-standard environmental conditions revealed distinct as well as overlapping phenotype. Single and double *sep* mutants showed organ specific phenotype, especially at elevated temperature (Biewers, 2014). When single and double *sep* mutants were grown in a screenhouse containment facility that allowed exposure to real-world environmental fluctuations, they showed variable phenotypes (Unpublished, Davies and Kauffman labs). These observations suggest that the duplicate *SEP* genes may have a possible relationship with regulating the robustness of flower development in Arabidopsis. Thus, this chapter aimed at identifying whether different *sep* mutant flowers showed distinct

and variable phenotype when subjected to variable temperature conditions and assessing whether they were truly functionally redundant.

4.7.2 Individual Arabidopsis SEPs show different phenotypes

Characterisation of *sep* single and double mutants described in Section 4.1 clearly disprove the functional redundancy of *SEP*s. These results show that *sep1* and *sep2* alleles exhibit a skewed petal phenotype with a higher penetrance in variable environment (Figure 4-3, Table 4.2). Whereas *sep3* and *sep4* showed environment-independent phenotypes. Flowers from *sep3-2* plants showed occasional development of *sep*alloid petals. *sep4-2* flowers showed additional *sep*als and petals (Section 4.1.2). Although these alleles have been studied before (Ditta et al., 2004; Jack, 2001; Pelaz, Gustafson-Brown, et al., 2001a), these phenotypes for the *sep* mutants were never described in literature. This could be due to the subtle nature of the single mutant phenotypes compared to the striking phenotype exhibited by the higher order mutants and mutants of A, B, and C activity genes. Moreover, although T-DNA insertion lines are gene-specific and stable mutants, they might show pleotropic effects (Monroe et al., 2020). Thus, it was important to ensure that the phenotypes observed in this study were specific to the loss of *SEP* function and were not results of a pleotropic effect. This was done by characterizing additional T-DNA insertion lines, i.e, *sep1-2, sep1-3, sep2-3, sep2-4,* and *sep4-1* (Table 4-2). Phenotypic characterisation of the new *sep* alleles reinforced the results obtained from the primary analysis. Additionally, complementation analysis for *sep1-1* and *sep2-1* was performed (Section 4.3.2). Successful complementation of *sep1* by *pSEP1::SEP1-GFP* and *sep2* by *pSEP2::SEP2-GFP* confirmed that the skewed petal phenotype was indeed linked to the loss of *SEP1* and *SEP2*.

The *sep*arate phenotypes demonstrated by individual *sep* mutants clearly indicate that *SEP1/SEP2* have functions *sep*arate from *SEP3,* and *SEP4.* These results are in accordance with multiple *SEP* genes from other species that have been reported to have *sep*arate functions. For instance, the four *SEP*s that have been identified from *Thalictrum thalictroides* (Ranunculaceae), an apetalous, early diverging eudicot, showed sub-functionalization leading to divergent functions (Soza et al., 2016). *ThtSEP1* and *ThtSEP2,* showed cadastral roles in determining the *sep*al-stamen and stamen-carpel boundaries, respectively. *ThSEP3*, a homologue of the Arabidopsis SEP3 functioned in determining carpel identity (Soza et al., 2016). Similarly, the five tomato

SEP homologues show overlapping as well as *sep*arate functions. The *SEP3* orthologue *LeTM5* is necessary for specification of whorls 2, 3, and 4. Downregulation of *LeTM5* leads to an increase in the floral meristem size along with an increase in the number of petals, stamens, and carpels (Pnueli et al., 1991, 1994). The *SEP1* orthologue *LeTM29* plays a role in floral meristem specification, *sep*al identity, and fertilization. Downregulation of *LeTM29* results in a phenotype affecting whorls 2, 3, and 4. Whorl 2 shows *sep*aloid petals; whorls 3 and 4 showed infertile organs that lead to development of parthenocarpic fruits (Ampomah-Dwamena et al., 2002). The other tomato SEP, *LeMADS-RIN*, is an orthologue of SEP4. The *rin* mutant plants displayed affected inflorescence determinacy along with enlarged *sep*als. The fruits from *rin* plants failed to ripen (Vrebalov et al., 2002). Two more tomato SEPs, *LeMADS1* and *SlMBP21* belong to the *FBP9/FBP23* subclade of *SEP*s. *SlMBP21* is involved in the development of the flower abscission zone. Antisense *SlMBP21* plants showed complete or partial disappearance of the abscission zone, along with jointless pedicels. Antisense *LeMADS1* plants showed normal pedicels but had enlarged *sep*als (Liu et al., 2014).

Similarly, the six orthologues of *SEP*s from Petunia viz. *FLORAL BINDNG PROTEIN 2 (FBP2), FBP4, FBP5, FBP9, FBP23*, and *pMADS12* show different gene expression patterns and protein interactions (Ferrario et al., 2003). *FBP2*, the *SEP3* homologue, functions in specifying the identity of whorls 2, 3, and 4 in Petunia (Ferrario et al., 2003). The *fbp2* mutant showed *sep*aloid petals with trichomes on both adaxial and abaxial sides, along with secondary flowers in whorl 3 (Vandenbussche et al., 2003). The *fbp5* mutant flowers showed reduced female fertility but were devoid of any morphological aberrations. However, the co-suppression double mutant *fbp2 fbp5* showed an increase in the *sep*aloid nature of petals compared to *fbp2*, the anthers were covered with *sep*al-like structures with trichomes, and a huge pistil with trichomes (Vandenbussche et al., 2003). This suggests that *FBP2* and *FBP5* show partial redundancy. Although the exact functions of *FBP4, FBP9, FBP23*, and *pMADS12* are not known, all Petunia SEPs have different spatiotemporal patterns of gene expression. For example, *FBP2, FBP5, FBP23*, and *pMADS12* are only expressed in the floral organs, while *FBP4* and *FBP9* are expressed in vegetative tissues as well. *FBP4* and *FBP23* are expressed in seed pods. *FBP5* and *pMADS12* are expressed in the inflorescence meristem, while *FBP2* is restricted to the central dome of the floral

meristem (Ferrario et al., 2003). These expression patterns suggest that these genes function in different tissues and at different stages of development, thereby implying that they are not fully redundant.

Right after a duplication event, generally the resultant duplicated genes have the same functions and thus, are considered to be redundant in theory. However, diversification of duplicate gene families may lead to sub-functionalisation or neo-functionalisation, resulting in them being only partially redundant or completely non-redundant. During sub- and neo- functionalisation, there is a possibility of the gene copies retaining a very similar sequence. Thus, a high percentage of sequence similarity does not necessarily imply functional redundancy, especially in genes comprised of multiple functional domains. For example, two closely related MADS-box genes *PLENA (PLE)* and *FARINELLI (FAR)* from Antirrhinum cannot functionally substitute for one another (Davies et al., 1999). *PLE* and *FAR* also showed different gene expression patterns as well as differences in protein interaction patterns (Bradley et al., 1993). The difference in their function can be attributed to a single amino acid change (Airoldi et al., 2010). Although the MADS-domain in Arabidopsis SEPs is highly conserved, the K-domain shows differences which might be associated with different functional roles of the SEP genes. Sub- and neo-functionalisation may also occur via mutations in regulatory sequences (Langham et al., 2004). This warrants further research into determining the cause underlying sub-functionalisation of Arabidopsis SEPs.

4.7.3 *SEP1* and *SEP2* function redundantly to govern robustness of decussate floral symmetry

Both *sep1* and *sep2* mutants show a subtle skewed arrangement of petals in ST. The variability of angle and the percentage of flowers with skewed petals both increase in *sep1* and *sep2* plants grown under VT (Section 4.2.1). Additionally, the phenotype was stronger in *sep1* compared to *sep2* (Section 4.2.1). The *sep1 sep2* double mutant showed a more intense version of the skewed petal phenotype, such that it was immeasurable in most flowers. Additionally, the angle between adjacent petals was found to be variable and the variability was increased in response to VT. The variability in distribution of phenotypes is often ignored due to the mean-centric approach used to quantify most phenotypes related to developmental biology (Geiler-Samerotte et al., 2013). However, to identify traits related to robustness, it is essential to identify mutants that affect the phenotypic variance (coefficient of variation, CV) while keeping the

mean constant (Boukhibar and Barkoulas, 2016). Mutant phenotypes generally tend to be more variable compared to the wild type (Waddington, 1942), which means that any mutant phenotype with a mean different from the wild type mean would be accompanied with changes in variance. This might lead to wrongly associating a phenotype with robustness. However, genuinely large changes in CV accompanied by a different trait mean could be still linked to robustness; in this case, it is important to identify the difference in phenotypic variability demonstrated by wild type and mutants (Levy and Siegal, 2008). With respect to the *sep1* and *sep2* skewed petal phenotype, the mean of the ABAP for a flower constituting of 4 petals will theoretically always be 90°. However, the individual ABAP was found to be variable in *sep1* and *sep2* mutant flowers. This indicates that the skewed petals phenotype in *sep1* and *sep2* is associated with robustness of decussate symmetry. Complementation of *sep1* by *pSEP1:SEP-GFP* and of *sep2* by *pSEP2:SEP2-GFP* led to decrease in variability of ABAP (Section 4.3.2). The data suggests that *SEP1* and *SEP2* might be involved in buffering the variability caused by stochastic environmental conditions to produce an ideal cruciferous flower. Functional redundancy confers developmental robustness upon a biological system as it provides back-up mechanisms that ensure production of a stable output by buffering the stochastic perturbations (Masel and Siegal, 2009). Biological systems are redundant at different levels, such as in cells, genes and regulatory elements (Wagner, 2007). For instance, in the nematode *Caenorhabditis elegans,* environmental perturbations affect the development of vulva. The anchor cell located above the P6.p cell can be mis-centered and the new anchor cell is established above the P5.p cell due to environmental variation. However, three competent cells P(3,4,8).p act redundantly to buffer the mis-centring thereby resulting in normal development of the vulva. Similarly, genetic redundancy can bestow robustness when a duplicate gene substitutes for a paralogue that is affected by genetic or environmental perturbations (Hsiao and Vitkup, 2008; Keane et al., 2014). Furthermore, redundant regulatory elements such as transcription factors act as 'master regulators' or 'network hubs' to avert massive changes in gene expression in response to environmental perturbations (Frankel et al., 2010; Perry et al., 2010).

The skewed petals in *SEP1* and *SEP2* also seem to affect the phyllotaxy at floral organ level. In Arabidopsis, the shoot apical meristem and inflorescence meristem have a spiral phyllotaxy wherein new leaves/flowers arise at 137.5˚ angle from the previous

one. There is a sudden transition from this spiral phyllotaxy to an opposite decussate phyllotaxy at the floral meristem level, such that four *sep*als and four petals are placed opposite each other (Bartlett and Thompson, 2014; Sun and Ito, 2015). The skewed petal phenotype of *sep1* and *sep2* mutants leads to a hypothesis that they are deficient in completing this transition. This functional deficiency is aggravated by VT. Ideally both genes are required to give more normality under fluctuating conditions, bestowing robustness upon flower development.

Loss of both *SEP1* and *SEP2* leads to suppression of lateral *sep*al development (Section 4.3). This phenotype is observed only in the double *sep1 sep2* mutants and not in the single *sep1* and *sep2* mutants. *pSEP1:SEP1-GFP* and *pSEP2:SEP2-GFP* transgenes complemented the suppression of lateral *sep*als phenotype in *sep1 sep2*. This suggest that *SEP1* and *SEP2* act redundantly to regulate lateral *sep*al expansion. As this phenotype is observed both in ST and VT, and does not show any variability, it does not conform to the definition of a trait associated with classical biological robustness (Levy and Siegal, 2008). This shows that SEP1/SEP2 regulate two *sep*arate processes in flower development, one that confers robustness upon the symmetry while other that regulates development of lateral *sep*als.

4.7.4 *sep3* and *sep4* phenotypes are not affected by environmental perturbations

As seen in Section 4.4, *sep3-2* flowers were mostly aphenotypic in both ST and VT conditions, except for the rare and occasional formation of early flowers with *sep*alloid petals. This suggests that the partial conversion of petals to *sep*al like structures in *sep3-2*, as previously reported could be associated with a particular environmental or developmental stage that could not be reproduced in our experiments. The strong phenotypes reported for *35S:SEP3* sense and *antisense* lines could be attributed to the constitutive expression leading to ectopic activation (Castillejo et al., 2005). However, this study aimed at only determining the molecular interactions of *SEP3.* Interestingly, most studies aiming to characterize the function and interactions of SEPs have been conducted by using SEP3 as a representative (Castillejo et al., 2005; Immink et al., 2009; Käppel et al., 2018; Kaufmann et al., 2009b; Lai et al., 2020; Melzer et al., 2009; Pelaz, Gustafson-Brown, et al., 2001a). The fact that *sep1, sep2,* and *sep4* showed more significant and different phenotypes compared to *sep3* highlight the necessity to include other SEPs in further studies.

Additionally, the extra organs in *sep4-1* and *sep4-2* mutants under ST as well as VT conditions point towards the role of SEP4 in regulating organ number. The increase in organ numbers could be either due to an increase in meristem size, increase in number floral meristem cells that turn into organ primordia, or decrease in the distance between organ primordia to accommodate additional primordia. *CLAVATA1-3 (CLV1-3)* genes that function in stem cell specification and regulating meristem size. Similar phenotypes showing increased floral organ numbers are observed in *clv* mutants; however, *clv* flowers show extra whorls as well as extra organs (Clark et al., 1996; DeYoung & Clark, 2008), which is not observed in *sep4. PERIANTHIA (PAN)* is a bZIP-transcription factor that regulates stem cell fate and determines floral organ patterning. *pan* mutants produce flowers with five *sep*als, five petals, five stamens and two carpels (Running and Meyerowitz, 1996). However, *sep4* flowers differ from *pan* as they show a variable number of *sep*als and petals, ranging from 5-7. SEP4 is required for specification of meristem identity as well as floral organ identity (Ditta et al., 2004). SEPs are involved in feedback regulation of *WUSCHEL (WUS)*, that is also regulated by *CLV*. However, direct interactions of *SEP4* and *CLV* genes are yet unknown. Similarly, *PAN* has been shown to act downstream of *AP1* and *AP2* and upstream of *AG*, the possibility of its interaction with *SEP4* is unknown (Running and Meyerowitz, 1996; Das et al., 2009). Interestingly, the members of the *miRNA164* family, viz., *miR164a, miR164b*, and *miR164c* redundantly control floral organ number. The *mir164abc* triple mutant showed an increased and variable number of perianth organs, but fewer stamens compared to the wild type (Sieber et al., 2007). Additionally, the size of organs varied, as well as, a reduction in fertility was observed. miR164 family contributes to the robustness of flower development by preventing fluctuations in target gene expression despite genetic noise and perturbations created by processes such as transcription and translation (Sieber et al., 2007).

4.7.5 SEP genes are partially redundant

The phenotypes observed in single *sep1* and *sep2* mutants and the *sep1 sep2* double mutant both indicate the *SEP1* and *SEP2* are functionally redundant. The lack of a significant phenotype in *sep3* and the extra floral organ phenotype in *sep4* shows that *SEP3* and *SEP4* are non-redundant with *SEP1/SEP2.* The promoter swap experiments showed that the skewed petal phenotype was complemented by *pSEP1:SEP1* and *pSEP1:SEP2* such that the complementation lines showed less variability in ABAP. Replacement of *SEP1/SEP2* by *SEP3* and *SEP4*, that is, *pSEP1:SEP3* and *pSEP1:SEP4* did not complement this phenotype. Thus, *SEP1* and *SEP2* genes are necessary for specifying the decussate symmetry in Arabidopsis petals. This suggests that the differences in the gene sequence are significant enough that *SEP3, SEP4* cannot substitute for *SEP1/SEP2* in this case. Thus, further research needs to be carried to determine which domain in *SEP1/SEP2* functions in regulating petal angle symmetry. In contrast, the suppression of lateral *sep*als phenotype was complemented by any *SEP* driven by *pSEP1* or *pSEP2* promoter, that is, *pSEP1:SEP1/2/3/4* and *pSEP2:SEP1/2/3/4*. This suggests that the activity of SEP1 and SEP2 in regulating lateral *sep*al development is either promoter dependent or is influenced by a conserved domain between all four SEPs.

5 Chapter 5: Targets of *SEP1* and *SEP2* associated with suppressed lateral *sep*als in *sep1 sep2*

5.1 Introduction

Flower development comprises different stages; initiation of flowering, floral meristem (FM) specification and formation, organ identity specification, and organ development. Different floral regulators hierarchically govern each stage. Genes that regulate FM formation and specify organ identity have been well studied well and reviewed (Weigel and Meyerowitz, 1994; Causier et al., 2010; Wellmer and Riechmann, 2010; Murai, 2013). Post organ identity specification, genes that govern organ polarity, boundaries, and cell division and expansion are essential for successfully developing flowers with precise size, shape, and symmetry. In Arabidopsis, genes from the HD-Zip III, YABBY and KANADI families have been reported to specify organ polarity in leaves and flowers (Bowman et al., 2002). The organ boundaries are established by the expression of boundary specific *CUP-SHAPED COTYLEDON 1/2/3* (*CUC 1/2/3*) and *JAGGED (JAG)* genes (Aida and Tasaka, 2006). An excellent example of genes associated with cell expansion and division regulating organ size and shape can be seen in *sep*als.

Once the *sep*al primordia are initiated, appropriate cell division and expansion is essential for *sep*al development. *FRILL 1* (*FRL1)* regulates *sep*al morphology by maintaining the mitotic stage during cell division, affecting the number of cell divisions and subsequent cell expansion (Hase et al., 2000). The size and curvature of *sep*als are regulated by giant cells found in the *sep*al epidermis. CDK inhibitors such as *KRP 1* and *LOSS OF GIANT CELLS FROM ORGANS (LGO)* control the cell cycle by stopping mitotic division so that the cell expands but fails to divide, resulting in giant cells (Bemis and Torii, 2007; Roeder et al., 2010). The stochastic patterning of giant and small cells contributes to ideal *sep*al size and shape. The identity of giant cells is controlled by the epidermal specification pathway that includes cell cycle genes such as *DEFECTIVE KERNEL 1 (DEK1), MERISTEM LAYER 1 (ATML1),* Arabidopsis *CRINKLY 4 (ACR4)* and *HOMEODOMAIN GLABROUS 11 (HDG11)* (Roeder et al., 2012). Apart from giant cells, *sep*al expansion is also regulated by mechanical feedback. Microtubules act as stress sensors and growth regulators for initiation and

termination of *sep*al expansion, guided by the tensile stress in the organ (Hervieux et al., 2016).

As described in Chapter 4, flowers from the *sep1 sep2* double mutant showed suppression of lateral *sep*als. The *sep*al primordia originate but fail to expand fully into a mature *sep*al in *sep1 sep2* flowers. This phenotype was absent in *sep1* and *sep2* single mutant flowers, comprising four *sep*als, suggesting that both *SEP1* and *SEP2* must be required for expression of genes underlying lateral *sep*al expansion. Lateral *sep*al development in Arabidopsis has been linked to the homeobox gene *PRESSED FLOWER (PRS)*. The flowers lack lateral *sep*als in *prs* flowers. However, unlike the *sep1 sep2* phenotype, the lateral *sep*al primordia do not form in *prs* (Matsumoto and Okada, 2001). *PRS* is involved in cell proliferation in lateral organs. Apart from *PRS*, little is known about the lateral axis dependent development of organs in the floral meristem.

On the contrary, genes related to adaxial-abaxial axis dependent organ formation have been well studied. *REVOLUTA (REV), PHABULOSA (PHB) AND PHAVOLUTA (PHV)* from the HD-Zip III subfamily is expressed on the adaxial side of floral organs, while *FILAMENTOUS FLOWER (FIL)* and *YABBY3 (YAB3)* are expressed on the abaxial side of floral organs (Sawa et al., 1999; Siegfried et al., 1999; Otsuga et al., 2001). The combinatorial expression of these genes specific to a side of the axis is necessary to establish correct organ polarity. Although these genes have been associated with lateral *sep*al development, their relationship with SEPs has not been explored. Moreover, SEP1 and SEP2 may govern lateral *sep*al development by regulating other genes. This warrants further investigation to identify genes regulated by SEP1 and SEP2 associated with lateral *sep*al development.

Several genes governing organ identity specification and further development have been identified through forward and reverse genetic approaches. A prominent example of this was identifying homeotic transcription factors from the ABCE model of flower development that specify floral organ identity in Arabidopsis and Antirrhinum (Bowman et al., 1989; Carpenter & Coen, 1990; Hill & Lord, 1989; Pelaz et al., 2000; Schwarz-Sommer et al.,1990; Yanofsky et al., 1990). Their immediate interactions in the gene regulatory networks (GRN) were identified through reverse genetics, and the network was further enriched by studying protein-protein interactions and expression

of downstream genes (Immink et al., 2010). Genes associated with organ polarity have been identified using similar approaches and methods (Kerstetter et al., 2001; Otsuga et al., 2001; Siegfried et al., 1999). However, little is known about the detailed mechanism and pathways through which these genes regulate the interaction and expression of downstream genes that contribute to flower development. In the past decade, studies using high-throughput omics methods such as RNA-seq and ChIP-seq have helped delineate the GRN and create a global view of molecular interactions during flower development. RNA-seq experiments have helped identify hundreds of genes associated with specific developmental stages, organs and cell types (Jiao and Meyerowitz, 2010; Zhang et al., 2015).

This chapter aimed to identify genes regulated by SEP1 and SEP2 involved in lateral *sep*al development. Targets of SEP1 and SEP2 was identified by performing RNAseq analysis. Differentially expressed genes (DEGs) in *sep1, sep2,* and *sep1 sep2* inflorescences was identified by normalisation to Col-0. Further, various strategies were used to focus on the genes most likely to function in flower and lateral *sep*al development. The role of a few selected target genes was validated by characterising phenotypes of their existing mutant lines or new KO mutants generated by using CRISPR/Cas9 genome editing.

Objectives

- To identify targets of SEP1 and SEP2 by using RNAseq analysis
- To determine which target genes of SEP1 and SEP2 are associated with suppression of lateral *sep*als in *sep1 sep2*
- To experimentally validate whether the selected target genes contribute to lateral *sep*al development.

5.2 Quality control for RNA-seq analysis

High-quality RNA was extracted from inflorescences of *sep1, sep2, sep1 sep2,* and Col-0 plants grown in standard conditions. The samples contained a mixture of stage 1-12 flowers and the floral meristem, but open flowers and large buds were excluded. The sample was thus considered an average of different flower developmental stages (Smyth et al., 1990). The RNA was used to prepare cDNA libraries and sequenced using high-throughput next-generation Illumina sequencing (Smyth et al., 1990). Each sequenced library yielded between 30 to 33 million reads of 76 bases each. The reads were aligned to the indexed Arabidopsis genome (v. TAIR 10, GFF3 annotation file) using the STAR aligner (Dobin et al., 2013). The TAIR10 genome annotation includes 33,602 genes, including 27,416 protein-coding genes. The libraries showed 70 to 75 % uniquely aligned reads (Table 3.6). The read alignments and gene expression patterns for each gene were compared between the mutant and wild-type inflorescences using Cuffdiff (Trapnell et al., 2013). The number of single-mapping overlapping reads for each gene were used to generate raw count-based and normalised expression values. Normalised expression values calculated for each gene included fragments per million (FPM) and fragments per kilobase million (FPKM), equal to FPM divided by the largest transcript size per gene in kilobases. In order to identify differentially expressed genes (DEG), the average FPKM values from mutant samples were compared to the average wild type FPKM to generate $\log_2$(fold change) values. A multiple-test corrected p-value (P_{adj}) of 0.01 was employed (Benjamini, 2010).

Table 5-1: Number of reads and percentage alignment with the indexed Arabidopsis genome for each sample. Three biological replicates of inflorescences from Col-0 (WT), *sep1-1, sep2-1*, and *sep1 sep2* were sequenced and analysed.

Sample	Replicate	Number of Reads (million)	% aligned
Col-0	1	31.69	74.56
Col-0	2	31.65	74.25
Col-0	3	31.79	73.91
sep1-1	1	31.14	74.34
sep1-1	2	31.75	73.76
sep1-1	3	33.71	70.74
sep2-1	1	31.35	72.46
sep2-1	2	31.24	74.78
sep2-1	3	31.79	73.34
sep1 sep2	1	31.27	70.45
sep1 sep2	2	30.63	71.34
sep1 sep2	3	30.79	73.45

Visualisation of data by using CummeRbund showed good quality, devoid of any erroneous points. Although CummeRbund is used to consolidate and organise the vast amount of data generated from CuffDiff, it produces many redundant graphs for each dataset. The global statistics and quality control for *sep1 sep2* normalised to Col-0 are shown below to represent the output obtained for all datasets.

Differentially expressed genes in *sep1 sep2* compared to Col-0 were visualised using a log adjusted P-value versus log fold-change scatter plot. Each point represents the statistical significance relative to the magnitude of differential expression for a single gene. The P-values have a negative transformation; thus, the data points corresponding to higher values along the y-axis have smaller P-values and are more statistically significant (points shown in red, Figure 5-1-A). The log fold-change along the x-axis shows substantial differences in expression levels, with data points closer to 0 representing genes with similar mean expression levels. The plot confirms the presence of statistically significant DEGs (with $-\log_{10}$(P-value) > -2) with large fold changes (FC

> 2) in *sep1 sep2* (Figure 5-1-A). The upregulated genes are shown towards the right of the axis, and the downregulated genes are towards the left.

The cross-replicate variability across Col-0 samples was found to be low, indicating good quality of RNA-seq data (Figure 5-1-B). The squared coefficient of variation (CV^2) is a normalised measure of variance between replicate values per condition across the range of FPKM estimates. The CV^2 was higher across *sep1 sep2* samples compared to Col-0, indicating the presence of significant DEGs. Additionally, both samples lacked very high CV^2 values, which indicated a low probability of erroneous differential expression. A higher degree of variability between replicate FPKM estimates can result in lower numbers of differentially expressed genes; however, this quality control step eliminated false DEGs from the data. Overall, the FPKM and FC values produced were confirmed to pass all quality control requirements and could be used for further analysis.

A principal component analysis of 5000 representative genes per sample showed that Col-0, *sep1*, *sep2*, and *sep1 sep2* samples formed *sep*arate clusters (Figure 5-1-C). However, all biological replicates of the samples clustered together, affirming good quality of data. Finally, a list of DEG, with FC and corresponding P and P_{adj}-values was generated. Genes with P_{adj}-values < 0.01 were considered to be statistically significant for this analysis. Overall, *sep1, sep2* and *sep1 sep2* showed 6440, 5231, and 2981 differentially expressed genes compared to Col-0.

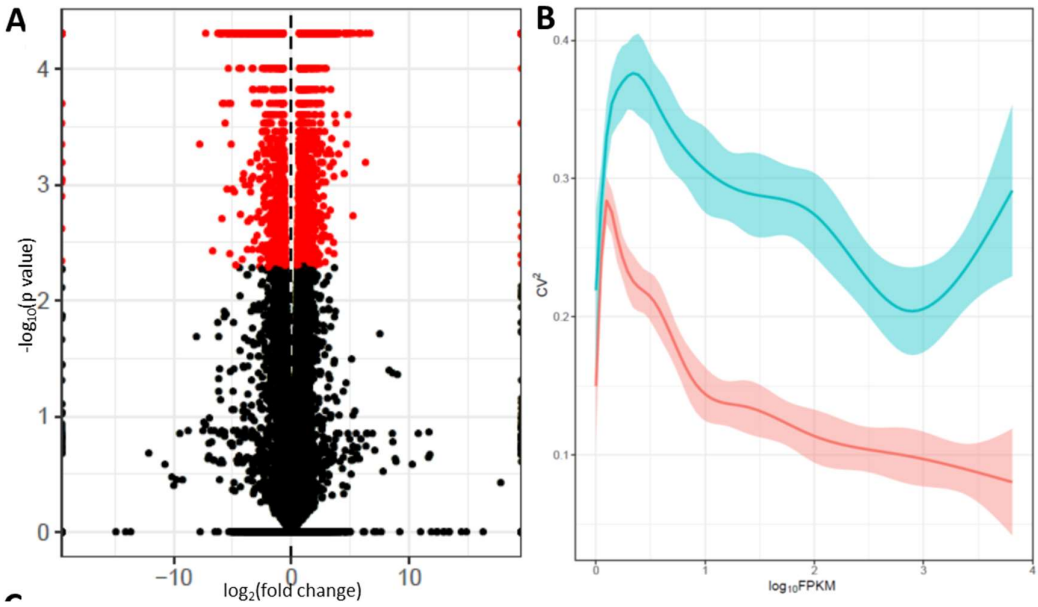

Figure 5-1**:** Quality control of RNAseq analysis by using CummeRbund visualisation (A) Volcano scatter plot of Col-0 and *sep1 sep2* samples with red dots showing statistically significant (P<0.01) genes that were differentially expressed in Col-0 and *sep1 sep2* (B) The coefficient of variation (CV^2) between empirical replicate FPKM values per sample, across the range of FPKM estimates for genes in Col-0 (pink) and *sep1 sep2* (blue) (n=3).

5.1 **Putative targets of SEP1 and SEP2 involved in lateral *sep*al development**

As described in Chapter 4, loss of either *SEP1* or *SEP2* resulted in the development of flowers with compromised decussate petal symmetry. *sep1* and *sep2* flowers showed a skewed arrangement of petals that indicated defective phyllotaxy. Loss of both *SEP1* and *SEP2* enhanced the penetrance of this phenotype. Additionally, *sep1 sep2* flowers showed a lack of fully developed lateral *sep*als. In order to identify genes associated with lateral *sep*al development from the extensive list of DEGs from in *sep1 sep2,* two strategies were used-

Strategy A: The hypothesis was that the suppression of *sep*als could exacerbate the skewed petal arrangement phenotype observed in the single mutant flowers. The loss of SEP1 and SEP2 may lead to more defects in the phyllotaxy, affecting the number of *sep*als. As this phenotype is observed in *sep1, sep2,* and *sep1 sep2*, the associated genes would be differentially expressed in all three mutants (Figure 5-2, strategy A). Thus, a list of 131 common DEGs between *sep1, sep2* and *sep1 sep2* was generated (Appendix 5-I). Out of these, 40 genes expressed in the floral tissues according to the eFP browser were selected. From this list, candidate genes associated with lateral *sep*al development were selected based on their annotated function on databases such as TAIR and Araport, gene ontology analysis, or available relevant literature (described in Section 0).

Strategy B: Alternative to strategy A, it was hypothesised that the suppression of lateral *sep*als phenotype was independent of the defective petal phyllotaxy observed in single mutants. Thus, genes exclusively differentially expressed only in *sep1 sep2* and NOT in *sep1* or *sep2* were selected for further analysis (Figure 5-2, Strategy B). *sep1 sep2* showed 2510 unique DEGs. In order to identify genes relevant to lateral *sep*al expansion, the first step was to identify genes specific to flower development. In order to achieve this, a *pin-1* RNAseq dataset was used to identify DEGs from *sep1 sep2* not expressed in *pin-1* (Appendix 5-II). The *pin-1* plants do not produce any flowers; they are less likely to express flower development-related genes. Although this is not a foolproof method, it narrowed down the list to 718 genes. This list of 718 genes was further narrowed by selecting genes that were regulated by prominent floral transcription factors SEP3, AP1, AP3, PI, AG, LFY or JAG, based on information from ChIP-seq datasets (Chen et al., 2018) (described in Section 0).

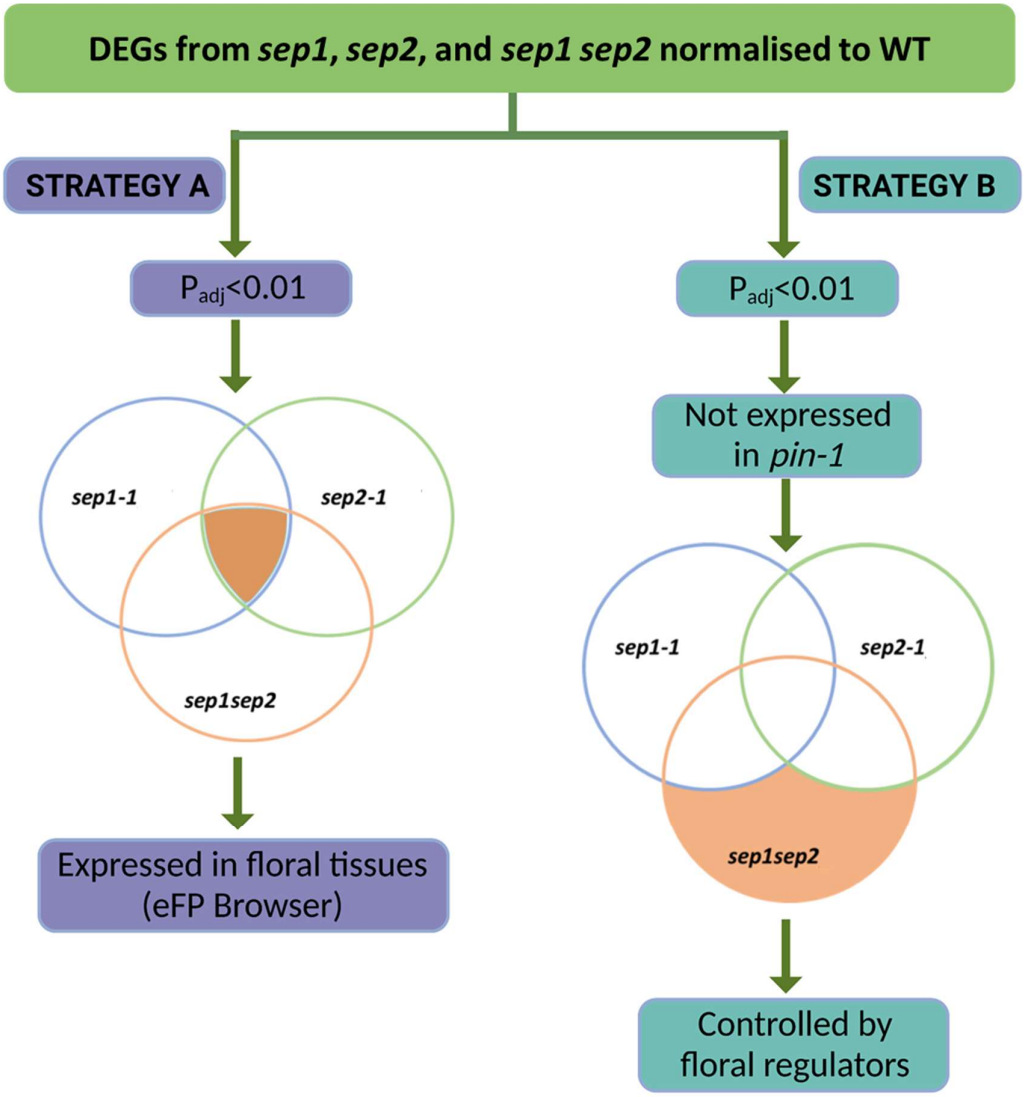

Figure 5-2: Schematic of approaches used to identify target genes that may play a role in developing lateral *sep*als in Arabidopsis flowers. DEGs from *sep1-1*, *sep2-1*, and *sep1 sep2* with P_{adj}<0.01 were selected. Strategy (A) identified DEGs common between *sep1-1*, *sep2-1*, and *sep1 sep2* and expressed in floral tissues; whereas, strategy (B) identified DEGs unique to *sep1 sep2* and reported to be controlled by other floral regulators.

5.1.1 Strategy A: Differentially expressed genes common in *sep1-1*, *sep2-1,* and *sep1 sep2*

131 DEGs were common between *sep1-1, sep2-1*, and *sep1 sep2* such that 34 genes were upregulated, and 97 genes were downregulated (Figure 5-3). Out of these, DEGs expressed in the flowers according to the Klepikova Atlas on the Arabidopsis eFP Browser 2.0 were selected for further analysis (Winter et al., 2007; Klepikova et al., 2016) (Appendix 5-I). A few genes from this list were found to have annotations related to reproduction and flower development. The conditions used to select candidate genes associated with lateral *sep*al development were the fold change in *sep1 sep2* and expression in floral meristems and organs. Candidate genes belonging to families with characterised functions were prioritised.

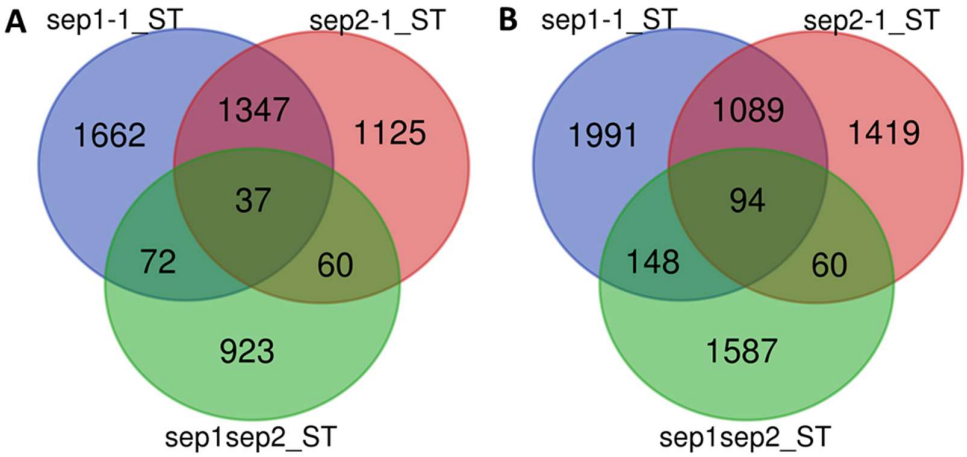

Figure 5-3: Number of common and unique differentially expressed genes between *sep1-1*, *sep2-1* and *sep1 sep2* (A) number of upregulated genes and (B) number of downregulated genes (P_{adj}<0.01)

From the 34 upregulated genes, *REPRODUCTIVE MERISTEM LIKE 3* (*REML3;* AT5G32460) was found to show the highest (28-fold) upregulation in *sep1 sep2. REML3* was expressed in the inflorescence meristem and all floral organs. *REML3* belongs to the transcription factor B3 family that encompasses distinctive gene families such as ARF (*AUXIN RESPONSE FACTOR*), AV (*LEAFY COTYLEDON2–ABSCISIC ACID INSENSITIVE3–VAL*), RAV (*RELATED TO ABI3* and *VP1*) and REM (*REPRODUCTIVE MERISTEM*) (Swaminathan et al., 2008). The REM family comprises around 76 genes, out of which only one, VERNALIZATION1 (VRN1), has been functionally characterised to maintain the vernalisation response and flowering

time in Arabidopsis (Y. Y. Levy et al., 2002). All characterised *REM* and *REM-like* genes are highly expressed in the shoot apical meristem (SAM), inflorescence meristem, and floral buds. Some are also known to be regulated by AP1, AP, PI, LFY, SVP, and AG (Mantegazza et al., 2014). However, the *rem1* mutant or ectopic expression of 35S::*REM1* have been reported to lack conspicuous developmental phenotypes (Franco-Zorrilla et al., 2002). This suggests that *REML3* could function in flower development in association with other floral genes.

The *F-BOX/RNI-LIKE (FBRI;* AT3G59190*)* gene was upregulated 3.1-fold in *sep1 sep2.* According to the eFP Browser, it is expressed in the SAM, inflorescence meristem, floral buds, and stamens and carpels in open flowers. *FBRI* is comprised of two distinct domains, the F-box and Leucine-rich repeats (LRR). F-box proteins are generally associated with regulating the activity of transcription factors and co-factors through ubiquitylation or proteasome-mediated degradation (Ni et al., 2004). Other F-box genes are known to regulate flower development; for example, *UNUSUAL FLORAL ORGANS* (*UFO*) interacts with AP1 and LFY to regulate the expression of *AP3* (Chae et al., 2008). Additionally, MADS-box proteins such as AG show interaction with LRR domains (Gamboa et al., 2001). Although the exact function of *FBRI* has not been deciphered yet, possessing these two domains highlights its potential for interaction with MADS-box proteins contributing to floral regulation.

PROLINE-RICH PROTEIN 2 (PRP2; AT2G21140*)* was found to be upregulated 2.47-fold in *sep1 sep2.* Plant *PRP*s function as cell wall proteins and contribute to development through spatio-temporal expression (Stein et al., 2011). *PRP2* was found to be expressed in young buds and anthers of open flowers. Although Arabidopsis *PRP2* has not been functionally characterised, its rice homolog, *OsPRP3,* plays a role in flower development and cold tolerance (Gothandam et al., 2009). This warrants further investigation into the role of *PRP2*.

O-ACYLTRANSFERASE or *FOLDED PETALS (FOP;* AT5G53390*)* was found to be expressed in the floral meristem, young buds, petals, and carpel in open flowers. It was upregulated 1.6 times in *sep1 sep2. FOP* encodes an ester synthase/diacylglycerol acyltransferase that is localised to the plasma membrane. It functions in petal elongation by acting as a lubricant in the petal epidermis (Takeda et al., 2013). These four genes, i.e., *REML3, FBRI, PRP2,* and *FOP,* were thought to be the most promising candidates

relevant to lateral *sep*al development from the list of genes upregulated in *sep1, sep2* and *sep1 sep2*

A few other genes, such as an *O-METHYLTRANSFERASE*, *PECTIN LYASE, EARLY LIGHT-INDUCABLE PROTEIN,* and *CYTOCHROME P450 CYP71B31*, would also make interesting candidate for further investigation, but there was insufficient time to follow these up. *O-METHYLTRANSFERASE (OMT;* AT5G53810*)* was upregulated 4.5-fold in *sep1 sep2.* The eFP browser showed that the gene was expressed exclusively in the petals. *OMT*s play a role in lignin biosynthesis, thereby controlling cell wall structure and composition. Moreover, OMTs methylate several different flavonoid compounds that play diverse roles, such as generating flower pigments, pollen tube growth, auxin transport, and antimicrobial activity, depending upon the tissue they are expressed in. Petal specific OMTs play a role in determining petal structure by modulating cell wall composition, pigmentation, and fragrance (Ibrahim et al., 1998; Fellenberg et al., 2012).

Similarly, *PECTIN LYASE* (AT1G60590) is another cell wall modifying enzyme that may affect organ initiation, expansion, and rigidity (Xiao et al., 2014). It was found to be expressed exclusively in the petals. Although these genes have functions linked to cell wall modification and cell expansion, they were not expressed in the *sep*als and thus, were not pursued further. Other genes from this list include *EARLY LIGHT-INDUCABLE PROTEIN* (AT3G22840) and *CYTOCHROME P450 CYP71B31* (AT3G53300), which showed petal-specific expression too. However, as these two genes have multiple functions in photosynthesis, hormone regulation, and metabolic regulation, they were not considered for further studies.

Table 5-2: Selected upregulated genes common in *sep1-1*, *sep2-1*, and *sep1 sep2* inflorescences, sorted in descending order of fold change (FC) in *sep1 sep2*. Genes highlighted in pink were used as candidates in further experiments

Gene ID	Annotation	FC *sep1-1* ST	FC *sep2-1* ST	*FC sep1 sep2* ST	Expressed in flowers
AT5G32460	*REPRODUCTIVE MERISTEM LIKE 3*	58.96	2.47	28.48	Yes
AT5G53810	*O-METHYLTRANSFERASE*	138.44	80.01	4.54	Yes
AT3G59190	*F-BOX/RNI-LIKE*	1.80	2.46	3.16	Yes
AT1G60590	*PECTIN LYASE*	2.84	2.51	2.72	Yes
AT2G21140	*PROLINE-RICH PROTEIN 2 (PRP2)*	2.23	1.73	2.47	Yes
AT3G22840	*EARLY LIGHT-INDUCABLE PROTEIN*	2.88	3.68	2.10	Yes
AT3G53300	*CYTOCHROME P450 CYP71B31*	99.31	93.14	2.06	Yes
AT5G53390	*O-ACYLTRANSFERASE (FOLDED PETALS)*	1.55	2.07	1.67	Yes

From the 97 downregulated genes commonly in *sep1*, *sep2*, and *sep1 sep2*, 49 were expressed in the inflorescence meristem and floral organs according to the eFP Browser Although these genes were downregulated in all three genotypes, the fold change was not significantly lower in *sep1 sep2.* None of the downregulated genes showed gene ontology corresponding to reproduction or flower development. Thus, to identify promising candidate genes associated with lateral *sep*al development, genes that could be linked with cell development, transcription regulation or auxin signalling were found by manually going through the annotation files.

Out of the 49 downregulated genes, *LOB DOMAIN CONTAINING PROTEIN 41* (*LBD 41 or ASL38;* AT3G02550) was a promising candidate due to its interactions with genes specifying organ primordia initiation as well as organ polarity. Members of the *LATERAL ORGAN BOUNDARIES (LOB)* domain *(LBD)* family are expressed at the SAM and organ primordia boundary. LBD 41 is known to interact with TOPLESS, TPR 1, TPR 2, and TPR 3 and other proteins such as SUMO 1, SUMO 3, and WSIP 2 that contribute to the TPL complex (Causier et al., 2012). The TPL complex is involved in diverse functions such as meristem maintenance, auxin signalling, initiation of flowering, and defence response. Additionally, *LBD 41* is involved in adaxial-abaxial patterning in lateral organs (Y.-B. Wang et al., 2015). Other members of the LBD

family include *ASYMMETRIC LEAVES 1* (*AS1*) and *AS2,* which repress class I *KNOX* genes to initiate organ primordia (Ha et al., 2007). Thus, *LBD 41* makes an attractive candidate related to the development of lateral *sep*als in *sep1 sep2.* Similarly, *MYB 77* (AT3G50060), a gene found in the TOPLESS interactome and abscisic acid interaction network, was downregulated in *sep1, sep2* and *sep1 sep2* (Causier et al., 2012; Carianopol et al., 2020). Thus, MYB 77 was selected as a candidate for further studies.

REGULATOR OF CHROMATIN CONDENSATION 1 (RCC 1; AT5G11580*)* was downregulated 0.68-fold in *sep1 sep2. RCC 1* is involved in cell cycle regulation. It acts as a signal to inhibit mitosis (Dasso, 1993). Although *RCC 1* is not well-characterised in Arabidopsis, other genes related to cell cycle regulation, such as *ATML 1, FRIL 1* and *LGO,* have been associated with *sep*al development (Roeder et al., 2010, 2012). This supports the likelihood of *RCC 1* being involved in lateral *sep*al development and, thus, was selected for further studies. Similarly, *ETHYLENE RESPONSIVE ELEMENT BINDING FACTOR 1 (ERF1;* AT4G17500), a member of the *AP2/ERF* transcription factor family, was downregulated 0.51-fold in *sep1 sep2. ERF1* and the floral homeotic gene *APETALA2 (AP2)* are known to regulate each other mutually. *AP2* is necessary for *sep*al specification, but it also regulates other floral homeotic genes such as *AG*. Thus, *ERF1* was considered to be an essential candidate for experimental validation. Other interesting genes such as *ACTIN-RELATED PROTEIN 9* (*ARP9*; AT5G43500)*, 1-AMINOCYCLOPROPANE-1-CARBOXYLIC ACID SYNTHASE 6* (*ACS6*; AT4G11280)*, INTEGRASE* (AT5G61590)*, and CML 42* (AT2G46600) were also related to functions of interest. However, these genes are a part of large gene families and are associated with multiple functions such as phytohormone signalling and cell structural regulation. As mutants of these genes were likely to have no significant phenotyping as they were parts of large gene families, they were not chosen for further experimental validation.

Table 5-3: Selected downregulated genes common

: Selected downregulated genes common in *sep1*, *sep2*, and *sep1 sep2* inflorescences, sorted in descending order of fold change (FC) in *sep1 sep2*. Genes highlighted in pink were used as candidates in further experiments

Gene ID	Annotation	FC *sep1*	FC *sep2*	FC *sep1 sep2*	Expressed in flowers
AT3G02550	*LOB DOMAIN CONTAINING PROTEIN 41*	-1.38	-3.45	-0.68	yes
AT5G11580	*REGULATOR OF CHROMOSOME CONDENSATION 1 (RCC1)*	-2.31	-1.32	-0.64	yes
AT5G43500	*ACTIN-RELATED PROTEIN 9*	-2.11	-1.20	-0.58	yes
AT4G11280	*1-AMINOCYCLOPROPANE-1-CARBOXYLIC ACID SYNTHASE 6*	-4.24	-4.89	-0.55	yes
AT3G50060	*MYB 77*	-5.59	-4.76	-0.55	yes
AT5G61590	*INTEGRASE*	-1.93	-1.89	-0.55	yes
AT2G46600	*CML 42*	-2.67	-2.71	-0.53	yes
AT4G17500	*ETHYLENE RESPONSIVE ELEMENT BINDING FACTOR 1*	-5.39	-6.33	-0.51	yes

5.1.2 Strategy B: Targets of SEP1 and SEP2 that are differentially expressed only in *sep1 sep2*

The previous section focused on identifying putative genes related to lateral *sep*al development that were commonly differentially expressed in *sep1-1*, *sep2-1*, and *sep1 sep2.* However, the expansion of lateral *sep*als was suppressed only in *sep1 sep2* and not in the single mutants. Thus, it was essential to sift through DEGs unique to *sep1 sep2.* As SEP1 and SEP2 are functionally redundant, it can be assumed that common targets of both SEP1 and SEP2 will not be differentially expressed on the loss of only SEP1 or SEP2. That is, expression of either SEP1 or SEP2 should be enough to regulate the expression of these common targets. However, loss of both SEP1 and SEP2 would lead to differential expression of these target genes.

Determination of DEGs unique to *sep1 sep2* presented many candidate genes that were difficult to examine manually. Thus, a number of parameters were used at different steps to obtain maximum relevant information from this dataset. 1350 DEGs showed a significant P-value (P_{adj}<0.01). GO analysis of these DEGs revealed that they were mapped to specific biological processes such as reproduction (GO:0000003), reproductive process (GO:0022414), developmental process (GO:0032502), and growth (GO:0040007) (Figure 5-4-A). Genes such as *YABBY1, CRABSCLAW, OLEOSIN*s, and *GIBBERELLIN RECEPTOR 18* were mapped to reproduction. Additionally, the developmental process included *TRICHOME DIFFERENTIATION PROTEIN GL1,* various transcription factors such as MYB23, *B-BOX ZINC FINGER 24* and *18,* and *GRF1-INTERACTING FACTOR 1.* The GO analysis also shed light upon different classes of proteins that comprised the DEGs (Figure 5-4-B). Most proteins belonged to relevant classes such as metabolite interconversion enzyme (PC00262), gene-specific transcriptional regulator (PC00264), transporter (PC00227), protein modifying enzyme (PC00260), chromatin/chromatin-binding (PC00077), and protein-binding activity modulator (PC00095). The transcriptional regulators included a variety of Homeobox Leucine Zipper, Myb, WRKY, Ethylene response factor and MADS-box TFs. Other regulatory proteins such as histone-binding or centromere-binding proteins mapped to the class chromatin/chromatin-binding proteins. Additionally, the DEGs included transmembrane proteins such as *POLLEN RECEPTOR-LIKE KINASE 2*, cell wall and structural proteins such as *EXTENSIN3*,

calcium-binding proteins, and different ribosomal proteins. This suggests that both SEP1 and SEP2 together regulate a collection of genes governing flower development.

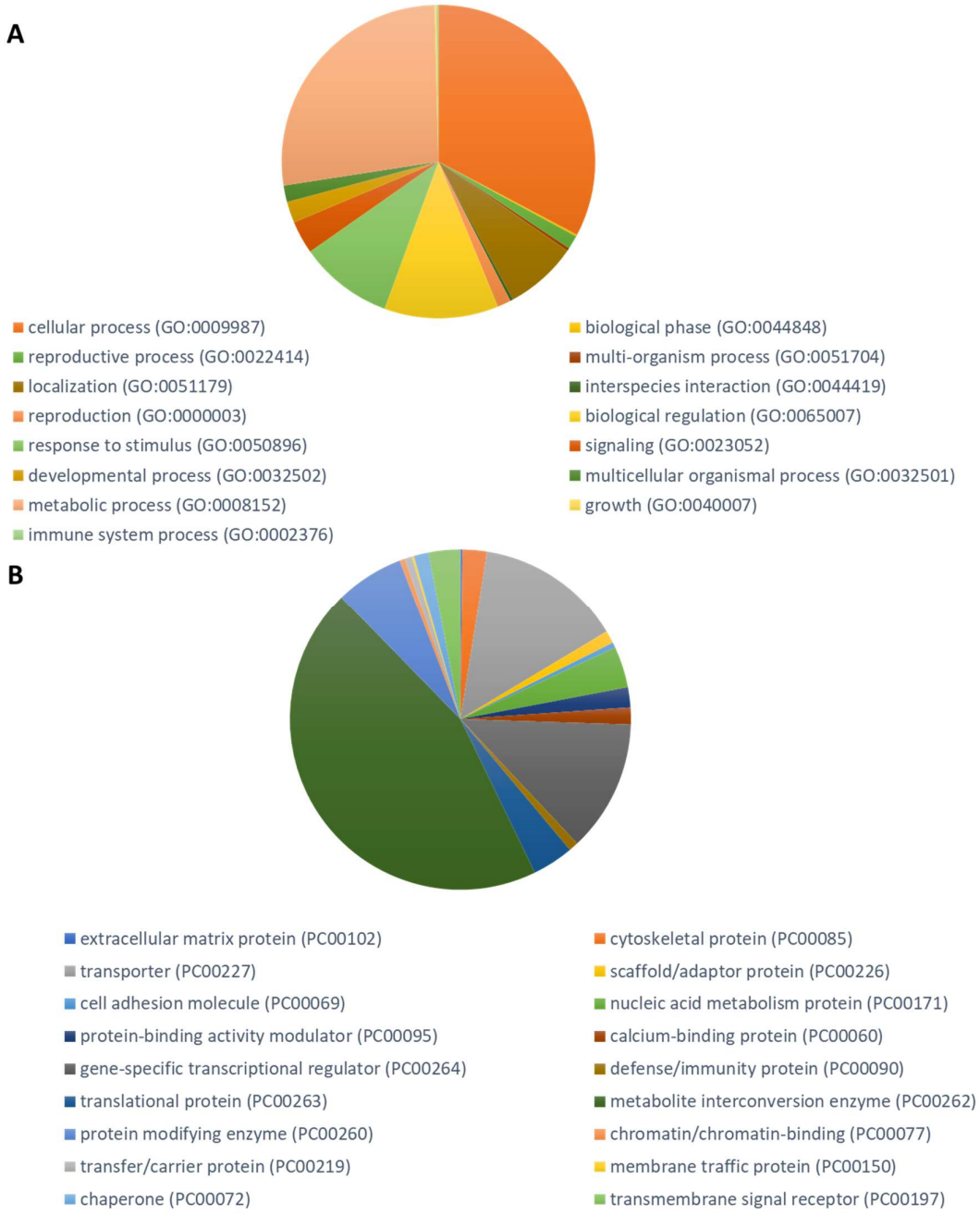

Figure 5-4: Gene Ontology analysis of DEGs from *sep1 sep2* (A) distribution of genes enriched in specific biological processes and (B) distribution of genes mapping to specific protein classes.

To narrow down the number of DEGs to be examined, 718 genes that were not expressed in the *pin1* dataset, that is, were largely flower specific, were selected. The exclusion of differentially expressed genes in *sep1-1* and *sep2-1* led to a dataset of 299 upregulated genes and 287 downregulated genes unique to *sep1 sep2.* To further focus on genes that were related to flower development, a ChIPseq dataset of targets of floral regulators was obtained (Chen et al., 2018). This led to the identification of 178 upregulated (Appendix 5-III) and 246 downregulated (Appendix 5-IV) DEGs controlled by different floral regulators.

Table 5-4: Selection criteria for candidate genes to generate more insight into the role of SEP1 and SEP2 in specifying lateral *sep*als

Selection Factor	**Np. of genes**	
Padj_value<0.01	1350	
Not expressed in *pin*	718	
	Upregulated	Downregulated
	341	377
Not DE in *sep1-1* and *sep2-1*	299	287
Controlled by a floral regulator	178	246

The candidate DEGs obtained were either regulated by LFY, SVP, BLR and ETT, indicating association with initiation of flowering, or showed interaction with ABCE TFs (AP1, AP2, AP3, PI, AG, SEP3), suggesting that they functioned in floral organ initiation and development. Out of the top 20 upregulated candidates, four well-characterised genes were recognised. These included *STERILE APETALA (SAP), NUBBIN/JAGGED-like (NUB), TERMINAL EAR1-LIKE 2 (TEL2),* and *UNUSUAL FLORAL ORGANS (UFO)* (Table 5-5).

NUBBIN (NUB) or *JAGGED-like* functions with *JAGGED (JAG),* a regulator of lateral organ growth (Dinneny et al., 2006; Ha et al., 2007). A mutation in *JAG* results in conspicuous *sep*al and petal phenotypes, while a phenotype for *nub* has not been described in the literature. However, *NUB* is expressed clearly in lateral organs on the interior adaxial side. Together, *NUB* and *JAG* regulate the number of cell layers and promote the differentiation of adaxial-abaxial cells (Dinneny et al., 2004). As *sep1 sep2*

flowers lack proliferation of lateral *sep*als, *NUB* proves to be an excellent candidate that could be involved in this GRN.

UNUSUAL FLORAL ORGANS (UFO) is required for normal patterning and growth in the floral meristem. It regulates the expression of AP3 in conjugation with LFY and regulates complex mechanisms such as meristem and organ primordia fate (Wilkinson and Haughn, 1995). Loss of function *ufo-1* flowers show altered organ numbers in all whorls. *STERILE APETALA (SAP)* or *SUPPRESSOR OF DA1 (SOD3)* is an F-box gene that regulates meristem proliferation and organ size by regulating the stability of PEAPODs transcription regulators. SAP forms a repressor complex with PEAPODs, KIX, and TOPLESS to control organ growth (Li et al., 2018). It also affects the organisation of floral whorls. *sap* flowers show carpelloid *sep*als, short or absent petals, and degenerated anthers (Byzova, Franken, , & 1999, 1999). Thus, *UFO* and *SAP* are crucial nodes in the SEP1/SEP2 gene network.

Other upregulated genes such as *TASTY, ERF15, MYB20, IAA29, GA2OX4,* and *LFY* also made exciting candidates. *TASTY* (AT1G54040), encoding for an epithiospecifier protein, was exclusively expressed in *sep*als according to the Klepikova Atlas. Although TASTY is mainly known to function in pathogen resistance and leaf senescence, it also interacts with RACK1, a WD40 repeat-containing protein that regulates gibberellin sensitivity and functions in flowering (Chen et al., 2006). *ERF15* (AT2G31230) is an AP2/ERF transcription factor that interacts with *PHYTOCHROME AND FLOWERING TIME 1* (*PFT1*). *MYB0* encodes GL1, a protein that is linked with trichome development. MYB0 interacts with other proteins involved in trichome development, such as GLABRA, GL3, JAZ, and DELLA. MYB0 also interacts with *GIBBERELLIC ACID INSENSITIVE 1 (GAI 1)* and *REPRESSOR OF GAI 1 (RGA1)* to regulate flowering. Other genes such as *IAA29* and *GA2OX4* showed annotations associated with auxin and gibberellin production, respectively. Most interestingly, the floral meristem identity control gene, *LEAFY,* was found to be upregulated in *sep1 sep2. LEAFY* interacts with AP1 to specify the floral meristem. It also regulates the expression of AP3, thereby regulating the B-function. Moreover, LEAFY interacts with BRM and UFO to specify organ boundaries and polarity. Although *LEAFY* makes an interesting candidate, *lfy* mutants show a severe phenotype of transforming flowers to inflorescence shoots. This would interfere with the objective of testing targets of SEP1

and SEP2 associated with lateral *sep*al development. Thus, *LEAFY* was not selected for further experiments.

Table 5-5: Selected upregulated candidate genes unique to *sep1 sep2* that are not expressed in *sep1-1* and *sep2-1* and interact with floral regulators

Gene ID	Annotation	FC *sep1 sep2*	Regulated by
AT1G54040	*TASTY*	63.313	ETT
AT2G31230	*ERF15*	12.214	AP1, AP2, BLR, ETT, LFY, RGA, SEP3
AT3G27920	*MYB0*	9.574	AG, AP3, BLR, JAG, PI, RGA, SEP3
AT5G35770	*SAP*	6.516	AG, AP1, AP3, BLR, ETT, PI, SEP3
AT1G13400	*NUB*	5.752	AG, AP1, AP3, BLR, PI, SEP3
AT1G67770	*TEL2*	5.612	AG, AP1, AP3, BLR, LFY, PI, SEP3
AT1G30950	*UFO*	4.981	AG, AP1, AP3, BLR, PI, SEP3
AT4G32280	IAA29	3.95	AP1,BLR,ETT,JAG,SVP
AT1G47990	GA2OX4	3.89	AG,AP2,AP3,BLR,LFY,PI,RGA,SEP3,SOC1
AT5G61850	LEAFY	3.49	AP1,AP3,BLR,ETT,JAG,LFY,PI,RGA,SEP3

Out of the top downregulated candidates, only two genes, *REPRESSOR OF GA1-like 2 (RGL2)* and *APETALA1 (AP1),* were well characterised (Appendix 5-IV). *RGL2* is a DELLA protein that regulates gibberellic acid response and represses cell proliferation and expansion (Tyler et al., 2004). It also represses GA-induced flower initiation. *RGL2* also regulates the floral homeotic genes via GA signalling (Yu et al., 2004). Thus, by regulating *RGL2* expression, SEP1 and SEP2 have control over GA mediated flower development. The other significant gene downregulated in *sep1 sep2* is *AP1*. *AP1* plays many vital roles, from specifying the floral meristem, initiation of flowering to specifying A-activity in floral organ specification and development. AP1 interacts with many floral regulators, such as AP1 itself, FLM, LFY, CAL, SVP, AP2, AP3, PI, and SEP3 (Chen et al., 2018; Pelaz, Gustafson-Brown, et al., 2001a). It also self regulates through a feedback mechanism. Along with *AP1, SEP3* was also found to be downregulated in *sep1 sep2*. The regulation of *AP1* and *SEP3* by SEP1 and SEP2 emphasises the complexity of the GRNs associated with flower development.

Table 5-6: Selected downregulated candidate genes unique to *sep1 sep2* that are not expressed in *sep1-1* and *sep2-1* and interact with floral regulators

Gene ID	Annotation	FC	Regulated by
AT3G53420	PIP2A	-0.73	BLR, FLM, LFY, RGA, SEP3, SVP
AT1G12440	A20 zinc finger	-0.73	BLR, ETT, FLM, LFY, RGA, SEP3, SVP
AT4G18970	GDSL-like Lipase	-0.72	AG, SEP3
AT1G69120	AP1	-0.69	AG, AP1, AP2, AP3, BLR, ETT, FLM, JAG, LFY, PI, SEP3, SVP
AT1G24260	SEP3	-0.68	AG,AP1,AP2,AP3,BLR, ETT,FLC,FLM,JAG,LFY,PI,RGA,SEP3,SOC1,SVP
AT2G13680	callose synthase 5	-0.67	LFY
AT5G13400	Major facilitator protein	-0.64	AG,AP1,AP2,AP3,BLR, ETT,JAG,PI,SEP3
AT2G46720	3-ketoacyl-CoA synthase 3 (KCS 13)	-0.62	AP3,BLR,ETT,PI,SEP3
AT2G32530	cellulose synthase-like B3	-0.61	BLR,FLM,SEP3
AT1G33240	GT-2-like 1 (GTL1)	-0.53	AP1,AP2,BLR,ETT,FLM,JAG,LFY,RGA,SEP3

Table 5-7: Selected genes for experimental validation

Gene ID	Gene Name	FC *sep1* *sep2*	Function	Homologue	Function of gene/ homolog	Reference
AT5G32460	*REPRODUCTIVE MERISTEM LIKE 3*	28.48	Unknown	*VERNALISATION 1*	regulates flowering time	Levy et al., 2002
AT3G59190	*F-BOX/RNI-LIKE*	3.16	Unknown	-	-	-
AT2G21140	*PROLINE-RICH PROTEIN 2*	2.47	Unknown	OsPRP3	Flower development	Gothandam et al., 2009
AT5G53390	*O-ACYLTRANSFERASE (FOLDED PETALS)*	1.67	Petal elongation	-	-	Takeda et al., 2013
AT5G35770	*STERILE APETALA*	6.51	Regulates meristem proliferation and organ size	-	-	Li et al., 2018
AT1G13400	*NUBBIN*	5.75	Adaxial side specification	JAGGED	Homolog *JAGGED* - Adaxial/abaxial polarity specification	Dinneny et al., 2006
AT1G67770	*TERMINAL EAR1-LIKE 2*	5.61	Meristem indeterminacy	*ZmEar1*	leaf development and tassel feminisation	Anderson et al., 2004; Charon et al., 2012
AT1G30950	*UNUSUAL FLORAL ORGANS*	4.98	Meristem identity and organ primordia fate	-	-	Wilkinson and Haughn, 1995
AT3G02550	*LOB DOMAIN-CONTAINING PROTEIN 41*	-0.68	Adaxial-abaxial organ polarity	-	-	Ha et al., 2007
AT5G11580	*REGULATOR OF CHROMOSOME CONDENSATION 1 (RCC1)*	-0.64	Cell cycle regulation(Dasso, 1993)	-	-	

AT3G50060	*MYB 77*	-0.53	Unknown	MYB family	Development, metabolism, response to stress	Dubos et al., 2010
AT4G17500	*ETHYLENE RESPONSIVE ELEMENT BINDING FACTOR 1*	-0.51	Regulation of AP2	ERF family	Transcription activation or repression	Fujimoto et al., 2000; Ogawa et al., 2007
AT3G53420	*PIP2A*	-0.73	Cell wall ultrastructure and plasma membrane traffic	-	-	Thompson and Wolniak, 2008
AT1G12440	*A20 zinc finger*	-0.73	Unknown	A20/AN1 OSDOG	Regulates cell elongation	Liu et al., 2011
AT4G18970	*GDSL-like Lipase*	-0.72	Unknown	GDSL lipase family	Regulation of GA signalling in epidermal cells	Rombolá-Caldentey et al., 2014
AT3G03450	*REPRESSOR OF GA1-like 2*	-0.70	Cell proliferation and expansion	-	-	Tyler et al., 2004

5.3 Experimental validation of putative candidate genes involved in lateral *sep*al development

The different strategies used to identify DEGs from *sep1 sep2* led to selecting 16 genes putatively associated with lateral *sep*al suppression. However, the exact function of some of these genes is unknown. Thus, it was crucial to evaluate the function of the selected genes in *sep1 sep2* experimentally. It was hypothesised that (i) generation of KO mutants of selected upregulated genes in *sep1 sep2* background would reverse the suppression of lateral *sep*als and lead to the formation of four fully developed *sep*als; and (ii) existing mutants of the selected down-regulated genes would show a phenotype similar to *sep1 sep2*, that is, suppressed lateral *sep*als. Eight upregulated genes in *sep1 sep2* were knocked out (KO) in the *sep1 sep2* background.

5.3.1 Generation of KO mutants of selected candidate genes upregulated in *sep1 sep2* by using CRISPR/Cas9 editing

Gene KO studies are valuable components of the functional genomics toolbox and are essential in determining the function of genes. In this study, we aimed to determine whether the function of selected upregulated genes from strategies A and B were associated with lateral *sep*al development in *sep1 sep2*. The number of *sep*als in a triple mutant consisting of KO mutants of a selected upregulated gene, *sep1,* and *sep2* (for example, *reml3 sep1 sep2*) was evaluated to determine if the lateral *sep*al suppression phenotype seen in *sep1 sep2* was rescued. The simplest and most efficient way of performing a triple KO experiment, within a limited time frame, was by using the CRISPR/Cas9 system to KO one gene within a homozygous and stable *sep1 sep2* double T-DNA mutant. Thus, a single guide RNA (sgRNA) was designed for each target gene using the CCTop tool (Table 5-8). The sgRNA protospacer was designed to be 20 nucleotides long with a GC content between 40-60%. The sgRNAs were selected such that they targeted the first exon of the selected gene with the number of mismatches limited to <4. It was confirmed that the sgRNA did not have any off-targets in Arabidopsis by using the CCTop off-target prediction tool (Labuhn et al., 2017) and running BLAST search on the TDNA Express website. However, sgRNAs for two genes, *FOP* and *PRP2,* had off-targets due to the unavailability of another suitable and efficient sgRNA (Table 5-8). FOP-sgRNA showed AT4G39420, a protein of uncharacterised function, as an off-target with more than 4 mismatches, thereby reducing the possibility of being targeted.

Similarly, PRP2-sgRNA showed AT2G42200 (*SPL9)* as an off-target with 4 mismatches. *SPL9* (squamosa promoter binding protein-like 9) is involved in the transition from the vegetative phase to the reproductive phase by inhibiting the initiation of new leaves at the shoot apical meristem. Although the function of *SPL9* is relevant to flower development, this sgRNA was selected as it had the least number of off-targets and high efficiency. The sgRNA-Cas9 construct was used to transform Agrobacterium, which was subsequently used to transform *sep1 sep2* plants.

Table 5-8: Characteristics of sgRNAs designed to target the selected genes

Gene	AGI	Target region	Sequence	CRISPRater score	% GC	PAM	Off-targets
PRS	AT2G28610	Exon	TCGGAGTCCGTATACCACTC	0.70	55	CGG	0
NUB	AT1G13400	Exon	AGCCACTGGTGCACCGATGA	0.66	60	AGG	0
UFO	AT1G30950	Exon	TGACTCACGGATCCGACAAG	0.8	55	AGG	0
HB4	AT2G44910	Exon	CGTGAACAGAGCTCAGTCTT	0.61	50	CGG	0
REML3	AT5G32460	Exon	AGGCTTGATGAAGTGTGGCT	0.69	50	TGG	0
FBRI	AT3G59190	Exon	TCCGATAGTGAATGCTAGAG	0.61	41.2	AGG	0
FOP	AT5G53390	Exon	TCAAGGCCGTGGATGATGGC	0.75	60	TGG	AT4G39420 (uncharacterized), >4 MM
PRP2	AT2G21140	Exon	AGGATATTACCGAAAAGCGG	0.67	45	AGG	AT2G42200 (SPL9), 4 MM

5.3.2 **Phenotypic characterisation of T1 sgRNA/*sep1 sep2* transgenic plants**

Seeds harvested from T0 plants were sown on the soil. The seedlings were sprayed with 120 mg/L of Basta every three days until non-transformed plants showed yellowing of cotyledons. At least 30 Basta resistant T1 plants were selected per construct, except for *ufo sep1 sep2* which failed to produce any transformants. Due to the limited time available for this experiment, it was impossible to genotype and characterise every T1 plant. However, measuring the number of *sep*als was an amenable approach to validate whether the selected target genes of SEP1 and SEP2 could rescue the suppressed lateral *sep*als phenotype observed in *sep1 sep2* flowers (Figure 5-5-A). Thus, the selected T1 transformants were first subjected to phenotypic analysis, followed by the genotypic analysis of the transformants that showed recovery of the *sep1 sep2* phenotype. T1 transformants were screened to identify plants that produced flowers with more than two *sep*als. Three independent T1 lines per construct with flowers showing more than two *sep*als were selected. Flowers from all three independent lines of *fbri sep1 sep2* and *nub sep1 sep2* showed four *sep*als (Figure 5-5 B, C). Flowers from *prp2 sep1 sep2* Line 1 and Line 2 showed four *sep*als (Figure 5-5 D), while 20% of flowers from Line 3 showed three *sep*als (Figure 5-5 E) (More than two *sep*als were considered to rescue the *sep1 sep2* phenotype). Flowers from other CRISPR mutants, that is, *prs sep1 sep2*, *hb4 sep1 sep2*, *reml3 sep1 sep2*, and *fop sep1 sep2* showed the *sep1 sep2* phenotype of only two *sep*als (Figure 5-5 E). To confirm that transformation with the sgRNA-pDeCas9 had resulted in homozygous mutations in *fbri sep1 sep2*, *nub sep1 sep2,* and *prp2 sep1 sep2,* the selected T1 lines were subjected to genotypic analysis.

Table 5-9: T1 transformants with flowers showing >2 *sep*als. Flowers from three independent T1 lines of *fbri sep1 sep2*, *nub sep1 sep2*, and *prp2 sep1 sep2* showed more than two *sep*als.

Genotype	Line	% Flowers with >2 *sep*als	% Flowers with 2 *sep*als
fbri sep1 sep2	Line 1 (n=6)	100	0
	Line 2 (n=6)	100	0
	Line 3 (n=6)	100	0
nub sep1 sep2	Line 1 (n=6)	100	0
	Line 2 (n=6)	100	0
	Line 3 (n=6)	100	0
prp2 sep1 sep2	Line 1 (n=6)	100	0
	Line 2 (n=6)	100	0
	Line 3 (n=8)	100	0

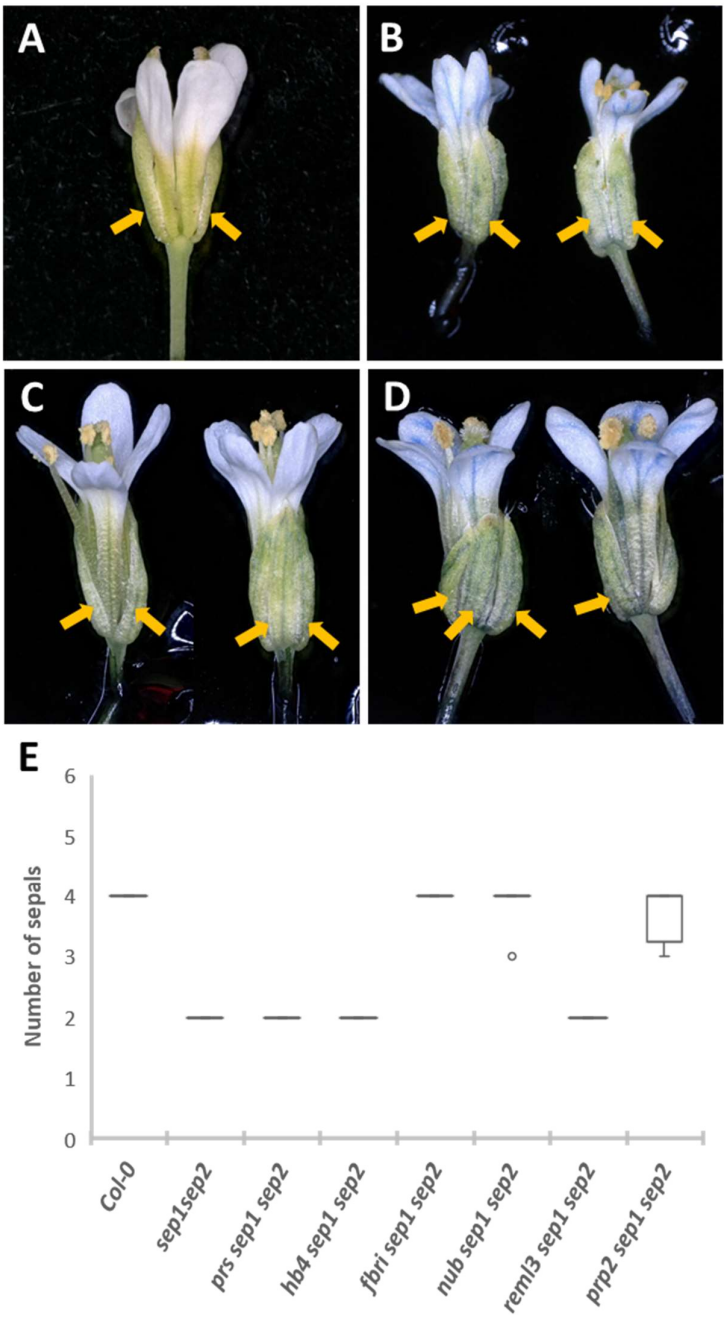

Figure 5-5: Phenotypic characterisation of flowers from T1 CRISPR mutants in *sep1 sep2* background. (A) A representative *sep1 sep2* flower showed two *sep*als where an arrow indicates each *sep*al. Images presenting two different sides of the same flower are included for each CRISPR mutant for ease of displaying all *sep*als, with individual *sep*als indicated by orange arrows - (B) *fbri sep1 sep2*, (C) *nub sep1 sep2*, and (D) *prp2 sep1 sep2* showing four *sep*als. (E) The number of *sep*als observed in sgRNA-*sep1 sep2* T1 plants (3 T1 lines, n=6 per line).

5.3.3 **High-resolution melting-curve (HRM) analysis confirmed CRISPR/Cas9 induced mutation in T1 transformants**

High-resolution melting-curve (HRM) analysis is used to detect single nucleotide polymorphisms (SNPs) and small indels (Simko, 2016). It is sensitive enough to determine mutations caused by the CRISPR/Cas9 system and whether the mutation is homozygous or heterozygous (Price et al., 2007). Thus, HRM was used to perform genotypic analysis of T1 lines from *fbri sep1 sep2*, *nub sep1 sep2*, and *prp2 sep1 sep2* to validate the presence of Cas9 induced mutations. Firstly, HRM primers were designed to amplify an 80-100 bp long fragment, including the Cas9 target site. The GC content of the amplicons ranged from 35 to 45% to avoid non-specific amplification. Real-time PCR reactions were performed on genomic DNA isolated from the selected T1 leaves using Precision Melt Supermix. Following real-time PCR, CRISPR products were subjected to high-resolution melt (HRM) analysis. Samples showing a divergent melting curve with respect to the wild type were indicative of Cas9 induced mutations. HRM analyses revealed clear differences between the melt curves of amplicons from the wild-type and T1 transgenic lines of *fbri sep1 sep2* and *nub sep1 sep2* (Figure 5-6 A, B). The shift of the melt-curve peak indicates mutation. Unfortunately, this data could not be obtained for samples from *prp2 sep1 sep2* due to poor priming. Although HRM analysis confirms the presence of Cas9-induced mutation, it is essential to identify the mutation using sequencing.

This evidence indicated that *FBRI*, *NUB*, and *PRP2* indeed contribute to the expansion of lateral *sep*als. As these three genes were upregulated in *sep1 sep2*, it also points towards the role of *SEP*s in regulating downstream targets by suppressing their expression.

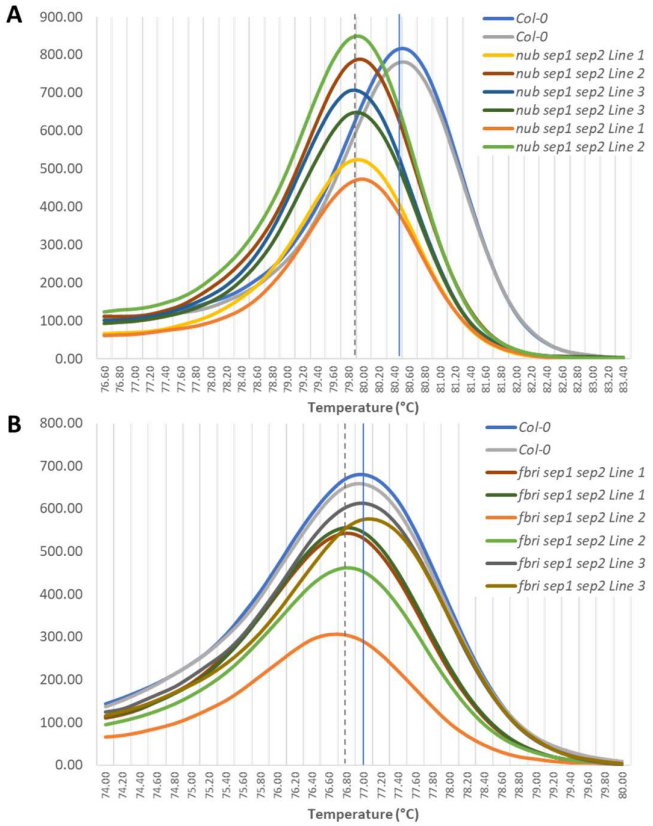

Figure 5-6: Genotypic analysis of T1 CRISPR/Cas9 mutants using High-resolution melting-curve (HRM) analysis. (A) The melting curve of a 100 bp fragment corresponding to NUB exon 1, amplified from Col-0, showed a relative fluorescence peak at 80.50 ºC (indicated by a solid blue line —). Melting curves for the same fragment amplified from *nub sep1 sep2*, Line 1, Line 2, and Line 3 showed peaks at 79.90 ºC (indicated by a dotted blue line ---) (B) Melting curve of a 100 bp fragment corresponding to FBRI exon 1, amplified from Col-0 showed a relative fluorescence peak at 77.00 ºC (indicated by a solid blue line —). Melting curves for the same fragment amplified from *fbri sep1 sep2*, Line 1, and Line 2 showed peaks at 76.70 ºC (indicated by a dotted blue line ---). The melt-curve peaks for technical replicates from Line 3 showed non-overlapping peaks at 77.00 and 77.20ºC, suggesting that Line 3 could be a heterozygous mutant.

5.3.4 **Phenotypic characterisation of flowers from mutant lines of selected candidate genes downregulated in *sep1 sep2***

To determine if the downregulated targets of SEP1 and SEP2 that were selected from both strategy A and strategy B analyses contributed to lateral *sep*al expansion. T-DNA insertion line mutants of the selected genes were characterized to determine if they showed a *sep1 sep2*-like loss of lateral *sep*als phenotype (Table 5-10). *LOB DOMAIN CONTAINING PROTEIN 41* (AT3G02550), *REGULATOR OF CHROMOSOME CONDENSATION 1* (*RCC1*; AT5G11580), *MYB 77* (AT3G50060), and *ETHYLENE RESPONSIVE ELEMENT BINDING FACTOR 1* (AT4G17500) were selected from the analysis that followed strategy A, that is, they were downregulated in *sep1*, *sep2,* and *sep1 sep2*. *Major facilitator protein* (AT5G13400), 3-KETOACYL-COA SYNTHASE 13 (*KCS13*; AT2G46720), *GTL1* (AT1G33240), and *CALLOSE SYNTHASE 5* (AT2G13680) were selected from the analysis that followed strategy B, that is, they were downregulated in only in *sep1 sep2* and not in *sep1* or *sep2*. Homozygous plants were used for the analysis. However, flowers from all the mutants showed 4 fully grown *sep*als. This suggests that none of these selected genes solely contribute to lateral *sep*al expansion.

Table 5-10: Selection of mutant lines for selected downregulated target genes. Homozygous T-DNA insertion lines with the insertion mostly in the exon (except for SALK_056243 and SALKseq_127555 which had the insertions in the 5' UTR and the promoter) were obtained f

Gene ID	Annotation	Stock ID	Zygosity	T-DNA Position	Insertion Co-ordinates	NASC ID
AT5G13400	*MAJOR FACILITATOR PROTEIN*	GABI_259D10	Homozygous	Exon	C/4297995-4298094	N424814
AT2G46720	*3-KETOACYL-COA SYNTHASE 13 (KCS13)*	SAIL_205_E06	Homozygous	Exon	C/19198584-19198837	N809612
AT1G33240	*GTL1*	WiscDsLox413-416C9	Homozygous	Exon	C/12052792-12053081	N854627
AT2G13680	*CALLOSE SYNTHASE 5*	SALK_056243	Homozygous	5' UTR	C/23270-23270	N556243
AT3G02550	*LOB DOMAIN CONTAINING PROTEIN 41*	SALK_144556	Homozygous	Exon	W/536767-536877	N644556
AT5G11580	*REGULATOR OF CHROMOSOME CONDENSATION 1 (RCC1)*	GABI_158F11	Homozygous	Exon	W/3718959-3719178	N737660
AT3G50060	*MYB 77*	WiscDsLox445B08	Homozygous	Exon	C/7695726-7696509	N856205
AT4G17500	*ETHYLENE RESPONSIVE ELEMENT BINDING FACTOR 1*	SALKseq_127555	Homozygous	Promoter	C/9758761-9758761	N627555

5.4 Discussion

5.4.1 Employing RNAseq to understand flower development gene network

Flower development being a crucial aspect of plant development, many efforts have been made to identify the underlying molecular mechanisms and gene networks associated with it. Over the past three decades, the genes involved in flower development have been identified by either reverse genetics methods or by more extensive genome-wide methods (Ó'Maoiléidigh et al., 2014; Becker and Ehlers, 2015). A large number of genes regulating floral meristem specification, and organ identity specification have been identified and characterised (Weigel and Meyerowitz, 1994; Causier et al., 2010; Wellmer and Riechmann, 2010; Murai, 2013). Genome-wide methods have made identification of genetic network involved at a particular time and developmental stage of flower development possible. Previously, methods such as cDNA and oligonucleotide arrays were used to determine large-scale transcript enrichment in flower development. Array based techniques utilise hybridization methods that have made identification of genes important for flower development. However, hybridization-based techniques have several drawbacks such as non-specific hybridization and insensitivity to low transcript levels (Marioni et al., 2008). Moreover, hybridization requires prior knowledge of genes in order to design probes. RNA-sequencing offers a great alternative to gene expression arrays and other hybridization-based approaches. RNA-seq data shows much more sensitivity by detecting low levels of transcripts with higher levels of reproducibility (Marioni et al., 2008). As the ease of sequencing and analysis has increased over the past few years, RNA-seq has been extensively used to generate transcriptomal data pertaining to various developmental stages in plant species (Martin et al., 2013). To date, RNA-seq has not only been used to study gene expression relevant to different floral organs but has also been used for cell-specific analysis in developing flowers, offering insights and resources to further study flower development (Jiao and Meyerowitz, 2010b). So far, the regulatory networks and targets associated with genes specifying floral organ identity or floral meristem specification, for example, AP1, SEP3, and LFY, have added much value to better understanding of the molecular mechanisms underlying specific flower developmental process (Kaufmann et al., 2009b; C. M. Winter et al., 2015).

5.4.2 **RNAseq analysis revealed targets of SEP1 and SEP2 relevant to lateral organ polarity**

Redundant transcription factors have been known to contribute to the development of adaxial, abaxial, and lateral organ polarity. For example, the members of the HD-Zip III gene family, *REV*, *PHV* and *PHB* redundantly lead to the establishment of adaxial domains in organs. Members of the *KANADI (KAN1-3)* and *YABBY* (*YAB1-3*) families function in establishment of the adaxial organ polarity (McConnell et al., 2001; Emery et al., 2003; Yamaguchi et al., 2012). These adaxial and abaxial polarity determining genes inhibit each other to specify boundaries (Yamaguchi et al., 2012). As the genes act redundantly to specify organ polarity, loss of a single gene usually does not lead to complete loss of patterning (Eshed et al., 2001). In this study, a similar phenomenon was observed in SEP1 and SEP2, wherein loss of both *SEP1* and *SEP2* led to suppression of lateral *sep*als. Although, *sep1* and *sep2* single mutants showed defective phyllotaxy in petal arrangement, the lateral *sep*als were not affected (Section 4.3). So far none of the Arabidopsis SEPs have been reported to regulate or interact with organ polarity specifying genes. Thus, RNAseq analysis of *sep1, sep2,* and *sep1 sep2* provided a good opportunity to identify targets of SEP1 and SEP2 relevant to organ polarity specification. However, it was unclear if the loss of lateral *sep*als in the double *sep1 sep2* was a severe version of the defective phyllotaxy in single mutants or whether it was a completely different phenotype. The two strategies employed in this chapter – strategy A (Section 5.3.1) and strategy B (Section 5.3.2) allowed identification of genes that could be associated with lateral *sep*al growth.

Organ polarity specifying genes

Interestingly, three genes – AFO/*YAB1, LBD 41, and NUB,* that could be associated wit organ polarity were identified to be upregulated only in *sep1 sep2*. Thus, either SEP1 or SEP2 is sufficient for regulation of these three genes, as they were not differentially expressed in the single mutants. AFO/*YAB1* specifies abaxial cell fate in leaf and floral organs in Arabidopsis (Siegfried et al., 1999). Similarly, *LBD 41* and *NUB* functions as regulators of lateral organ growth (Dinneny et al., 2006; Ha et al., 2007). The expression of *NUB* on the interior adaxial side lateral organs and co-regulation of the number of cell layers and cell differentiation with *JAG* led to the hypothesis that *NUB* was responsible for suppression of lateral *sep*als in *sep1 sep2*. CRISPR/Cas9 KO triple mutant *nub sep1 sep2* showed complete growth of lateral

*sep*als demonstrating that *NUB* was regulated by SEP1 and SEP2 (Section 5.4.2). The only other mutant reported that does not show lateral *sep*als is PRS (Matsumoto and Okada, 2001). However, the *sep*al primordia fail to form in *prs* whereas in *sep1 sep2*, the *sep*al primordia are formed, and they remain rudimentary. PRS is known to activate *AFO/YAB1* (Matsumoto and Okada, 2001). SEP1 and SEP2 in turn suppress *AFO*. However, PRS was not found to be upregulated in *sep1 sep2*. This suggests that PRS might act upstream or independently of *SEP1* and *SEP2* (Figure 5-7).

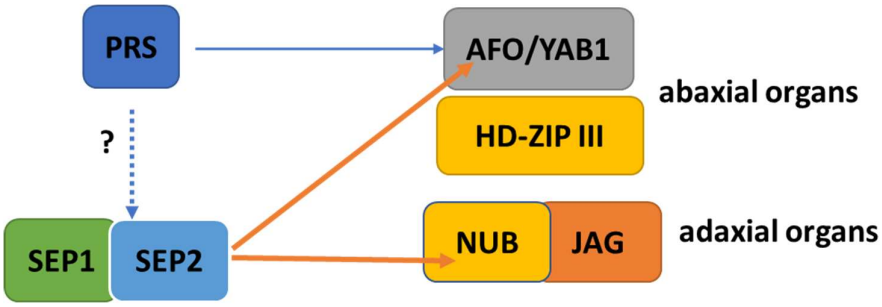

Figure 5-7: Schematic presentation of the proposed approach in which SEP1 and SEP2 regulate lateral *sep*al growth. PRS is known to regulate *AFO* (shown by a blue arrow). SEP1 and SEP2 suppress *AFO* and *NUB* (shown by a blue arrow).

Regulation of genes involved in cell expansion

SEP1 and SEP2 supressed genes such as *PRP2, FOP, PECTIN LYASE*, that are related to cell expansion. PRP2 is part of the extensin family, that modify cell wall for cell expansion (Stein et al., 2011). However, FOP, an *O-ACETYLTRANSFERASE* and *PECTIN LYASE* function in petal elongation and are not expressed in *sep*als. CRISPR/Cas9 KO triple mutant *prp2 sep1 sep2* showed four fully expanded lateral *sep*als demonstrating that *PRP2* was regulated by SEP1 and SEP2 (Section 5.4.2)

Regulation of *LEAFY*, *AP1*, and *SEP3*

Apart from genes involved in organ polarity specification, other genes important for floral meristem and organ identity specification were also differentially expressed in *sep1 sep2* (Section 5.3.2). *LFY* was found to be upregulated in *sep1 sep2* while *AP1* and *SEP3* were downregulated. Together, *LFY* and *AP1* regulate crucial pathways such as auxin response, flowering time, and floral meristem identity specification (Nilsson et al., 1998; Winter et al., 2015; Goslin et al., 2017; N, 2021). *LFY* and *AP1* together induce the expression of *SEP3* (Winter et al., 2015). However, *SEP3* was also found to be downregulated in *sep1 sep2*. The regulation of *LFY*, *AP1* and *SEP3* by *SEP1* and

SEP2 underlines the intricacy of the gene network associated with flower development. This shows that *SEP1* and *SEP2* play a greater role in flower development, contrary to the belief that they only act redundantly to specify E function. Further studies are necessary to shed more light upon the role of SEP1 and SEP2 in controlling the expression of these genes.

6 Chapter 6: Targets of SEP1 and SEP2 associated with robustness of decussate petal symmetry

6.1 Introduction

Gene regulatory networks (GRN) regulate plant development by synchronising internal plant signals and external environmental cues. Reproduction, a crucial aspect of plant development, is significantly affected by both internal and external signals. The process comprises multiple developmental stages that involve complex interactions from the GRN. The interactions are controlled by master floral regulators that are comprised of various transcription factors (TFs), co-factors, miRNAs, epigenetic and post-transcriptional regulators (Thomson and Wellmer, 2019). Floral regulators act hierarchically at different stages of reproduction, i.e., initiation of flowering, floral meristem specification and formation, organ identity specification, morphogenesis, and termination of flowering. A number of these regulators have been identified through forward and reverse genetic approaches.

A prominent example of this was identifying homeotic transcription factors from the ABCE model of flower development that specify floral organ identity in Arabidopsis and Antirrhinum (Bowman et al., 1989; Carpenter & Coen, 1990; Hill & Lord, 1989; S Pelaz et al., 2000; Schwarz-Sommer et al., 1990; Yanofsky et al., 1990). The homeotic TFs work by regulating the expression of specific genes necessary for the regulation of organ development and morphogenesis. The immediate interactions of these TFs in the GRN were identified through reverse genetics, and the network was further enriched by studying protein-protein interactions and expression of downstream genes (Blázquez et al., 2006.; Immink et al., 2010). The interactions between A, B, C, and E-activity homeotic TFs was characterised, leading to the proposal of the floral quartet model (Theißen and Saedler, 2001). However, relatively little is yet known about the detailed mechanisms and pathways through which these TFs regulate the expression of the downstream genes/miRNAs that contribute to flower development.

The advent of genome-wide molecular approaches such as transcriptome profiling, chromatin immunoprecipitation (ChIP), and interactome mapping, coupled with next-generation sequencing (NGS), offers global snapshots of the interactions in GRNs (Pajoro et al., 2014). These sophisticated techniques generate large-scale data while

also capturing the dynamic spatio-temporal changes in the GRN. They also identify non-linear aspects of GRNs, such as regulatory feedback loops that are difficult to characterise using a classical approach. Identifying secondary and tertiary connections of the 'master regulator' nodes, their expression profiles, and combinatorial interactions, improve our understanding of network connectivity and the molecular mechanisms underlying developmental processes. Some of these approaches have been employed to further our understanding of the part of GRN underlying flower development (Pajoro et al., 2014; Wellmer et al., 2014). Insights into spatio-temporal expression patterns of genes regulated by homeotic TFs at different stages of flower development were generated by using floral induction systems and translating ribosome affinity purification sequencing (TRAP-seq) approaches (Wellmer et al., 2006; Jiao and Meyerowitz, 2010c). Microarray based gene expression profiling of transgenics mis-expressing homeotic genes led to identification of hundreds of genes that were directly or indirectly controlled by the floral regulators (Zik and Irish, 2003; Alves-Ferreira et al., 2007). Direct targets of homeotic TFs, AP1, AP2, AP3, PI, and AG were detected by using a combination of gene expression profiling and genome-wide TF binding localisation studies (Kaufmann et al., 2010; Yant et al., 2010; Wuest et al., 2012; Ó'Maoiléidigh et al., 2013). Out of the four duplicate E-activity SEP TFs in Arabidopsis, the direct targets of SEP3 were determined by using ChIP-seq (Kaufmann et al., 2009b).

SEP TFs regulate flower development by modulating the expression of target genes through their ability to bind CArG boxes in promoter regions (Kaufmann et al., 2009a; Lai et al., 2020). They form tetrameric complexes with other MADS-box TFs, and multimeric, higher-order complexes with other MADS and non-MADS proteins (Kaufmann et al., 2005b; Hugouvieux and Zubieta, 2018; Rümpler et al., 2018). They can form multiple connections and function as network hubs in the GRN (Immink et al., 2009).

As seen in Chapter 4, single and double *sep* mutants exhibit subtle phenotypes that significantly vary from each other. Mutant phenotype characterisation, complementation, and promoter swap studies show that the SEPs are not entirely functionally redundant, implying that each SEP regulates common and unique parts of a larger GRN. However, most molecular studies have been carried out with SEP3 as the representative of the *A. thaliana* SEP family (Sridhar et al., 2006; Immink et al., 2009;

Kaufmann et al., 2009b; Käppel et al., 2018; Lai et al., 2020). Although these studies provide a great insight into the actions of SEP3, we can not necessarily extrapolate these findings to the other *A. thaliana* SEPs.

Amongst the four duplicate SEPs in Arabidopsis, SEP1 and SEP2 are phylogenetically closely related genes that have evolved through a recent duplication, and they share synteny (Section 3.4). The skewed petal arrangement phenotype in *sep1* and *sep2* shows that SEP1 and SEP2 ensure robust production of decussate petal symmetry. Thus, determining the targets of SEP1 and SEP2 will further our understanding of the molecular mechanisms underlying their function. In this chapter, the targets of SEP1 and SEP2 was investigated by performing RNAseq analysis on *sep1-1 and sep2-1* inflorescences grown in the natural environment in screenhouse, and in standard, controlled conditions in the growth chamber. The two different RNAseq datasets for the same mutant was used to determine high confidence candidate targets of SEP1 and SEP2. The RNAseq data from *sep1-1* and *sep2-1* grown in the screenhouse was used to investigate any robustness related targets. Candidate targets was screened for further study by efficient CRISPR/mutant analyses in chapter X.

Objectives

- To determine high confidence targets of SEP1 and SEP2
- To identify the targets of SEP1 and SEP2 that may be associated with biological robustness

6.2 High confidence targets of SEP1 and SEP2

Although RNAseq analysis generated a list of DEGs from each sample, each DEG was not necessarily a target of SEP1 or SEP2. However, the availability of two RNAseq datasets per *sep* mutant, that is, samples from ST and VT conditions, presented an advantage towards identifying high confidence targets of SEP1 or SEP2. Common DEGs in samples from both ST and VT had a higher likelihood of being direct or indirect SEP1 or SEP2 targets. Thus, to identify high confidence targets of SEP1, a two-step approach was used (Figure 6-1). Firstly, FPKM values from *sep1-1* grown in ST were normalized to FPKM values of from Col-0 grown in ST conditions to DEGs in *sep1-1*_ST. This eliminated any DEGs irrelevant to the analysis. Similarly, FPKM values *sep1-1* grown in VT were normalized to FPKM values from Col-0 grown in VT conditions to identify *sep1-1*_VT DEGs (n.b. the abbreviation VT is used in this chapter to denote screenhouse conditions for consistency and ease of reading). In the second step, DEGs common to *sep1-1*_ST and *sep1-1*_VT were determined to be high confidence targets of SEP1. A list of 429 common DEGs between *sep1-1*_ST and *sep1-1*_VT was generated. A similar approach was used to determine high confidence targets of SEP2, to generate a list of 681 common DEGs between *sep2-1*_ST and *sep2-1*_VT.

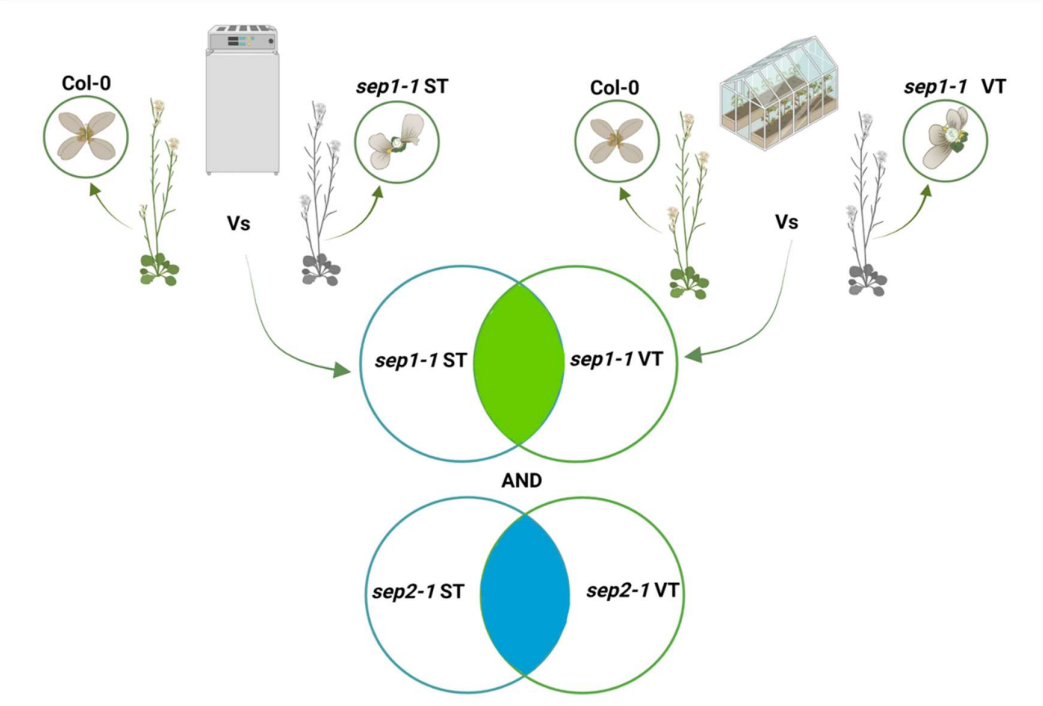

Figure 6-1: Schematic of the approach used to identify high confidence targets of SEP1 and SEP2. FPKM values *sep1-1* grown in ST were normalized to FPKM values of wild

type (Col-0) grown in ST conditions to identify *sep1-1*_ST DEGs. Similarly, FPKM values *sep1-1* grown in VT were normalized to FPKM values of wild type (Col-0) grown in VT conditions to identify *sep1-1*_VT DEGs. Common DEGs from *sep1-1*_ST and *sep1-1*_VT were determined to be high confidence targets of SEP1. Similarly, common DEGs from *sep2-1*_ST and *sep2-1*_VT were designated as high confidence targets of SEP2.

As described in Chapter 4, SEP1 and SEP2 act redundantly to regulate the decussate petal arrangement in stable and variable temperature conditions (Chapter 4, Section 4. 7). Loss of either SEP1 or SEP2 affected this decussate petal arrangement resulting in a skewed petal phenotype, which is observed in both stable and variable environments. Thus, by comparing DEGs in *sep1-1* and *sep2-1* grown in standard temperature conditions (ST) to their counterparts grown in natural screenhouse conditions (VT), more insight was gained regarding high confidence targets of SEP1 and SEP2. The number of DEG in *sep1-1*_ST and *sep1-1*_VT was 6440 and 2798, and 5231 and 5333 in *sep2-1*_ST and *sep2-1*_VT, respectively (Table 6-1). As the samples were inflorescences, containing meristems and flower buds at different developmental stages (Chapter 5, Section 5.2), and, in some samples, were also subjected to variable temperature conditions, it would not be surprising for genes to have highly variable FPKM values. Genes showing high variability in FPKM and P-values were eliminated during quality control. Thus, a lower number of DEG was detected in *sep1-1*_VT possibly due to the elimination of candidates during quality control steps. An overlap of 1273 DEGs was seen in *sep1-1*_ST and *sep1-1*_VT. Comparatively, only 681 genes were common between *sep2-1*_ST and *sep2-1*_VT. This indicates that in ST conditions, *sep1-1* and *sep2-1* had 1384 upregulated and 1183 downregulated common DEGs. Comparatively, in VT conditions, they showed 439 upregulated and 509 downregulated DEGs. As SEP1 and SEP2 are hypothesized to redundantly act as a buffer against external environmental perturbations to produce a decussate flower, this finding was surprising. This suggests that SEP1 and SEP2 might show differential regulation of their targets, possibly influenced by cell and time specific expression, and differences in associated cis-regulatory elements.

Table 6-1: Details of *sep* genotypes and conditions used in this study, along with the corresponding number of relevant DEGs.

Sample	Genotype	Condition	DEG (P_{adj}<0.01)
*sep1-1*_ST	*sep1-1*	Standard	6440
*sep2-1*_ST	*sep2-1*	Standard	5231
*sep1-1*_VT	*sep1-1*	Screenhouse	2798
*sep2-1*_VT	*sep2-1*	Screenhouse	5333

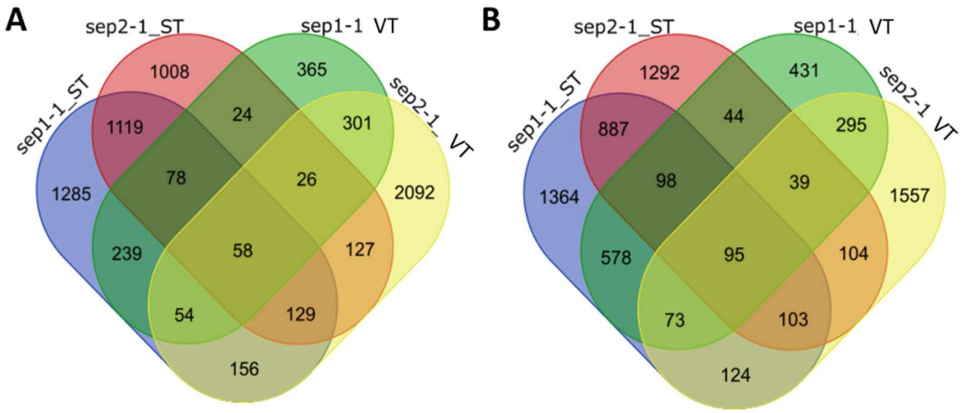

Figure 6-2: Number of common and unique differentially expressed genes between *sep1-1* and *sep2-1* grown in standard and screenhouse growth conditions (A) number of upregulated genes and (B) number of downregulated genes across *sep1-1*_ST, *sep2-1_ST*, *sep1-1*_VT, and *sep2-1*_VT (P_{adj}<0.01)

There were 429 common DEGs between *sep1-1*_ST and *sep1-1*_VT, and 681 common DEGs between *sep2-1*_ST and *sep2-1*_VT. However, most of these genes had annotations related to disease resistance (NBS-LRR), ribosomal proteins, or retrotransposons. We were interested in DEGs that played a role specifically in floral development. Thus, an RNAseq dataset of the *pin-1* mutant was obtained from Dr Antoine Larrieu, Davies Lab. The *PIN-1* gene in Arabidopsis encodes an auxin efflux carrier and *pin-1* lacks the ability to produce floral meristems (Vernoux et al., 2000). This dataset therefore provides the ability to filter the SEP DEGs to identify genes that are both SEP-regulated and flower specific. Genes that were not expressed in the *pin* mutant but were differentially expressed in the *sep* mutants were selected for further analysis. Although this method has an obvious flaw, since it ignores genes that are

expressed both florally and vegetatively, it significantly narrowed down the number of DEGs for further analysis.

6.2.1 Differentially expressed genes common to *sep1-1* ST and VT

Out of the 1237 common DEGs between *sep1-1*_ST and *sep1-1*_VT, only 278 were not expressed in *pin-1*. This subset constituted 71 upregulated genes and 207 downregulated genes. Gene ontology (GO) analysis of these genes showed enrichment for biological processes such as reproductive process (GO:0022414), multi-organism process (GO:0051704), reproduction (GO:0000003), developmental process (GO:0032502), signalling (GO:0023052), and metabolic process (GO:0008152) (Figure 6-3 A). Genes such as *AGAMOUS-LIKE 27 (AGL27)*, *AGL31*, and *MULTIPOLAR SPINDLE 1* mapped to GO reproduction terms. Genes mapping to signalling and metabolic process included transcription factors, enzymes such as oxidoreductases, oxygenases, dehydrogenase, methyltransferase, RNA polymerases. This indicates that SEP1 regulates a lot of other regulators of biological processes. A few significant DEGs were found to have functions relevant to flower development (Table 6-2). Out of these *MAF3* was found to be upregulated while *MAF4* was downregulated. MAF3 and MAF4 regulate flowering time as a part of the ambient temperature pathway (Blázquez et al., 2003). The upregulated genes included *BRASSINOSTEROID-6-OXIDASE 2 (BR6OX2),* a cytochrome P450 enzyme that catalyses the last step in the brassinolide synthesis pathway (Domagalska et al., 2010). Although *BR6OX2* is widely known for its role in circadian and light control, it is also known to interact with *SEUSS* to regulate ovule development (Nole-Wilson et al., 2010). Other upregulated genes included *PROLINE RICH PROTEIN 2* (*PRP2*) and *PROLINE-RICH PROTEIN 4* (*PRP4*), which are extensin-like genes, generally known to be expressed in pollen (Gothandam et al., 2009). *LOSS OF GIANT CELLS FROM ORGANS (LGO)* functions in giant cell development in *sep*als, thereby regulating *sep*al structure (Roeder et al., 2010). Genes that are commonly downregulated between *sep1-1*_ST and *sep1-1*_VT include *AGL31, AP2/B3-like, ARGONUTE9,* and *AUXIN RESISTANT1.* Out of these, *AGL31* and *AP2/B3*-like encode transcription factors from families that play significant roles in flower development. *ARGONAUTE9* (*AGO9)* dependent sRNA silencing plays a role in germ cell specification (Durán-Figueroa & Jean-Philippe, 2010), and *AUXIN RESISTANT1(AXR1)* which primarily, but not exclusively affects auxin response (del Pozo and Estelle, 1999). This suggests that SEP1

may function via regulating the activity of other transcription factors, miRNAs, and phytohormones.

Table 6-2: Selected high confidence targets of SEP1, differentially expressed in *sep1-1* under ST and VT conditions

Gene ID	Annotation	*sep1-1*_ST	*sep1-1*_VT
AT3G30180	*BRASSINOSTEROID-6-OXIDASE 2*	2.43	1.34
AT2G21140	*PROLINE RICH PROTEIN 2*	2.23	2.15
AT5G65060	*MADS AFFECTING FLOWERING 3*	1.71	1.80
AT3G10525	*LOSS OF GIANT CELLS FROM ORGANS*	1.68	1.65
AT4G38770	*PROLINE-RICH PROTEIN 4*	1.35	1.51
AT5G65070	*MADS AFFECTING FLOWERING 4*	-15.21	-15.20
AT5G42700	*AP2/B3*-like transcriptional factor family protein	-3.90	-3.87
AT5G21150	*ARGONAUTE 9*	-2.09	-2.29
AT5G65050	*AGAMOUS-like 31*	-1.51	-1.28
AT5G01240	*AUXIN RESISTANT 1*	-1.36	-1.29

6.2.2 Differentially expressed genes common to *sep2-1* ST and VT

Out of the 681 common DEG between *sep2-1*_ST and *sep2-1*_VT, 526 genes were not expressed in the *pin-1* dataset, out of which 183 genes were upregulated, and 343 genes were downregulated. GO analysis mapped these to biological processes such as developmental process (GO:0032502), localisation (GO:0051179), multicellular organismal process (GO:0032501), reproduction (GO:0000003), signalling (GO:0023052), response to stimulus (GO:0050896) and metabolic process (GO:0008152) (Figure 6-3 B). Genes classified under reproductive process included *YABBY 3 (YAB3)*, *YABBY 5* (*YAB5*), *BUB1*, and *GAMMA-TUBULIN COMPLEX COMPONENT 4 (GCP4)*. *YABBY3* encodes a polarity regulator that determines abaxial cell fate during organogenesis and embryogenesis (Siegfried et al., 1999). *YAB5* is a YAB3 homolog with an unknown function. *BUB1,* a mitotic checkpoint serine/threonine-protein kinase and *GCP4,* play roles in microtubule assembly during gametophyte development (Zhang et al., 2018a). Genes enriched under developmental process include *FAR-RED ELONGATED HYPOCOTYL 1 (FHY1)* which positively regulates photomorphogenesis, epigenetic regulators such as various histones H2As, kinase regulators such as *CYCLIN*s, and transporters such as *CHLOROPLASTIC*

IMPORT INNER MEMBRANE TRANSLOCASE SUBUNIT (TIM22-2), PEROXISOMAL ADENINE NUCLEOTIDE CARRIER 1, and *MITOCHONDRIAL INNER MEMBRANE PROTEIN* (Yang et al., 2009). Certain DEGs that were identified had functions relevant to flowering time and flower development (Table 6-3). *FLOWERING PROMOTING FACTOR 1 (FPF1)* is expressed in the inflorescence meristem and is known to work together with flowering time genes such as VRN2 and FRIGIDA, as well as floral organ identity genes such as *LFY* and *AP1* (Melzer et al, 2002). *PHYTOCHROME AND FLOWERING TIME 1 (PFT1)* promotes flowering in CO dependent and independent pathways (Cerdan and Chory, 2003). *DWARF AND DELAYED FLOWERING 1 (DDF1)* contains one AP2 domain and results in delayed flowering (Magome et al., 2004). *SERRATED LEAVES AND EARLY FLOWERING (SEF)* is known to interact with FLC and MAF4. The *sef* mutant shows flowers with increased number of organs and altered shape (March-Diaz et al, 2007). *EARLY BOLTING IN SHORT DAYS (EBS)* encodes a chromatin remodelling factor that regulates flowering time by repressing *FT* (Pinero et al, 2003). *EMBRYONIC FLOWER 2 (EMF2)* is part of a polycomb complex with FIE, CLF, and MSI1 to negatively regulate floral organ identity genes such as *AP3*, *PI* and *AG* (Calonje et al, 2008). Thus, targets of SEP2 predominantly include various flowering time genes. The GO analysis shows that although *SEP1* and *SEP2* are considered to be functionally redundant, the type of genes they regulate largely vary in their functions.

Table 6-3: Selected high confidence targets of SEP2, differentially expressed in *sep2-1* under ST and VT conditions.

Gene ID	Annotation	*sep2-1*_ST	*sep2-1*_VT
AT5G24860	*FLOWERING PROMOTING FACTOR 1*	3.58	1.11
AT1G25540	*PHYTOCHROME AND FLOWERING TIME 1*	1.35	1.30
AT1G12610	*DWARF AND DELAYED FLOWERING 1*	-46.91	-3.41
AT2G38810	Histone *H2A 8*	-1.40	-1.79
AT3G54560	Histone *H2A 11*	-1.35	-1.49
AT5G37055	*SERRATED LEAVES AND EARLY FLOWERING*	-1.28	-1.30
AT4G22140	*EARLY BOLTING IN SHORT DAYS*	-1.16	-1.04
AT5G51230	*EMBRYONIC FLOWER 2*	-1.11	-1.13

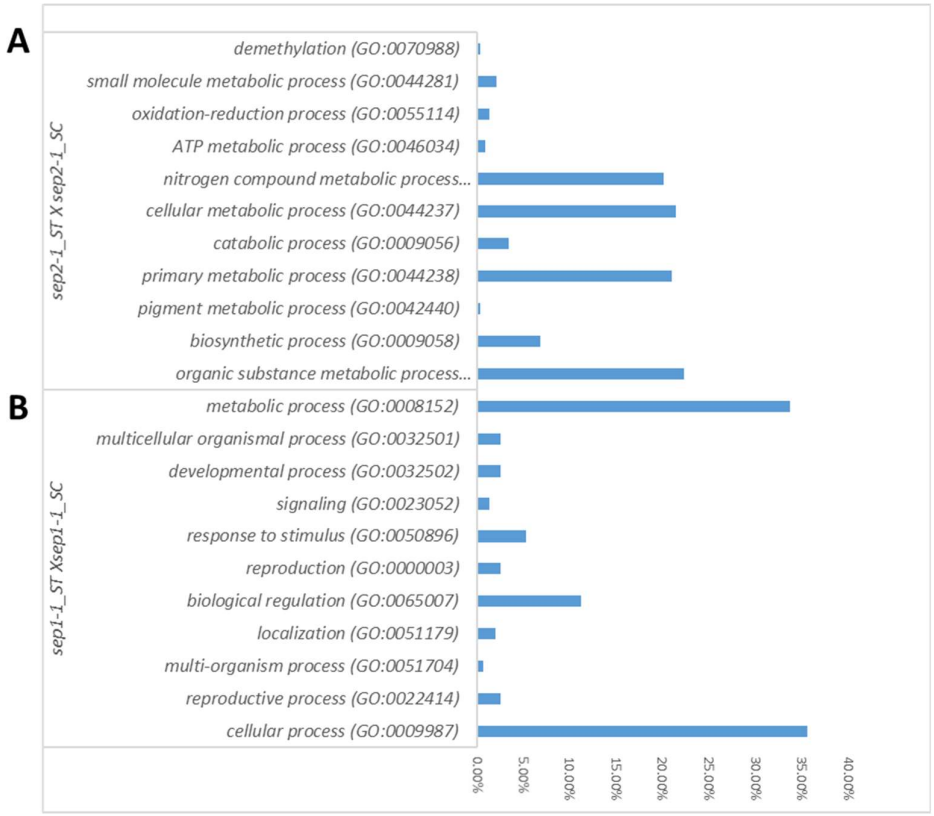

Figure 6-3: Gene Ontology analysis of high confidence targets of SEP1 and SEP2. Distribution of genes mapped to different GO terms for DEGs common (A) in *sep1-1*_ST and *sep1-1*_VT and (B) *sep2-1*_ST and *sep2-1*_VT.

6.2.3 Differentially expressed genes common in *sep1-1* and *sep2-1*, in both ST and VT conditions

Although *sep1-1* and *sep2-1* showed differences in the type of their downstream targets, *sep1-1*_ST, *sep1-1*_VT, *sep2-1*_ST and *sep2-1*_VT had 153 DEGs in common, out of which 58 were upregulated and 95 were downregulated (Figure 6-2). GO analysis of these genes did not result in significant enrichment. However, a closer manual look at the annotations revealed that most of them are uncharacterised, unknown proteins. A few candidates such as *LGO, BR6OX2, PRP2, AP2/B3*-like protein were identified in *sep1-1* or *sep2-1* datasets and were discussed earlier. This dataset contained genes such as the *PLATZ* transcription factor, *RNI* protein, P-loop containing nucleoside triphosphate hydrolases, *LSD1-like 3,* and *SGF29 Tudor-like* protein. Most of these proteins play a role in cell cycle regulation. Although the families these proteins belong to have been identified, the exact function of most of these genes have not been validated). Overall, this analysis confirms that SEP1 and SEP2 regulate the expression

of other regulators, highlighting the complex nature of Arabidopsis GRN. This analysis also indicates that SEP1 and SEP2 occupy master regulator positions in this network as they regulate other regulators in the GRN.

Table 6-4: Differentially expressed genes of biological significance, common in *sep1-1* and *sep2-1* inflorescences from plants grown under standard (ST) and screenhouse (VT) conditions.

Gene ID	Annotation	FC_*sep1-1*_ST	FC_*sep1-1*_VT	FC_*sep2-1*_ST	FC_*sep2-1*_VT
AT3G30180	*BRASSINOSTEROID-6-OXIDASE 2*	2.43	1.99	1.34	1.00
AT2G21140	*PROLINE-RICH PROTEIN 2*	2.23	1.73	2.15	1.47
AT4G06598	*bZIP transcription factor*	2.02	1.87	1.39	1.39
AT3G10525	*LOSS OF GIANT CELLS FROM ORGANS*	1.68	1.61	1.65	1.43
AT3G25870	*hypothetical protein*	1.67	2.05	1.35	1.05
AT4G00400	*GLYCEROL-3-PHOSPHATE ACYLTRANSFERASE 8*	1.44	1.40	1.41	1.17
AT5G60250	*ZINC FINGER PROTEIN*	1.42	1.93	1.50	3.36
AT4G08580	*MICROFIBRILLAR-ASSOCIATED PROTEIN*	1.29	1.16	1.37	1.06
AT4G16310	*LSD1-like 3*	1.12	1.08	1.15	1.08
AT3G18530	*ARM repeat protein*	-1752.01	-2.44	-511.20	-1.24
AT4G05631	*hypothetical protein*	-482.49	-1005.23	-613.36	-523.65
AT3G41979	*5.8SrRNA*	-104.63	-111.92	-238.27	-203.42
AT5G10400	*Histone superfamily protein*	-15.61	-1.15	-14.80	-2.05
AT5G22794	*hypothetical protein*	-5.46	-1.37	-3.04	-1.36
AT3G60930	*Transposable element*	-5.31	-6.45	-11.64	-20.75
AT5G46710	*PLATZ transcription factor*	-5.07	-4.92	-1.81	-1.06
AT5G56550	*OXIDATIVE STRESS 3*	-4.72	-5.60	-2.93	-1.39
AT5G42700	*AP2/B3-like transcriptional factor*	-3.90	-1.39	-3.87	-1.15
AT4G07825	*unknown protein*	-2.36	-2.63	-1.51	-1.57
AT4G13500	*transmembrane protein*	-2.34	-1.54	-3.73	-1.06
AT5G54569	*unknown protein*	-1.90	-1.84	-1.71	-1.89

6.3 Putative targets of SEP1 and SEP2 associated with governing the robustness of decussate petal arrangement

In Arabidopsis, *SEP1* or *SEP2* act redundantly to govern the robustness of decussate petal arrangement (Chapter 4, Section 4.7). The skewed arrangement of petals in *sep1-1* and *sep2-1* worsened, that is, the degree of variability of the angle and the number of flowers showing this phenotype increased, in plants grown in variable temperature conditions. This indicated the role of SEP1 and SEP2 in buffering external environmental perturbations in order to ensure robust development of flowers with invariant cruciferous symmetry. To gain more insight into the function of SEP1 and SEP2 in governing robustness of flower development, genes differentially expressed only under VT conditions were identified as robustness associated targets of SEP1 or SEP2. This was achieved via a two-step approach (Figure 6-4). In the first step, *sep1-1*_ST was normalized to Col-0_ST to eliminate extraneous DEGs. Similarly, DEGs from *sep1-1*_VT normalized to Col-0 VT were identified. After this, a list of DEGs unique to *sep1-1*_VT was generated and assessed to identify possible robustness associated targets of SEP1. A similar approach was used to narrow down possible robustness associated targets of SEP2.

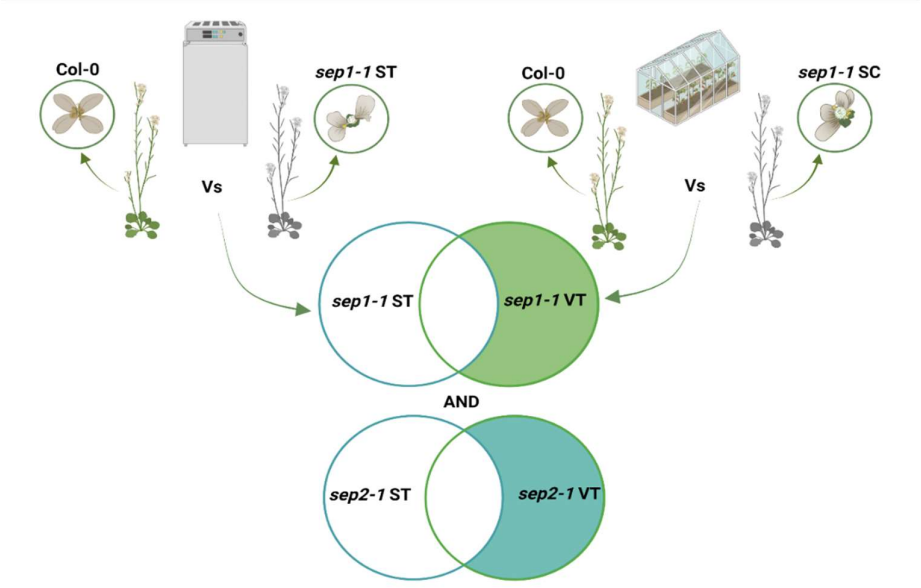

Figure 6-4: Schematic representation of the approach used to identify robustness related targets of SEP1 and SEP2, i.e, DEGs unique to screenhouse samples. *sep1-1*_ST and *sep1-1*_VT were normalized to Col-0_ST and Col-0_VT respectively. Unique DEGs from the normalized *sep1-1*_VT were chosen for further analysis to identify robustness

associated genes. A similar approach was used to determine robustness associated genes targets of SEP2.

6.3.1 Differentially expressed genes unique to *sep1-1* VT

In total 1525 DEGs were unique to *sep1-1*_VT, with 1386 DEGs that were not expressed in *pin-1*. Out of these, 676 were upregulated and 711 were downregulated. This was a large number of genes to inspect in order to find genes associated with robustness. To generate an overview of what genes were differentially expressed, a few filters such as 'regulation by floral transcription factors' and 'regulated by SEP3' were used wherever required. Although these steps may result in missing certain genes, they allowed us to zoom in on different genes and gene families to broaden our understanding of molecular mechanisms underlying SEP1/SEP2 associated robustness.

Table 6-5: Selection criteria for candidate genes to generate more insight into the role of SEP1 in VT conditions

Condition		**Number of unique DEG (*sep1-1* VT)**	
P<0.01		1525	
Not expressed in *pin-1*		1386	
Upregulated	676	Downregulated	711
Regulated by floral TFs	401	Regulated by floral TFs	461
Regulated by SEP3	147	Regulated by SEP3	198

Firstly, a GO analysis of the upregulated genes in *sep1-1*_VT showed enrichment of two broad categories, cellular component organization (GO0016043) and nitrogen compound metabolic process (GO0006807) (Figure 6-5). 'Cellular component organization' was linked to the prominent category organelle organization (GO0006996) that was linked to 30 genes, constituting chromosome organization (GO0051276), and chromatin organization (GO0006325). These terms were linked to genes such as *ASYNAPTIC1* (AT1G67370, *ASY1*), *HISTONE MONO-UBIQUITINATION 1* (AT2G44950, *HUB1*), *HUB2* (AT1G55250), *PICKLE* (AT2G25170; *PKL*), which are involved in chromatin modification and transcription regulation. Interestingly, other genes included *EARLY FLOWERING 7* (AT2G06210; *ELF 7*) and *ELF 8* (AT1G79730) that are involved in controlling flowering time by

elevating FLC expression to a level that creates a vernalization response. The post embryonic development (GO0009791) was associated with genes such as *SEUSS* (AT1G43850; *SEU*), and *TERMINAL FLOWER 2* (AT5G17690; *TFL2*). *TFL2* regulates the meristem response to light signals, the maintenance of inflorescence meristem identity and influences the activity of *AP1*. *SEU* encodes a transcriptional co-regulator of *AGAMOUS*, that functions with *LEUNIG* to repress *AG* in the outer floral whorls. The other enriched term 'nitrogen compound metabolic process', with 98 associated genes, was linked to nucleotide and nucleic acid metabolic processes (Figure 6-5). This included a variety of genes involved in transcription initiation, regulation of transcription and RNA-binding (Table 6-6). The prominent genes included *ALWAYS EARLY 2* (AT3G05380), involved in DNA metabolism and *LEO1* (AT5G61150), a DNA-directed RNA polymerase. Multiple RNA splicing and processing factors were also found. Overall, genes associated with transcription regulation are upregulated in *sep1-1.* A full list of transcription associated genes upregulated in *sep1-1* is listed (Appendix 6-I)

Table 6-6: Selected genes upregulated in *sep1-1* VT with GO terms mapping to chromatin and transcriptional regulation

Gene ID	Annotation	Protein Class
AT3G05380	Protein ALWAYS EARLY 2;ALY2;ortholog	DNA metabolism protein(PC00009)
AT2G30320	Putative tRNA pseudouridine synthase;TAIR:locus:2065748;ortholog	lyase(PC00144)
AT1G08370	mRNA-decapping enzyme-like protein;TAIR:locus:2201821;ortholog	mRNA capping factor(PC00145)
AT5G13010	Pre-mRNA-splicing factor ATP-dependent RNA helicase DEAH7;CUV;ortholog	RNA helicase(PC00032)
AT5G19040	Adenylate isopentenyltransferase 5, chloroplastic;IPT5;ortholog	RNA processing factor(PC00147)
AT4G21660	PSP domain-containing protein;At4g21660;ortholog	RNA splicing factor(PC00148)
AT1G10320	Zinc finger CCCH domain-containing protein 5;TAIR:locus:2012843;ortholog	RNA splicing factor(PC00148)
AT4G03430	Protein STABILIZED1;STA1;ortholog	RNA splicing factor(PC00148)
AT1G03910	Cactin;CTN;ortholog	scaffold/adaptor protein(PC00226)
AT5G60870	RCC1 domain-containing protein RUG3, mitochondrial;RUG3;ortholog	ubiquitin-protein ligase(PC00234)
AT1G67370	Meiosis-specific protein ASY1;ASY1;ortholog	cysteine protease(PC00081)
AT3G24870	Chromatin modification-related protein EAF1 B;EAF1B;ortholog	chromatin/chromatin-binding, or -regulatory protein(PC00077)

AT1G21610	Ubinuclein-1;UBN1;ortholog	scaffold/adaptor protein(PC00226)
AT5G61150	Protein LEO1 homolog;VIP4;ortholog	DNA-directed RNA polymerase(PC00019)

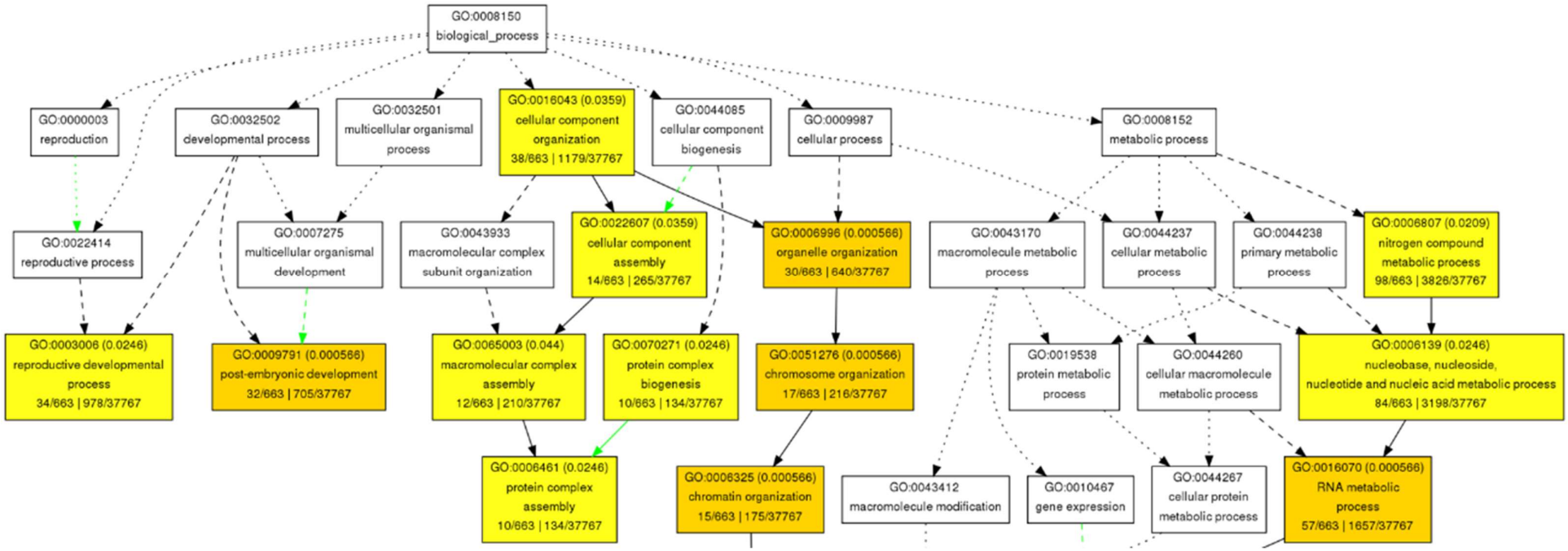

Figure 6-5: A graphical hierarchical image of GO analysis of genes upregulated in *sep1-1* under VT. (Coloured boxes denote significant terms. Darker box colour denotes a lower p-value). Biological processes under "GO0016043: cellular component organization", and "GO0006807: nitrogen compound metabolic process" are show enrichment in the dataset.

Genes downregulated in *sep1-1*_VT did not yield any significant GO terms associated with flower development or robustnes. Instead, the enriched GO terms were sterol metabolic process (GO:0016125), phospholipid biosynthetic process (GO:0008654), glycerophospholipid biosynthetic process (GO:0046474), and phosphoinositide biosynthetic process (GO:0046489). The genes associated with these terms included *AMINOALCOHOLPHOSPHOTRANSFERASE 1* (AT3G25585; *AAPT 1*), *AAPT 2* (AT1G13560), *PHOSPHATIDYLINOSITOL SYNTHASE 1* (AT1G68000; *ATPIS1*).

As the GO analysis did not yield satisfactory results, the list of genes downregulated in *sep1-1*_VT was filtered to identify genes that were regulated by SEP3 (Table 6-7). The top 10 candidates from this list included a CLAVATA3/ESR-RELATED 20 (AT1G05065; CLE20) with an unknown function. CLE20 is a member of the *CLAVATA3-LIKE* family. The remaining genes included four transcription factors, and other genes with unknown functions. Overall, the analysis of genes downregulated in *sep1-1*_VT led to insignificant results.

Table 6-7: Selected genes downregulated in *sep1-1* VT that are known to be regulated by SEP3

AGI	Annotation	FC
AT1G05065	CLAVATA3/ESR-RELATED 20	-2.52
AT1G14685	basic pentacysteine 2	-1.27
AT1G21150	Mitochondrial transcription termination factor family protein	-1.74
AT1G35516	myb-like transcription factor family protein	-1.93
AT1G67060	peptidase M50B-like protein	-1.35
AT2G34750	RNA polymerase I specific transcription initiation factor RRN3 protein	-1.27
AT3G06240	F-box family protein	-1.23
AT3G25020	receptor like protein 42	-14.4
AT3G27870	ATPase E1-E2 type family protein / haloacid dehalogenase-like hydrolase family protein	-1.47
AT5G18940	Mo25 family protein	-1.46

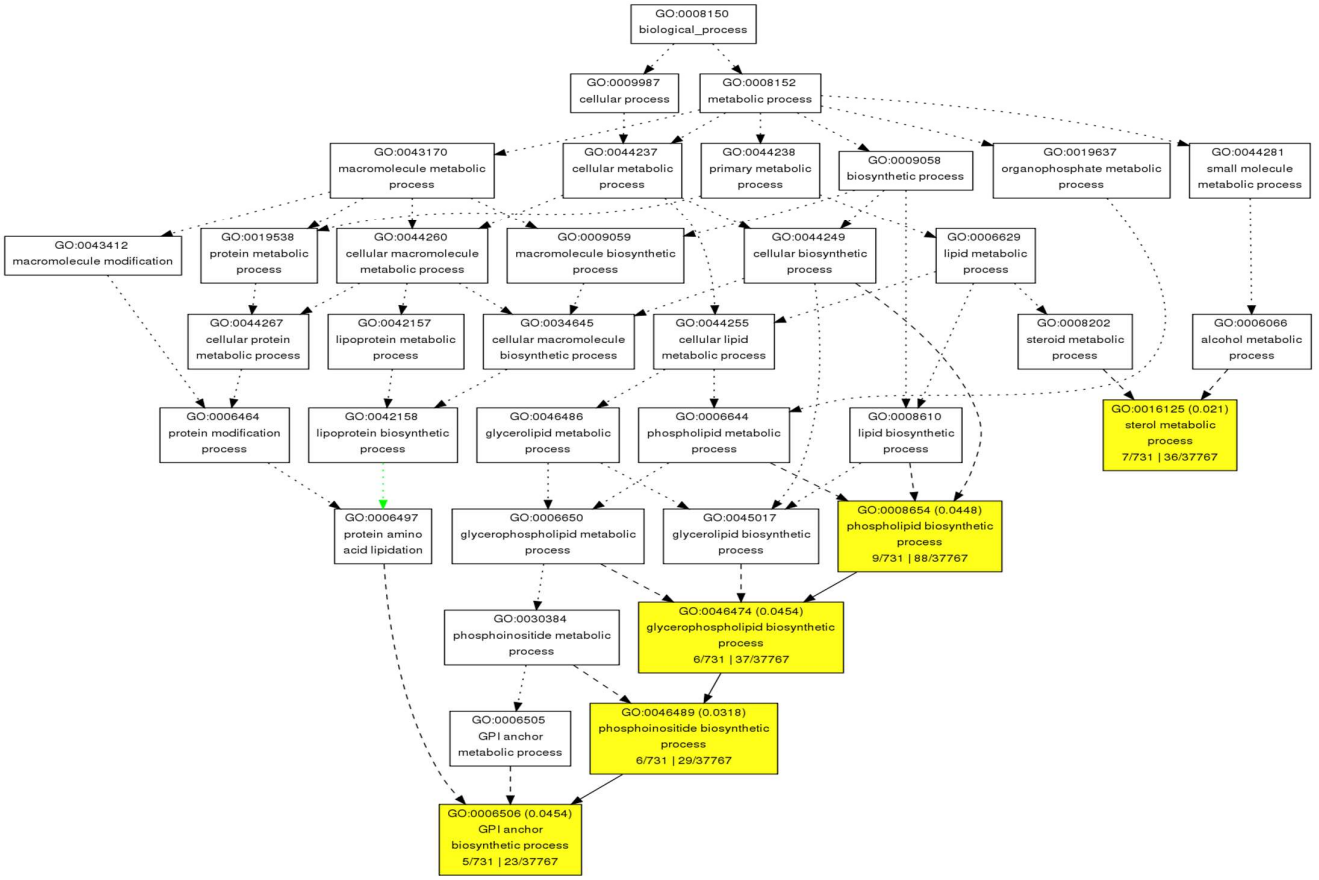

Figure 6-6: A graphical hierarchical image of GO analysis of genes downregulated in *sep1-1* under VT. (Coloured boxes denote significant terms). Biological processes under "GO0016125: sterol metabolic processes", and "GO0008654: phospholipid biosynthetic process" show enrichment in the dataset.

6.3.2 Differentially expressed genes unique to *sep2-1* VT

Genes upregulated in *sep2-1*_VT showed enrichment of a variety of GO terms. The most significantly enrich GO term was photosynthesis (GO:0015979) with 16 genes and plastid organization (GO:0009657). The genes in this list included *VARIEGATED 2* (AT2G30950; *VAR2*), a metalloprotease that functions in thylakoid membrane biogenesis and repair of PSII following damaged incurred during photoinhibition. Components of photosystem II, *PHOTOSYSTEM II SUBUNIT O-2* (AT3G50820), photosystem II subunit R (AT1G79040) are also downregulated in *sep2-1*_VT. Additionally, chloroplast proteins such as *ALBINO AND PALE GREEN 2* (AT2G01110), *PLASTID TRANSCRIPTIONALLY ACTIVE4* (AT1G65260), *PHOTOTROPIN 2* (AT5G58140), *SUPPRESSOR OF VARIEGATION 1* (AT2G39140), *J-DOMAIN PROTEIN REQUIRED FOR CHLOROPLAST ACCUMULATION RESPONSE 1* (AT1G75100), and *PLASTID MOVEMENT IMPAIRED1* (AT1G42550) were also found to be upregulated in *sep2-1*_VT. These genes play import roles in chloroplast organisation, thereby aiding photosynthesis.

Another enriched GO term was 'response to stimulus' (GO:0050896) with a 124 associated genes. However, the more enriched secondary branch, 'response to light stimulus' (GO:0009416) showed 32 genes. For example, *PHYTOCHROME-INTERACTING FACTOR7* (AT5G61270), functions in far-red light absorption. *MORE AXILLARY BRANCHES 2* (AT2G42620) is a ubiquitin-protein ligase that supresses hypocotyl and petiole elongation in light-grown seedlings. Similarly, *LIGHT-DEPENDENT SHORT HYPOCOTYLS 1* (AT5G28490) mediates light regulation of seedling development in a phytochrome-dependent manner. *X-RAY INDUCED TRANSCRIPT 1* (AT5G48720) functions in post-meiotic stages of pollen development and male and female meiosis.

The development-related GO term, 'post-embryonic development' (GO:0009791) led to identification of some flowering associated genes in the list. *ENHANCER OF AG-4 2* (AT5G23150; *HUA*) *HUA* is associated with the floral homeotic *AG* pathway and it enhances the phenotypes of the mild *ag-4* allele. Additionally, HUA also regulates flowering time genes such as *FLM* and *MAF2*. *HUA ENHANCER 4* (AT5G64390; *HEN4*) encodes a putative RNA binding protein that interacts with HUA and acts redundantly with *HUA1* and *HUA2* in the specification of floral organ identity in the third whorl.

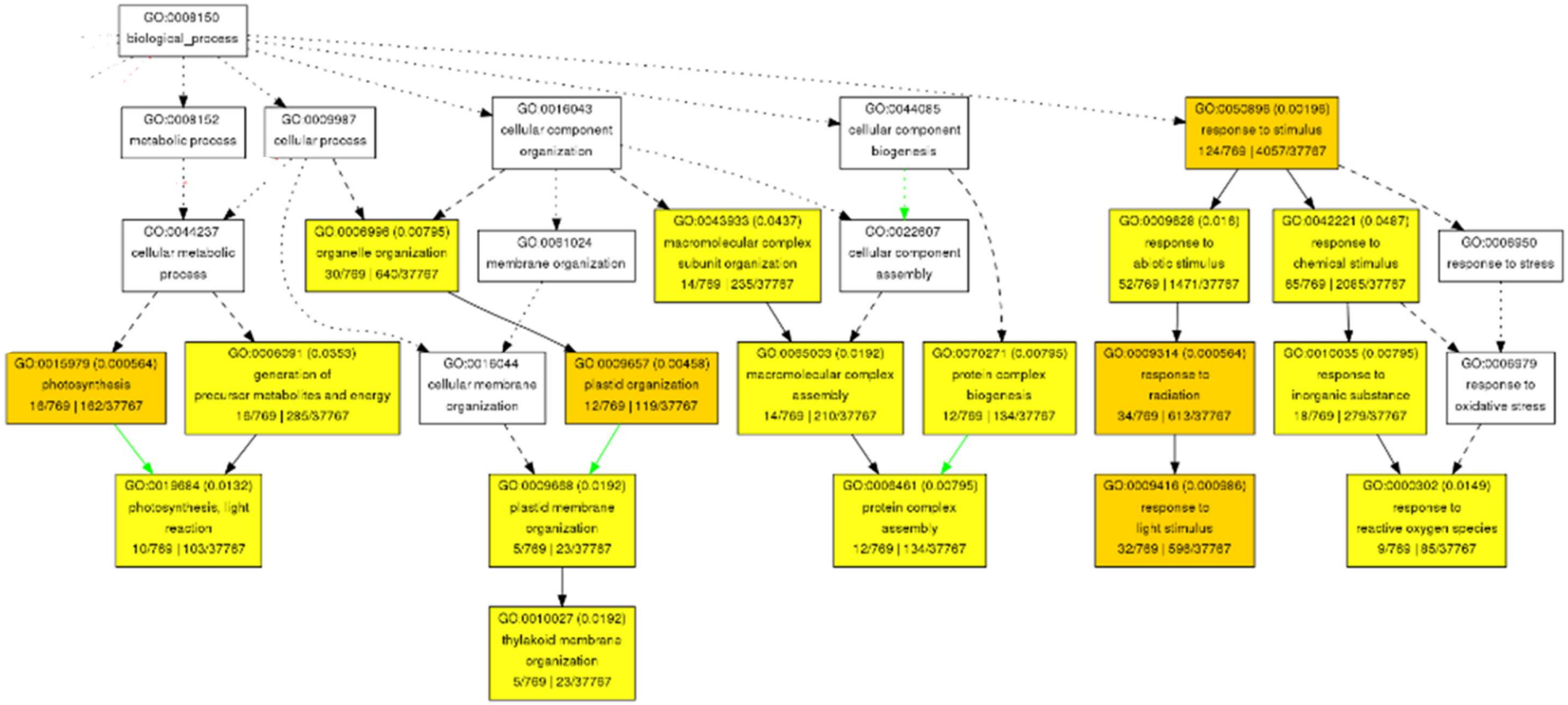

Figure 6-7: Snapshot of a graphical hierarchical image of GO analysis of genes upregulated in *sep2-1* VT. (Coloured boxes denote significant terms. Darker box colour denotes a lower p-value). Biological processes under "GO0065007: biological regulation", and "GO000198: response to stimulus" show enrichment in the dataset.

Manual analysis of the list of genes upregulated in *sep2-1*_VT indicated that 19 different Heat Shock Proteins (HSPs) or Chaperones were upregulated (Table 6-8). These contained large HSPs such as HSP70 (AT1G16030) and small HSPs such as HSP20 (AT1G52560, AT2G19310). HSPs are a big gene family associated with biological robustness. This suggests that SEP2 might act through HSPs in order to regulate robustness of flower development.

Table 6-8: Genes belonging to the heat shock protein (HSP) family, upregulated in *sep2-1* VT

Gene ID	Annotation	FC
AT1G71000	Chaperone DnaJ-domain superfamily protein	45.06
AT1G16030	heat shock protein 70B	23.88
AT3G14200	Chaperone DnaJ-domain superfamily protein	16.63
AT1G52560	HSP20-like chaperones superfamily protein	11.97
AT1G72416	Chaperone DnaJ-domain superfamily protein	10.92
AT2G19310	HSP20-like chaperones superfamily protein	8.61
AT5G62020	heat shock transcription factor B2A	6.31
AT1G56300	Chaperone DnaJ-domain superfamily protein	2.37
AT3G02990	heat shock transcription factor A1E	1.93
AT2G20920	chaperone (DUF3353)	1.91
AT1G77930	Chaperone DnaJ-domain superfamily protein	1.77
AT1G12520	copper chaperone for SOD1	1.65
AT2G22360	DNAJ heat shock family protein	1.50
AT5G01970	heat-inducible transcription repressor	1.46
AT1G65280	DNAJ heat shock N-terminal domain-containing protein	1.42
AT5G53150	DnaJ heat shock amino-terminal domain protein	1.40
AT5G37380	Chaperone DnaJ-domain superfamily protein	1.36
AT5G22080	Chaperone DnaJ-domain superfamily protein	1.28
AT5G49580	Chaperone DnaJ-domain superfamily protein	1.21

Genes downregulated in *sep2-1*_VT show significant enrichment of the GO term 'translation' (GO:0006412) (Figure 6-8), with 41 genes in the list (Appendix 6-II). Translation related genes predominantly contain four different classes (Table 6-9). The first is translation initiation factor, that contains prominent members such as *EUKARYOTIC TRANSLATION INITATION FACTOR 4E* (AT4G18040), *TRANSLATION INITIATION FACTOR 3* (AT5G44320), *TRANSLATION INITIATION*

FACTOR 6 (AT2G39820). These proteins function in ribosome assembly and initiation of translation. The second and third classes are comprised of 40S and 60S ribosomal proteins, respectively. The 40S ribosomal proteins play a role in biogenesis of the small unit of ribosome while the 60S proteins are structural constituents of the large subunit of ribosome. The fourth class is aminoacyl-tRNA synthetase. tRNA-synthetases specific to cysteine, aspargine, and phenylalanine were downregulated in *sep2-1*_VT.

Table 6-9: Selected candidates from GO analysis of genes downregulated in *sep2-1* VT, related to regulation of translation

Gene ID	Annotation	Protein Class
AT5G38830	Cysteine--tRNA ligase 2, cytoplasmic	aminoacyl-tRNA synthetase(PC00047)
AT5G35620	Eukaryotic translation initiation factor isoform 4E;EIF	translation initiation factor(PC00224)
AT1G34030	40S ribosomal protein S18;RPS18A	ribosomal protein(PC00202)
AT2G32220	60S ribosomal protein L27-1;RPL27A	ribosomal protein(PC00202)

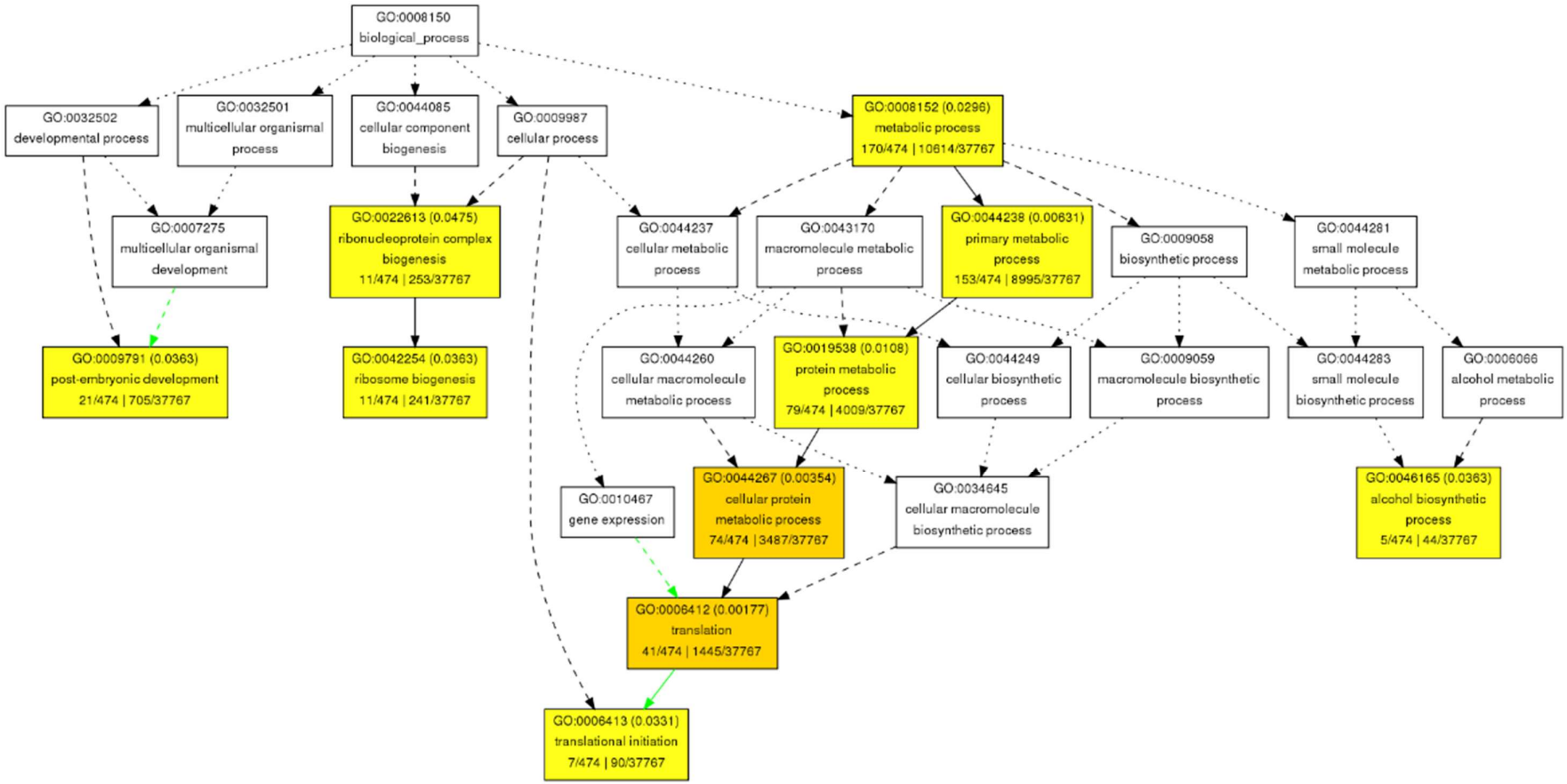

Figure 6-8: A graphical hierarchical image of GO analysis of genes in *sep2-1* VT. Coloured boxes denote significant terms. Darker box colour denotes a lower p-value. Biological processes under 'translation' (GO:0006412) show enrichment in the dataset

6.4 Discussion

6.4.1 High confidence targets of SEP1 and SEP2

As Arabidopsis SEPs have been reported as redundant, SEP3 has been used as a representative of the SEP gene family for most molecular research relevant to flower development in Arabidopsis. The targets of SEP3 have been identified by using ChIPseq (Kaufmann et al., 2009a) and its role in protein-protein interactions have been studied (Pelaz et al., 2001c). Furthermore, the role of SEP3 in forming complexes with other transcription factors that bind to DNA to regulate gene expression has been described (Sridhar et al., 2006; Immink et al., 2009; Melzer et al., 2009; Lai et al., 2020). The mechanisms employed by SEP3 for recognising and binding target DNA sequences has also been studied (Käppel et al., 2018). Although the yeast two hybrid (Y2H) studies that used SEP1, SEP2, and SEP4 along with SEP3 as baits provide insight into the protein-protein interactions of other Arabidopsis SEPs (de Folter et al., 2005b; Kaufmann et al., 2005a), information about the targets of SEP1 and SEP2 transcription factors is lacking.

Results from Chapter 4 show that SEP1 and SEP2 are non-redundant with SEP3 and SEP4 (Section 4.1, 4.4). Thus, it is important to identify the targets of SEP1 and SEP2 to further our understanding of their functions. Additionally, individual SEP transcription factors have different preferences for co-operative DNA binding and bind to target genes that differ in the arrangement and spacing of the CArG-boxes in their cis-regulatory regions (Jetha et al., 2014). Moreover, the SEPs have two domains that might directly or indirectly affect binding to targets – (i) the highly conserved MADS domain that binds to CArG domains in the promoter region of target genes, and (ii) K-domain that facilitates protein-protein interaction to form complexes with other transcription factors which in turn regulate gene expression. Based on the different expression patterns and protein-protein interactions of SEPs (de Folter et al., 2005b; Kaufmann et al., 2005a), it is evident that different SEPs may regulate expression of target genes that are largely overlapping, but not identical sets. This highlights the importance of finding targets of SEP1 and SEP2.

Thus, in this study, RNAseq data was generated and analysed for *sep1-1* and *sep2-1*. Moreover, the availability of two different datasets for each *sep1-1* and *sep2-1*, grown in either ST or VT presented an opportunity to determine high-confidence targets of SEP1 and SEP2. SEP1 regulates targets involved in flowering time, flower

development, *sep*al development, and phytohormone synthesis pathways (Section 6.2.1). The targets of SEP2 predominantly include genes functioning in flowering time, organ polarity specification, and metabolic processes (Section 6.2.1). In addition to MADS-box transcription factors, they also regulate other transcription factors such as bZIP and PLATZ. Thus, SEP1 and SEP2 are not only involved in regulating downstream transcription factors that in turn, directly or indirectly control metabolic processes, but they themselves also regulate other genes involved in metabolism and signalling. They also regulate genes involved in brassinosteroid synthesis and auxin signalling, indicating that SEP1 and SEP2 are involved in the regulation of responses toward the phytohormones brassinosteroids (*BR6OX2*) and auxin (*AUXIN RESISTANT 1*). Overall, both SEP1 and SEP2, like other MADS-box transcription factors, either activate or repress expression of downstream genes in order to regulate flower development.

6.4.2 Common and different targets of SEP1 and SEP2

As SEP1 and SEP2 have been shown to act redundantly to regulate the robustness of decussate petal arrangement in both ST and VT (Chapter 4). Thus, it was important to analyse the overlapping set of target genes regulated by SEP1 and SEP2 in both ST and VT conditions. Overlapping genes between *sep1-1* and *sep2-1* from both ST and VT showed a very small overlap. This could be due to including RNAseq datasets from VT conditions, as natural environmental conditions might result in a lot of variability in gene expression levels. As the RNAseq analysis tool Cuffdiff eliminates genes that show high variability between replicates, these genes must have been excluded, resulting in a low overlap. The small number of overlapping genes showed genes that function in *sep*al growth (*LGO, PRP2*). Most target genes had unannotated functions. Although the motive behind identifying overlapping DEGs from *sep1-1* and *sep2-1* was to identify genes relevant to robustness, the obtained dataset did not offer any conclusive information.

6.4.3 Targets of SEP1 and SEP2 that aid with robustness

According to our hypothesis (Section 1.6), SEP1 and SEP2 buffer the stochastic perturbations caused by changing environment to produce a robust decussate flower. An attempt towards identifying targets of SEP1 and SEP2 related to robustness was made by analysing the list of DEGs exclusive to *sep1-1* and *sep2-1* VT. RNAseq analysis of *sep1-1* and *sep2-1* mutants grown in variable environments allows us to

view a snapshot of the genes that would act downstream of SEP1 and SEP2 in the mechanism of conferring robustness. Genes upregulated in *sep1-1* VT could be broadly categorised as (i) transcription initiation factors, (ii) RNA processing factor, (iii) RNA splicing factor, and (iv) chromatin regulatory proteins (Appendix 6-I). This suggests the possibility of SEP1 directly or indirectly regulating the expression of its targets through transcriptional regulation and chromatin modification. In Arabidopsis, several components of flowering time and flower development pathways are involved in regulating the expression by modifying the chromatin of target genes (He and Amasino, 2005). In contrast, the downregulation of genes related to translation in *sep2-1* VT suggests the SEP2 regulates protein levels of targets at a post-transcriptional level. Moreover, upregulation of ~ 20 HSP/Chaperone genes in *sep2-1* VT hints towards a molecular link between SEP2 and HSPs that might play a role in robustness. HSPs are considered to be master regulators that govern the robustness of systems. The most prominent example is HSP90, that functions across various species. HSPs are molecular chaperones responsible for folding and localization of proteins as well as for regulation of protein accumulation and denaturation. The HSP family contributes to various functions such as abiotic stress tolerance, in particular heat stress and various developmental stage (Queitsch and Hong, 2000). HSP90 functions as a network hub in gene regulatory networks and has the capacity to buffer many developmental phenotypes (Sangster and Queitsch, 2005). In Arabidopsis, perturbing HSP90 resulted in phenotypic variation with respect to multiple traits such as root elongation, defense and response to stress. Additionally, it is also speculated that in regulators connected to multiple genetic networks, their contribution to each network is balanced. If this balance is disrupted, phenotypic variance is seen. Further investigation into the role of different small HSPs and Chaperones is necessary to understand how SEP2 and HSPs regulate robustness in flower development.

In summary, the RNAseq analyses identified targets of SEP1 and SEP2, relevant to flower development as well as robustness. The results allow some general conclusions as to how SEP1 and SEP2 regulate floral organ identity, organ patterning, as well as robustness of flower development. First, SEP1 and SEP2 regulate other transcription factors involved in flower development (LFY, SEP3, AP1; Section 5.3), suggesting autoregulation action. Other targets of SEP1 and SEP2 include genes that are involved in *sep*al growth, organ boundaries and position, hormone response (Appendix 5-I, 5-II,

Table 6-2, Table 6-3, and Table 6-9). Second, SEP1 and SEP2 may act as activators or repressors of transcription and translation (Table 6-9). They regulate not only DNA-binding TFs such as MADS box proteins, but also chromatin remodelers, transcription initiation factors and RNA-polymerase subunits. Third, SEP1 and SEP2 have mostly been reported to be a part of the E-function gene specifying floral organ identity, but their regulatory functions are also indispensable for further growth and differentiation of the floral organs.

7 General Discussion

The primary objective of the work described in this thesis has been to determine whether *SEPs* play a role in developmental robustness of flower development in Arabidopsis and to identify the molecular mechanisms underlying the phenomenon. In this process, I investigated the evolution and diversification of the *SEP* gene family in Angiosperms (Chapter 3). I then performed phenotypic characterization of the Arabidopsis *sep* mutants to conclude that they show distinct and significant phenotypes and that individual *SEPs* showed redundant as well as non-redundant functions (Chapter 4). Subsequent work then focused on understanding the molecular mechanisms underlying the function of *SEP1* and *SEP2* (Chapter 5 and Chapter 6). This chapter aims to highlight key outcomes from this thesis and to provide scope for future research.

7.1 SEP1 and SEP2 contribute to a robust decussate petal arrangement

The phenotypic characterization and RNAseq analysis of *sep1* and *sep2* shows that they exhibit robustness related traits. *sep1* and *sep2* mutants showed a variability in petal arrangement producing flowers with skewed petals in stable temperature (ST) conditions (Section 4.2). The increase in variance and penetrance of this phenotype in variable temperature (VT) conditions while keeping a constant theoretical and experimental mean of 90° shows a typical characteristic of mutants associated with robustness (Boukhibar and Barkoulas, 2016). Thus, increased trait variability, rather than simple enhancement of trait severity, is the critical measure of robustness of decussate *sep*al arrangement. *sep1 sep2* plants produced flowers with skewed petal angles in both ST and VT. Although the phenotypic variance in *sep1 sep2* could not be quantified due to the extreme deformation of the flowers, it is evident SEP1 and SEP2 act redundantly to govern the robustness of forming decussate flowers. Angiosperms have a large number of redundant duplicate genes. Most of these are a result of small and/or large-scale genome duplications, and the whole-genome duplication (WGD) events that occurred during the evolution of flowering plants (Hanada et al., 2009; Kuzmin et al., 2020). Although duplicate genes undergo non-functionalisation or sub- and neo-functionalisation, the paralogues that are retained often have at least partly overlapped functions (Veitia, 2005). Such redundancy is important for developmental

robustness or canalization (Whitacre, 2012) as redundant transcription factors involved in developmental robustness could reduce variability caused by environmental changes and other stochastic perturbations (Gu et al., 2003).

Due to the temporal, physical, developmental and biochemical constraints required to optimise the reproductive potential of the flower, mechanisms that reproducibly and robustly deliver a uniform flower despite changing environments may be under stringent selection. Recent studies aiming to characterise different aspects of development in flower development have highlighted the role of redundant genes. For example, the *miRNA164* family has been shown to redundantly control floral organ number (Sieber et al., 2007). Redundant miRNAs - *miR164A, miR164B*, and *miR164C* regulate gene expression to reproducibly produce a fixed number of perianth organs. Similarly, duplicate *SHATTERPROOF 1 (SHP 1)* and *SHP 2* genes in Arabidopsis show overlapping functions in carpel and ovule identity along with AG and *SEEDSTICK* (Pinyopich et al., 2003). Some studies on developmental robustness hypothesise that for redundant genes, the stochastic amount each individual protein produced would be buffered at the level of downstream gene expression. At a given time, the output would be relative to the total level of protein, allowing the effects of stochastic bursts in the production of each one to be averaged out across the different proteins (Qian et al., 2010). This is reflected in the unaffected expression levels of *SEP1* in *sep2-1* mutants and of *SEP2* in *sep1-1* mutant (as seen from the RNAseq data in this study). Taken together, examples like these suggest that the robustness originally caused by a duplication has facilitated evolutionary diversification on the molecular level. Such diversification is a prerequisite for morphological evolution.

Although SEP1 and SEP2 are redundant, unique genes and gene families were found to be differentially expressed exclusively in either *sep1-1* or *sep2-1* grown in the screenhouse (Section 6.3). This suggests the possibility of SEP1 and SEP2 employing *sep*arate molecular mechanisms to safeguard the robustness of developing flowers with decussate petal arrangement. In screenhouse growth conditions, loss of *SEP1* resulted in upregulation of genes involved in transcription initiation, regulation of transcription and RNA-binding. On the contrary, loss of *SEP2* resulted in upregulation of Heat Shock Proteins (HSPs) and Chaperones. Members of the HSP family ae known to contribute to robustness by aiding protein folding and transcriptional regulation by RNA polymerase II pausing (El-Samad et al., 2005; Siegal and Rushlow, 2012). Genes

associated with initiation of translation and ribosome synthesis were downregulated in *sep2-1* grown in the screenhouse. Overall, loss of SEP1 or SEP2 affected the expression of network elements that are essential for transcriptional and post-transcriptional regulation. This showed that SEP1 and SEP2 act upstream of regulatory genes and gene families in the GRN. Thus, SEP1 and SEP2 govern the robustness of decussate petal symmetry through combinatorial activity of genetic redundancy, regulation of gene expression and by acting as master regulators, functioning upstream of other regulators. The skewed petal phenotype in *sep1-1* and *sep2-1* could be complemented by *pSEP1:SEP1* and *pSEP1:SEP2*, but not by *pSEP1:SEP3/4*, which makes two points. Firstly, even if *SEP1* and *SEP2* potentially confer robustness by regulating different targets, robustness can be more or less restored by adding in a duplicate of the retained gene, which suggests that robustness is a quantitative trait or that there is actually an undiscovered common mechanism. Secondly, it is the SEP protein that functions in robustness of decussate petal arrangement, and not the promoter *pSEP1* or *pSEP2* that makes the difference. Thus, further investigation is necessary to identify the properties of SEP1 and SEP2 have that are not found in SEP3 and SEP4, that allows them to promote robustness in petal angle.

7.2 Redundant function of SEP1 and SEP2 in lateral *sep*al growth

In addition to their role in robustness of petal angle, SEP1 and SEP2 act redundantly to regulate growth of lateral *sep*als (Section 4.3). Single *sep-1* and *sep2-1* mutants do not show loss of lateral *sep*als. However, the *sep1-1 sep2-1* double mutant is characterised by the presence of rudimentary lateral *sep*als that fail to grow further. Complementation of this phenotype by *pSEP1:SEP1* and *pSEP2:SEP* confirmed that it was attributable to the loss of *SEP1* and *SEP2* (Section 4.5.1). However, more detailed characterisation of double mutants formed by different *sep1* and *sep2* alleles is necessary. Additionally, the loss of lateral *sep*als phenotype was also complemented by promoter swap constructs *pSEP1:SEP2/3/4* and *pSEP2:SEP1/3/4* (Section 4.5.2). This showed that the activity of the protein was essential to regulate growth of lateral *sep*als and that the SEP1-4 could contribute redundantly to it. Redundant transcription factors are known to regulate the development of plant lateral organs (Eshed et al., 2001). Single mutants of these redundant transcription factors seldom cause a comprehensive loss of patterning (Eshed et al., 2001; Husbands et al., 2009). This points towards robustness of the network in terms of changes in the amount of its components.

One of the most interesting outcomes in this study has been identification and experimental validation of targets of SEP1 and SEP2 that contribute to lateral *sep*al development. RNAseq analysis revealed a large number of interesting genes that could play a possible role in the growth of lateral *sep*als. Two different strategies were used to narrow down upon a few high-confidence targets that link expression of *SEP1* and *SEP2* to outgrowth of lateral *sep*als. Since the loss of lateral *sep*als is not observed in *sep1-1* or *sep2-1* single mutants, it could either be a more severe version of the individual single mutant phenotypes or be a completely unrelated phenotype, only present when both SEP1 and SEP2 are compromised. RNAseq analysis based on strategy A (Section 5.3.1) showed that a variety of genes with functions related to meristem identity specification, cell wall modification, cell cycle regulation and cell proliferation, were commonly differentially expressed in *sep1-1, sep2-1* and *sep1 sep2*. Targeted candidate gene testing by CRISPR and mutant analysis revealed that two genes of unknown function, *FBRI* and *PRP2,* both of which were upregulated in *sep1*, *sep2* and *sep1 sep2*, play a key role in lateral *sep*al expansion. Flowers from *sep1 sep2 fbri* and *sep1 sep2 prp2* revert to have four *sep*als, including two fully grown lateral *sep*als (Section 5.4.2). This supports the hypothesis that overexpression of one or other of these genes in the *sep1 sep2* double mutant is a causative factor in the failure of lateral *sep*als to develop normally. Removal of either gene, via CRISPR deletion, restores normal lateral *sep*al development in *sep1 sep2*. Although the *FBRI* is not functionally characterised, its constitutive domains, F-box and LRR, show potential for regulating the activity of transcription factors and co-factors through ubiquitylation and interaction with MADS-box transcription factors (Gamboa et al., 2001; Ni et al., 2004). The homologues of the uncharacterised *PRP2* function as extensins in cell wall modification (Stein et al., 2011). RNAseq analysis based on strategy B, that is, differentially expressed only in *sep1 sep2* identified many genes associated with determining organ polarity (Section 5.3.2). Out of these, *NUBBIN*, a homologue of *JAGGED* was identified as a putative target of *SEP1* and *SEP2*. *nub sep1 sep2* flowers also showed a reversal of the *sep1 sep2* lateral *sep*al phenotype to wild type (Section 5.4.2). SEP1 and SEP2 together regulate organ polarity genes, such as *YABBY1, CRABSCLAW, NUBBIN* and *HD-ZIPIII* that function in controlling appropriate cell division and expansion that is necessary for organ development. Overall, this shows that SEP1 and SEP2 not only function during specification of organ identity, but their regulatory action is crucial for further growth and differentiation of the floral organs. It

also suggests that the expression SEP1 and SEP2 persists even after initiation of organ primordia.

7.3 .Functional diversification and partial redundancy of Arabidopsis SEPs

In this study, the phenotypic characterization of *sep1-4* mutants in stable and variable temperatures has revealed *sep*arate and significant phenotypes for each individual mutant. The skewed petal phenotype of *sep1* and *sep2* alleles was affected by the environmental conditions, whereas the loss of lateral *sep*als described in *sep1 sep2* was environment independent. Although *sep3-2* did not show a significant phenotype, it showed occasional conversion of petals to *sep*alloid petals. The extra floral organs phenotype of *sep4* was environment independent (Section 4.1). This study also showed that *SEP1* and *SEP2* are partially redundant with each other; whereas, *SEP1/2, SEP3* and *SEP4* are non-redundant (Chapter 4). This is supported by the fact that *SEP1/2, SEP3* and *SEP4* form different subclades in the phylogenetic analysis (Section 3.3). This is in concurrence with the reported evolutionary analysis showing that *SEP3* forms a different subclade while *SEP1/2/4* belong to the LOFSEP subclade (Malcomber and Kellogg, 2005; Zahn et al., 2005). Additionally, *SEP1/2/4* and *SEP3* share different syntenic blocks with the two Amborella SEPs, showing independent evolution (Section 3.4). This is supported by the difference in reported expression patterns of *SEP* genes. *SEP1, SEP2*, and *SEP4* are expressed throughout the floral meristems and in all four floral whorls from stage 2 onwards (Flanagan and Ma, 1994; Savidge et al., 1995; Mandel and Yanofsky, 1999; Ditta et al., 2004). In contrast, *SEP3* is expressed only in whorls 1, 2, and 3 before specification of floral organ primordia. Furthermore, individual SEPs form *sep*arate protein-protein interactions, for examples, ARABIDOPSIS B-SISTER I (ABS-I) forms ternary complexes with the dimers SEP1-SEP2, SEP2-AGL74, SEP3-PI and SEP3-AGL16 (Immink et al., 2009). The independent individual phenotypes for each gene combined with the reported difference in expression patterns and different protein-protein interactions show that these genes have independent functions. Additionally, the RNAseq analysis for *sep1-1* and *sep2-1* showed differential expression of common as well as unique targets. Analysis of the unique targets, as mentioned earlier in Section 7.2, shows that SEP1 and SEP2 are associated with target genes that have very different functions. This indicates that despite being functionally redundant, SEP1 and SEP2 might have different molecular mechanisms underlying their function. Overall, the outcomes from the present study

suggest that the Arabidopsis SEPs have undergone sub-functionalisation, wherein SEP1 and SEP2 have functions relevant to organ growth and patterning and SEP4 is involved in regulating organ number.

7.4 Future prospects

The outcomes from this thesis lead to further questions –

7.4.1 Identification of protein domains or amino acids responsible for phenotypes of individual SEPs

This work has shown that the Arabidopsis *SEP* genes are not functionally redundant. Further, promoter swap experiments identified that the loss of lateral *sep*als in *sep1 sep2* could be complemented by *pSEP1* or *pSEP2* driving the expression of any Arabidopsis *SEP* (*pSEP1:SEP1/2/3/4-GFP* and *pSEP2:SEP1/2/3/4-GFP* constructs). This showed that any Arabidopsis SEP protein could redundantly function to regulate lateral *sep*al growth under if expressed using *pSEP1* or *pSEP2* promoters. In contrast, *SEP3* and *SEP4* driven by *pSEP1* or *pSEP2* promoters cannot complement the skewed petal phenotype in *sep1-1* and *sep2-1*. This raises a question about which domains confer specific functions to *SEPs*. Domain swap assays could be performed to investigate this.

7.4.2 Analysis of suppressed lateral *sep*al phenotype in *sep1 sep2*

The flowers from *sep1-1 sep2-1* double mutant plants showed suppressed growth of lateral *sep*als. However, due to the difficulty in identifying homozygous double mutants for other alleles, the occurrence of this phenotype in double mutants of different *sep1* and *sep2* alleles was not confirmed. Confidence that the suppressed lateral petal phenotype is specifically dependent on the loss of both *SEP1* and *SEP2* comes from the fact that normal lateral *sep*al development is restored when *sep1-1 sep2-1* is complemented by *SEP1* or *SEP2* under the control of their native promoters. Nevertheless, new crosses with the other alleles of *sep1* (*sep1-2, sep1-3*) and *sep2* (*sep2-3, sep2-4*) need to be generated to provide more evidence supporting this phenotype. Alternatively, novel *sep1 sep2* knockout lines could be generated by using the CRISPR/Cas9 genome editing tool.

7.4.3 Further examination of targets of SEP1 and SEP2

This study provided the identification of targets of SEP1 and SEP2 by RNAseq analysis of *sep1-1* and *sep2-1,* grown in standard and screenhouse conditions, respectively. It also determined the common targets of SEP1 and SEP2 from *sep1 sep2*. Out of the few

target genes selected for experimental validation, three genes – *NUB, FBRI,* and *PRP2* were found to reverse the *sep1 sep2* phenotype. However, due to time constraints caused by the COVID pandemic, this experiment was carried out only on T1 plants from the CRISPR/Cas9 KO lines generated for *nub sep1 sep2*, *fbri sep1 sep2,* and *prp2 sep1 sep2.* Further experiments are necessary for molecular and phenotypic characterisation of these lines. Additionally, RNAseq data from *sep3* and *sep4* alleles grown in standard and screenhouse conditions could be used to broaden our understanding of molecular mechanisms underlying the function of SEPs. These datasets, in combination with the RNAseq datasets from this study could be used to further identify-
(i) DEGs common to *sep1, sep2, sep3,* and *sep4* in order to determine common targets of SEPs1-4

(ii) DEGs contributing to the extra organ phenotype in *sep4.*

7.4.4 **Investigation of reproductive fitness in *sep* mutants**

A major conclusion from this thesis is that *SEPs*, especially *SEP1* and *SEP2* ensure robust flower development in Arabidopsis. Flower development is thought to be robust as it is a crucial aspect of reproduction. Thus, it was interesting to evaluate the effect of loss of SEPs on the reproductive fitness of plants in natural environmental conditions. The resources generated from the present study, that is, the complementation lines *pSEP1:SEP1/2/3/4-GFP* in *sep1-1* and *sep1 sep2* background and *pSEP2:SEP1/2/3/4-GFP* in *sep2-1* and *sep1 sep2* background could be used for this experiment.

8 Appendix

Appendix 5-I: List of genes upregulated in *sep1*, *sep2*, and *sep1 sep2*. The list is sorted according to expression in flowers followed by fold change (FC) in *sep1 sep2* in ascending order.

Gene ID	Annotation	FC *sep1*	FC *sep2*	FC *sep1 sep2*	Expressed in flowers
AT5G32460	Reproductive meristem like 3	58.96	2.47	28.48	yes
AT5G53810	O-methyltransferase	138.44	80.01	4.54	yes
AT5G17780	alpha/beta-Hydrolases	2.62	1.72	3.23	yes
AT3G59190	F-box/RNI-like	1.80	2.46	3.16	yes
AT2G35700	ERF 38	2.01	2.14	3.07	yes
AT5G55560	Protein kinase	1.72	2.15	3.00	yes
AT3G08860	PYRIMIDINE 4	3.50	5.69	2.80	yes
AT1G60590	Pectin lyase-like	2.84	2.51	2.72	yes
AT5G60250	zinc finger	1.42	1.93	2.66	yes
AT3G45060	high affinity nitrate transporter 2.6	2.13	3.17	2.48	yes
AT2G21140	proline-rich protein 2	2.23	1.73	2.47	yes
AT3G22840	Chlorophyll A-B binding	2.88	3.68	2.10	yes
AT3G53300	cytochrome P450	99.31	93.14	2.06	yes
AT4G08870	Arginase/deacetylase	1.58	2.03	1.85	yes
AT5G20150	SPX domain-containing protein 1	1.33	1.99	1.77	yes
AT5G53390	O-acyltransferase (WSD1-like)	1.55	2.07	1.67	yes
AT4G08580	microfibrillar-associated protein	1.29	1.16	1.63	yes
AT5G16990	Zinc-binding dehydrogenase	1.91	1.18	1.55	yes
AT5G28300	Duplicated homeodomain-like	1.58	1.73	1.53	yes
AT4G02390	poly(ADP-ribose) polymerase	1.64	1.89	1.52	yes
AT2G40940	ethylene response sensor 1	1.29	1.38	1.47	yes
AT5G03340	ATPase CDC48 protein	1.25	1.35	1.43	yes
AT5G52540	keratin-associated (DUF819)	1.60	1.57	1.42	yes
AT5G56500	TCP-1/cpn60 chaperonin	1.45	1.57	1.38	yes
AT5G56330	alpha carbonic anhydrase 8	353.26	406.48	218.33	no
AT5G37940	Zinc-binding dehydrogenase	2.39	2.72	9.92	no
AT5G50360	von willebrand factor A domain protein	6.69	5.56	3.00	no
AT4G11530	cysteine-rich RLK (RECEPTOR-like protein kinase) 34	2.26	1.63	2.82	no
AT5G51480	SKU5 similar 2	1.63	2.14	2.58	no

AT5G24240	phosphatidylinositol 4-kinase gamma-like protein	3.74	1.97	2.58	no
AT3G21560	UDP-Glycosyltransferase	1.61	2.37	2.18	no
AT2G16660	Major facilitator	1.84	2.88	1.73	no
AT5G43340	phosphate transporter	1.52	1.78	1.68	no
AT1G67990	S-adenosyl-L-methionine-dependent methyltransferase	1.61	1.99	1.55	no

Appendix 5-II: List of genes downregulated in *sep1, sep2*, and *sep1 sep2*. The list is sorted according to expression in flowers followed by fold change (FC) in *sep1 sep2* in descending order.

Gene ID	Annotation	FC *sep1*	FC *sep2*	FC *sep1 sep2*	Expressed in flowers
AT2G43550	scorpion toxin-like knottin	-1.45	-1.41	-0.72	yes
AT5G46430	Ribosomal protein L32e	-2.07	-1.21	-0.72	yes
AT5G52390	PAR1 protein	-3.51	-1.99	-0.68	yes
AT5G22580	Stress responsive A/B Barrel Domain-containing protein	-1.43	-1.35	-0.68	yes
AT3G02550	LOB domain-containing protein 41	-1.38	-3.45	-0.68	yes
AT5G11580	Regulator of chromosome condensation (RCC1)	-2.31	-1.32	-0.64	yes
AT5G13240	transcription regulator	-1.48	-1.21	-0.64	yes
AT5G04720	ADR1-like 2	-1.88	-1.84	-0.63	yes
AT4G16690	methyl esterase 16	-1.84	-1.62	-0.61	yes
AT5G54630	zinc finger protein-like protein	-1.43	-1.69	-0.61	yes
AT2G30600	BTB/POZ domain-containing protein	-1.99	-2.15	-0.61	yes
AT2G02710	PAS/LOV protein B	-1.93	-2.45	-0.61	yes
AT5G45110	NPR1-like protein 3	-2.36	-2.10	-0.60	yes
AT3G55630	DHFS-FPGS homolog D	-1.39	-1.60	-0.60	yes
AT4G37240	HTH-type transcriptional regulator	-1.97	-1.61	-0.59	yes
AT5G53050	alpha/beta-Hydrolases	-3.66	-3.17	-0.58	yes
AT1G33600	Leucine-rich repeat (LRR)	-2.82	-2.49	-0.58	yes
AT1G69890	actin cross-linking protein (DUF569)	-1.75	-1.69	-0.58	yes
AT5G43500	actin-related protein 9	-2.11	-1.20	-0.58	yes
AT5G40910	Disease resistance protein (TIR-NBS-LRR class)	-2.49	-1.46	-0.58	yes
AT4G02130	galacturonosyltransferase 6	-1.96	-2.24	-0.57	yes
AT5G53880	hypothetical protein	-1.47	-1.53	-0.56	yes
AT4G11280	1-aminocyclopropane-1-carboxylic acid synthase 6	-4.24	-4.89	-0.55	yes
AT5G62020	heat shock transcription factor B2A	-2.70	-2.29	-0.55	yes
AT2G28660	Chloroplast-targeted copper chaperone protein	-1.24	-1.29	-0.55	yes
AT3G50060	myb domain protein 77	-5.59	-4.76	-0.55	yes
AT5G61590	Integrase-type DNA-binding	-1.93	-1.89	-0.55	yes
AT4G07825	transmembrane protein	-2.36	-2.63	-0.53	yes
AT2G46600	Calcium-binding EF-hand	-2.67	-2.71	-0.53	yes

AT3G23080	Polyketide cyclase/dehydrase and lipid transport	-2.03	-1.66	-0.53	yes
AT2G40000	ortholog of sugar beet HS1 PRO-1 2	-5.08	-5.98	-0.53	yes
AT4G17500	ethylene responsive element binding factor 1	-5.39	-6.33	-0.51	yes
AT5G17870	plastid-specific 50S ribosomal protein 6	-4.38	-1.28	-0.51	yes
AT3G16720	TOXICOS EN LEVADURA 2	-3.21	-4.26	-0.50	yes
AT3G51860	cation exchanger 3	-1.52	-1.43	-0.50	yes
AT5G41080	PLC-like phosphodiesterases	-2.12	-2.19	-0.44	yes
AT5G41740	Disease resistance protein (TIR-NBS-LRR class)	-11.26	-6.95	-0.42	yes
AT2G32140	transmembrane receptor	-8.56	-4.59	-0.39	yes
AT4G01590	DNA-directed RNA polymerase III subunit	-2.97	-2.76	-0.38	yes
AT3G55980	salt-inducible zinc finger 1	-7.26	-4.50	-0.37	yes
AT4G29780	nuclease	-7.91	-10.07	-0.35	yes
AT4G27280	Calcium-binding EF-hand	-12.68	-5.88	-0.35	yes
AT5G43440	2-oxoglutarate (2OG) and Fe(II)-dependent oxygenase	-5.30	-1.37	-0.34	yes
AT1G78450	SOUL heme-binding	-1.66	-1.78	-0.33	yes
AT2G32150	Haloacid dehalogenase-like hydrolase (HAD)	-2.06	-2.03	-0.30	yes
AT5G56910	Proteinase inhibitor	-2.81	-2.53	-0.21	yes
AT3G60930	unknown protein	-5.31	-6.45	-0.18	yes
AT5G56370	F-box/RNI-like/FBD-like domains-containing protein	-4.12	-3.59	-0.15	yes
AT1G76650	calmodulin-like 38	-5.26	-9.56	-0.15	yes
AT5G48412	unknown protein	-1.90	-1.38	-0.63	no
AT5G56760	serine acetyltransferase	-1.20	-1.42	-0.58	no
AT5G26800	xaa-pro aminopeptidase P	-2.68	-1.34	-0.57	no
AT1G49130	B-box type zinc finger protein with CCT domain-containing protein	-1.94	-3.99	-0.57	no
AT4G32480	sugar phosphate exchanger (DUF506)	-2.65	-3.68	-0.56	no
AT5G39210	chlororespiratory reduction 7	-1.91	-1.33	-0.54	no
AT1G51405	myosin-like protein	-1.47	-1.87	-0.50	no
AT5G55060	Rab3 GTPase-activating protein catalytic subunit	-1.62	-1.72	-0.47	no
AT3G44260	Polynucleotidyl transferase ribonuclease H-like	-6.16	-5.61	-0.47	no
AT5G14740	carbonic anhydrase 2	-2.06	-2.96	-0.46	no
AT4G24570	dicarboxylate carrier 2	-9.71	-8.70	-0.46	no
AT5G42200	RING/U-box	-1.46	-1.77	-0.46	no

AT5G51720	iron sulfur cluster binding protein	-2.61	-2.70	-0.45	no
AT5G52547	hypothetical protein	-4.37	-3.96	-0.40	no
AT1G22590	AGAMOUS-like 87	-2.12	-1.48	-0.40	no
AT5G53700	RNA-binding (RRM/RBD/RNP motifs)	-2.86	-1.97	-0.38	no
AT1G07135	glycine-rich protein	-5.71	-6.95	-0.28	no
AT1G29600	Zinc finger C-x8-C-x5-C-x3-H type	-206.08	-3.51	-0.28	no
AT4G17490	ethylene responsive element binding factor 6	-34.95	-20.26	-0.27	no
AT4G08035	unknown protein	-3.05	-3.53	-0.23	no
AT1G78990	HXXXD-type acyl-transferase	-2.80	-1.88	-0.23	no
AT3G48360	BTB and TAZ domain protein 2	-6.94	-6.46	-0.21	no
AT3G13662	Disease resistance-responsive (dirigent-like protein)	-3.48	-10.63	-0.17	no
AT5G51790	basic helix-loop-helix (bHLH) DNA-binding	-9.28	-8.68	-0.16	no
AT4G06536	SPla/RYanodine receptor (SPRY) domain-containing protein	-14.88	-12.11	-0.15	no
AT4G09190	F-box and associated interaction domains-containing protein	-14.37	-4.52	-0.11	no
AT3G49270	extensin-like protein	-1.46	-1.69	-0.11	no
AT4G06534	transmembrane protein	-5.91	-10.47	-0.10	no
AT5G10400	Histone	-15.61	-1.15	-0.09	no
AT4G02540	Cysteine/Histidine-rich C1 domain	-80.57	-71.12	-0.09	no
AT5G54190	protochlorophyllide oxidoreductase A	-48.87	-52.58	-0.08	no
AT2G34600	jasmonate-zim-domain protein 7	-4.31	-3.33	-0.07	no
AT5G56747	unknown protein	-12.16	-44.32	-0.03	no
AT5G55896	unknown protein	-5.20	-4.83	-0.02	no

Appendix 5-III: List of genes upregulated in and unique to *sep1 sep2*. The list is sorted by fold change (FC) in *sep1 sep2* in descending order.

Gene ID	Annotation	FC *sep1 sep2*	Regulators
AT1G54040	epithiospecifier (TASTY)	63.31	ETT
AT2G31230	ethylene-responsive element binding factor 15 (ERF15)	12.21	AP1,AP2,BLR,ETT,LFY,RGA,SEP3
AT1G65500	transmembrane	10.91	BLR,LFY
AT4G13840	HXXXD-type acyl-transferase (CER26)	10.61	AP1,AP3,BLR,ETT,JAG,PI,SEP3
AT2G07698	ATPase alpha subunit	10.28	AP1,SEP3
AT3G27920	myb domain 0 (MYB0)	9.57	AG,AP3,BLR,JAG,PI,RGA,SEP3
AT1G15330	Cystathionine beta-synthase (CBS)	7.58	LFY,PI
AT4G25430	hypothetical (TRM23)	7.16	AP1,BLR,JAG,LFY,RGA
AT2G05380	glycine-rich 3 short isoform (GRP3S)	7.00	FLM,LFY,RGA,SEP3,SVP
AT5G07760	FH2 domain-containing	6.58	LFY
AT5G35770	Transducin/WD40 repeat-like (SAP)	6.52	AG,AP1,AP3,BLR,ETT,PI,SEP3
AT1G13400	C2H2 and C2HC zinc fingers (NUB)	5.75	AG,AP1,AP3,BLR,PI,SEP3
AT1G67770	terminal EAR1-like 2 (TEL2)	5.61	AG,AP1,AP3,BLR,LFY,PI,SEP3
AT1G30950	F-box (UFO)	4.98	AG,AP1,AP3,BLR,PI,SEP3
AT1G67330	glucuronoxylan 4-O-methyltransferase-like (DUF579)	4.85	LFY,SVP
AT4G19030	NOD26-like major intrinsic 1 (NLM1)	4.81	LFY
AT5G23000	myb domain 37 (RAX1)	4.64	AP1,AP3,BLR,ETT,JAG,LFY,PI,RGA,SEP3
AT1G13110	cytochrome P450 (CYP71B7)	4.64	BLR,ETT
AT2G15080	receptor like 19 (RLP19)	4.58	LFY
AT1G21130	O-methyltransferase (IGMT4)	4.58	BLR,LFY
AT1G33790	jacalin lectin	4.45	AP1,BLR,ETT,RGA,SEP3
AT5G49525	transmembrane	4.44	BLR,LFY

AT5G66270	Zinc finger C-x8-C-x5-C-x3-H type	4.41	BLR,SEP3
AT4G25100	Fe superoxide dismutase 1 (FSD1)	4.37	BLR,SEP3
AT1G75490	Integrase-type DNA-binding	4.15	AP1,BLR,ETT,JAG,LFY,RGA,SEP3,SOC1
AT3G60670	PLATZ transcription factor	3.96	AG,AP3,LFY,PI,RGA,SEP3
AT4G32280	indole-3-acetic acid inducible 29 (IAA29)	3.95	AP1,BLR,ETT,JAG,SVP
AT1G47990	gibberellin 2-oxidase 4 (GA2OX4)	3.89	AG,AP2,AP3,BLR,LFY,PI,RGA,SEP3,SOC1
AT4G29190	Zinc finger C-x8-C-x5-C-x3-H type (TZF3)	3.86	AP1,AP2,BLR,ETT,FLM,JAG,LFY,RGA,SEP3,SOC1,SVP
AT5G10100	Haloacid dehalogenase-like hydrolase (HAD) (TPPI)	3.85	AP1,BLR,ETT,JAG,RGA,SEP3
AT2G26560	phospholipase A 2A (PLP2)	3.85	BLR,LFY,RGA,SEP3
AT4G25480	dehydration response element B1A (DREB1A)	3.64	AG,AP1,AP2,AP3,BLR,ETT,FLC,FLM,JAG,LFY,PI,RGA,SEP3,SOC1,SVP
AT1G13710	cytochrome P450 polypeptide 5 (KLU)	3.61	AG,AP1,AP3,BLR,PI,SEP3
AT5G61850	floral meristem identity control LEAFY (LFY)	3.49	AP1,AP3,BLR,ETT,JAG,LFY,PI,RGA,SEP3
AT2G17770	basic region/leucine zipper motif 27 (FDP)	3.46	AG,AP1,BLR,LFY,SEP3
AT5G14070	Thioredoxin (ROXY2)	3.46	BLR
AT2G05520	glycine-rich 3 (GRP3)	3.41	AG,AP1,FLM,SEP3,SVP
AT5G14010	C2H2 and C2HC zinc fingers (KNU)	3.38	AP2,AP3,BLR,FLM,PI,SOC1
AT4G37580	Acyl-CoA N-acyltransferases (NAT) (UNS2)	3.36	AP1,BLR,JAG,LFY,PI,RGA,SEP3
AT3G14210	GDSL-like lipase/acylhydrolase (ESM1)	3.35	AG,AP3,FLC,FLM,LFY,PI,RGA,SEP3,SOC1,SVP
AT1G21310	extensin 3 (RSH)	3.27	BLR,FLM,SEP3
AT3G13960	growth-regulating factor 5 (GRF5)	3.27	AG,AP1,AP2,AP3,BLR,ETT,FLC,FLM,JAG,LFY,PI,RGA,SEP3,SOC1
AT3G12970	serine/arginine repetitive matrix-like	3.21	AP3,BLR,LFY,PI,RGA,SEP3

AT5G62630	hipl2 precursor (HIPL2)	3.17	BLR,LFY,SEP3
AT4G32540	Flavin-binding monooxygenase (YUC1)	3.09	AP3,BLR,PI,SEP3
AT4G34400	AP2/B3-like transcriptional factor	3.08	FLM,SEP3,SOC1,SVP
AT4G29030	Putative membrane lipo	3.02	AP3,JAG,SEP3
AT3G26760	NAD(P)-binding Rossmann-fold	3.01	BLR,ETT,RGA
AT4G14400	ankyrin repeat (ACD6)	3.00	LFY,RGA,SEP3
AT1G18710	myb domain 47 (MYB47)	2.99	BLR,FLM,SEP3
AT1G23000	Heavy metal transport/detoxification	2.96	AP1,AP3,BLR,JAG,LFY,PI,RGA,SEP3
AT1G78850	D-mannose binding lectin	2.96	BLR,ETT,FLM,LFY
AT3G29300	transmembrane	2.92	SEP3
AT2G35750	transmembrane	2.91	BLR
AT4G23130	cysteine-rich RLK (RECEPTOR-like kinase) 5 (RLK6)	2.87	BLR
AT3G55560	AT-hook of GA feedback 2 (AHL15)	2.86	AP1,AP2,BLR,ETT,LFY,PI,RGA,SEP3,SOC1,SVP
AT5G66940	Dof-type zinc finger DNA-binding	2.86	AP1,AP3,BLR,ETT,JAG,LFY,RGA,SEP3
AT5G48540	receptor-like kinase-related	2.77	ETT,SVP
AT4G36740	homeobox 40 (HB40)	2.73	AP1,BLR,ETT,JAG,LFY,RGA,SEP3
AT4G27300	S-locus lectin kinase	2.73	AP1,BLR,ETT,FLC,FLM,LFY,RGA,SVP
AT1G53080	Legume lectin	2.71	AG,AP1,AP2,AP3,BLR,ETT,FLC,FLM,JAG,LFY,RGA,SEP3,SOC1,SVP
AT1G65780	P-loop containing nucleoside triphosphate hydrolases	2.66	BLR
AT3G63010	alpha/beta-Hydrolases (GID1B)	2.66	AG,AP1,AP2,AP3,BLR,ETT,FLM,LFY,PI,RGA,SEP3
AT5G42530	hypothetical	2.64	LFY
AT1G61810	beta-glucosidase 45 (BGLU45)	2.63	AP1,BLR,LFY,RGA,SEP3
AT2G19810	CCCH-type zinc finger (TZF2)	2.61	AP3,BLR,ETT,LFY,PI,RGA,SEP3
AT1G68640	bZIP transcription factor (TGA8)	2.50	AG,AP3,BLR,PI,SEP3
AT3G28220	TRAF-like	2.49	BLR,JAG,RGA,SOC1
AT3G12420	Polynucleotidyl transferase	2.49	BLR

AT4G37390	Auxin-responsive GH3 (YDK1)	2.44	AP3,BLR,ETT,FLM,RGA,SEP3
AT3G27250	hypothetical	2.41	BLR,ETT,LFY,RGA,SEP3
AT3G59480	pfkB-like carbohydrate kinase	2.39	AG,LFY
AT4G16750	Integrase-type DNA-binding	2.37	AG,AP1,AP3,BLR,ETT,JAG,LFY,PI,RGA,SEP3,SOC1
AT1G28360	ERF domain 12 (ERF12)	2.36	AG,AP1,AP2,AP3,BLR,ETT,JAG,PI,RGA,SEP3
AT1G15320	seed dormancy control	2.35	LFY
AT1G70890	MLP-like 43 (MLP43)	2.32	AG,AP1,AP2,AP3,BLR,JAG,LFY,PI,SEP3
AT2G18050	histone H1-3 (HIS1-3)	2.32	SVP
AT3G52525	ovate 6 (OFP6)	2.32	AP1,BLR,LFY
AT1G02065	squamosa promoter binding -like 8 (SPL8)	2.29	AG,AP1,AP2,AP3,BLR,ETT,FLM,JAG,PI,RGA,SEP3
AT5G49120	DUF581 (DUF581)	2.23	AP3,BLR,LFY
AT2G24700	Transcriptional factor B3	2.20	AP1,BLR,PI,SEP3
AT1G29910	chlorophyll A/B binding 3 (LHCB1.2)	2.20	LFY,RGA
AT2G44910	homeobox-leucine zipper 4 (HB4)	2.14	AP1,AP2,BLR,ETT,FLM,JAG,LFY,RGA,SEP3
AT4G30720	FAD/NAD(P)-binding oxidoreductase (PDE327)	2.13	RGA
AT5G48820	inhibitor/interactor with cyclin-dependent kinase (KRP3)	2.12	AP1,AP2,AP3,BLR,JAG,LFY,PI,SEP3
AT5G24470	two-component response regulator-like (PRR5)	2.11	AP1,BLR,ETT,FLM,LFY,RGA,SEP3,SOC1,SVP
AT5G05860	UDP-glucosyl transferase 76C2 (UGT76C2)	2.09	BLR,LFY
AT1G71030	MYB-like 2 (MYBL2)	2.07	AP2,BLR,ETT,FLM,LFY,SEP3,SOC1,SVP
AT5G06510	nuclear factor Y subunit A10 (NF-YA10)	2.05	AP1,BLR,JAG,SEP3
AT5G03790	homeobox 51 (LMI1)	2.02	AP1,BLR,JAG,PI,RGA,SEP3
AT4G28100	transmembrane	2.02	AP3,LFY,PI,SEP3
AT1G26780	myb domain 117 (MYB117)	2.01	AG,AP1,AP3,BLR,LFY,PI,SEP3
AT1G78860	D-mannose binding lectin	1.99	AG,AP1,AP3,BLR,ETT,LFY,PI,SEP3

AT5G02810	pseudo-response regulator 7 (PRR7)	1.99	LFY
AT1G52000	Mannose-binding lectin	1.97	SEP3
AT2G42840	protodermal factor 1 (PDF1)	1.96	AP1,AP3,ETT,RGA,SEP3
AT2G43520	trypsin inhibitor 2 (TI2)	1.96	BLR,JAG,SEP3
AT1G29920	chlorophyll A/B-binding 2 (LHCB1.1)	1.95	FLM,LFY,RGA,SEP3
AT2G05100	photosystem II light harvesting complex 2.1 (LHCB2.1)	1.93	RGA,SVP
AT4G24150	growth-regulating factor 8 (GRF8)	1.93	AP2,BLR,ETT,JAG,RGA,SEP3
AT1G11600	cytochrome P450 polypeptide 1 (CYP77B1)	1.91	BLR,SEP3
AT4G32295	histone acetyltransferase	1.89	AG,AP1,AP2,AP3,BLR,FLM,PI,RGA,SEP3
AT2G34650	kinase (PID)	1.89	AP1,AP3,BLR,ETT,JAG,LFY,RGA,SEP3
AT5G51600	Microtubule associated (MAP65/ASE1) (PLE)	1.88	AP3,BLR,PI
AT5G56220	P-loop containing nucleoside triphosphate hydrolases	1.88	AP1,BLR,JAG,LFY,RGA,SEP3
AT1G64080	membrane-associated kinase regulator (MAKR2)	1.88	BLR,FLM,JAG,LFY,RGA
AT4G30250	P-loop containing nucleoside triphosphate hydrolases	1.84	AG,AP1,AP3,BLR,LFY,PI,RGA,SEP3
AT5G17150	Cystatin/monellin	1.83	BLR,FLM,PI
AT3G61250	myb domain 17 (MYB17)	1.83	AG,AP1,AP3,BLR,ETT,JAG,LFY,PI,RGA,SEP3
AT3G50410	OBF binding 1 (OBP1)	1.78	AG,AP1,BLR,LFY,PI,SEP3
AT5G07180	ERECTA-like 2 (ERL2)	1.78	AG,AP1,AP3,BLR,ETT,PI,RGA,SEP3
AT2G25900	Zinc finger C-x8-C-x5-C-x3-H type (ATTZF1)	1.77	LFY,PI,RGA,SVP
AT1G03230	Eukaryotic aspartyl protease	1.77	FLM,LFY
AT1G14440	homeobox 31 (ZHD4)	1.77	AG,BLR,SEP3
AT1G62830	LSD1-like 1 (SWP1)	1.77	BLR,PI
AT4G17090	chloroplast beta-amylase (CT-BMY)	1.77	AP2,BLR,JAG,LFY,RGA,SEP3,SVP
AT5G67260	CYCLIN D3 (CYCD3;2)	1.76	AG,AP1,AP3,BLR,ETT,LFY,PI,RGA,SEP3
AT2G45190	Plant-specific transcription factor YABBY (YAB1)	1.75	AP1,BLR,LFY,SEP3

AT1G44760	Adenine nucleotide alpha hydrolases-like	1.75	AP1,AP3,BLR,FLM,PI,RGA,SEP3
AT3G53310	AP2/B3-like transcriptional factor	1.72	AP1
AT2G31220	basic helix-loop-helix (bHLH) DNA-binding	1.72	BLR,RGA,SEP3
AT1G47530	MATE efflux	1.71	SEP3
AT5G47600	HSP20-like chaperones	1.70	AP2,AP3,FLM,LFY,PI,RGA,SEP3,SVP
AT2G26330	Leucine-rich receptor-like kinase (QRP1)	1.70	AP1,BLR,ETT,FLM,JAG,LFY,RGA,SEP3
AT3G53650	Histone	1.70	BLR
AT5G54260	DNA repair and meiosis (Mre11) (MRE11)	1.69	BLR,JAG
AT5G63920	topoisomerase 3alpha (TOP3A)	1.68	BLR
AT4G27870	Vacuolar iron transporter (VIT)	1.67	AP1,AP2,BLR,LFY,SEP3
AT5G10180	slufate transporter 2 (SULTR2;1)	1.67	BLR
AT5G43020	Leucine-rich repeat kinase	1.67	JAG,RGA,SEP3
AT4G00480	basic helix-loop-helix (bHLH) DNA-binding (myc1)	1.66	BLR,LFY
AT1G02800	cellulase 2 (CEL2)	1.65	SEP3
AT1G15570	CYCLIN A2 (CYCA2;3)	1.65	BLR,FLM,LFY
AT1G31310	hydroxyproline-rich glyco	1.64	BLR,SEP3
AT1G56660	MAEBL domain	1.63	AP2,ETT,PI,SEP3,SOC1,SVP
AT4G31290	ChaC-like (GGCT2;2)	1.63	BLR
AT3G27050	plant/	1.62	BLR,LFY,RGA
AT5G60150	hypothetical	1.61	SEP3
AT5G54270	light-harvesting chlorophyll B-binding 3 (LHCB3*1)	1.60	LFY
AT3G50570	hydroxyproline-rich glyco	1.59	LFY,SEP3
AT3G13190	WEB (DUF827)	1.59	AG,AP3,FLM,PI,SEP3,SOC1
AT3G23670	phragmoplast-associated kinesin-related (PAKRP1L)	1.59	FLM,SVP
AT3G23890	topoisomerase II (TOPII)	1.58	LFY,SEP3,SVP
AT1G73590	Auxin efflux carrier (PIN1)	1.57	AP1,BLR,ETT,SEP3
AT1G60160	Potassium transporter	1.56	AG,SEP3
AT3G18524	MUTS homolog 2 (MSH2)	1.56	AP1,AP2,AP3,FLM,RGA,SEP3
AT1G67040	DnaA initiator-associating (TRM22)	1.56	AP1,AP3,BLR,LFY,PI,SEP3
AT5G04130	DNA GYRASE B2 (GYRB2)	1.56	AP2,BLR,FLM,LFY,RGA,SEP3

AT5G03450	Transducin/WD40 repeat-like	1.55	BLR,FLM
AT5G55120	VITAMIN C DEFECTIVE 5 (VTC5)	1.55	AP2,BLR,FLC,FLM,LFY,RGA,SOC1,SVP
AT1G67340	HCP-like with MYND-type zinc finger	1.54	AG,AP3,BLR,ETT,LFY,PI,RGA,SEP3
AT5G07280	Leucine-rich repeat transmembrane kinase (EXS)	1.54	AG,AP1,AP3,ETT,FLM,PI,SEP3,SOC1
AT4G23800	HMG (high mobility group) box (3xHMG-box2)	1.54	FLM,LFY,RGA
AT5G57660	CONSTANS-like 5 (COL5)	1.52	AG,AP1,AP2,AP3,BLR,ETT,FLM,LFY,RGA,SEP3,SVP
AT1G49650	alpha/beta-Hydrolases	1.49	AP1,ETT,FLM,JAG,RGA,SEP3
AT3G26810	auxin signaling F-box 2 (AFB2)	1.49	AP1,AP2,BLR,ETT,SEP3
AT4G14330	P-loop containing nucleoside triphosphate	1.49	FLM,LFY
AT1G75640	Leucine-rich receptor-like kinase	1.48	AP3,BLR,FLM
AT1G78820	D-mannose binding lectin	1.47	BLR,ETT,FLM,LFY,PI,RGA
AT2G42600	phosphoenolpyruvate carboxylase 2 (PPC2)	1.47	AP1,AP2,FLC,SEP3
AT1G53160	squamosa promoter binding -like 4 (SPL4)	1.46	AP1,AP2,BLR,JAG,PI,RGA,SEP3
AT4G31820	Phototropic-responsive NPH3 (NPY1)	1.46	AG,AP1,AP2,AP3,BLR,ETT,FLC,FLM,LFY,PI,RGA,SEP3
AT5G08000	glucan endo-1-beta-glucosidase-like 3 (PDCB2)	1.44	AG,AP1,BLR,ETT,FLC,FLM,JAG,PI,RGA,SEP3,SOC1
AT4G33400	Vacuolar import/degradation Vid27-related	1.44	SVP
AT1G14410	ssDNA-binding transcriptional regulator (WHY1)	1.43	ETT,JAG,LFY,SEP3,SVP
AT1G19850	Transcriptional factor B3 AUX/IAA-like (MP)	1.43	AP3,BLR,ETT,LFY,PI,RGA,SEP3
AT2G02070	indeterminate(ID)-domain 5 (IDD5)	1.43	AP1,AP3,BLR,ETT,PI,SEP3
AT2G31070	TCP domain 10 (TCP10)	1.42	AP1,BLR,ETT,FLM,SEP3
AT5G06150	Cyclin (CYCB1;2)	1.42	LFY

AT1G11820	O-Glycosyl hydrolases family 17	1.42	AP3,ETT,FLM,LFY,RGA
AT3G57060	binding	1.41	FLM,RGA,SEP3
AT1G68400	leucine-rich repeat transmembrane kinase	1.40	BLR,SEP3
AT1G15500	TLC ATP/ADP transporter (ATNTT2)	1.38	LFY,SEP3
AT4G37210	Tetratricopeptide repeat (TPR)-like	1.38	SEP3
AT4G37550	Acetamidase/Formamidase	1.37	AP1,AP2,BLR,ETT,JAG,LFY,PI,RGA,SEP3
AT5G04290	kow domain-containing transcription factor 1 (SPT5L)	1.36	SVP
AT3G04260	plastid transcriptionally active 3 (PTAC3)	1.36	BLR

Appendix 5-IV: List of genes downregulated in and unique to *sep1 sep2*. The list is sorted by fold change (FC) in *sep1 sep2* in descending order.

Gene ID	Annotation	FC	Regulators
AT3G53420	plasma membrane intrinsic 2A (PIP2A)	-0.74	BLR,FLM,LFY,RGA,SEP3,SVP
AT1G12440	A20/AN1-like zinc finger	-0.74	BLR,ETT,FLM,LFY,RGA,SEP3,SVP
AT4G18970	GDSL-like Lipase/Acylhydrolase	-0.73	AG,JAG,SEP3
AT3G51840	acyl-CoA oxidase 4 (ATSCX)	-0.73	AG,AP1,AP3,BLR,FLC,FLM,PI,RGA,SEP3,SOC1
AT2G45740	peroxin 11D (PEX11D)	-0.73	RGA
AT1G61900	hypothetical	-0.72	BLR,LFY
AT1G01610	glycerol-3-phosphate acyltransferase 4 (GPAT4)	-0.72	BLR,ETT,LFY,SEP3,SVP
AT1G02190	Fatty acid hydroxylase superfamily	-0.72	AP2,BLR,ETT,FLM,JAG,LFY,RGA,SEP3
AT3G47340	glutamine-dependent asparagine synthase 1 (DIN6)	-0.71	LFY,SEP3,SVP
AT2G45970	cytochrome P450 (LCR)	-0.71	AP2,AP3,BLR,ETT,FLM,JAG,LFY,PI,RGA,SEP3,SVP
AT3G03450	RGA-like 2 (RGL2)	-0.70	AG,AP1,AP2,BLR,ETT,FLC,FLM,JAG,PI,RGA,SEP3,SOC1,SVP
AT1G07040	plant/	-0.70	AP1,AP2,BLR,FLM,JAG,SEP3,SOC1,SVP
AT3G05880	Low temperature and salt responsive family (RCI2A)	-0.70	BLR,FLM,SEP3,SVP
AT5G40450	A-kinase anchor-like	-0.70	BLR
AT5G66310	ATP binding microtubule motor	-0.70	AP2,BLR,ETT,FLM,JAG,LFY,RGA,SEP3,SVP
AT4G14990	Topoisomerase II-associated PAT1	-0.70	AP3,SVP
AT5G25220	homeobox knotted-1-like 3 (KNAT3)	-0.70	BLR,LFY,SEP3,SVP
AT1G15980	NDH-dependent cyclic electron flow 1 (PnsB1)	-0.69	RGA
AT1G69120	MADS-box transcription factor (AP1)	-0.69	AG,AP1,AP2,AP3,BLR,ETT,FLM,JAG,LFY,PI,SEP3,SVP
AT1G19660	Wound-responsive (BBD2)	-0.69	AP2,BLR,ETT,LFY,RGA,SVP

AT5G09660	peroxisomal NAD-malate dehydrogenase 2 (PMDH2)	-0.69	LFY,RGA
AT5G16240	Plant stearoyl-acyl-carrier- desaturase	-0.69	AG,AP3,BLR,FLM,PI,RGA, SEP3
AT3G19930	sugar transporter 4 (STP4)	-0.69	BLR
AT1G78670	gamma-glutamyl hydrolase 3 (GGH3)	-0.68	BLR,JAG,RGA,SEP3
AT1G03590	phosphatase 2C	-0.68	ETT,SEP3
AT1G24260	MADS-box transcription factor (SEP3)	-0.68	AG,AP1,AP2,AP3,BLR,ETT, FLC,FLM,JAG,LFY,PI,RGA ,SEP3,SOC1,SVP
AT1G03090	methylcrotonyl-CoA carboxylase alpha chain (MCCA)	-0.68	BLR,SEP3
AT1G10060	branched-chain amino acid transaminase 1 (BCAT1)	-0.68	AP1,AP2,BLR,ETT,JAG,RG A,SEP3
AT4G34920	PLC-like phosphodiesterases	-0.68	BLR,RGA
AT1G12460	Leucine-rich repeat kinase	-0.67	AP3,BLR,ETT,JAG,PI,RGA, SEP3
AT2G36270	Basic-leucine zipper (bZIP) transcription factor (GIA1)	-0.67	AG,AP1,AP3,BLR,ETT,FLM ,JAG,LFY,PI,RGA,SEP3,SO C1
AT1G53840	pectin methylesterase 1 (PME1)	-0.67	FLM,SVP
AT4G13530	transmembrane	-0.67	AG,AP1,AP3,BLR,ETT,JAG ,PI,RGA,SEP3,SVP
AT5G12950	proline-tRNA ligase (DUF1680)	-0.67	BLR,RGA,SEP3
AT3G48460	GDSL-like Lipase/Acylhydrolase	-0.67	LFY,SEP3,SOC1
AT2G36320	A20/AN1-like zinc finger	-0.67	BLR,FLC,FLM,SOC1,SVP
AT5G49740	ferric reduction oxidase 7 (FRO7)	-0.67	BLR,FLM,SVP
AT1G02640	beta-xylosidase 2 (BXL2)	-0.67	AP3,BLR,FLM,JAG,LFY,PI, RGA,SVP
AT3G04910	with no lysine (K) kinase 1 (ZIK4)	-0.67	BLR,ETT,JAG,RGA,SEP3
AT1G80460	Actin-like ATPase (NHO1)	-0.67	LFY,RGA
AT2G13680	callose synthase 5 (GLS2)	-0.67	LFY
AT3G52840	beta-galactosidase 2 (BGAL2)	-0.66	BLR,FLC,FLM,SVP
AT2G39010	plasma membrane intrinsic 2E (PIP2E)	-0.66	AP1,AP2,BLR,ETT,FLC,FL M,JAG,RGA,SEP3,SOC1,SV P
AT4G37470	alpha/beta-Hydrolases (KAI2)	-0.66	AP1,BLR,ETT,FLM,JAG,RG A,SEP3,SVP

AT5G65110	acyl-CoA oxidase 2 (ATACX2)	-0.66	AG,AP3,BLR,ETT,LFY,PI,RGA,SEP3
AT1G64680	beta-carotene isomerase D27	-0.66	AG,AP1,AP2,AP3,BLR,ETT,JAG,PI,SEP3
AT4G35470	plant intracellular ras group-related LRR 4 (PIRL4)	-0.65	BLR,ETT,FLM,LFY,SVP
AT1G27100	Actin cross-linking	-0.65	AP3,BLR,ETT,LFY,PI,SEP3,SVP
AT1G32700	PLATZ transcription factor	-0.65	BLR,FLM,SEP3,SVP
AT2G13360	alanine:glyoxylate aminotransferase (SGAT)	-0.65	BLR,SVP
AT5G25280	serine-rich -like	-0.65	AP3,BLR,ETT,FLM,LFY,SEP3,SVP
AT4G32150	vesicle-associated membrane 711 (VAMP711)	-0.65	LFY,RGA
AT1G11260	sugar transporter 1 (STP1)	-0.65	BLR,FLM,LFY,SEP3,SVP
AT5G13400	Major facilitator	-0.64	AG,AP1,AP2,AP3,BLR,ETT,JAG,PI,SEP3
AT5G07440	glutamate dehydrogenase 2 (GDH2)	-0.64	FLM,LFY,RGA
AT3G14990	Class I glutamine amidotransferase-like (DJ1A)	-0.64	AG,AP1,AP3,BLR,ETT,LFY,PI,RGA,SEP3
AT2G39510	nodulin MtN21 /EamA-like transporter (UMAMIT14)	-0.64	BLR
AT1G29390	cold regulated 314 thylakoid membrane 2 (COR413IM2)	-0.64	BLR
AT1G63710	cytochrome P450 polypeptide 7 (CYP86A7)	-0.63	BLR,LFY,RGA
AT3G05900	neurofilament -like	-0.63	JAG
AT1G03440	Leucine-rich repeat (LRR)	-0.63	ETT,FLM,RGA,SEP3
AT1G78240	S-adenosyl-L-methionine methyltransferases (TSD2)	-0.63	AP1,BLR,LFY,SEP3
AT3G61260	Remorin	-0.63	AP3,BLR,ETT,PI,RGA,SEP3,SVP
AT4G34750	SAUR-like auxin-responsive family (SAUR49)	-0.63	AP1,BLR,RGA
AT2G19800	myo-inositol oxygenase 2 (MIOX2)	-0.62	FLM,LFY,SEP3,SOC1,SVP
AT2G16760	Calcium-dependent phosphotriesterase	-0.62	AP2,SEP3
AT4G36540	BR enhanced expression 2 (BEE2)	-0.62	BLR,FLM
AT1G57680	plasminogen activator inhibitor (Cand1)	-0.62	ETT,FLM,JAG,RGA,SEP3

AT1G16880	uridylyltransferase-like (ACR11)	-0.62	BLR,FLM,SVP
AT4G19400	Profilin	-0.62	AP1,AP3,BLR,ETT,FLM,JAG,PI,SEP3,SVP
AT1G07720	3-ketoacyl-CoA synthase 3 (KCS3)	-0.62	AP3,BLR,ETT,PI,SEP3
AT3G60130	beta glucosidase 16 (BGLU16)	-0.62	AG,SEP3,SVP
AT1G21460	Nodulin MtN3 (SWEET1)	-0.62	AG,AP2,AP3,BLR,JAG,PI,RGA,SEP3
AT3G55710	UDP-Glycosyltransferase	-0.61	AP2,BLR,SEP3
AT2G31800	Integrin-linked kinase family	-0.61	BLR,ETT,PI,RGA,SEP3
AT2G32530	cellulose synthase-like B3 (CSLB03)	-0.61	BLR,FLM,SEP3
AT1G01240	transmembrane	-0.61	BLR,ETT,JAG,RGA
AT2G23790	calcium uniporter (DUF607)	-0.61	AP2,ETT,JAG,RGA,SEP3
AT1G30540	Actin-like ATPase	-0.61	BLR
AT1G65590	beta-hexosaminidase 3 (HEXO3)	-0.61	BLR,ETT,JAG,RGA,SEP3
AT3G47600	myb domain 94 (MYB94)	-0.60	JAG
AT2G40110	Yippee family putative zinc-binding	-0.60	AP1,AP2,BLR,ETT,FLM,JAG,RGA,SEP3
AT2G23760	BEL1-like homeodomain 4 (SAW2)	-0.60	BLR,ETT,SEP3
AT4G38810	Calcium-binding EF-hand	-0.60	AP1,LFY,SEP3
AT5G16370	acyl activating enzyme 5 (AAE5)	-0.60	AP2,AP3,BLR,FLM,RGA
AT2G46720	3-ketoacyl-CoA synthase 13 (KCS13)	-0.60	AG,AP1,AP2,AP3,ETT,FLC,JAG,PI,RGA,SEP3,SOC1,SVP
AT3G55130	white-brown complex homolog 19 (WBC19)	-0.59	BLR,ETT,JAG,SEP3,SOC1
AT5G48900	Pectin lyase-like	-0.59	ETT,LFY
AT2G45180	lipid-transfer 2S albumin	-0.59	AP1,BLR,LFY,SEP3,SVP
AT1G71960	ATP-binding casette family G25 (ATABCG25)	-0.59	AP1,AP2,BLR,ETT,JAG,RGA,SEP3
AT1G25275	thionin-like	-0.59	FLM,LFY,SVP
AT1G75460	ATP-dependent protease La (LON) domain	-0.59	BLR,RGA,SEP3
AT3G10570	cytochrome P450 polypeptide 6 (CYP77A6)	-0.59	BLR,SEP3
AT2G46870	AP2/B3-like transcriptional factor (NGA1)	-0.59	AP1,BLR,PI,SEP3
AT5G15310	myb domain 16 (MYB16)	-0.59	AP2,JAG,SEP3
AT4G15160	Bifunctional inhibitor/lipid-transfer	-0.58	LFY
AT3G23450	transmembrane	-0.58	BLR,SVP

AT3G23410	fatty alcohol oxidase 3 (FAO3)	-0.58	Sep-03
AT3G62650	hypothetical	-0.58	AP2,BLR,JAG,PI,RGA,SEP3,SVP
AT5G01075	Glycosyl hydrolase family 35	-0.58	RGA
AT3G11773	Thioredoxin	-0.58	BLR,JAG
AT1G58180	beta carbonic anhydrase 6 (BCA6)	-0.58	BLR,LFY
AT1G77210	sugar transporter 14 (STP14)	-0.58	AG,PI,SEP3,SOC1
AT1G67560	PLAT/LH2 domain-containing lipoxygenase (LOX6)	-0.57	AG,AP1,AP3,BLR,FLC,FLM,PI,SEP3,SOC1,SVP
AT4G34138	UDP-glucosyl transferase 73B1 (UGT73B1)	-0.57	BLR,SEP3
AT2G15880	Leucine-rich repeat (LRR)	-0.57	BLR,FLM,SEP3,SVP
AT1G25230	Calcineurin-like metallo-phosphoesterase	-0.57	AG,AP1,AP2,AP3,BLR,ETT,LFY,PI,SEP3
AT1G22640	myb domain 3 (MYB3)	-0.57	AP1,BLR,ETT,JAG,SEP3
AT5G64410	oligopeptide transporter 4 (OPT4)	-0.57	JAG
AT5G15530	biotin carboxyl carrier 2 (CAC1-B)	-0.57	BLR,LFY
AT2G38110	glycerol-3-phosphate acyltransferase 6 (GPAT6)	-0.57	AP2,BLR,JAG,SEP3
AT2G28630	3-ketoacyl-CoA synthase 12 (KCS12)	-0.57	RGA,SEP3
AT5G59570	Homeodomain-like (BOA)	-0.56	LFY
AT2G42890	MEI2-like 2 (ML2)	-0.56	BLR,JAG,SEP3
AT2G38060	phosphate transporter 4%3B2 (PHT4;2)	-0.56	AG,AP1,BLR,ETT,FLM,JAG,PI,SEP3
AT1G26945	basic helix-loop-helix (bHLH) DNA-binding (PRE6)	-0.56	BLR,ETT,FLM,JAG,RGA,SEP3
AT3G20520	SHV3-like 3 (SVL3)	-0.56	BLR,ETT
AT3G22750	kinase	-0.55	BLR
AT4G14750	IQ-domain 19 (IQD19)	-0.55	BLR,ETT,FLM,SEP3
AT2G39360	kinase	-0.55	BLR,SEP3
AT1G21540	AMP-dependent synthetase and ligase	-0.55	AP1,AP2,BLR,JAG,LFY,PI,RGA,SEP3
AT5G07580	ethylene-responsive transcription factor	-0.54	AP1,AP3,BLR,ETT,FLM,PI,RGA,SEP3,SVP
AT1G78960	lupeol synthase 2 (LUP2)	-0.54	AP2,SEP3
AT4G24140	alpha/beta-Hydrolases	-0.54	AP2,BLR,ETT,JAG,RGA,SEP3
AT4G37520	Peroxidase	-0.54	RGA,SEP3
AT3G16570	rapid alkalinization factor 23 (RALF23)	-0.54	FLM,LFY,RGA

AT2G23290	myb domain 70 (MYB70)	-0.53	AG,AP1,BLR,ETT,JAG,PI,RGA,SEP3,SVP
AT1G01600	cytochrome P450 polypeptide 4 (CYP86A4)	-0.53	ETT,JAG,RGA,SEP3,SVP
AT1G33240	GT-2-like 1 (GTL1)	-0.53	AP1,AP2,BLR,ETT,FLM,JAG,LFY,RGA,SEP3
AT1G35310	MLP-like 168 (MLP168)	-0.53	AP2
AT2G36420	nucleolin-like (TRM27)	-0.53	AG,AP1,AP2,AP3,BLR,ETT,FLC,FLM,JAG,LFY,PI,RGA,SEP3,SVP
AT2G41170	F-box	-0.53	AG,BLR,LFY,PI,RGA,SEP3
AT1G78830	Curculin-like (mannose-binding) lectin	-0.52	BLR,ETT,FLM,LFY,PI,RGA
AT2G27920	serine carboxypeptidase-like 51 (SCPL51)	-0.52	AP3,BLR,PI,RGA,SEP3
AT3G50660	Cytochrome P450 (SNP2)	-0.52	BLR,ETT,JAG,LFY,SEP3
AT5G22430	Pollen Ole e 1 allergen and extensin	-0.52	AG,AP1,AP3,PI,SEP3
AT4G19200	proline-rich	-0.52	ETT,SVP
AT1G14280	phytochrome kinase substrate 2 (PKS2)	-0.52	AP2,BLR,ETT,FLC,FLM,JAG,RGA,SVP
AT4G24130	DUF538 (DUF538)	-0.51	LFY,SEP3
AT1G22370	UDP-glucosyl transferase 85A5 (UGT85A5)	-0.51	Sep-03
AT4G35110	phospholipase-like (PEARLI 4)	-0.51	BLR,ETT,LFY,SEP3
AT4G24040	trehalase 1 (TRE1)	-0.51	AP3,BLR,FLC,FLM,LFY,PI,RGA,SEP3,SVP
AT5G40890	chloride channel A (CLCA)	-0.51	BLR,LFY,SEP3,SVP
AT5G64570	beta-D-xylosidase 4 (XYL4)	-0.51	AP1,BLR,ETT,JAG,SEP3,SOC1
AT5G05440	Polyketide cyclase/dehydrase (RCAR8)	-0.51	AP1,AP2,BLR,ETT,FLM,LFY,SEP3
AT1G22330	RNA-binding (RRM/RBD/RNP motifs)	-0.51	AP1,BLR,FLM,JAG,LFY,SEP3,SVP
AT3G30775	Methylenetetrahydrofolate reductase (PRODH)	-0.50	AP1,BLR,ETT,FLC,FLM,JAG,LFY,RGA,SEP3,SOC1,SVP
AT4G19960	K+ uptake permease 9 (KUP9)	-0.50	BLR,ETT,JAG,SEP3
AT3G59350	kinase	-0.50	BLR,ETT,JAG,SEP3,SVP
AT1G75380	basal defense response 1 (BBD1)	-0.50	BLR,FLM,SVP

AT3G43720	Bifunctional inhibitor/lipid-transfer (LTPG2)	-0.50	BLR,LFY
AT5G22940	glucuronoxylan glucuronosyltransferase (F8H)	-0.50	AP2,AP3,ETT,LFY,PI,RGA, SEP3
AT3G62410	CP12 domain-containing 2 (CP12-2)	-0.49	FLM,LFY,SVP
AT5G19190	hypothetical	-0.49	AP1,BLR,FLM,LFY,SEP3,SVP
AT1G15360	Integrase-type DNA-binding (WIN1)	-0.49	AP1,AP2,BLR,JAG,LFY,RGA,SEP3
AT1G72130	Major facilitator	-0.49	BLR
AT3G61430	plasma membrane intrinsic 1A (PIP1A)	-0.48	AP1,BLR,JAG,SEP3
AT1G22910	RNA-binding (RRM/RBD/RNP motifs)	-0.48	BLR,LFY,RGA,SVP
AT2G27830	hypothetical	-0.48	BLR,FLM,LFY,PI,RGA,SEP3,SVP
AT1G12780	UDP-D-glucose/UDP-D-galactose 4-epimerase 1 (UGE1)	-0.48	BLR,PI,SEP3
AT4G01330	kinase	-0.48	ETT,LFY,RGA
AT1G11850	transmembrane	-0.48	Sep-03
AT1G74020	strictosidine synthase 2 (SS2)	-0.48	BLR,ETT,LFY,SEP3
AT1G23050	hydroxyproline-rich glyco	-0.48	BLR,SVP
AT3G07010	Pectin lyase-like	-0.47	BLR,ETT,SEP3
AT5G04770	cationic amino acid transporter 6 (CAT6)	-0.47	AP1,AP2,BLR,ETT,FLC,FLM,JAG,LFY,RGA,SEP3,SVP
AT5G09440	EXORDIUM like 4 (EXL4)	-0.47	AG,AP1,AP2,AP3,BLR,ETT,FLM,JAG,LFY,PI,RGA,SEP3
AT2G17550	RB1-inducible coiled-coil (TRM26)	-0.47	BLR,ETT
AT1G78460	SOUL heme-binding	-0.47	BLR,FLM,RGA
AT3G62570	Tetratricopeptide repeat (TPR)-like	-0.47	BLR,RGA,SEP3
AT5G22500	fatty acid reductase 1 (FAR1)	-0.46	AP1,BLR,ETT,JAG,SEP3
AT3G12110	actin-11 (ACT11)	-0.46	AP3,BLR,ETT,JAG,LFY,PI,SEP3
AT1G20190	expansin 11 (EXPA11)	-0.46	LFY
AT5G62100	BCL-2-associated athanogene 2 (BAG2)	-0.46	BLR,LFY,RGA,SVP
AT2G37170	plasma membrane intrinsic 2 (PIP2B)	-0.46	AP3,ETT,JAG,LFY,RGA,SEP3
AT1G15670	Galactose oxidase/kelch repeat (KMD2)	-0.45	AG,BLR,LFY,RGA,SEP3
AT2G40610	expansin A8 (EXPA8)	-0.45	BLR,LFY,SEP3
AT1G50830	Aminotransferase-like	-0.45	BLR

AT4G20260	plasma-membrane associated cation-binding 1 (PCAP1)	-0.45	AP3,BLR,RGA,SEP3,SVP
AT1G12080	Vacuolar calcium-binding -like	-0.45	AP1,AP2,BLR,FLC,FLM,LFY,SEP3,SOC1,SVP
AT1G55850	cellulose synthase like E1 (CSLE1)	-0.45	FLM
AT3G51070	S-adenosyl-L-methionine-dependent methyltransferases	-0.45	BLR
AT5G06860	polygalacturonase inhibiting 1 (PGIP1)	-0.44	AG,BLR,ETT,FLM,LFY,PI,SEP3
AT5G23210	serine carboxypeptidase-like 34 (SCPL34)	-0.44	ETT,LFY,RGA
AT1G72610	germin-like 1 (GLP1)	-0.44	AP2,BLR,FLM,SEP3,SVP
AT3G17580	SsrA-binding	-0.43	BLR,JAG,RGA
AT5G37740	Calcium-dependent lipid-binding (CaLB domain)	-0.43	BLR
AT2G17880	Chaperone DnaJ-domain (DJC24)	-0.43	AP3,FLM,PI,SEP3
AT2G48030	DNAse I-like	-0.42	ETT,SEP3
AT3G02140	AFP2 (ABI five-binding 2) (TMAC2)	-0.42	AP1,AP2,BLR,ETT,FLM,LFY,RGA,SEP3,SVP
AT3G54830	Transmembrane amino acid transporter	-0.42	LFY
AT2G23690	HTH-type transcriptional regulator	-0.41	AP1,AP3,BLR,ETT,JAG,PI,RGA,SEP3
AT4G39480	cytochrome P450 polypeptide 9 (CYP96A9)	-0.41	AG,AP1,AP2,AP3,BLR,ETT,LFY,PI,SEP3
AT5G62360	Plant invertase/pectin methylesterase inhibitor	-0.41	AG,AP1,AP3,BLR,ETT,FLM,JAG,PI,SEP3,SVP
AT5G50950	FUMARASE 2 (FUM2)	-0.41	BLR,ETT,JAG,LFY,SEP3,SVP
AT1G22400	UDP-Glycosyltransferase (UGT85A1)	-0.40	AP1,AP2,ETT,FLM,LFY,SEP3,SVP
AT1G11080	serine carboxypeptidase-like 31 (scpl31)	-0.40	BLR
AT4G16563	Eukaryotic aspartyl protease	-0.40	LFY,PI
AT1G52190	Major facilitator (NRT1.11)	-0.40	AP1,BLR,ETT,PI,SEP3
AT1G75880	SGNH hydrolase-type esterase	-0.39	AP1,FLM,RGA,SEP3
AT1G61740	Sulfite exporter TauE/SafE	-0.39	AG,ETT,FLM,SEP3
AT4G36410	ubiquitin-conjugating enzyme 17 (UBC17)	-0.39	BLR
AT4G39070	B-box zinc finger (BZS1)	-0.39	AG,AP1,BLR,ETT,JAG,PI,RGA,SEP3

AT3G62550	Adenine nucleotide alpha hydrolases-like	-0.39	BLR,FLM,LFY,SVP
AT5G43870	auxin canalization (DUF828)	-0.38	AP3,BLR,LFY,PI,SEP3,SVP
AT4G33150	saccharopine dehydrogenase (SDH)	-0.38	AP1,BLR,ETT,LFY,PI,RGA,SEP3
AT5G01740	Nuclear transport factor 2 (NTF2)	-0.38	BLR,ETT,LFY
AT1G80180	hypothetical	-0.38	SVP
AT4G38690	PLC-like phosphodiesterases	-0.38	AG,AP3,BLR,JAG,PI,SEP3
AT5G45920	SGNH hydrolase-type esterase	-0.37	Sep-03
AT4G34790	SAUR-like auxin-responsive family (SAUR3)	-0.37	AG,AP1,BLR,FLC,FLM,JAG,RGA,SEP3
AT5G45960	GDSL-like Lipase/Acylhydrolase	-0.36	BLR,SEP3
AT1G10070	branched-chain amino acid transaminase 2 (BCAT2)	-0.36	AG,AP1,AP2,AP3,BLR,ETT,LFY,PI,RGA,SEP3
AT1G74670	Gibberellin-regulated (GASA6)	-0.36	BLR,LFY,SEP3,SVP
AT3G29370	hypothetical (P1R3)	-0.36	AP2,SEP3
AT1G68500	hypothetical	-0.36	AP1,BLR,ETT,FLM,LFY,SEP3
AT3G19390	Granulin repeat cysteine protease	-0.35	BLR,ETT,FLM,JAG,LFY,RGA,SEP3,SVP
AT1G67265	ROTUNDIFOLIA like 21 (RTFL21)	-0.34	BLR,LFY,SEP3
AT3G06490	myb domain 108 (MYB108)	-0.34	AG,BLR,ETT,SEP3
AT1G72240	hypothetical	-0.34	BLR,FLM,JAG,SVP
AT1G27045	Homeobox-leucine zipper family (HB54)	-0.34	AP2,BLR,FLM,LFY,RGA,SEP3
AT3G11930	Adenine nucleotide alpha hydrolases-like	-0.33	Sep-03
AT1G21910	Integrase-type DNA-binding (DREB26)	-0.32	BLR,ETT
AT3G12160	RAB GTPase homolog A4D (RABA4D)	-0.31	FLM,JAG,LFY,RGA
AT1G25340	myb domain 116 (MYB116)	-0.31	AG,AP2,BLR,ETT,RGA,SEP3
AT5G14000	NAC domain containing 84 (NAC084)	-0.31	BLR,FLM,SEP3
AT4G21870	HSP20-like chaperones	-0.30	AG,AP1,AP2,AP3,BLR,ETT,FLC,FLM,LFY,PI,SEP3,SVP
AT4G30270	xyloglucan endotransglucosylase/hydrolase 24 (XTH24)	-0.29	BLR,ETT,LFY,PI,SEP3
AT5G01610	hypothetical (DUF538)	-0.29	AG,AP1,AP3,BLR,LFY,PI,RGA,SEP3,SVP

AT1G30040	gibberellin 2-oxidase (GA2OX2)	-0.29	ETT,FLM,LFY,SEP3
AT3G07340	basic helix-loop-helix (bHLH) DNA-binding	-0.29	AP1,BLR,ETT,JAG,LFY,PI,RGA,SEP3
AT1G02610	RING/FYVE/PHD zinc finger	-0.28	AG,AP3,BLR,ETT,FLM,PI,RGA,SEP3,SVP
AT2G38400	alanine:glyoxylate aminotransferase 3 (AGT3)	-0.27	BLR
AT3G15500	NAC domain containing 3 (NAC3)	-0.27	AG,AP1,AP3,ETT,FLC,FLM,LFY,PI,RGA,SEP3,SOC1,SVP
AT4G19840	phloem 2-A1 (PP2-A1)	-0.27	AP1,BLR
AT1G75750	GAST1 homolog 1 (GASA1)	-0.27	AP1,AP3,BLR,PI,SEP3
AT1G56250	phloem 2-B14 (VBF)	-0.25	BLR,LFY,SEP3
AT2G43610	Chitinase	-0.24	AG,SVP
AT5G62730	Major facilitator	-0.23	ETT,FLM,LFY,RGA,SEP3,SVP
AT1G57990	purine permease 18 (PUP18)	-0.21	BLR,ETT,LFY,SEP3,SVP
AT1G54050	HSP20-like chaperones	-0.21	ETT,JAG,RGA
AT4G34510	3-ketoacyl-CoA synthase 17 (KCS17)	-0.20	PI
AT5G49360	beta-xylosidase 1 (BXL1)	-0.18	AP2,BLR,ETT,FLC,FLM,LFY,RGA,SEP3,SVP
AT1G10220	ZCF37	-0.15	AG,AP3,BLR,ETT,LFY,PI,SEP3,SVP
AT5G18600	Thioredoxin	-0.13	BLR,FLM,PI
AT5G23530	carboxyesterase 18 (CXE18)	-0.08	BLR,ETT,JAG,RGA,SEP3

Appendix 6-I: GO terms mapped to transcription regulation in genes upregulated in *sep1-1* VT

Gene ID	Annotation	Protein Class
AT3G05380	Protein ALWAYS EARLY 2;ALY2;ortholog	DNA metabolism protein(PC00009)
AT5G60040	DNA-directed RNA polymerase III subunit 1;NRPC1;ortholog	DNA-directed RNA polymerase(PC00019)
AT4G35800	DNA-directed RNA polymerase II subunit RPB1;NRPB1;ortholog	DNA-directed RNA polymerase(PC00019)
AT5G61150	Protein LEO1 homolog;VIP4;ortholog	DNA-directed RNA polymerase(PC00019)
AT1G65440	Transcription elongation factor SPT6 homolog;SPT6;ortholog	general transcription factor(PC00259)
AT1G73960	Transcription initiation factor TFIID subunit 2;TAF2;ortholog	general transcription factor(PC00259)
AT1G04950	Transcription initiation factor TFIID subunit 6;TAF6;ortholog	general transcription factor(PC00259)
AT4G12610	Transcription initiation factor IIF subunit alpha;RAP74;ortholog	general transcription factor(PC00259)
AT2G30320	Putative tRNA pseudouridine synthase;TAIR:locus:2065748;ortholog	lyase(PC00144)
AT1G08370	mRNA-decapping enzyme-like protein;TAIR:locus:2201821;ortholog	mRNA capping factor(PC00145)
AT5G13010	Pre-mRNA-splicing factor ATP-dependent RNA helicase DEAH7;CUV;ortholog	RNA helicase(PC00032)
AT1G32490	Pre-mRNA-splicing factor ATP-dependent RNA helicase DEAH1;ESP3;ortholog	RNA helicase(PC00032)
AT3G55200	Spliceosome-associated protein 130 A;SAP130A;ortholog	RNA processing factor(PC00147)
AT5G13480	Flowering time control protein FY;FY;ortholog	RNA processing factor(PC00147)
AT5G19040	Adenylate isopentenyltransferase 5, chloroplastic;IPT5;ortholog	RNA processing factor(PC00147)
AT4G21660	PSP domain-containing protein;At4g21660;ortholog	RNA splicing factor(PC00148)
AT5G27720	Sm-like protein LSM4;LSM4;ortholog	RNA splicing factor(PC00148)
AT4G37120	Pre-mRNA-splicing factor SLU7-B;TAIR:locus:2115115;ortholog	RNA splicing factor(PC00148)
AT1G77180	SNW/SKI-interacting protein;SKIP;ortholog	RNA splicing factor(PC00148)
AT3G50670	U1 small nuclear ribonucleoprotein 70 kDa;RNU1;ortholog	RNA splicing factor(PC00148)
AT1G65700	Sm-like protein LSM8;LSM8;ortholog	RNA splicing factor(PC00148)
AT3G20550	FHA domain-containing protein DDL;DDL;ortholog	RNA splicing factor(PC00148)
AT5G06160	Splicing factor SF3a60 homolog;ATO;ortholog	RNA splicing factor(PC00148)
AT1G65660	Pre-mRNA-splicing factor SLU7-A;TAIR:locus:2018496;ortholog	RNA splicing factor(PC00148)

AT1G10320	Zinc finger CCCH domain-containing protein 5;TAIR:locus:2012843;ortholog	RNA splicing factor(PC00148)
AT4G03430	Protein STABILIZED1;STA1;ortholog	RNA splicing factor(PC00148)
AT1G03910	Cactin;CTN;ortholog	scaffold/adaptor protein(PC00226)
AT1G20960	DExH-box ATP-dependent RNA helicase DExH12;BRR2A;ortholog	scaffold/adaptor protein(PC00226)
AT5G60870	RCC1 domain-containing protein RUG3, mitochondrial;RUG3;ortholog	ubiquitin-protein ligase(PC00234)
AT1G67370	Meiosis-specific protein ASY1;ASY1;ortholog	cysteine protease(PC00081)
AT1G08600	Protein CHROMATIN REMODELING 20;ATRX;ortholog	
AT3G24870	Chromatin modification-related protein EAF1 B;EAF1B;ortholog	chromatin/chromatin-binding, or -regulatory protein(PC00077)
AT4G29940	Pathogenesis-related homeodomain protein;PRH;ortholog	chromatin/chromatin-binding, or -regulatory protein(PC00077)
AT5G46030	Transcription elongation factor 1 homolog;TAIR:locus:2161418;ortholog	
AT5G61070	Histone deacetylase 18;HDA18;ortholog	
AT1G21610	Ubinuclein-1;UBN1;ortholog	scaffold/adaptor protein(PC00226)
AT2G44950	E3 ubiquitin-protein ligase BRE1-like 1;HUB1;ortholog	
AT5G17690	Chromo domain-containing protein LHP1;LHP1;ortholog	
AT5G56950	Nucleosome assembly protein 1;3;NAP1;3;ortholog	chromatin/chromatin-binding, or -regulatory protein(PC00077)
AT1G55250	E3 ubiquitin-protein ligase BRE1-like 2;HUB2;ortholog	
AT5G67320	WD40 repeat-containing protein HOS15;HOS15;ortholog	
AT5G61150	Protein LEO1 homolog;VIP4;ortholog	DNA-directed RNA polymerase(PC00019)
AT3G52280	Transcription factor GTE6;GTE6;ortholog	
AT3G19960	Myosin-1;VIII-1;ortholog	actin binding motor protein(PC00040)
AT5G02560	Probable histone H2A.4;AT5G02560;ortholog	histone(PC00118)
AT2G25170	CHD3-type chromatin-remodeling factor PICKLE;PKL;ortholog	
AT1G54140	Transcription initiation factor TFIID subunit 9;TAF9;ortholog	
AT5G54260	Double-strand break repair protein MRE11;MRE11;ortholog	
AT1G21700	SWI/SNF complex subunit SWI3C;SWI3C;ortholog	chromatin/chromatin-binding, or -regulatory protein(PC00077)
AT2G19480	Nucleosome assembly protein 1;2;NAP1;2;ortholog	chromatin/chromatin-binding, or -regulatory protein(PC00077)

Appendix 6-II: GO terms mapped to translation in genes downregulated in *sep2-1* VT

Gene ID	Annotation	Protein Class
AT5G38830	Cysteine--tRNA ligase 2, cytoplasmic;TAIR:locus:2152237;ortholog	aminoacyl-tRNA synthetase(PC00047)
AT5G35620	Eukaryotic translation initiation factor isoform 4E;EIF(ISO)4E;ortholog	translation initiation factor(PC00224)
AT4G18040	Eukaryotic translation initiation factor 4E-1;EIF4E1;ortholog	translation initiation factor(PC00224)
AT1G34030	40S ribosomal protein S18;RPS18A;ortholog	ribosomal protein(PC00202)
AT5G64140	40S ribosomal protein S28-2;RPS28C;ortholog	ribosomal protein(PC00202)
AT3G13920	Eukaryotic initiation factor 4A-1;EIF4A1;ortholog	
AT5G59850	40S ribosomal protein S15a-1;RPS15AA;ortholog	ribosomal protein(PC00202)
AT4G18100	60S ribosomal protein L32-1;RPL32A;ortholog	ribosomal protein(PC00202)
AT1G70600	60S ribosomal protein L27a-3;RPL27AC;ortholog	ribosomal protein(PC00202)
AT4G20980	Eukaryotic translation initiation factor 3 subunit D;TIF3D1;ortholog	translation initiation factor(PC00224)
AT5G18380	40S ribosomal protein S16-3;RPS16C;ortholog	ribosomal protein(PC00202)
AT3G02190	60S ribosomal protein L39-2;RPL39B;ortholog	ribosomal protein(PC00202)
AT1G66580	60S ribosomal protein L10-3;RPL10C;ortholog	ribosomal protein(PC00202)
AT1G48630	Receptor for activated C kinase 1B;RACK1B;ortholog	
AT1G48830	40S ribosomal protein S7-1;RPS7A;ortholog	ribosomal protein(PC00202)
AT5G67510	60S ribosomal protein L26-2;RPL26B;ortholog	ribosomal protein(PC00202)
AT5G39850	40S ribosomal protein S9-2;RPS9C;ortholog	ribosomal protein(PC00202)
AT5G09510	40S ribosomal protein S15-4;RPS15D;ortholog	ribosomal protein(PC00202)
AT1G23290	60S ribosomal protein L27a-2;RPL27AB;ortholog	ribosomal protein(PC00202)
AT3G44590	60S acidic ribosomal protein P2-4;RPP2D;ortholog	ribosomal protein(PC00202)
AT5G02610	60S ribosomal protein L35-4;RPL35D;ortholog	ribosomal protein(PC00202)
AT3G53890	40S ribosomal protein S21-1;RPS21B;ortholog	ribosomal protein(PC00202)
AT3G55280	60S ribosomal protein L23a-2;RPL23AB;ortholog	ribosomal protein(PC00202)
AT3G04230	40S ribosomal protein S16-2;RPS16B;ortholog	ribosomal protein(PC00202)
AT1G72550	Phenylalanine--tRNA ligase beta subunit, cytoplasmic;TAIR:locus:2030290;ortholog	aminoacyl-tRNA synthetase(PC00047)
AT2G09990	40S ribosomal protein S16-1;RPS16A;ortholog	ribosomal protein(PC00202)
AT2G32220	60S ribosomal protein L27-1;RPL27A;ortholog	ribosomal protein(PC00202)
AT2G32060	40S ribosomal protein S12-2;RPS12C;ortholog	ribosomal protein(PC00202)

AT2G34520	At2g34520;rps14;ortholog	ribosomal protein(PC00202)
AT5G56680	Asparagine--tRNA ligase, cytoplasmic 1;SYNC1;ortholog	aminoacyl-tRNA synthetase(PC00047)
AT4G10450	60S ribosomal protein L9-2;RPL9D;ortholog	ribosomal protein(PC00202)
AT4G39280	Phenylalanine--tRNA ligase alpha subunit, cytoplasmic;TAIR:locus:2136328;ortholog	aminoacyl-tRNA synthetase(PC00047)

Bibliography

Abley, K., Locke, J. C. W., and Leyser, H. M. O. (2016a). Developmental mechanisms underlying variable, invariant and plastic phenotypes. *Annals of Botany* 117, 733–748. doi:10.1093/aob/mcw016.

Abley, K., Locke, J. C. W., and Leyser, H. M. O. (2016b). Developmental mechanisms underlying variable, invariant and plastic phenotypes. *Annals of Botany* 117, 733–748. doi:10.1093/aob/mcw016.

Acajjaoui, S., Zubieta, C., and IUCr (2013). Crystallization studies of the keratin-like domain from *Arabidopsis thaliana* SEPALLATA 3. *Acta Crystallographica Section F Structural Biology and Crystallization Communications* 69, 997–1000. doi:10.1107/S174430911302006X.

Aida, M., and Tasaka, M. (2006). Genetic control of shoot organ boundaries. *Current Opinion in Plant Biology* 9, 72–77. doi:10.1016/J.PBI.2005.11.011.

Airoldi, C. A., Bergonzi, S., and Davies, B. (2010). Single amino acid change alters the ability to specify male or female organ identity. *Proceedings of the National Academy of Sciences* 107, 18898–18902. doi:10.1073/PNAS.1009050107.

Airoldi, C. A., and Davies, B. (2012). Gene Duplication and the Evolution of Plant MADS-box Transcription Factors. *Journal of Genetics and Genomics* 39, 157–165. doi:10.1016/j.jgg.2012.02.008.

Alejandra Mandel, M., Gustafson-Brown, C., Savidge, B., and Yanofsky, M. F. (1992). Molecular characterization of the Arabidopsis floral homeotic gene APETALA1. *Nature 1992 360:6401* 360, 273–277. doi:10.1038/360273a0.

Alvarez-Buylla, E. R., Pelaz, S., Liljegren, S. J., Gold, S. E., Burgeff, C., Ditta, G. S., et al. (2000). An ancestral MADS-box gene duplication occurred before the divergence of plants and animals. *Proceedings of the National Academy of Sciences* 97, 5328–5333. doi:10.1073/PNAS.97.10.5328.

Alves-Ferreira, M., Wellmer, F., Banhara, A., Kumar, V., Riechmann, J. L., and Meyerowitz, E. M. (2007). Global expression profiling applied to the analysis of arabidopsis stamen development. *Plant Physiology* 145, 747–762. doi:10.1104/pp.107.104422.

Ampomah-Dwamena, C., Morris, B. A., Sutherland, P., Veit, B., and Yao, J.-L. (2002). Down-Regulation of TM29, a TomatoSEPALLATA Homolog, Causes Parthenocarpic Fruit Development and Floral Reversion. *Plant Physiology* 130, 605–617. doi:10.1104/PP.005223.

Anderson, G. H., Alvarez, N. D. G., Gilman, C., Jeffares, D. C., Trainor, V. C. W., Hanson, M. R., et al. (2004). Diversification of Genes Encoding Mei2-Like RNA Binding Proteins in Plants. *Plant Molecular Biology 2004 54:5* 54, 653–670. doi:10.1023/B:PLAN.0000040819.33383.B6.

Assis, R., and Bachtrog, D. (2013). Neofunctionalization of young duplicate genes in Drosophila. *Proceedings of the National Academy of Sciences* 110, 17409–17414. doi:10.1073/PNAS.1313759110.

Bacilio, M., Moreno, M., Raul Lopez-Aguilar, D., and Bashan, Y. (2017). Scaling from the growth chamber to the greenhouse to the field: Demonstration of diminishing effects of mitigation of salinity in peppers inoculated with plant growth-promoting bacterium and humic acids. doi:10.1016/j.apsoil.2017.07.002.

Bailey, T. L., Johnson, J., Grant, C. E., and Noble, W. S. (2015). The MEME Suite. *Nucleic Acids Research* 43, W39–W49. doi:10.1093/NAR/GKV416.

Bao, S., Hua, C., Shen, L., and Yu, H. (2020). New insights into gibberellin signaling in regulating flowering in Arabidopsis. *Journal of Integrative Plant Biology* 62, 118–131. doi:10.1111/JIPB.12892.

Bateman, A., Coin, L., Durbin, R., Finn, R. D., Hollich, V., Griffiths-Jones, S., et al. (2004). The Pfam protein families database. *Nucleic Acids Research* 32, D138–D141. doi:10.1093/NAR/GKH121.

Bateson, P. P. G. (Paul P. G., and Gluckman, P. D. *Plasticity, Robustness, Development and Evolution*. Available at: http://www.cambridge.org/us/academic/subjects/life-sciences/evolutionary-biology/plasticity-robustness-development-and-evolution?format=HB&isbn=9780521516297#0e14WTIBz172tFta.97 [Accessed January 29, 2018].

Becker, A., and Ehlers, K. (2015). Arabidopsis flower development—of protein complexes, targets, and transport. *Protoplasma 2015 253:2* 253, 219–230. doi:10.1007/S00709-015-0812-7.

Becker, A., Winter, K. U., Meyer, B., Saedler, H., and Theißen, G. (2000). MADS-box gene diversity in seed plants 300 million years ago. *Molecular Biology and Evolution* 17, 1425–1434. doi:10.1093/oxfordjournals.molbev.a026243.

Bemis, S. M., and Torii, K. U. (2007). Autonomy of cell proliferation and developmental programs during Arabidopsis aboveground organ morphogenesis. *Developmental Biology* 304, 367–381. doi:10.1016/J.YDBIO.2006.12.049.

Benjamini, Y. (2010). Discovering the false discovery rate. *Journal of the Royal Statistical Society. Series B: Statistical Methodology* 72, 405–416. doi:10.1111/J.1467-9868.2010.00746.X.

Besnard, F., Refahi, Y., Morin, V., Marteaux, B., Brunoud, G., Chambrier, P., et al. (2013). Cytokinin signalling inhibitory fields provide robustness to phyllotaxis. *Nature 2013 505:7483* 505, 417–421. doi:10.1038/nature12791.

Biewers, S. M. (2014). Sepallata genes and their role during floral organ formation. Available at: http://etheses.whiterose.ac.uk/8965/1/Sepallata%20genes%20and%20their%20role%20during%20floral%20organ%20development.pdf [Accessed January 29, 2018].

Blackman, B. K. (2017). Changing Responses to Changing Seasons: Natural Variation in the Plasticity of Flowering Time. *Plant Physiology* 173, 16–26. doi:10.1104/PP.16.01683.

Blázquez, M. A., Ahn, J. H., and Weigel, D. (2003). A thermosensory pathway controlling flowering time in Arabidopsis thaliana. *Nature Genetics 2003 33:2* 33, 168–171. doi:10.1038/ng1085.

Blázquez, M. A., Ferrándiz, C., and Madueño, F. How Floral Meristems are Built New DELLA-based biotechnological tools for sustainable agriculture View project ABA Signalling View project. doi:10.1007/s11103-006-0013-z.

Blum, A. (2014). Genomics for drought resistance-getting down to earth. in *Functional Plant Biology* (CSIRO), 1191–1198. doi:10.1071/FP14018.

Boukhibar, L. M., and Barkoulas, M. (2016). The developmental genetics of biological robustness. *Annals of Botany* 117, 699. doi:10.1093/AOB/MCV128.

Bowman, J. L., Eshed, Y., and Baum, S. F. (2002). Establishment of polarity in angiosperm lateral organs. *Trends in Genetics* 18, 134–141. doi:10.1016/S0168-9525(01)02601-4.

Bowman, J. L., Smyth, D. R., and Meyerowitz, E. M. (1991). Genetic interactions among floral homeotic genes of Arabidopsis. *Development* 112, 1–20. doi:10.1242/dev.112.1.1.

Bowman, J., Smyth, D., and Meyerowitz, E. (1989). Genes directing flower development in Arabidopsis. *Plant Cell* 1.

Bradley, D., Carpenter, R., Sommer, H., Hartley, N., and Coen, E. (1993). Complementary floral homeotic phenotypes result from opposite orientations of a transposon at the plena locus of antirrhinum. *Cell* 72, 85–95. doi:10.1016/0092-8674(93)90052-R.

Buide, M. L. (2004). Intra-inflorescence variation in floral traits and reproductive success of the hermaphrodite Silene acutifolia. *Annals of Botany* 94, 441–448. doi:10.1093/aob/mch164.

Byzova, M., Franken, J., … M. A.-G. &, and 1999, undefined (1999). Arabidopsis STERILE APETALA, a multifunctional gene regulating inflorescence, flower, and ovule development. *genesdev.cshlp.org*. Available at: http://genesdev.cshlp.org/content/13/8/1002.short [Accessed July 15, 2021].

Carianopol, C. S., Chan, A. L., Dong, S., Provart, N. J., Lumba, S., and Gazzarrini, S. (2020). An abscisic acid-responsive protein interaction network for sucrose non-fermenting related kinase1 in abiotic stress response. *Communications Biology 2020 3:1* 3, 1–15. doi:10.1038/s42003-020-0866-8.

Carpenter, R., and Coen, E. S. (1990). Floral homeotic mutations produced by transposon-mutagenesis in Antirrhinum majus. *Genes and Development* 4, 1483–1493. doi:10.1101/gad.4.9.1483.

Castillejo, C., Romera-Branchat, M., and Pelaz, S. (2005). A new role of the Arabidopsis SEPALLATA3 gene revealed by its constitutive expression. *Plant Journal* 43, 586–596. doi:10.1111/j.1365-313X.2005.02476.x.

Causier, B., Ashworth, M., Guo, W., and Davies, B. (2012). The TOPLESS Interactome: A Framework for Gene Repression in Arabidopsis. *Plant Physiology* 158, 423–438. doi:10.1104/PP.111.186999.

Causier, B., Cook, H., and Davies, B. (2003). An Antirrhinum ternary complex factor specifically interacts with C-function and SEPALLATA-like MADS-box factors. *Plant Molecular Biology* 52, 1051–1062. doi:10.1023/A:1025426016267.

Causier, B., and Davies, B. (2014). Flower Development in the Asterid Lineage. *Methods in Molecular Biology* 1110, 35–55. doi:10.1007/978-1-4614-9408-9_2.

Causier, B., Schwarz-Sommer, Z., and Davies, B. (2010). Floral organ identity: 20 years of ABCs. *Seminars in Cell & Developmental Biology* 21, 73–79. doi:10.1016/J.SEMCDB.2009.10.005.

Chae, E., Tan, Q. K.-G., Hill, T. A., and Irish, V. F. (2008). An Arabidopsis F-box protein acts as a transcriptional co-factor to regulate floral development. *Development* 135, 1235–1245. doi:10.1242/DEV.015842.

Charon, C., Bruggeman, Q., Thareau, V., and Henry, Y. (2012). Gene duplication within the Green Lineage: the case of TEL genes. *Journal of Experimental Botany* 63, 5061–5077. doi:10.1093/JXB/ERS181.

Chen, D., Yan, W., Fu, L. Y., and Kaufmann, K. (2018). Architecture of gene regulatory networks controlling flower development in Arabidopsis thaliana. *Nature Communications* 9, 1–13. doi:10.1038/s41467-018-06772-3.

Chen, F., Zhang, X., Liu, X., and Zhang, L. (2017). Evolutionary analysis of MIKCc - type MADS-Box genes in gymnosperms and angiosperms. *Frontiers in Plant Science* 8, 895. doi:10.3389/fpls.2017.00895.

Chen, J.-G., Ullah, H., Temple, B., Liang, J., Guo, J., Alonso, J. M., et al. (2006). RACK1 mediates multiple hormone responsiveness and developmental processes in Arabidopsis. *Journal of Experimental Botany* 57, 2697–2708. doi:10.1093/JXB/ERL035.

Christensen, A. R., and Malcomber, S. T. (2012). Duplication and diversification of the LEAFY HULL STERILE1 and Oryza sativa MADS5 SEPALLATA lineages in graminoid Poales. *EvoDevo 2012 3:1* 3, 1–15. doi:10.1186/2041-9139-3-4.

Clark, S. E., Jacobsen, S. E., Levin, J. Z., and Meyerowitz, E. M. (1996). The CLAVATA and SHOOT MERISTEMLESS loci competitively regulate meristem activity in Arabidopsis. *Development* 122, 1567–1575. doi:10.1242/DEV.122.5.1567.

Clarke, G. M. (1998). The genetic basis of developmental stability. V. Inter- and intra-individual character variation. *Heredity* 80, 562–567. doi:10.1046/j.1365-2540.1998.00294.x.

Coen, E. S., and Meyerowitz, E. M. (1991). The war of the whorls: genetic interactions controlling flower development. *Nature* 353, 31–37. doi:10.1038/353031a0.

Corbesier, L., Vincent, C., Jang, S., Fornara, F., Fan, Q., Searle, I., et al. (2007). FT protein movement contributes to long-distance signaling in floral induction of Arabidopsis. *Science* 316, 1030–1033. doi:10.1126/SCIENCE.1141752.

Dai, C., Liang, X., Ren, J., Liao, M., Li, J., and Galloway, L. F. (2016). The mean and variability of a floral trait have opposing effects on fitness traits. *Annals of Botany* 117, 421–429. doi:10.1093/aob/mcv189.

Das, P., Ito, T., Wellmer, F., Vernoux, T., Dedieu, A., Traas, J., et al. (2009). Floral stem cell termination involves the direct regulation of AGAMOUS by PERIANTHIA. *Development* 136, 1605–1611. doi:10.1242/DEV.035436.

Dasso, M. (1993). RCC1 in the cell cycle: the regulator of chromosome condensation takes on new roles. *Trends in Biochemical Sciences* 18, 96–101. doi:10.1016/0968-0004(93)90161-F.

Davies, B., Egea-Cortines, M., Silva, E. de A., Saedler, H., and Sommer, H. (1996). Multiple interactions amongst floral homeotic MADS box proteins. *The EMBO Journal* 15, 4330–4343. doi:10.1002/J.1460-2075.1996.TB00807.X.

Davies, B., Motte, P., Keck, E., Saedler, H., Sommer, H., and Schwarz-Sommer, Z. (1999). PLENA and FARINELLI: redundancy and regulatory interactions

between two Antirrhinum MADS-box factors controlling flower development. *The EMBO Journal* 18, 4023–4034. doi:10.1093/EMBOJ/18.14.4023.

de Folter, S., Immink, R. G. H., Kieffer, M., Pařenicová, L., Henz, S. R., Weigel, D., et al. (2005a). Comprehensive Interaction Map of the Arabidopsis MADS Box Transcription Factors. *The Plant Cell* 17, 1424–1433. doi:10.1105/TPC.105.031831.

de Folter, S., Immink, R. G. H., Kieffer, M., Pařenicová, L., Henz, S. R., Weigel, D., et al. (2005b). Comprehensive Interaction Map of the Arabidopsis MADS Box Transcription Factors. *The Plant Cell* 17, 1424–1433. doi:10.1105/TPC.105.031831.

del Pozo, J. C., and Estelle, M. (1999). Function of the ubiquitin–proteosome pathway in auxin response. *Trends in Plant Science* 4, 107–112. doi:10.1016/S1360-1385(99)01382-5.

DeYoung, B. J., and Clark, S. E. (2008). BAM Receptors Regulate Stem Cell Specification and Organ Development Through Complex Interactions With CLAVATA Signaling. *Genetics* 180, 895–904. doi:10.1534/GENETICS.108.091108.

Diggle, P. K. ARCHITECTURAL EFFECTS AND THE INTERPRETATION OF PATTERNS OF FRUIT AND SEED DEVELOPMENT. Available at: www.annualreviews.org [Accessed May 11, 2021].

Dinneny, J. R., Weigel, D., and Yanofsky, M. F. (2006). NUBBIN and JAGGED define stamen and carpel shape in Arabidopsis. *Development* 133, 1645–1655. doi:10.1242/DEV.02335.

Ditta, G., Pinyopich, A., Robles, P., Pelaz, S., and Yanofsky, M. F. (2004). The SEP4 Gene of Arabidopsis thaliana Functions in Floral Organ and Meristem Identity. *Current Biology* 14, 1935–1940. doi:10.1016/j.cub.2004.10.028.

Domagalska, M. A., Sarnowska, E., Nagy, F., and Davis, S. J. (2010). Genetic Analyses of Interactions among Gibberellin, Abscisic Acid, and Brassinosteroids in the Control of Flowering Time in Arabidopsis thaliana. *PLOS ONE* 5, e14012. doi:10.1371/JOURNAL.PONE.0014012.

Dubos, C., Stracke, R., Grotewold, E., Weisshaar, B., Martin, C., and Lepiniec, L. (2010). MYB transcription factors in Arabidopsis. *Trends in Plant Science* 15, 573–581. doi:10.1016/J.TPLANTS.2010.06.005.

Egea-Cortines, M., Saedler, H., and Sommer, H. (1999). Ternary complex formation between the MADS-box proteins SQUAMOSA, DEFICIENS and GLOBOSA is involved in the control of floral architecture in Antirrhinum majus. *EMBO Journal* 18, 5370–5379. doi:10.1093/emboj/18.19.5370.

El-Samad, H., Kurata, H., Doyle, J. C., Gross, C. A., and Khammash, M. (2005). Surviving heat shock: Control strategies for robustness and performance. *Proceedings of the National Academy of Sciences* 102, 2736–2741. doi:10.1073/PNAS.0403510102.

Emery, J. F., Floyd, S. K., Alvarez, J., Eshed, Y., Hawker, N. P., Izhaki, A., et al. (2003). Radial Patterning of Arabidopsis Shoots by Class III HD-ZIP and KANADI Genes. *Current Biology* 13, 1768–1774. doi:10.1016/J.CUB.2003.09.035.

Endress, P. K. (1992). Evolution and Floral Diversity: The Phylogenetic Surroundings of Arabidopsis and Antirrhinum. Available at: https://www.jstor.org/stable/2995533 [Accessed May 11, 2021].

Ermolaeva, M. D., Wu, M., Eisen, J. A., and Salzberg, S. L. (2003). The age of the Arabidopsis thaliana genome duplication. *Plant Molecular Biology 2003 51:6* 51, 859–866. doi:10.1023/A:1023001130337.

Eshed, Y., Baum, S. F., Perea, J. v., and Bowman, J. L. (2001). Establishment of polarity in lateral organs of plants. *Current Biology* 11, 1251–1260. doi:10.1016/S0960-9822(01)00392-X.

Espinosa-Soto, C., Padilla-Longoria, P., and Alvarez-Buylla, E. R. (2004). A gene regulatory network model for cell-fate determination during Arabidopsis thaliana flower development that is robust and recovers experimental gene expression profiles. *Plant Cell* 16, 2923–2939. doi:10.1105/tpc.104.021725.

Félix, M. A., and Barkoulas, M. (2015a). Pervasive robustness in biological systems. *Nature Reviews Genetics* 16, 483–496. doi:10.1038/nrg3949.

Félix, M.-A., and Barkoulas, M. (2015b). Pervasive robustness in biological systems. *Nature Reviews Genetics* 16, 483–496. doi:10.1038/nrg3949.

Fellenberg, C., Ohlen, M. van, Handrick, V., and Vogt, T. (2012). The role of CCoAOMT1 and COMT1 in Arabidopsis anthers. *Planta 2012 236:1* 236, 51–61. doi:10.1007/S00425-011-1586-6.

Ferrandiz, C., Gu, Q., Martienssen, R., and Yanofsky, M. F. (2000). Redundant regulation of meristem identity and plant architecture by FRUITFULL, APETALA1 and CAULIFLOWER. *Development* 127, 725–734. doi:10.1242/DEV.127.4.725.

Ferrario, S., Immink, R. G. H., Shchennikova, A., Busscher-Lange, J., and Angenent, G. C. (2003). The MADS Box Gene FBP2 Is Required for SEPALLATA Function in Petunia. *The Plant Cell* 15, 914–925. doi:10.1105/TPC.010280.

FILAMENTOUS FLOWER, a meristem and organ identity gene of Arabidopsis, encodes a protein with a zinc finger and HMG-related domains Available at: http://genesdev.cshlp.org/content/13/9/1079.short [Accessed August 17, 2021].

Flanagan, C. A., and Ma, H. (1994). Spatially and temporally regulated expression of the MADS-box gene AGL2 in wild-type and mutant arabidopsis flowers. *Plant Molecular Biology* 26, 581–595.

Forde, B. G. (2009). Is it good noise? The role of developmental instability in the shaping of a root system. *Journal of Experimental Botany* 60, 3989–4002. doi:10.1093/jxb/erp265.

Franco-Zorrilla, J. M., Cubas, P., Jarillo, J. A., Fernández-Calvín, B., Salinas, J., and Martínez-Zapater, J. M. (2002). AtREM1, a Member of a New Family of B3 Domain-Containing Genes, Is Preferentially Expressed in Reproductive Meristems. *Plant Physiology* 128, 418–427. doi:10.1104/PP.010323.

Fujimoto, S. Y., Ohta, M., Usui, A., Shinshi, H., and Ohme-Takagi, M. (2000). Arabidopsis Ethylene-Responsive Element Binding Factors Act as Transcriptional Activators or Repressors of GCC Box–Mediated Gene Expression. *The Plant Cell* 12, 393–404. doi:10.1105/TPC.12.3.393.

Gamboa, A., Paéz-Valencia, J., Acevedo, G. F., Vázquez-Moreno, L., and Alvarez-Buylla, R. E. (2001). Floral Transcription Factor AGAMOUS Interacts in Vitro with a Leucine-Rich Repeat and an Acid Phosphatase Protein Complex. *Biochemical and Biophysical Research Communications* 288, 1018–1026. doi:10.1006/BBRC.2001.5875.

Gao, X., Liang, W., Yin, C., Ji, S., Wang, H., Su, X., et al. (2010). The SEPALLATA-like gene OsMADS34 is required for rice inflorescence and spikelet development. *Plant physiology* 153, 728–40. doi:10.1104/pp.110.156711.

Geiler-Samerotte, K. A., Bauer, C. R., Li, S., Ziv, N., Gresham, D., and Siegal, M. L. (2013). The details in the distributions: why and how to study phenotypic variability. *Current Opinion in Biotechnology* 24, 752–759. doi:10.1016/J.COPBIO.2013.03.010.

Geuten, K., Viaene, T., and Irish, V. F. (2011). Robustness and evolvability in the B-system of flower development. *Annals of Botany* 107, 1545–1556. doi:10.1093/AOB/MCR061.

Goslin, K., Zheng, B., Serrano-Mislata, A., Rae, L., Ryan, P. T., Kwaśniewska, K., et al. (2017). Transcription Factor Interplay between LEAFY and APETALA1/CAULIFLOWER during Floral Initiation. *Plant Physiology* 174, 1097–1109. doi:10.1104/PP.17.00098.

Gothandam, K. M., Nalini, E., Karthikeyan, S., and Shin, J. S. (2009). OsPRP3, a flower specific proline-rich protein of rice, determines extracellular matrix structure of floral organs and its overexpression confers cold-tolerance. *Plant Molecular Biology 2009 72:1* 72, 125–135. doi:10.1007/S11103-009-9557-Z.

Gramzow, L., Ritz, M. S., and Theißen, G. (2010). On the origin of MADS-domain transcription factors. *Trends in Genetics* 26, 149–153. doi:10.1016/j.tig.2010.01.004.

Gramzow, L., and Theissen, G. (2010). A hitchhiker's guide to the MADS world of plants. *Genome Biology* 11, 214. doi:10.1186/gb-2010-11-6-214.

Gu, Z., Steinmetz, L. M., Gu, X., Scharfe, C., Davis, R. W., and Li, W.-H. (2003). Role of duplicate genes in genetic robustness against null mutations. *Nature* 421, 63–66. doi:10.1038/nature01198.

Gustafson-Brown, C., Savidge, B., and Yanofsky, M. F. (1994). Regulation of the arabidopsis floral homeotic gene APETALA1. *Cell* 76, 131–143. doi:10.1016/0092-8674(94)90178-3.

Ha, C. M., Jun, J. H., Nam, H. G., and Fletcher, J. C. (2007). BLADE-ON-PETIOLE1 and 2 Control Arabidopsis Lateral Organ Fate through Regulation of LOB Domain and Adaxial-Abaxial Polarity Genes. *The Plant Cell* 19, 1809–1825. doi:10.1105/TPC.107.051938.

Hanada, K., Kuromori, T., Myouga, F., Toyoda, T., Li, W.-H., and Shinozaki, K. (2009). Evolutionary Persistence of Functional Compensation by Duplicate Genes in Arabidopsis. *Genome Biology and Evolution* 1, 409–414. doi:10.1093/GBE/EVP043.

Hase, Y., Tanaka, A., Baba, T., and Watanabe, H. (2000). FRL1 is required for petal and sepal development in Arabidopsis. *The Plant Journal* 24, 21–32. doi:10.1046/J.1365-313X.2000.00851.X.

He, Y., and Amasino, R. M. (2005). Role of chromatin modification in flowering-time control. *Trends in Plant Science* 10, 30–35. doi:10.1016/J.TPLANTS.2004.11.003.

Heijmans, K., Morel, P., and Vandenbussche, M. (2012). MADS-box Genes and Floral Development: the Dark Side. *Journal of Experimental Botany* 63, 5397–5404. doi:10.1093/JXB/ERS233.

Hervieux, N., Dumond, M., Sapala, A., Routier-Kierzkowska, A. L., Kierzkowski, D., Roeder, A. H. K., et al. (2016). A Mechanical Feedback Restricts Sepal Growth and Shape in Arabidopsis. *Current Biology* 26, 1019–1028. doi:10.1016/J.CUB.2016.03.004.

Hill, J. P., and Lord, E. M. (1989). Floral development in Arabidopsis thaliana : a comparison of the wild type and the homeotic pistillata mutant . *Canadian Journal of Botany* 67, 2922–2936. doi:10.1139/b89-375.

Honma, T., and Goto, K. (2001). Complexes of MADS-box proteins are sufficient to convert leaves into floral organs. *Nature* 409.

Hornstein, E., and Shomron, N. (2006). Canalization of development by microRNAs. *Nature Genetics* 38, S20–S24. doi:10.1038/ng1803.

Hugouvieux, V., and Zubieta, C. (2018). MADS transcription factors cooperate: complexities of complex formation. *Journal of Experimental Botany* 69, 1821–1823. doi:10.1093/jxb/ery099.

Hulo, N., Bairoch, A., Bulliard, V., Cerutti, L., de Castro, E., Langendijk-Genevaux, P. S., et al. (2006). The PROSITE database. *Nucleic Acids Research* 34, D227–D230. doi:10.1093/NAR/GKJ063.

Husbands, A. Y., Chitwood, D. H., Plavskin, Y., and Timmermans, M. C. P. (2009). Signals and prepatterns: new insights into organ polarity in plants. *Genes & Development* 23, 1986–1997. doi:10.1101/GAD.1819909.

Immink, R. G. H., Kaufmann, K., and Angenent, G. C. (2010). The "ABC" of MADS domain protein behaviour and interactions. *Seminars in Cell and Developmental Biology* 21, 87–93. doi:10.1016/j.semcdb.2009.10.004.

Immink, R. G. H., Tonaco, I. A. N., de Folter, S., Shchennikova, A., van Dijk, A. D. J., Busscher-Lange, J., et al. (2009). SEPALLATA3: The "glue" for MADS box transcription factor complex formation. *Genome Biology* 10, 1–16. doi:10.1186/gb-2009-10-2-r24.

Irish, V. F., and Sussex, I. M. (1990). Function of the apetala-1 gene during Arabidopsis floral development. *The Plant Cell* 2, 741–753. doi:10.1105/TPC.2.8.741.

Jack, T. (2001). Relearning our ABCs: New twists on an old model. *Trends in Plant Science* 6, 310–316. doi:10.1016/S1360-1385(01)01987-2.

Jack, T., Brockman, L. L., and Meyerowitz, E. M. (1992). The homeotic gene APETALA3 of Arabidopsis thaliana encodes a MADS box and is expressed in petals and stamens. *Cell* 68, 683–697. doi:10.1016/0092-8674(92)90144-2.

Jetha, K., Theißen, G., and Melzer, R. (2014). Arabidopsis SEPALLATA proteins differ in cooperative DNA-binding during the formation of floral quartet-like complexes. *Nucleic Acids Research* 42, 10927–10942. doi:10.1093/nar/gku755.

Jiao, Y., and Meyerowitz, E. M. (2010a). Cell-type specific analysis of translating RNAs in developing flowers reveals new levels of control. *Molecular Systems Biology* 6, 419. doi:10.1038/MSB.2010.76.

Jiao, Y., and Meyerowitz, E. M. (2010b). Cell-type specific analysis of translating RNAs in developing flowers reveals new levels of control. *Molecular Systems Biology* 6, 419. doi:10.1038/MSB.2010.76.

Jiao, Y., and Meyerowitz, E. M. (2010c). Cell-type specific analysis of translating RNAs in developing flowers reveals new levels of control. *Molecular Systems Biology* 6, 419. doi:10.1038/msb.2010.76.

Jofuku, K. D., den Boer, B. G., van Montagu, M., and Okamuro, J. K. (1994). Control of Arabidopsis flower and seed development by the homeotic gene APETALA2. *The Plant Cell* 6, 1211–1225. doi:10.1105/TPC.6.9.1211.

Juarez, M. T., Kui, J. S., Thomas, J., Heller, B. A., and Timmermans, M. C. P. (2004). microRNA-mediated repression of rolled leaf1 specifies maize leaf polarity. *Nature* 428, 84–88. doi:10.1038/nature02363.

Käppel, S., Melzer, R., Rümpler, F., Gafert, C., and Theißen, G. (2018). The floral homeotic protein SEPALLATA3 recognizes target DNA sequences by shape readout involving a conserved arginine residue in the MADS-domain. *The Plant Journal* 95, 341–357. doi:10.1111/tpj.13954.

Kaufmann, K., Anfang, N., Saedler, H., and Theissen, G. (2005a). Mutant analysis, protein–protein interactions and subcellular localization of the Arabidopsis Bsister (ABS) protein. *Molecular Genetics and Genomics 2005 274:2* 274, 103–118. doi:10.1007/S00438-005-0010-Y.

Kaufmann, K., Melzer, R., and Theißen, G. (2005b). MIKC-type MADS-domain proteins: Structural modularity, protein interactions and network evolution in land plants. *Gene* 347, 183–198. doi:10.1016/j.gene.2004.12.014.

Kaufmann, K., Muiño, J. M., Jauregui, R., Airoldi, C. A., Smaczniak, C., Krajewski, P., et al. (2009a). Target genes of the MADS transcription factor sepallata3: Integration of developmental and hormonal pathways in the arabidopsis flower. *PLoS Biology* 7, 0854–0875. doi:10.1371/journal.pbio.1000090.

Kaufmann, K., Muiño, J. M., Jauregui, R., Airoldi, C. A., Smaczniak, C., Krajewski, P., et al. (2009b). Target genes of the MADS transcription factor sepallata3: Integration of developmental and hormonal pathways in the arabidopsis flower. *PLoS Biology* 7, 0854–0875. doi:10.1371/journal.pbio.1000090.

Kaufmann, K., Wellmer, F., Muiñ, J. M., Ferner, T., Wuest, S. E., Kumar, V., et al. (2010). Orchestration of floral initiation by APETALA1. *Science* 328, 85–89. doi:10.1126/science.1185244.

Kerstetter, R. A., Bollman, K., Taylor, R. A., Bomblies, K., and Poethig, R. S. (2001). KANADI regulates organ polarity in Arabidopsis. *Nature 2001 411:6838* 411, 706–709. doi:10.1038/35079629.

Kidner, C. A., and Martienssen, R. A. (2004). Spatially restricted microRNA directs leaf polarity through ARGONAUTE1. *Nature 2004 428:6978* 428, 81–84. doi:10.1038/nature02366.

Kieffer, M., Master, V., Waites, R., and Davies, B. (2011). TCP14 and TCP15 affect internode length and leaf shape in Arabidopsis. *The Plant Journal* 68, 147–158. doi:10.1111/J.1365-313X.2011.04674.X.

Klepikova, A. v., Kasianov, A. S., Gerasimov, E. S., Logacheva, M. D., and Penin, A. A. (2016). A high resolution map of the Arabidopsis thaliana developmental transcriptome based on RNA-seq profiling. *The Plant Journal* 88, 1058–1070. doi:10.1111/TPJ.13312.

Komaki, M. K., Okada, K., Nishino, E., and Shimura, Y. (1988). Isolation and characterization of novel mutants of Arabidopsis thaliana defective in flower development. *Development* 104, 195–203. doi:10.1242/DEV.104.2.195.

Krizek, B. A., and Fletcher, J. C. (2005). Molecular mechanisms of flower development: An armchair guide. *Nature Reviews Genetics* 6, 688–698. doi:10.1038/nrg1675.

Kunst, L., Klenz, J. E., Martinez-Zapater, J., and Haughn, G. W. (1989). AP2 Gene Determines the Identity of Perianth Organs in Flowers of Arabidopsis thaliana. *The Plant Cell* 1, 1195–1208. doi:10.1105/TPC.1.12.1195.

Kuzmin, E., Vandersluis, B., Ba, A. N. N., Wang, W., Koch, E. N., Usaj, M., et al. (2020). Exploring whole-genome duplicate gene retention with complex genetic interaction analysis. *Science* 368. doi:10.1126/SCIENCE.AAZ5667.

Lachowiec, J., Mason, G. A., Schultz, K., and Queitsch, C. (2018). Redundancy, Feedback, and Robustness in the Arabidopsis thaliana BZR/BEH Gene Family. *Frontiers in Genetics* 9. doi:10.3389/FGENE.2018.00523.

Lai, X., Stigliani, A., Lucas, J., Hugouvieux, V., Parcy, F., and Zubieta, C. (2020). Genome-wide binding of SEPALLATA3 and AGAMOUS complexes determined by sequential DNA-affinity purification sequencing. *Nucleic Acids Research* 48, 9637–9648. doi:10.1093/nar/gkaa729.

Landscapes and Labscapes: Exploring the Lab-Field Border in Biology - Robert E. Kohler - Google Books Available at: https://books.google.co.uk/books?hl=en&lr=&id=eeyPEcen1toC&oi=fnd&pg=PR7&ots=nVaNIDT6kT&sig=a9Lxfo9uO5O5OK3mVhh5kHUqSms&redir_esc=y#v=onepage&q&f=false [Accessed May 4, 2021].

Lee, J. H., Yoo, S. J., Park, S. H., Hwang, I., Lee, J. S., and Ahn, J. H. (2007). Role of SVP in the control of flowering time by ambient temperature in Arabidopsis. *Genes & Development* 21, 397–402. doi:10.1101/GAD.1518407.

Lenski, R. E., Barrick, J. E., and Ofria, C. (2006). Balancing Robustness and Evolvability. *PLoS Biology* 4, e428. doi:10.1371/journal.pbio.0040428.

Levy, S. F., and Siegal, M. L. (2008). Network hubs buffer environmental variation in Saccharomyces cerevisiae. *PLoS biology* 6, e264. doi:10.1371/journal.pbio.0060264.

Levy, Y. Y., Mesnage, S., Mylne, J. S., Gendall, A. R., and Dean, C. (2002). Multiple Roles of Arabidopsis VRN1 in Vernalization and Flowering Time Control. *Science* 297, 243–246. doi:10.1126/SCIENCE.1072147.

Li, N., Liu, Z., Wang, Z., Ru, L., Gonzalez, N., Baekelandt, A., et al. (2018). STERILE APETALA modulates the stability of a repressor protein complex to control organ size in Arabidopsis thaliana. *PLOS Genetics* 14, e1007218. doi:10.1371/JOURNAL.PGEN.1007218.

Litt, A. (2015). An Evaluation of A-Function: Evidence from the APETALA1 and APETALA2 Gene Lineages. *https://doi.org/10.1086/509662* 168, 73–91. doi:10.1086/509662.

Liu, D., Wang, D., Qin, Z., Zhang, D., Yin, L., Wu, L., et al. (2014). The SEPALLATA MADS-box protein SLMBP21 forms protein complexes with JOINTLESS and MACROCALYX as a transcription activator for development of the tomato flower abscission zone. *The Plant Journal* 77, 284–296. doi:10.1111/TPJ.12387.

Liu, Y., Xu, Y., Xiao, J., Ma, Q., Li, D., Xue, Z., et al. (2011). OsDOG, a gibberellin-induced A20/AN1 zinc-finger protein, negatively regulates gibberellin-mediated cell elongation in rice. *Journal of Plant Physiology* 168, 1098–1105. doi:10.1016/J.JPLPH.2010.12.013.

Lloyd, J., and Meinke, D. Genome Analysis A Comprehensive Dataset of Genes with a Loss-of-Function Mutant Phenotype in Arabidopsis 1[W][OA]. doi:10.1104/pp.111.192393.

Lynch, M., and Conery, J. S. (2000). The Evolutionary Fate and Consequences of Duplicate Genes. *Science* 290. Available at: http://science.sciencemag.org/content/290/5494/1151 [Accessed May 18, 2017].

Lynch, M., and Force, A. (2000). The Probability of Duplicate Gene Preservation by Subfunctionalization. *Genetics* 154, 459–473. doi:10.1093/GENETICS/154.1.459.

Magome, H., Yamaguchi, S., Hanada, A., Kamiya, Y., and Oda, K. (2004). dwarf and delayed-flowering 1, a novel Arabidopsis mutant deficient in gibberellin biosynthesis because of overexpression of a putative AP2 transcription factor. *The Plant Journal* 37, 720–729. doi:10.1111/J.1365-313X.2003.01998.X.

Malcomber, S. T., and Kellogg, E. A. (2005). SEPALLATA gene diversification: brave new whorls. *Trends in Plant Science* 10, 427–435. doi:10.1016/J.TPLANTS.2005.07.008.

Mandel, M. A., and Yanofsky, M. F. (1998). The Arabidopsis AGL9 MADS box gene is expressed in young flower primordia. *Sexual Plant Reproduction 1998 11:1* 11, 22–28. doi:10.1007/S004970050116.

Mandel, M., and Yanofsky, M. (1999). The Arabidopsis AGL 9 MADS box gene is expressed in young flower primordia. *Sex Plant Reprod* 11.

Mantegazza, O., Gregis, V., Mendes, M. A., Morandini, P., Alves-Ferreira, M., Patreze, C. M., et al. (2014). Analysis of the arabidopsis REM gene family predicts functions during flower development. *Annals of Botany* 114, 1507–1515. doi:10.1093/AOB/MCU124.

Marioni, J. C., Mason, C. E., Mane, S. M., Stephens, M., and Gilad, Y. (2008). RNA-seq: An assessment of technical reproducibility and comparison with gene expression arrays. *Genome Research* 18, 1509–1517. doi:10.1101/GR.079558.108.

Martin, L., Fei, Z., Giovannoni, J., and Rose, J. K. C. (2013). Catalyzing plant science research with RNA-seq. *Frontiers in Plant Science* 0, 66. doi:10.3389/FPLS.2013.00066.

Masel, J., and Siegal, M. L. (2009). Robustness: mechanisms and consequences. *Trends in Genetics* 25, 395–403. doi:10.1016/j.tig.2009.07.005.

Masters, M. T. (2011). Vegetable teratology, an account of the principal deviations from the usual construction of plants, by Maxwell T. Masters ... With numerous illus. by E.M. Williams. *Vegetable teratology, an account of the principal deviations from the usual construction of plants, by Maxwell T. Masters ... With numerous illus. by E.M. Williams.* doi:10.5962/BHL.TITLE.17149.

Matsumoto, N., and Okada, K. (2001). A homeobox gene, PRESSED FLOWER, regulates lateral axis-dependent development of Arabidopsis flowers. *Genes & Development* 15, 3355–3364. doi:10.1101/GAD.931001.

McConnell, J. R., Emery, J., Eshed, Y., Bao, N., Bowman, J., and Barton, M. K. (2001). Role of PHABULOSA and PHAVOLUTA in determining radial patterning in shoots. *Nature 2001 411:6838* 411, 709–713. doi:10.1038/35079635.

Mead, J., Bruning, A. R., Gill, M. K., Steiner, A. M., Acton, T. B., and Vershon, A. K. (2002). Interactions of the Mcm1 MADS Box Protein with Cofactors That Regulate Mating in Yeast. *Molecular and Cellular Biology* 22, 4607–4621. doi:10.1128/MCB.22.13.4607-4621.2002.

Melzer, R., Verelst, W., and Theißen, G. (2009). The class E floral homeotic protein SEPALLATA3 is sufficient to loop DNA in 'floral quartet'-like complexes in vitro. *Nucleic Acids Research* 37, 144–157. doi:10.1093/NAR/GKN900.

Mendel's Principles of Heredity (1913). *Nature 1913 91:2262* 91, 9–9. doi:10.1038/091009b0.

Mestek Boukhibar, L., and Barkoulas, M. (2016). The developmental genetics of biological robustness. *Annals of Botany* 117, 699–707. doi:10.1093/aob/mcv128.

Meyerowitz, E. M., Smyth, D. R., and Bowman, J. L. (1989). Abnormal flowers and pattern formation in floral. *Development* 106, 209–217. doi:10.1242/DEV.106.2.209.

Michaels, S. D., and Amasino, R. M. (1999). FLOWERING LOCUS C Encodes a Novel MADS Domain Protein That Acts as a Repressor of Flowering. *The Plant Cell* 11, 949–956. doi:10.1105/TPC.11.5.949.

Mirabet, V., Besnard, F., Vernoux, T., and Boudaoud, A. (2012). Noise and Robustness in Phyllotaxis. *PLOS Computational Biology* 8, e1002389. doi:10.1371/JOURNAL.PCBI.1002389.

Mockler, T., Yang, H., Yu, X., Parikh, D., Cheng, Y., Dolan, S., et al. (2003). Regulation of photoperiodic flowering by Arabidopsis photoreceptors. *Proceedings of the National Academy of Sciences* 100, 2140–2145. doi:10.1073/PNAS.0437826100.

Monroe, J. G., Srikant, T., Carbonell-Bejerano, P., Exposito-Alonso, M., Weng, M.-L., Rutter, M. T., et al. (2020). Mutation bias shapes gene evolution in Arabidopsis thaliana. *bioRxiv*, 2020.06.17.156752. doi:10.1101/2020.06.17.156752.

Murai, K. (2013). Homeotic genes and the ABCDE model for floral organ formation in wheat. *Plants* 2, 379–395. doi:10.3390/plants2030379.

N, D.-F., and JP, V.-C. (2010). ARGONAUTE9-dependent silencing of transposable elements in pericentromeric regions of Arabidopsis. *Plant signaling & behavior* 5, 628–632. doi:10.1038/NATURE08828.

N, Y. (2021). LEAFY, a Pioneer Transcription Factor in Plants: A Mini-Review. *Frontiers in plant science* 12. doi:10.3389/FPLS.2021.701406.

Nam, J., DePamphilis, C. W., Ma, H., and Nei, M. (2003). Antiquity and evolution of the MADS-box gene family controlling flower development in plants. *Molecular Biology and Evolution* 20, 1435–1447. doi:10.1093/molbev/msg152.

Nelson, T. J., Balza, R., Xiao, Q., and Misra, R. P. (2005). SRF-dependent gene expression in isolated cardiomyocytes: Regulation of genes involved in cardiac hypertrophy. *Journal of Molecular and Cellular Cardiology* 39, 479–489. doi:10.1016/J.YJMCC.2005.05.004.

Ni, W., Xie, D., Hobbie, L., Feng, B., Zhao, D., Akkara, J., et al. (2004). Regulation of Flower Development in Arabidopsis by SCF Complexes. *Plant Physiology* 134, 1574–1585. doi:10.1104/PP.103.031971.

Nikolov, L. A. (2019). Brassicaceae flowers: Diversity amid uniformity. *Journal of Experimental Botany* 70, 2623–2635. doi:10.1093/jxb/erz079.

Nilsson, O., Lee, I., Blázquez, M. A., and Weigel, D. (1998). Flowering-Time Genes Modulate the Response to LEAFY Activity. *Genetics* 150, 403–410. doi:10.1093/GENETICS/150.1.403.

Nole-Wilson, S., Rueschhoff, E. E., Bhatti, H., and Franks, R. G. (2010). Synergistic disruptions in seuss cyp85A2 double mutants reveal a role for brassinolide synthesis during gynoecium and ovule development. *BMC Plant Biology 2010 10:1* 10, 1–7. doi:10.1186/1471-2229-10-198.

Ogawa, T., Uchimiya, H., and Kawai-Yamada, M. (2007). Mutual Regulation of Arabidopsis thaliana Ethylene-responsive Element Binding Protein and a Plant Floral Homeotic Gene, APETALA2. *Annals of Botany* 99, 239–244. doi:10.1093/AOB/MCL265.

Ó'Maoiléidigh, D. S., Graciet, E., and Wellmer, F. (2014). Gene networks controlling Arabidopsis thaliana flower development. *New Phytologist* 201, 16–30. doi:10.1111/nph.12444.

Ó'Maoiléidigh, D. S., Wuest, S. E., Rae, L., Raganelli, A., Ryan, P. T., Kwaśniewska, K., et al. (2013). Control of reproductive floral organ identity specification in arabidopsis by the C function regulator AGAMOUS. *Plant Cell* 25, 2482–2503. doi:10.1105/tpc.113.113209.

Otsuga, D., DeGuzman, B., Prigge, M. J., Drews, G. N., and Clark, S. E. (2001). REVOLUTA regulates meristem initiation at lateral positions. *The Plant Journal* 25, 223–236. doi:10.1111/J.1365-313X.2001.00959.X.

Paaby, A. B., and Rockman, M. v. (2014). Cryptic genetic variation: evolution's hidden substrate. *Nature Reviews Genetics 2014 15:4* 15, 247–258. doi:10.1038/nrg3688.

Pajoro, A., Biewers, S., Dougali, E., Valentim, F. L., Mendes, M. A., Porri, A., et al. (2014). The (r)evolution of gene regulatory networks controlling Arabidopsis plant reproduction: A two-decade history. *Journal of Experimental Botany* 65, 4731–4745. doi:10.1093/jxb/eru233.

Pelaz, S., Ditta, G., Baumann, E., Wisman, E., and Yanofsky, M. (2000a). B and C floral organ identity functions require SEPALLATA MADS-box genes. *Nature* 405.

Pelaz, S., Ditta, G. S., Baumann, E., Wisman, E., and Yanofsky, M. F. (2000b). B and C floral organ identity functions require SEPALLATA MADS-box genes. *Nature* 405, 200–203. doi:10.1038/35012103.

Pelaz, S., Ditta, G. S., Baumann, E., Wisman, E., and Yanofsky, M. F. (2000c). B and C floral organ identity functions require SEPALLATA MADS-box genes. *Nature* 405, 200–203. doi:10.1038/35012103.

Pelaz, S., Gustafson-Brown, C., Kohalmi, S. E., Crosby, W. L., and Yanofsky, M. F. (2001a). APETALA1 and SEPALLATA3 interact to promote flower development . *The Plant Journal* 26, 385–394. doi:10.1046/j.1365-313x.2001.2641042.x.

Pelaz, S., Gustafson-Brown, C., Kohalmi, S. E., Crosby, W. L., and Yanofsky, M. F. (2001b). APETALA1 and SEPALLATA3 interact to promote flower development . *The Plant Journal* 26, 385–394. doi:10.1046/J.1365-313X.2001.2641042.X.

Pelaz, S., Gustafson-Brown, C., Kohalmi, S. E., Crosby, W. L., and Yanofsky, M. F. (2001c). APETALA1 and SEPALLATA3 interact to promote flower development . *The Plant Journal* 26, 385–394. doi:10.1046/j.1365-313x.2001.2641042.x.

Pelaz, S., Tapia-López, R., Alvarez-Buylla, E. R., and Yanofsky, M. F. (2001d). Conversion of leaves into petals in Arabidopsis. *Current Biology* 11, 182–184. doi:10.1016/S0960-9822(01)00024-0.

Pigliucci, M., Murren, C. J., and Schlichting, C. D. (2006). Phenotypic plasticity and evolution by genetic assimilation. *Journal of Experimental Biology* 209, 2362–2367. doi:10.1242/jeb.02070.

Pinyopich, A., Ditta, G. S., Savidge, B., Liljegren, S. J., Baumann, E., Wisman, E., et al. (2003). Assessing the redundancy of MADS-box genes during carpel and ovule development. *Nature 2003 424:6944* 424, 85–88. doi:10.1038/nature01741.

Piwarzyk, E., Yang, Y., and Jack, T. (2007). Conserved C-Terminal Motifs of the Arabidopsis Proteins APETALA3 and PISTILLATA Are Dispensable for Floral Organ Identity Function. *Plant Physiology* 145, 1495–1505. doi:10.1104/PP.107.105346.

Plavskin, Y., Nagashima, A., Perroud, P. F., Hasebe, M., Quatrano, R. S., Atwal, G. S., et al. (2016). Ancient trans-Acting siRNAs Confer Robustness and Sensitivity onto the Auxin Response. *Developmental Cell* 36, 276–289. doi:10.1016/J.DEVCEL.2016.01.010.

Pnueli, L., Abu-Abeid, M., Zamir, D., Nacken, W., Schwarz-Sommer, Zs., and Lifschitz, E. (1991). The MADS box gene family in tomato: temporal expression during floral development, conserved secondary structures and homology with homeotic genes from Antirrhinum and Arabidopsis. *The Plant Journal* 1, 255–266. doi:10.1111/J.1365-313X.1991.00255.X.

Pnueli, L., Hareven, D., Broday, L., Hurwitz, C., and Lifschitz, E. (1994). The TM5 MADS Box Gene Mediates Organ Differentiation in the Three Inner Whorls of Tomato Flowers. *The Plant Cell* 6, 175–186. doi:10.1105/TPC.6.2.175.

Poorter, H., Fiorani, F., Pieruschka, R., Wojciechowski, T., Putten, W. H., Kleyer, M., et al. (2016). Pampered inside, pestered outside? Differences and similarities between plants growing in controlled conditions and in the field. *New Phytologist* 212, 838–855. doi:10.1111/nph.14243.

Portereiko, M. F., Lloyd, A., Steffen, J. G., Punwani, J. A., Otsuga, D., and Drews, G. N. (2006). AGL80 Is Required for Central Cell and Endosperm Development in Arabidopsis. *The Plant Cell* 18, 1862–1872. doi:10.1105/TPC.106.040824.

Price, E. P., Smith, H., Huygens, F., and Giffard, P. M. (2007). High-Resolution DNA Melt Curve Analysis of the Clustered, Regularly Interspaced Short-Palindromic-Repeat Locus of Campylobacter jejuni. *Applied and Environmental Microbiology* 73, 3431. doi:10.1128/AEM.02702-06.

Puranik, S., Acajjaoui, S., Conn, S., Costa, L., Conn, V., Vial, A., et al. (2014). Structural Basis for the Oligomerization of the MADS Domain Transcription Factor SEPALLATA3 in Arabidopsis. *The Plant Cell* 26, 3603–3615. doi:10.1105/TPC.114.127910.

Putterill, J., Robson, F., Lee, K., Simon, R., and Coupland, G. (1995). The CONSTANS gene of arabidopsis promotes flowering and encodes a protein showing similarities to zinc finger transcription factors. *Cell* 80, 847–857. doi:10.1016/0092-8674(95)90288-0.

Qian, W., Liao, B.-Y., Chang, A. Y.-F., and Zhang, J. (2010). Maintenance of duplicate genes and their functional redundancy by reduced expression. *Trends in genetics : TIG* 26, 425–30. doi:10.1016/j.tig.2010.07.002.

Queitsch, C., Hong, S., Vierling, E., Cell, S. L.-T. P., and 2000, undefined Heat shock protein 101 plays a crucial role in thermotolerance in Arabidopsis. *Am Soc Plant Biol*. Available at: http://www.plantcell.org/user/logout?current=node/8384 [Accessed January 29, 2018].

Queitsch, C., Hong, S.-W., Vierling, E., and Lindquist, S. (2000). Heat Shock Protein 101 Plays a Crucial Role in Thermotolerance in Arabidopsis. *The Plant Cell* 12, 479–492. doi:10.1105/TPC.12.4.479.

Queitsch, C., Sangstert, T. A., and Lindquist, S. (2002). Hsp90 as a capacitor of phenotypic variation. *Nature* 417, 618–624. doi:10.1038/nature749.

Reynolds, Joan., and Tampion, John. (1983). Double flowers : a scientific study. 183.

RK, I., A, B., and B, B. (1998). Plant O-methyltransferases: molecular analysis, common signature and classification. *Plant molecular biology* 36, 1–10. doi:10.1023/A:1005939803300.

Rody, H. V. S., Baute, G. J., Rieseberg, L. H., and Oliveira, L. O. (2017). Both mechanism and age of duplications contribute to biased gene retention patterns in plants. *BMC Genomics* 18, 1–10. doi:10.1186/s12864-016-3423-6.

Roeder, A. H. K., Chickarmane, V., Cunha, A., Obara, B., Manjunath, B. S., and Meyerowitz, E. M. (2010). Variability in the Control of Cell Division Underlies Sepal Epidermal Patterning in Arabidopsis thaliana. *PLOS Biology* 8, e1000367. doi:10.1371/JOURNAL.PBIO.1000367.

Roeder, A. H. K., Cunha, A., Ohno, C. K., and Meyerowitz, E. M. (2012). Cell cycle regulates cell type in the Arabidopsis sepal. *Development* 139, 4416–4427. doi:10.1242/DEV.082925.

Rombolá-Caldentey, B., Rueda-Romero, P., Iglesias-Fernández, R., Carbonero, P., and Oñate-Sánchez, L. (2014). Arabidopsis DELLA and Two HD-ZIP Transcription Factors Regulate GA Signaling in the Epidermis through the L1 Box cis-Element. *The Plant Cell* 26, 2905–2919. doi:10.1105/TPC.114.127647.

Rounsley, S. D., Ditta, G. S., and Yanofsky, M. F. (1995). Diverse roles for MADS box genes in Arabidopsis development. *The Plant Cell* 7, 1259–1269. doi:10.1105/tpc.7.8.1259.

Rudall, P. J., and Bateman, R. M. (2003). Evolutionary change in flowers and inflorescences: Evidence from naturally occurring terata. *Trends in Plant Science* 8, 76–82. doi:10.1016/S1360-1385(02)00026-2.

Rümpler, F., Theißen, G., and Melzer, R. (2018). A conserved leucine zipper-like motif accounts for strong tetramerization capabilities of SEPALLATA-like MADS-domain transcription factors. *Journal of Experimental Botany* 69, 1943–1954. doi:10.1093/jxb/ery063.

Running, M. P., and Meyerowitz, E. M. (1996). Mutations in the PERIANTHIA gene of Arabidopsis specifically alter floral organ number and initiation pattern. *Development* 122, 1261–1269. doi:10.1242/DEV.122.4.1261.

Sangster, T. A., and Queitsch, C. (2005). The HSP90 chaperone complex, an emerging force in plant development and phenotypic plasticity. *Current Opinion in Plant Biology* 8, 86–92. doi:10.1016/J.PBI.2004.11.012.

Sangster, T. A., Salathia, N., Undurraga, S., Milo, R., Schellenberg, K., Lindquist, S., et al. HSP90 affects the expression of genetic variation and developmental stability in quantitative traits. Available at: http://www.pnas.org/content/pnas/105/8/2963.full.pdf [Accessed January 29, 2018].

Santelli, E., and Richmond, T. J. (2000). Crystal structure of MEF2A core bound to DNA at 1.5 Å resolution. *Journal of Molecular Biology* 297, 437–449. doi:10.1006/JMBI.2000.3568.

Saunders, E. R. (1921). NOTE ON THE EVOLUTION OF THE DOUBLE STOCK (MA TTItlOLA 1NCANA). *Journal of Genetics* 11, 69–74.

Savidge, B., Rounsley, S. D., and Yanofsky, M. F. (1995). Temporal relationship between the transcription of two Arabidopsis MADS box genes and the floral organ identity genes. *The Plant Cell* 7, 721–733. doi:10.1105/TPC.7.6.721.

Sawa, M., and Kay, S. A. (2011). GIGANTEA directly activates Flowering Locus T in Arabidopsis thaliana. *Proceedings of the National Academy of Sciences* 108, 11698–11703. doi:10.1073/PNAS.1106771108.

Schwarz-Sommer, Z., Hue, I., Huijser, P., Flor, P. J., Hansen, R., Tetens, F., et al. (1992). Characterization of the Antirrhinum floral homeotic MADS-box gene deficiens: evidence for DNA binding and autoregulation of its persistent expression throughout flower development. *The EMBO Journal* 11, 251–263. doi:10.1002/J.1460-2075.1992.TB05048.X.

Schwarz-Sommer, Z., Huijser, P., Nacken, W., Saedler, H., and Sommer, H. Genetic Control of Flower Development by Homeotic Genes in Antirrhinum majus. Available at: http://science.sciencemag.org/ [Accessed June 25, 2021].

Sémon, M., and Wolfe, K. H. (2007). Consequences of genome duplication. *Current Opinion in Genetics & Development* 17, 505–512. doi:10.1016/J.GDE.2007.09.007.

Sieber, P., Wellmer, F., Gheyselinck, J., Riechmann, J. L., and Meyerowitz, E. M. (2007). Redundancy and specialization among plant microRNAs: role of the

MIR164 family in developmental robustness. *Development* 134, 1051–1060. doi:10.1242/DEV.02817.

Siegal, M. L., and Rushlow, C. (2012). Pausing on the Path to Robustness. *Developmental Cell* 22, 905–906. doi:10.1016/J.DEVCEL.2012.04.020.

Siegfried, K. R., Eshed, Y., Baum, S. F., Otsuga, D., Drews, G. N., and Bowman, J. L. (1999). Members of the YABBY gene family specify abaxial cell fate in Arabidopsis. *Development* 126, 4117–4128. doi:10.1242/DEV.126.18.4117.

Simko, I. (2016). High-Resolution DNA Melting Analysis in Plant Research. *Trends in Plant Science* 21, 528–537. doi:10.1016/J.TPLANTS.2016.01.004.

Sink, K. C. (1973). The inheritance of apetalous flower type in Petunia hybrida Vilm. and linkage tests with the genes for flower doubleness and grandiflora characters and its use in hybrid seed production. *Euphytica 1973 22:3* 22, 520–526. doi:10.1007/BF00036650.

Smaczniak, C., Immink, R. G. H., Muiño, J. M., Blanvillain, R., Busscher, M., Busscher-Lange, J., et al. (2012). Characterization of MADS-domain transcription factor complexes in Arabidopsis flower development. *Proceedings of the National Academy of Sciences* 109, 1560–1565. doi:10.1073/PNAS.1112871109.

Smyth, D. R. (2018). Evolution and genetic control of the floral ground plan. *New Phytologist* 220, 70–86. doi:10.1111/nph.15282.

Smyth, D. R., Bowman, J. L., and Meyerowitz, E. M. (1990). Early flower development in Arabidopsis. *Plant Cell* 2, 755–767. doi:10.1105/tpc.2.8.755.

Soza, V. L., Snelson, C. D., Hewett Hazelton, K. D., and di Stilio, V. S. (2016). Partial redundancy and functional specialization of E-class SEPALLATA genes in an early-diverging eudicot. *Developmental Biology* 419, 143–155. doi:10.1016/J.YDBIO.2016.07.021.

Sridhar, V., Surendrarao, A., and Liu, Z. (2006). APETALA1 and SEPALLATA3 interact with SEUSS to mediate transcription repression during flower development. *Development* 133.

Stein, H., Honig, A., Miller, G., Erster, O., Eilenberg, H., Csonka, L. N., et al. (2011). Elevation of free proline and proline-rich protein levels by simultaneous

manipulations of proline biosynthesis and degradation in plants. *Plant Science* 181, 140–150. doi:10.1016/J.PLANTSCI.2011.04.013.

Su, K., Zhao, S., Shan, H., Kong, H., Lu, W., Theissen, G., et al. (2008). The MIK region rather than the C-terminal domain of AP3-like class B floral homeotic proteins determines functional specificity in the development and evolution of petals. *New Phytologist* 178, 544–558. doi:10.1111/J.1469-8137.2008.02382.X.

Swaminathan, K., Peterson, K., and Jack, T. (2008). The plant B3 superfamily. *Trends in Plant Science* 13, 647–655. doi:10.1016/J.TPLANTS.2008.09.006.

Takeda, S., Iwasaki, A., Matsumoto, N., Uemura, T., Tatematsu, K., and Okada, K. (2013). Physical Interaction of Floral Organs Controls Petal Morphogenesis in Arabidopsis. *Plant Physiology* 161, 1242–1250. doi:10.1104/PP.112.212084.

Taylor, M. A., Wilczek, A. M., Roe, J. L., Welch, S. M., Runcie, D. E., Cooper, M. D., et al. (2019). Large-effect flowering time mutations reveal conditionally adaptive paths through fitness landscapes in Arabidopsis thaliana. *Proceedings of the National Academy of Sciences of the United States of America* 116, 17890–17899. doi:10.1073/pnas.1902731116.

THATCHER, S. R., BURD, S., WRIGHT, C., LERS, A., and GREEN, P. J. (2015). Differential expression of miRNAs and their target genes in senescing leaves and siliques: insights from deep sequencing of small RNAs and cleaved target RNAs. *Plant, Cell & Environment* 38, 188–200. doi:10.1111/pce.12393.

Theißen, G. (2001). Development of floral organ identity: stories from the MADS house. *Current Opinion in Plant Biology* 4, 75–85. doi:10.1016/S1369-5266(00)00139-4.

Theissen, G., Becker, A., di Rosa, A., Kanno, A., Kim, J. T., Münster, T., et al. (2000a). A short history of MADS-box genes in plants. *Plant Molecular Biology* 42, 115–149. doi:10.1023/A:1006332105728.

Theissen, G., Becker, A., Rosa, A. di, Kanno, A., and Kim, J. (2000b). A short history of MADS-box genes in plants. *Plant Mol Biol* 42.

Theißen, G., and Gramzow, L. (2016). Structure and Evolution of Plant MADS Domain Transcription Factors. *Plant Transcription Factors: Evolutionary, Structural and Functional Aspects*, 127–138. doi:10.1016/B978-0-12-800854-6.00008-7.

Theißen, G., Kim, J. T., and Saedler, H. (1996). Classification and phylogeny of the MADS-box multigene family suggest defined roles of MADS-box gene subfamilies in the morphological evolution of eukaryotes. *Journal of Molecular Evolution 1996 43:5* 43, 484–516. doi:10.1007/BF02337521.

Theißen, G., and Saedler, H. (2001). Floral quartets. *Nature* 409, 469–471. doi:10.1038/35054172.

Thompson, M. v., and Wolniak, S. M. (2008). A Plasma Membrane-Anchored Fluorescent Protein Fusion Illuminates Sieve Element Plasma Membranes in Arabidopsis and Tobacco. *Plant Physiology* 146, 1599–1610. doi:10.1104/PP.107.113274.

Thomson, B., and Wellmer, F. (2019). "Molecular regulation of flower development," in *Current Topics in Developmental Biology* (Academic Press Inc.), 185–210. doi:10.1016/bs.ctdb.2018.11.007.

Tiwari, S., Spielman, M., Schulz, R., Oakey, R. J., Kelsey, G., Salazar, A., et al. (2010). Transcriptional profiles underlying parent-of-origin effects in seeds of Arabidopsis thaliana. *BMC Plant Biology 2010 10:1* 10, 1–22. doi:10.1186/1471-2229-10-72.

Trapnell, C., Hendrickson, D. G., Sauvageau, M., Goff, L., Rinn, J. L., and Pachter, L. (2013). Differential analysis of gene regulation at transcript resolution with RNA-seq. *Nature Biotechnology* 31, 46–53. doi:10.1038/nbt.2450.

Tyler, L., Thomas, S. G., Hu, J., Dill, A., Alonso, J. M., Ecker, J. R., et al. (2004). DELLA Proteins and Gibberellin-Regulated Seed Germination and Floral Development in Arabidopsis. *Plant Physiology* 135, 1008–1019. doi:10.1104/PP.104.039578.

Vandenbussche, M., Zethof, J., Souer, E., Koes, R., Tornielli, G. B., Pezzotti, M., et al. (2003). Toward the Analysis of the Petunia MADS Box Gene Family by Reverse and Forward Transposon Insertion Mutagenesis Approaches: B, C, and D Floral

Organ Identity Functions Require SEPALLATA-Like MADS Box Genes in Petunia. *The Plant Cell* 15, 2680–2693. doi:10.1105/TPC.017376.

Veitia, R. A. (2005). Paralogs in Polyploids: One for All and All for One? *The Plant Cell* 17, 4. doi:10.1105/TPC.104.170130.

Vernoux, T., Brunoud, G., Farcot, E., Morin, V., Daele, H. van den, Legrand, J., et al. (2011). The auxin signalling network translates dynamic input into robust patterning at the shoot apex. *Molecular Systems Biology* 7, 508. doi:10.1038/MSB.2011.39.

Vernoux, T., Kronenberger, J., Grandjean, O., Laufs, P., and Traas, J. (2000). PIN-FORMED 1 regulates cell fate at the periphery of the shoot apical meristem. *Development* 127, 5157–5165. doi:10.1242/dev.127.23.5157.

Vrebalov, J., Ruezinsky, D., Padmanabhan, V., White, R., Medrano, D., Drake, R., et al. (2002). A MADS-box gene necessary for fruit ripening at the tomato ripening-inhibitor (rin) locus. *Science* 296, 343–346. doi:10.1126/SCIENCE.1068181.

WADDINGTON, C. H. (1942). CANALIZATION OF DEVELOPMENT AND THE INHERITANCE OF ACQUIRED CHARACTERS. *Nature 1942 150:3811* 150, 563–565. doi:10.1038/150563a0.

Waddington, C. H. (1961). Genetic Assimilation. *Advances in Genetics* 10, 257–293. doi:10.1016/S0065-2660(08)60119-4.

Wagner, A. *Robustness and evolvability in living systems*. Available at: https://books.google.co.uk/books?hl=en&lr=&id=pRFYAQAAQBAJ&oi=fnd&pg=PP1&dq=Robustness+and+evolvability+in+living+system&ots=2TMqJlcPNY&sig=IaMUAfhUCRI7AOyOdrQ7l0xkUm8#v=onepage&q=Robustness%20and%20evolvability%20in%20living%20system&f=false [Accessed January 22, 2018].

Wang, D., Passier, R., Liu, Z. P., Shin, C. H., Wang, Z., Li, S., et al. (2002). Regulation of cardiac growth and development by SRF and its cofactors. *Cold Spring Harbor Symposia on Quantitative Biology* 67, 97–105. doi:10.1101/SQB.2002.67.97.

Wang, Y.-B., Song, J.-P., and Wang, Z.-B. (2015). ASYMMETRIC LEAVES2-LIKE38, one member of AS2/LOB gene family, involves in regulating ab-adaxial

patterning in Arabidopsis lateral organs. *Acta Physiologiae Plantarum 2015 37:9* 37, 1–11. doi:10.1007/S11738-015-1938-0.

Weigel, D., and Meyerowitz, E. M. (1994). The ABCs of floral homeotic genes. *Cell* 78, 203–209. doi:10.1016/0092-8674(94)90291-7.

Wellmer, F., Alves-Ferreira, M., Dubois, A., Riechmann, J. L., and Meyerowitz, E. M. (2006). Genome-wide analysis of gene expression during early Arabidopsis flower development. *PLoS Genetics* 2, 1012–1024. doi:10.1371/journal.pgen.0020117.

Wellmer, F., Graciet, E., and Riechmann, J. L. (2014). Specification of floral organs in Arabidopsis. *Journal of Experimental Botany* 65, 1–9. doi:10.1093/jxb/ert385.

Wellmer, F., and Riechmann, J. L. (2010). Gene networks controlling the initiation of flower development. *Trends in Genetics* 26, 519–527. doi:10.1016/J.TIG.2010.09.001.

Whitacre, J. M. (2012). Biological Robustness: Paradigms, Mechanisms, and Systems Principles. *Frontiers in Genetics* 3, 67. doi:10.3389/fgene.2012.00067.

Whitacre, J. M., and Bender, A. (2010). Networked buffering: a basic mechanism for distributed robustness in complex adaptive systems. *Theoretical Biology and Medical Modelling* 7, 20. doi:10.1186/1742-4682-7-20.

Wilkinson, M. D., and Haughn, G. W. (1995). UNUSUAL FLORAL ORGANS Controls Meristem Identity and Organ Primordia Fate in Arabidopsis. *The Plant Cell* 7, 1485–1499. doi:10.1105/TPC.7.9.1485.

Wils, C. R., and Kaufmann, K. (2017). Gene-regulatory networks controlling inflorescence and flower development in Arabidopsis thaliana. *Biochimica et Biophysica Acta - Gene Regulatory Mechanisms* 1860, 95–105. doi:10.1016/j.bbagrm.2016.07.014.

Winter, C. M., Yamaguchi, N., Wu, M.-F., and Wagner, D. (2015). Transcriptional programs regulated by both LEAFY and APETALA1 at the time of flower formation. *Physiologia Plantarum* 155, 55–73. doi:10.1111/PPL.12357.

Winter, D., Vinegar, B., Nahal, H., Ammar, R., Wilson, G. v., and Provart, N. J. (2007). An “Electronic Fluorescent Pictograph” Browser for Exploring and Analyzing

Large-Scale Biological Data Sets. *PLOS ONE* 2, e718. doi:10.1371/JOURNAL.PONE.0000718.

Wuest, S. E., O'Maoileidigh, D. S., Rae, L., Kwasniewska, K., Raganelli, A., Hanczaryk, K., et al. (2012). Molecular basis for the specification of floral organs by APETALA3 and PISTILLATA. *Proceedings of the National Academy of Sciences of the United States of America* 109, 13452–13457. doi:10.1073/pnas.1207075109.

Würschum, T., Groß-Hardt, R., and Laux, T. (2006). APETALA2 Regulates the Stem Cell Niche in the Arabidopsis Shoot Meristem. *The Plant Cell* 18, 295–307. doi:10.1105/TPC.105.038398.

Wyatt, R. (1982). INFLORESCENCE ARCHITECTURE: HOW FLOWER NUMBER, ARRANGEMENT, AND PHENOLOGY AFFECT POLLINATION AND FRUIT-SET. *American Journal of Botany* 69, 585–594. doi:10.1002/j.1537-2197.1982.tb13295.x.

Xiao, C., Somerville, C., and Anderson, C. T. (2014). POLYGALACTURONASE INVOLVED IN EXPANSION1 Functions in Cell Elongation and Flower Development in Arabidopsis. *The Plant Cell* 26, 1018–1035. doi:10.1105/TPC.114.123968.

Yamaguchi, T., Nukazuka, A., and Tsukaya, H. (2012). Leaf adaxial–abaxial polarity specification and lamina outgrowth: evolution and development. *Plant and Cell Physiology* 53, 1180–1194. doi:10.1093/PCP/PCS074.

Yang, S. W., Jang, I.-C., Henriques, R., and Chua, N.-H. (2009). FAR-RED ELONGATED HYPOCOTYL1 and FHY1-LIKE Associate with the Arabidopsis Transcription Factors LAF1 and HFR1 to Transmit Phytochrome A Signals for Inhibition of Hypocotyl Elongation. *The Plant Cell* 21, 1341–1359. doi:10.1105/TPC.109.067215.

Yang, Y. (2004). Defining subdomains of the K domain important for protein-protein interactions of plant MADS proteins. *Plant Molecular Biology* 55, 45–59.

Yang, Y., Fanning, L., and Jack, T. (2003). The K domain mediates heterodimerization of the Arabidopsis floral organ identity proteins, APETALA3 and PISTILLATA. *The Plant Journal* 33, 47–59. doi:10.1046/J.0960-7412.2003.01473.X.

Yanofsky, M. F., Ma, H., Bowman, J. L., Drews, G. N., Feldmann, K. A., and Meyerowitz, E. M. (1990). The protein encoded by the Arabidopsis homeotic gene agamous resembles transcription factors. *Nature* 346, 35–39. doi:10.1038/346035a0.

Yant, L., Mathieu, J., Dinh, T. T., Ott, F., Lanz, C., Wollmann, H., et al. (2010). Orchestration of the floral transition and floral development in arabidopsis by the bifunctional transcription factor APETALA2. *Plant Cell* 22, 2156–2170. doi:10.1105/tpc.110.075606.

Yoo, S. K., Chung, K. S., Kim, J., Lee, J. H., Hong, S. M., Yoo, S. J., et al. (2005). CONSTANS Activates SUPPRESSOR OF OVEREXPRESSION OF CONSTANS 1 through FLOWERING LOCUS T to Promote Flowering in Arabidopsis. *Plant Physiology* 139, 770–778. doi:10.1104/PP.105.066928.

Yu, H., and Goh, C. J. (2000). Identification and Characterization of Three Orchid MADS-Box Genes of the AP1/AGL9 Subfamily during Floral Transition. *Plant Physiology* 123, 1325–1336. doi:10.1104/PP.123.4.1325.

Yu, H., Ito, T., Zhao, Y., Peng, J., Kumar, P., and Meyerowitz, E. M. (2004). Floral homeotic genes are targets of gibberellin signaling in flower development. *Proceedings of the National Academy of Sciences* 101, 7827–7832. doi:10.1073/PNAS.0402377101.

Zahn, L. M., Kong, H., Leebens-Mack, J. H., Kim, S., Soltis, P. S., Landherr, L. L., et al. (2005). The evolution of the SEPALLATA subfamily of MADS-box genes: a preangiosperm origin with multiple duplications throughout angiosperm history. *Genetics* 169, 2209–23. doi:10.1534/genetics.104.037770.

Zahn, L. M., Leebens-Mack, J. H., Arrington, J. M., Hu, Y., Landherr, L. L., DePamphilis, C. W., et al. (2006). Conservation and divergence in the AGAMOUS subfamily of MADS-box genes: Evidence of independent sub- and neofunctionalization events. *Evolution and Development* 8, 30–45. doi:10.1111/J.1525-142X.2006.05073.X.

Zhang, H., Deng, X., Sun, B., Lee Van, S., Kang, Z., Lin, H., et al. (2018a). Role of the BUB3 protein in phragmoplast microtubule reorganization during cytokinesis. *Nature Plants 2018 4:7* 4, 485–494. doi:10.1038/s41477-018-0192-z.

Zhang, J., Hu, Z., Wang, Y., Yu, X., Liao, C., Zhu, M., et al. (2018b). Suppression of a tomato SEPALLATA MADS-box gene, SlCMB1, generates altered inflorescence architecture and enlarged sepals. *Plant Science* 272, 75–87. doi:10.1016/J.PLANTSCI.2018.03.031.

Zhang, L., Wang, L., Yang, Y., Cui, J., Chang, F., Wang, Y., et al. (2015). Analysis of Arabidopsis floral transcriptome: detection of new florally expressed genes and expansion of Brassicaceae-specific gene families. *Frontiers in Plant Science* 0, 802. doi:10.3389/FPLS.2014.00802.

Zhang, S., Lu, S., Yi, S., Han, H., Liu, L., Zhang, J., et al. (2016). Functional conservation and divergence of five SEPALLATA-like genes from a basal eudicot tree, Platanus acerifolia. *Planta 2016 245:2* 245, 439–457. doi:10.1007/S00425-016-2617-0.

Zhao, T., Holmer, R., de Bruijn, S., Angenent, G. C., van den Burg, H. A., and Schranz, M. E. (2017). Phylogenomic Synteny Network Analysis of MADS-Box Transcription Factor Genes Reveals Lineage-Specific Transpositions, Ancient Tandem Duplications, and Deep Positional Conservation. *The Plant Cell* 29, 1278–1292. doi:10.1105/TPC.17.00312.

Zhao, X. Y., Cheng, Z. J., and Zhang, X. S. (2006). Overexpression of TaMADS1, a SEPALLATA-like gene in wheat, causes early flowering and the abnormal development of floral organs in Arabidopsis. *Planta* 223, 698–707. doi:10.1007/s00425-005-0123-x.

Zhu, Q.-H., and Helliwell, C. A. (2011). Regulation of flowering time and floral patterning by miR172. *Journal of Experimental Botany* 62, 487–495. doi:10.1093/JXB/ERQ295.

Zik, M., and Irish, V. F. (2003). Global identification of target genes regulated by APETALA3 and PISTILLATA floral homeotic gene action. *Plant Cell* 15, 207–222. doi:10.1105/tpc.006353.